

UNIVERSIDAD COMPLUTENSE DE MADRID

FACULTAD DE CIENCIAS QUÍMICAS

Departamento de Ingeniería Química



TESIS DOCTORAL

**Estudio termodinámico del proceso de separación de
copolímero de Etileno-Vinil Acetato (EVA) en disolución**

MEMORIA PARA OPTAR AL GRADO DE DOCTOR

PRESENTADA POR

Javier Adolfo Camacho Adrianza

Directores

Gabriel Ovejero Escudero

Eduardo Díez Alcántara

Madrid, 2017

UNIVERSIDAD COMPLUTENSE DE MADRID

FACULTAD DE CIENCIAS QUÍMICAS

Departamento de Ingeniería Química



**Estudio termodinámico del proceso de
separación del copolímero de Etileno -
Vinil Acetato (EVA) en disolución**

TESIS DOCTORAL

Autor: Javier Adolfo Camacho Adrianza

Directores: Gabriel Ovejero Escudero / Eduardo Díez Alcántara

Madrid, 2015

UNIVERSIDAD COMPLUTENSE DE MADRID

FACULTAD DE CIENCIAS QUÍMICAS

Departamento de Ingeniería Química



**Thermodynamic study of the Ethylene -
Vinyl Acetate copolymer (EVA) solution
separation process**

PHD THESIS

Author: Javier Adolfo Camacho Adrianza

Directors: Gabriel Ovejero Escudero / Eduardo Díez Alcántara

Madrid, 2015

D. GABRIEL OVEJERO ESCUDERO, Catedrático, y D. EDUARDO DIEZ ALCÁNTARA, Profesor Contratado Doctor, del Departamento de Ingeniería Química de la Universidad Complutense de Madrid.

CERTIFICAN:

Que el presente trabajo de investigación titulado: “ESTUDIO TERMODINÁMICO DEL PROCESO DE SEPARACIÓN DEL COPOLÍMERO DE ETILENO – VINIL ACETATO (EVA) EN DISOLUCIÓN” constituye la memoria que presenta el ingeniero D. JAVIER ADOLFO CAMACHO ADRIANZA para aspirar al grado de *Doctor en Ingeniería Química*, y ha sido realizada en los laboratorios del Departamento de Ingeniería Química de la Universidad Complutense de Madrid bajo nuestra dirección.

Y para que conste, firmamos el presente certificado en Madrid, a veinte de octubre de dos mil quince.

Fdo. Gabriel Ovejero Escudero

Fdo. Eduardo Díez Alcántara

To my daughter, Andrea Valeria

Acknowledgments

Eduardo Díez

Gabriel Ovejero

M^a Dolores Romero

Ismael Díaz

José Luis Sotelo

Alicia Garcia

M^a Carmen Garcia

Ismael Águeda

Miguelangel Ocaña

Cesar Gómez

Manuel Consuegra

Jesus Plaza

Table of Contents

Abstract.....	ix
CHAPTER 1: Introduction	1
1.1 Ethylene – Vinyl Acetate Copolymer	1
1.1.1 Properties	1
1.1.2 Applications	3
1.1.3 EVA Production processes.	4
1.1.4 EVA Solution production process	5
1.1.5 Global market	7
1.1.6 References	9
1.2 Thermodynamics of polymer/solvent systems	10
1.2.1 Phase Equilibria in Polymer Systems	10
1.2.1.1 Polymer Solubility (Liquid-Liquid Equilibria)	10
1.2.1.2 Solvent Sorption in Polymers (Vapor-Liquid Equilibria)	11
1.2.2 Thermodynamic modeling.....	12
1.2.2.1 Gibbs energy models.....	12
1.2.2.1.1 Flory Huggins Model	12
1.2.2.1.2 Bernard Wolf Model.....	17
1.2.2.2 Equations of state.....	20
1.2.2.2.1 PC- SAFT model.....	21
1.2.3 References	25
1.3 Thermodynamic Characterization.....	28
1.3.1 Solvent/Solvent mixtures.....	28
1.3.1.1 Glass Ebullometer.....	28
1.3.1.2 Gas Chromatography (CG)	29
1.3.2 Polymer/Solvent mixtures	30
1.3.2.1 Intrinsic Viscosity (IV)	30
1.3.2.2 Inverse Gas Chromatography (IGC)	33
1.3.3 References	35

1.4 Polymer Characterization	37
1.4.1 Gel Permeation Chromatography (GPC)	37
1.4.2 Differential Scanning Calorimetry (DSC).....	38
1.4.3 Thermogravimetric Analysis (TGA).....	39
1.4.4 Scanning Electron Microscopy (SEM)	40
1.4.5 Intrinsic Viscosity (IV).....	40
1.4.6 References	41
1.5 Hypothesis and objectives	42
1.5.1 Overview	42
1.5.2 General Objective	45
1.5.3 Specific Objectives	45
1.5.4 Thesis structure	46
1.5.5 References	47

CHAPTER 2: Thermodynamics of EVA/solvents mixtures at infinite dilution of solvents49

2.1 Thermodynamic Interactions of EVA Copolymer-Solvent Systems by Inverse Gas Chromatography Measurements	51
2.2 Inverse Gas Chromatography study of Polyvinylacetate - solvent and Polyethylene - solvent systems	59
2.3 Bulk polymer/solvent interactions for Polyethylene and EVA copolymers, below their melting temperatures.....	69
2.4 Comparison between three predictive methods for the calculation of polymer solubility parameters	85
2.5 Summary and Discussion	93

CHAPTER 3: Thermodynamics of EVA/solvents mixtures at infinite dilution of polymer97

3.1 Turbidimetric and intrinsic viscosity study of EVA copolymer – solvent systems.....	99
3.2 Thermodynamic study of PVAc – solvent and PE – solvent diluted solutions	115
3.3 Generalization of a double-point method to determine the intrinsic viscosity in a polymer - solvent mixture	123
3.4 Summary and Discussion	131

CHAPTER 4: Thermodynamics of solvent/solvent mixtures involved in the EVA solution process133

4.1 Vapor–Liquid Equilibrium at $p/kPa = 101.3$ of the Binary Mixtures of Ethenyl Acetate with Methanol and Butan-1-ol.....	135
4.2 Summary and Discussion	143

CHAPTER 5: Thermodynamics of EVA/solvents mixtures at finite compositions of polymer145

5.1 Prediction of sorption curves from Flory Huggins parameters determined at solvent and polymer infinite dilution	147
5.2 PC-SAFT thermodynamics of ethylene vinyl acetate copolymer in a solution separation process.....	167
5.3 Summary and Discussion	191

CHAPTER 6: Conclusions195

CHAPTER 7: Appendix.....199

Abstract

This work presents a rigorous thermodynamic study for the interactions between the Ethylene Vinyl Acetate (EVA) copolymer and the solvents involved in the separation stage (recovery column) of an EVA solution production process; in order to model accurately this process and provide an industrial tool that allows the development of suitable prediction and optimization strategies. To achieve this goal, the EVA copolymer was splitted into its correspondent homopolymers, Polyethylene (PE) and Polyvinylacetate (PVA). The solvents participating in this process are methanol and vinyl acetate, plus the strategic consideration of cyclohexane.

Initially, the traditional thermodynamics parameters for these polymer/solvents systems (Flory Huggins parameters) were determined at infinite dilution of polymer and infinite dilution of solvent, by means of the Intrinsic Viscosity procedure and the Inverse Gas Chromatography Technique, respectively. In addition, the interaction between these polymers and other solvents (representing dispersion, association and polar solvents) were determined, in order to develop an intensive thermodynamic assessment at such infinite dilutions conditions; reporting and evaluating several crucial thermodynamic variables for the EVA copolymer, Polyethylene and Polyvinylacetate.

Then, a novel methodology to estimate the Flory Huggins – polymer concentration curve, and the subsequent solvent sorption curve (pressure – polymer composition curves), from the mentioned Flory Huggins data measured at the composition extremes of the binary mixture (infinite dilution of polymer and solvent) was proposed, based on the works of Bernard Wolf. This methodology was validated for ten different polymer/solvent systems in a range of molecular weights from 10 to 250 kg/mol, with an overall value of the average absolute deviation (%AAD) between the literature and estimated pressure values around 1%. Therefore, it is applicable for any typical polymer/solvent system.

Applying the mentioned methodology for the polymer/solvent mixtures strategically considered in the EVA separation solution process, the solvent sorption curves were determined and fitted to the PC-SAFT equation on state model, in order to determine each PC-SAFT binary interaction parameter (k_{ij}), previously defining the best scheme for the association's interactions. A good agreement has been shown in all cases. The k_{ij} between the solvents were fitted from the vapor-liquid equilibrium data, also determined in this work. Finally the main EVA separation solution process was simulated in a recovery column, obtaining an average of %AAD for the mass flows of each component participating in this process, bellow to 1%, regarding the literature data shown in patents.

Resumen

Este proyecto presenta un estudio termodinámico riguroso para las interacciones entre el Copolímero de Etileno- Acetato de Vinilo (EVA) y los disolventes participantes en la etapa de separación (columna de recuperación) del proceso de producción del copolímero EVA en disolución; con el objetivo de modelar dicho proceso y de proveer una herramienta que permita el desarrollo de estrategias adecuadas para la predicción y optimización industrial. Para alcanzar este objetivo, el copolímero EVA ha sido dividido en sus correspondientes homopolímeros, Polietileno y Polivinilacetato. Los disolventes participantes en el mencionado proceso son metanol y acetato de vinilo. Adicionalmente se ha considerado estratégicamente al disolvente ciclohexano.

Inicialmente, se han determinado los parámetros termodinámicos tradicionales para los sistemas polímero/disolventes (parámetros de Flory Huggins) a dilución infinita de polímero y de disolvente, a partir de los procedimientos experimentales de determinación de Viscosidad Intrínseca, y de la técnica de Cromatografía Inversa de Gases, respectivamente. Adicionalmente se han determinado las interacciones entre los polímeros mencionados y otros disolventes (representando a los disolventes con propiedades de dispersión, asociación y polares), con el objetivo de desarrollar una evaluación termodinámica intensiva a dichas condiciones diluidas, para reportar y evaluar variables termodinámicas fundamentales del copolímero EVA, el Polietileno y el Polivinilacetato.

Seguidamente, se ha propuesto una metodología, para estimar la curva parámetros de Flory Huggins – composición de polímero, y la subsecuente curva de absorción de disolvente (Presión – concentración de polímero), a partir de los parámetros de Flory Huggins obtenidos a los mencionados extremos de las mezclas binarias (dilución infinita de polímero y de disolvente). Dicha metodología se ha basado en los trabajos de Bernard Wolf y ha sido validada para diez sistemas de polímeros/disolventes diferentes, en el rango de pesos moleculares entre 10 y 250 kg/mol, obteniendo un valor promedio de la desviación absoluta (%AAD) alrededor de 1%, entre la presión estimada y bibliográfica. Por lo tanto esta metodología es aplicable para los sistemas polímero/disolvente comunes.

Aplicando la mencionada metodología par a las mezclas binarias de los polímeros/disolventes implicados en el proceso de separación del copolímero EVA en disolución, se han determinado las respectivas curvas de absorción y se han ajustado al modelo PC-SAFT; determinando los parámetros de interacción binaria (k_{ij}) y definiendo el mejor esquema para las interacciones de asociación. Se han obtenido ajustes favorables en todos los casos. El k_{ij} entre los disolventes participantes ha sido determinado a partir de la curva equilibrio liquido-vapor, determinada también experimentalmente. Finalmente se ha simulado la etapa principal del proceso de separación del copolímero EVA, obteniendo un valor promedio del %AAD para los flujos máxicos de cada componente participante, menor al 1%, con respecto a los valores de reportados en las patentes industriales.

1 Introduction

This thesis is included in the research program “Thermodynamic studies for polymer/solvent systems to model an industrial separation process” of the Catalysis and Separation Processes Research Group of the Chemical Engineering Department of the Complutense University of Madrid. The work presented here is concerned with the thermodynamics of EVA copolymers/solvents systems, aimed to model the separation stage in the production of EVA copolymer in a solution process.

The content presented in this chapter, is a summary of the EVA copolymers overview (properties, applications, productions processes and global market), plus the state of the art of the polymer/solvent thermodynamics, considered in this work, and the characterization techniques employed for the polymers, and the thermodynamic interactions with solvents. Finally, the hypothesis and objectives are presented.

1.1 Ethylene - Vinyl Acetate copolymer (EVA)

1.1.1 Properties

EVA copolymers represent the largest-volume segment of ethylene copolymers market [1], and they are the products of the radical random copolymerization of the monomers ethylene and vinyl acetate (VA) in a predetermined ratio [2], as is shown in Figure 1.1.1. Therefore, they are considered to be composed on polyethylene (LDPE) and polyvinyl acetate (PVA) homopolymers.

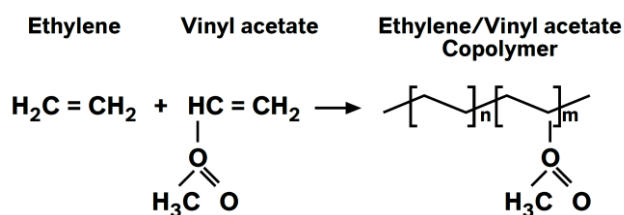


Figure 1.1.1. Radical polymerization and chemical structure of EVA copolymer

The presence of the acetoxy groups of VA disrupts the crystal structures that are present in LDPE [3] reducing its crystallinity and giving an amorphous character to the final EVA copolymer. Varying the percentage of VA in the composition, EVAs with significantly different properties are produced, which range from thermoplastic products (similar to LDPE) to rubber-like products [2].

The higher the proportion of vinyl acetate in the copolymer, the more the regularity of the ethylene chain is disturbed. Crystallization is increasingly hampered and is entirely absent from a copolymer with a vinyl acetate content of approx. 55 %. Copolymers with higher vinyl acetate content are therefore amorphous [4]. The presence of the PVA homopolymer, gives increasingly amorphous properties to the EVA copolymers, reducing the melt temperature (T_m), and appearing a glass transition temperature (T_g) as it is shown in Figure 1.1.2.

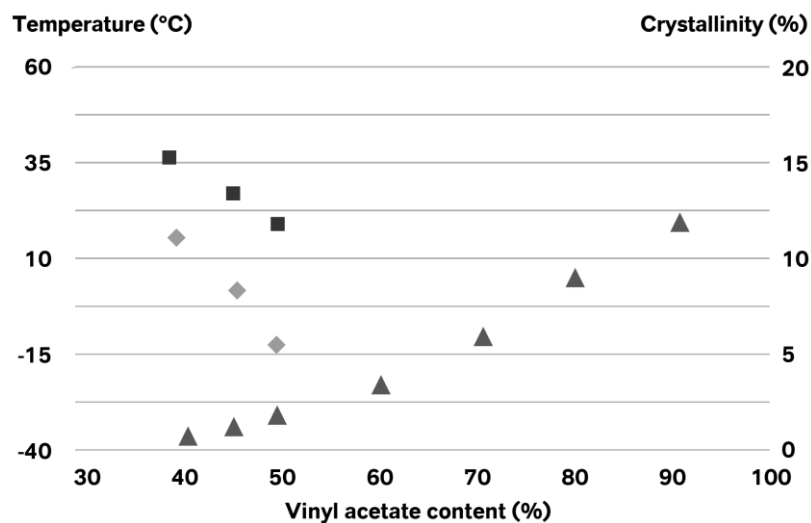


Figure 1.1.2. Influence of the VA content on EVA copolymers morphology [4]
 ▲ T_g (°C) ■ T_m (°C) ♦ Crystallinity (%)

A reduction of the crystallinity improves the flexibility, clarity, stress-crack and flex-crack resistance, low temperature flexibility and impact strength. However, the EVA copolymers exhibit reduced tensile strength, hardness, oil and grease resistance, melting point, heat seal temperature and dielectric properties versus the homopolymers LDPE, as well as greater permeability to gases and water vapor [3].

The polarity of the VA molecule also gives polarity to the resulting EVA, making these copolymers receptive to high filler loadings and to be combined with tackifiers and other adhesive components. Increased vinyl acetate content, in general, improves flexibility, elongation, adhesion, weathering properties and solubility in organic solvents. The flexibility imparted by the vinyl acetate gives EVA copolymers elastomer-like properties, and the ozone resistance is superior to most polymers [3].

EVA is thermally unstable above 220 °C, and so it has to be processed with care to avoid breakdown to acetic acid [3].

1.1.2 Applications

EVA copolymers with high VA content are typically used in adhesive applications (>20% VA), while low vinyl acetate copolymers, whose tensile moduli and surface hardness are greater, find greatest use in films (<20% VA), profile extrusions and injection molding (10-30% VA) [2]. EVA copolymers with only small vinyl acetate content (3% VA) are best considered as a modification of low-density polyethylene. These last copolymers have less crystallinity and greater flexibility, softness, and, in case of film, surface gloss [1].

Regarding the melt index (that describes the viscosity and the molecular weight of a polymer in the melt), as this property increases, the EVA copolymer exhibits improved flexibility, and declines in tensile strength, thermal stability and hardness. So, high melt flow rate grades are preferred for injection molding, since these grades fill mold cavities and solidify rapidly. Conversely, for extrusion processes, low melt flow rate grades are preferred to give the fabricator greater process flexibility and polymer melt strength before solidification [2]. Figure 1.1.3 shows the typical range of melt index and VA content of the EVA copolymers, by application.

In addition to specialty applications involving film and adhesives production, some typical end uses of EVAs resulting of molding, compounds, and extrusion applications, include flexible hose and tubing, footwear components, toys and athletic goods, wire and cable compounding, extruded gaskets, molded automotive parts (such as energy-absorbing bumper components), cap and closure seals [1].

EVA materials can be processed by all standard plastics processing techniques, including injection and blow molding, thermoforming, and extrusion into sheet and shapes. They accommodate high loadings of fillers, pigments, and carbon blacks. They are also compatible with other thermoplastics, and thus are frequently used for impact modification and improvement of stress-crack resistance. This combination of properties makes EVA copolymers highly adaptable vehicles for color concentrates.

Moreover, EVA resins can be formulated with blowing agents and cross-linking to produce low density foams via compression molding [1].

The EVA copolymers are slightly less flexible than normal rubber compounds but have the advantage of simpler processing since vulcanization is not always necessary. Typical applications include turntable mats, based pads for small items of office equipment, buttons, car door protection strips, and for other parts where a soft product of good appearance is required [1].

Another substantial use of EVA copolymers is as wax additives and additives for hot-melt coatings and adhesives [1].

In addition EVA is a copolymer encapsulant used as an interlayer in the industrial photovoltaic module encapsulation process. EVA serves to provide the functions of structural support, electrical isolation, physical isolation/protection and thermal conduction for the solar cell circuit [5].

Hydrolysis of EVA copolymers yields ethylene–vinyl alcohol copolymers (EVOH). EVOH material has exceptional gas barrier properties as well as oil and organic solvent resistance. The poor moisture resistance of EVOH is overcome by coating, coextrusion, and lamination with other substrates. Applications include containers for food, as well as chemicals and solvents [1].

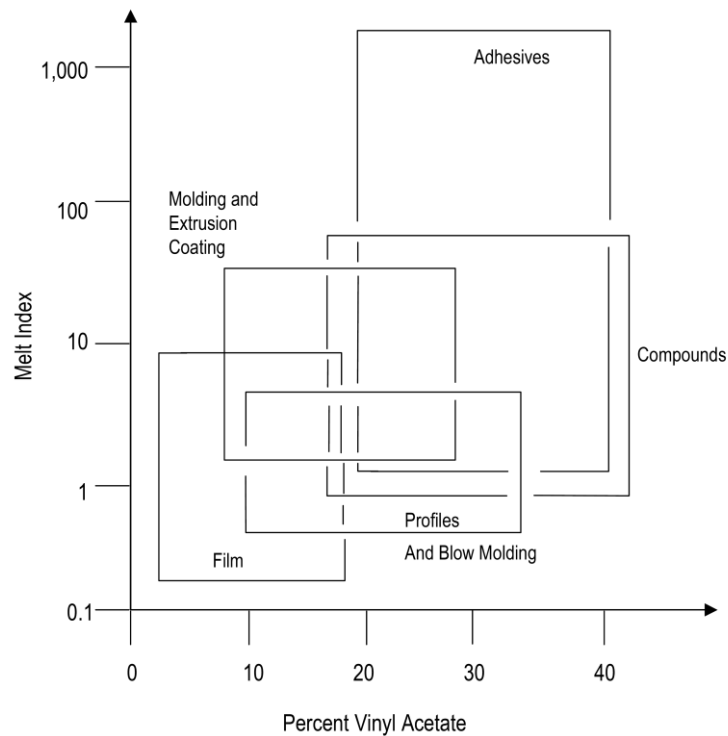


Figure 1.1.3. EVA copolymers applications range [2].

1.1.3 EVA Production processes

As previously stated, the vinyl acetate percentage in the EVA copolymer, will determine the final use of these polymers, and the final VA content will depend of the kind of polymerization process for the production of the EVA copolymer. It is known that ethylene and vinyl acetate may be radically copolymerized in varying proportions with random distribution of the monomers. The copolymerization may in principle be carried out by three different processes [6].

1. Emulsion polymerization
2. Solution polymerization
3. High pressure bulk polymerization.

EVA with low vinyl acetate content may be economically produced by high pressure bulk polymerization. If the VA content is low, the copolymers have the usual crystallinity of polyethylene at room temperature and are thermoplastic in character due to relatively long ethylene sequences. The polymerization is generally carried out at pressures from 1000 to 3000 bar and at temperatures from 150 to 280 °C. Products with vinyl acetate contents of up to 30% by weight prepared by this process may be used mainly, as hot melt adhesives and as rheology modifiers for crude oils and medium distillates and for cable sheaths. The high pressure process is not suitable for the preparation of EVA copolymers with medium to high VA contents (more than 30 %) [6]. Above this level the vinyl acetate acts increasingly as a telogen or chain stopper, thus making it difficult to make high average molecular weight resins (measured as low melt flow index) [3].

EVA copolymers with VA contents above 70% by weight are prepared predominantly by emulsion polymerization. The usual conditions are pressures from 30 to 500 bar and temperatures from 20 to 100 °C. The copolymer is generally not isolated from the dispersion obtained but directly used for further processing in the form of the aqueous dispersion (latex). Especially in this process, however, products with very high gel content are obtained which are not usable as elastomeric solid rubber on account of their poor processing properties. Their main use is in adhesives [6].

EVA copolymers having a VA content of at least 30% by weight may also be prepared by a solution polymerization process at medium pressure. The solvent used may be, for example, tertiary butanol or methanol, in which the polymers remain in solution throughout the polymerization process. The solution polymerization process is generally carried out in a train of 3 to 10 reactors at temperatures from 50° to 130° C. and pressures from 50 to 400 bar. The solvents are generally used in the presence of radical forming substances such as organic peroxides or azo-compounds as polymerization initiators. The products obtained by this process are high molecular weight, slightly branched thermoplastic elastomeric copolymers with low gel contents and VA contents of 30 to 75% by weight are obtained. The use of these copolymers is as rheology modifiers, adhesive binders and compounding components for thermoplasts and duroplasts, and for the production of vulcanisates [6].

1.1.4 EVA Solution production process

The following section describes a typical solution process for producing an ethylene-vinyl acetate copolymer based on the patents assigned to Kuraray Company [7,8]. This process comprises two main steps: copolymerizing ethylene and vinyl acetate in an alcohol based solvent and recovering unreacted vinyl acetate from a solution after copolymerizing. This EVA copolymer solution production process described below is shown in Figure 1.1.4 and its mass balance is presented in Table 1.1.1.

A stream containing ethylene, vinyl acetate and methanol is introduced in the polymerization vessel (R1). The methanol used as a solvent was previously deoxidized by nitrogen bubbling in advance, and its oxygen concentration was decreased to not more than 1 ppm. In the reactor, it is preferable that the polymerization temperature is at least 50 °C, but not more than 80 °C, and the pressure of the gaseous phase (ethylene pressure) is from 20 to 80 bar. In the case of batch type, it is preferable that the reaction

time is from 3 to 24 hours. In the case of continuous type, it is also preferable that the average residence time is in about the same range. The initiator usually employed is the 2,2'-azobis(2,4-dimethylvaleronitrile). Finally, the radical polymerization produces ethylene vinyl acetate (EVA) copolymers with a degree of polymerization about 30 to 80%, based on vinyl acetate.

Next, a polymerization inhibitor, as β -myrcene, is added to the solution containing an ethylene-vinyl acetate copolymer (copolymer solution), and the unreacted ethylene gas is evaporated from the copolymer solution in a flash tank (S1), and removed through the upper portion thereof.

The polymerization reaction solution (copolymer solution) drawn continuously from the polymerization vessel through its bottom portion, is fed into a recovery bubble-cap tower column (C1) filled with Rasching ring (e.g. 20 steps and diameter of 0.85), through the upper portion thereof, in order to extract the unreacted vinyl acetate from the copolymer solution. A vapor of the alcohol-based solvent (methanol) is continuously blown into the recovery column through the lower portion thereof. The methanol blown into the tower had been deoxidized by nitrogen bubbling in advance so that the oxygen concentration in the methanol was decreased to 10 ppm. Then, the unreacted vinyl acetate is taken out of the tower through the top portion thereof with part of the methanol, while the copolymer solution (EVA copolymer plus methanol) is taken out of the column through its bottom portion.

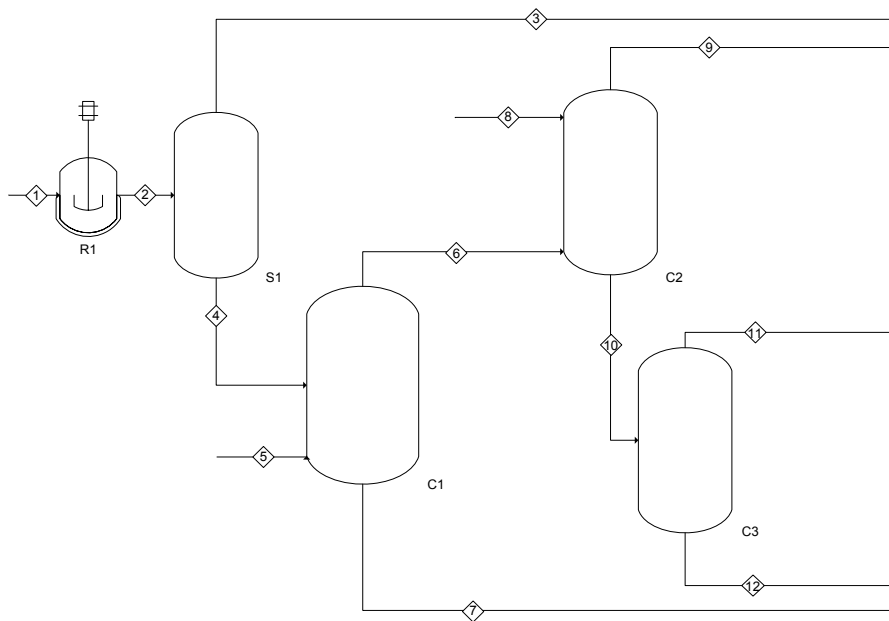


Figure 1.1.4. Process Diagram of an EVA copolymers solution production process [7,8]

Next, the mixture solution taken out of the recovery column through the top portion is introduced into another treatment column (C2), where vinyl acetate is separated from the mixture solution by extractive distillation with water, and it is taken out of the treatment column separated from a mixed solvent solution of alcohol and water. Furthermore, by separating and purifying this water/alcohol mixture solution in (C3), an

alcohol-based solvent can be recovered. The unreacted vinyl acetate and the alcohol-based solvent thus recovered are reused in the copolymerization. The alcohol-based solvent recovered also is reused in the above-mentioned recovery of vinyl acetate.

On the other hand, the ethylene-vinyl acetate copolymer contained in the methanol solution from which vinyl acetate had been separated can be separated in another column, or it is saponified to produce EVOH copolymers.

Table 1.1.1. Mass Balance of an EVA copolymers solution production process [7,8]

Stream	2	3	4	5	6	7	8	9	10	11	12
Temperature (°C)	60	60	60	60	60	60	60	60	60	60	60
Pressure (bar)	44.13	1.00	1.00	1.00	1.00	1.00	1.00	1.00	1.00	1.00	1.00
Mass Flow (kg/h)	1,333.3	133.3	1,200	474.0	927.3	746.7	865.5	556.4	1,236.4	865.5	370.9
% w/w Vinyl acet.	0.417	0.00	0.464	0.00	0.600	0.00	0.00	1.00	0.00	0.00	0.00
% w/w Methanol	0.231	0.00	0.256	1.00	0.400	0.550	0.00	0.00	0.300	1.00	0.00
% w/w Ethylene	0.100	1.00	0.00	0.00	0.00	0.00	0.00	0.00	0.00	0.00	0.00
% w/w EVA	0.256	0.00	0.280	0.00	0.000	0.450	0.00	0.00	0.00	0.00	0.00
% w/w Water	0.256	0.00	0.280	0.00	0.000	0.450	1.00	0.00	0.700	0.00	1.00

1.1.5 Global market

Ethylene vinyl acetate market is estimated to generate a global value of \$12,131.4 million by 2018, in applications such as film, injection molding, extrusion, non-extrusion, coating, and wire & cable [9].

The leading players of the EVA industry include: ExxonMobil Corporation (U.S), Lyondellbasell (The Netherlands), E.I. du Pont de Nemours & Co. (U.S), ENI S.p.A (Italy), and China Petroleum & Chemical Corporation (China) [9].

The global demand for EVA has growing sharply over the last decade, and it was 1.4 million tons in 2000. Global EVA capacity increased to 2.7 million tons in 2009 and it will grow and reach to 3.6 million tons in 2015 [10]. Much of the increase in demand for EVA came from the Asia-Pacific region, and the same trend is expected to continue in the near future. Asia-Pacific is expected to account for 52.4% of the global EVA demand in 2015.

Regarding the Global EVA demand by regions in 2009 (Figure 1.1.5), Asia-Pacific had the largest demand with 1,345,100 tons and a share of 51.3%. North America had a demand 858,600 tons and a share of 31.8% followed by Europe with a demand of 353,700 tons and a share of 13.1%. Middle East and Africa had a Demand of 83,700 tons and a share of 3.1% followed by South and Central America with a Demand of 78,300 tons and a share of 2.9%. The growth in Asian economies is seen as the main driver behind an increased global demand for EVA with the Chinese economy being the leader, followed by India and South Korea. As previously said, EVA foam and soles are extensively being used in shoe manufacturing industry, and over the last decade there has been a shift in manufacturing of shoe industries to Asian countries like China to

take advantage of low cost manufacturing facilities. This has created a demand growth in the Asia pacific region. The same trend is expected to continue in future [10].

The EVA global market, demand by end use in 2009 (Figure 1.1.6), leading end-use generally consisted on non film applications, flexible injection molding components, shoes foams and soles, thermosols and toys. It constituted 44.2% of the global EVA demand. Packaging (plastic films, hot melt adhesives etc) was the second leading market for EVA and accounts for 38.4% of global EVA end-use markets in 2009. Agriculture (films, etc) sector accounted for 9.2% share, and electrical (wires and cables, EVA sheet encapsulant for solar cells) sector accounted for 8.2% share in the global EVA demand, in 2009. The increased focus of world economies to invest in clean power is expected to increase the investments in the field of solar energy. EVA encapsulants currently have a market share of around 80% in this field (PV encapsulant). These increased investments in the sector will result in increasing of the overall EVA consumption and hence an increasing in the global EVA demand. Europe leads currently in this field but China and the US are expected to increase the investments in this sector [10].

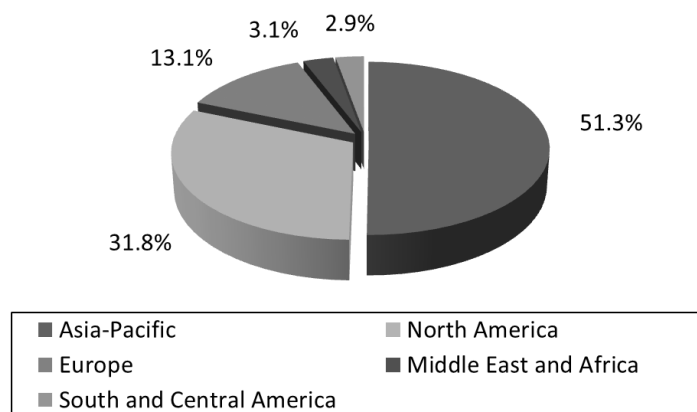


Figure 1.1.5. EVA copolymers global market demand (2.7 MT) by regions [10].

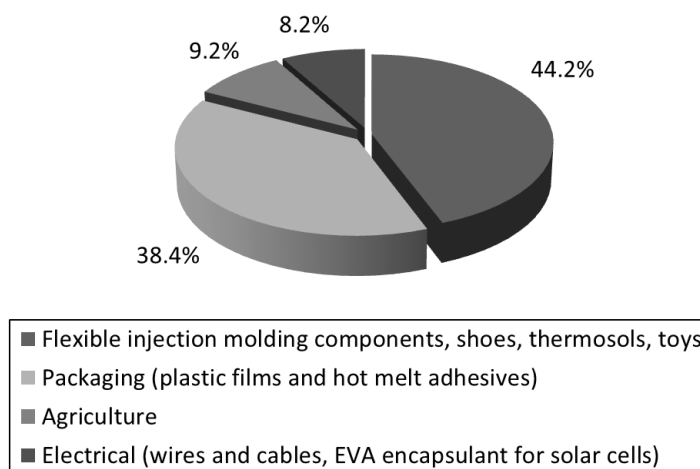


Figure 1.1.6. EVA copolymers global market demand by end use [10].

1.1.6 References

1. Chanda, M., & Roy, S. K. (2008). Industrial polymers, specialty polymers, and their applications (Vol. 74). CRC Press.
2. Anon. (2006). PERP Program—LDPE copolymers (03/04S9). Chem systems Reports. Nexant Inc., New York, USA
3. Whelan, A. (2012). Polymer technology dictionary. Springer Science & Business Media.
4. Anon. (2008). Levamelt. Lanxess Deutschland GmbH.
5. Agroui, K., Maallemi, A., Boumaour, M., Collins, G., & Salama, M. (2006). Thermal stability of slow and fast cure EVA encapsulant material for photovoltaic module manufacturing process. Solar energy materials and solar cells, 90(15), 2509-2514.
6. Baade, W., Obrecht, W., & Ohm, C. (1992). U.S. Patent No. 5,093,450. Washington, DC: U.S. Patent and Trademark Office.
7. Kawahara, T., & Hikasa, T. (2005). U.S. Patent No. 6,838,517. Washington, DC: U.S. Patent and Trademark Office.
8. Yanagida, N. (2004). U.S. Patent No. 6,683,148. Washington, DC: U.S. Patent and Trademark Office.
9. Ethylene Vinyl Acetate Market by Type (VLEVA, LEVA, MEVA, HEVA), Application (Film, Extrusion, Non-Extrusion, Injection Molding, Coating, Wire & Cable), by End-Uses (Shoes & Foams, Packaging, Photovoltaic Panels) & Geography - Trends & Forecasts to 2018. Markets and markets. Publishing Date: April 2014. Report Code: CH 2362
10. Ethylene Vinyl Acetate (EVA) Global Market to 2015 - Photovoltaic Encapsulants to Drive EVA Demand In The Future. GBI Research. 2011.

1.2 Thermodynamics of polymer/solvent systems

The knowledge of the mutual solubility of polymers and volatile organic substances is of importance for any applications in polymer chemistry and polymer engineering. Polymerizations, which should be performed in homogeneous phase, require the complete miscibility of monomer, polymer, solvent (liquid or supercritical) and other additives. Subsequently, the extraction of the polymer product from the reaction mixture requires a phase split (into two liquid phases or into a vapor and a liquid phase) to obtain a polymer product of high purity at one side as well as the unreacted monomer at the other side [1].

However, experimental data of polymer solubility is often scarce. Considerable experimental effort is generally required for determining these properties of polymer systems. Thermodynamics can provide powerful and robust tools for modeling of experimental data and even prediction of the thermodynamic behavior [1].

1.2.1 Phase Equilibria in Polymer Systems

1.2.1.1 Polymer Solubility (Liquid-Liquid Equilibria)

Polymers very often show only limited miscibility with liquid solvents. Moreover, miscibility is not only a function of temperature, pressure and polymer concentration, but also of molecular weight as well as of molecular-weight distribution of the polymer [1].

A typical phase behavior of a polymer/solvent system is shown in Figure 1.2.1 for the polystyrene/ methylcyclohexane system [2]. At low temperatures this system shows a region of demixing into two liquid phases (LL). In this region an increasing temperature leads to an improved miscibility. Above the critical temperature (Upper Critical Solution Temperature; UCST) the system is at first completely miscible and forms a homogeneous liquid solution (L). However, for polymer/solvent systems also a liquid-liquid demixing at high temperatures is typically observed. The reason is the so-called free-volume effect: At high temperatures, the density (inverse of "free volume") of the solvent decreases much more than that of the polymer. This causes a separation of polymer and solvent, showing a Lower Critical Solution Temperature (LCST). With further increasing temperature this effect becomes even more pronounced. UCST demixing is only slightly influenced by pressure, as it is typically the case for incompressible liquids. However, the LCST demixing shows pronounced pressure dependence because of the free-volume difference which at high temperature is directly determined by system pressure. In most cases an increasing pressure improves miscibility [1].

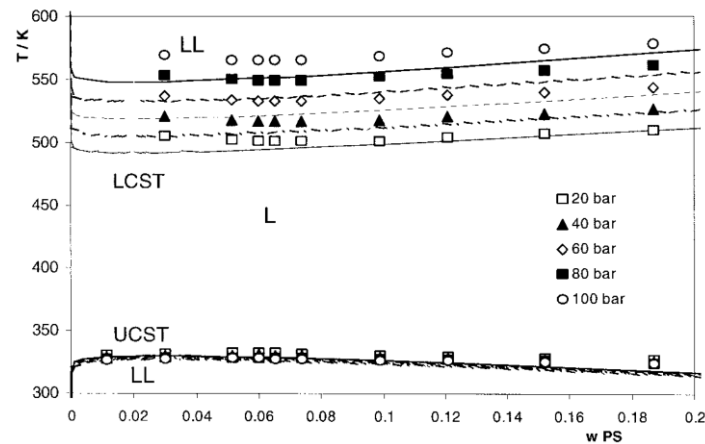


Figure 1.2.1. Polymer solubility (L-L) for methylcyclohexane/polystyrene system [2]

On the other hand, polymer solubility is a strong function of polymer molecular weight. Smaller polymers are better soluble and thus need a smaller pressure to be dissolved than large polymers. Therefore, for polydisperse polymers the molecular-weight distribution of the polymer has also to be considered in the modeling [3].

1.2.1.2 Solvent Sorption in Polymers (Vapor-Liquid Equilibria)

At low pressures (below the vapor pressure of the pure solvent), the solvent starts to evaporate from the polymer solution. On the other hand, solvent vapor of a given partial pressure may dissolve in the polymer. In these cases a liquid polymer/solvent mixture is in equilibrium with pure solvent vapor. An example is shown in figure 1.2.2 for the chlorobenzene/polystyrene system [4]. As it can be seen, the amount of solvent sorbed in the liquid polymer solution is a strong function of solvent partial pressure and temperature.

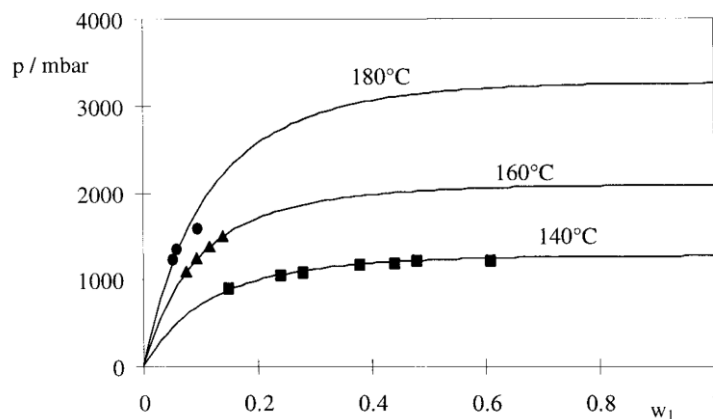


Figure 1.2.2. Sorption curves (V-L) for chlorobenzene/polystyrene system [4].

1.2.2 Thermodynamic modeling

1.2.2.1 Gibbs energy models

The sorption of a solvent vapor in a polymer can be described using [1]:

$$p = x_1 \gamma_1 p_{1,o} \quad (1)$$

where p is the pressure, x_1 is the solvent mole fraction and γ_1 the solvent activity coefficient, respectively. $p_{1,o}$ is the pure-component vapor pressure of the solvent at system temperature. Very often, instead of mole fraction x_1 , the weight fraction w_1 is used in (1):

$$p = x_1 \Omega_1 p_{1,o} \quad (2)$$

where Ω_1 , is the solvent weight-fraction activity coefficient.

For the description of liquid-liquid demixing, the thermodynamic phase-equilibrium conditions can be also formulated based on mole fractions or weight fractions, respectively,

$$x_i^I \gamma_i^I = x_i^{II} \gamma_i^{II} \quad (3)$$

or

$$w_i^I \Omega_i^I = w_i^{II} \Omega_i^{II} \quad (4)$$

The activity coefficients γ_i and Ω_i , in Equations (1) to (4) can be easily calculated from Gibbs energy models using classical thermodynamic relationships.

The first Gibbs energy model developed for polymer solutions is the well-known expression from Flory and Huggins [5], which was developed based on a lattice theory. Besides this, solvent activity coefficients can also be calculated using group-contribution methods. Some of them are based on the well-known UNIFAC model [6], which was originally proposed for low-molecular-weight substances, and later modified in order to consider the free-volume effect by the UNIFAC-FV models [7] and more recently by the Entropic FV models [8,9].

1.2.2.1.1 Flory Huggins Model

Processes taking place at constant temperature and constant pressure are normally dealt with in terms of changes in the Gibbs energy $\Delta \overline{G}$, which are made up of an enthalpy contribution $\Delta \overline{H}$, and an entropy contribution $\Delta \overline{S}$, according to:

$$\Delta \bar{G} = \Delta \bar{H} - T \Delta \bar{S} \quad (5)$$

where T is the absolute temperature. Quantities referring to one mole of mixture are characterized by a stroke above the symbol (\bar{X}).

Perfect mixing takes place athermally ($\Delta \bar{H} = 0$) and the volume of the mixture does not differ from the sum of the volumes of its constituents (change volume of mixing $\Delta \bar{V} = 0$). In this case the driving force for the formation of a molecularly disperse mixture consists exclusively of the changes in entropy associated with the mixing process. This described limiting situation is usually called perfect mixing (by similarity with the mixtures of gases or mixed crystals) and the following relation holds true [10]:

$$\frac{-\Delta \bar{S}^{perf}}{R} = x_1 \ln x_1 + x_2 \ln x_2 \quad (6)$$

where R is the universal gas constant and x_i are mole fractions of the two constituents of the mixture. The Gibbs energy of mixing can be expressed as:

$$\Delta \bar{G}^{perf} = -T \Delta \bar{S}^{perf} \quad (7)$$

However, real mixtures normally deviate considerably from the ideal behavior described above. In order to maintain a well-defined reference state the so called excess quantities (subscript E) are defined. They measure the deviation from perfect mixing, as formulated in the following equations.

$$\Delta \bar{G} = \Delta \bar{G}^{perf} + \Delta \bar{G}^E \quad (8)$$

This procedure is very useful for mixtures of low molecular weight compound. For polymer solutions and polymer blends the deviation from perfect behavior is, however, so pronounced that another reference state is advantageous.

So, for linear macromolecules Flory and Huggins have therefore developed the concept of combinatorial mixing. To this end, each molecule is subdivided into individual segments N_i that can be calculated as the quotient of the molar volume of the specie and the molar volume of the segment, as it is shown below:

$$N_i = \frac{\bar{V}_i}{V_{seg}} \quad (9)$$

Continuing with the approach, a lattice onto which the different segments of the individual molecules can be placed, is considered, as shown by the two-dimensional sketches of Fig. 1.2.3.

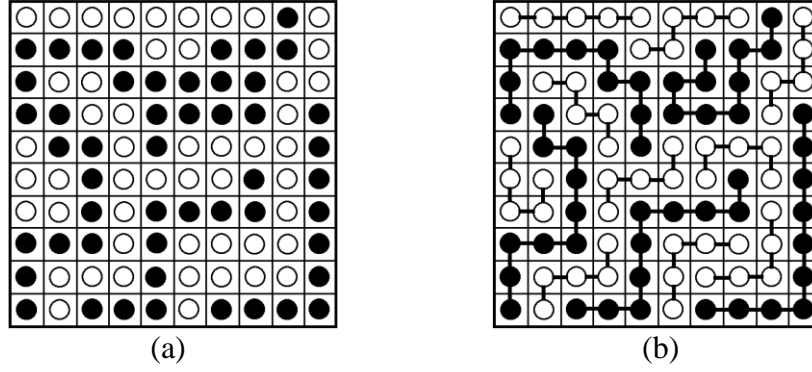


Figure 1.2.3. (a) Lattice model for a mixture of low molecular weight compounds.
(b) Lattice model for a mixture of chain molecules

The situation for a mixture of low molecular weight compounds ($N_1 = N_2 = 1$) is shown in part (a) of Figure 2.3 for an equal number of black and white entities, and assuming that this sketch stands for one 1 mole of mixture. Part (b) differs from part (a) only by the fact that the connection of 5 of the white molecules and 10 of the black molecules by a chemical bond to form a black penta-mer ($N_1 = 5$) and a white deca-mer ($N_1 = 10$). As a consequence of this action the number of moles has been reduced from 1 to 0.15, without changing the mass of the system. From the total of possibilities to place the segments of the chain molecules on the lattice, the authors have come to the following expression for the so-called combinatorial entropy of mixing for one mole of segments (instead of molecules), which is again an idealization like the corresponding expression for the perfect entropy of mixing (The quantities referring as a mole of segments are defined by a double stroke ($\overline{\overline{X}}$)).

$$\frac{-\Delta \overline{\overline{S}}}{R} = \frac{1}{N_1} \varphi_1 \ln \varphi_1 + \frac{1}{N_2} \varphi_2 \ln \varphi_2 \quad (10)$$

where φ_i represents the volume fraction of each mer. For many purposes volume fractions φ are employed as composition variables. For a binary mixture containing components that are made up of more than one segment, φ is given by:

$$\varphi_i = \frac{n_i N_i}{n_1 N_1 + n_2 N_2} \quad (11)$$

Where n_i are the moles of component i .

By analogy to mixtures of low molecular weight components, the deviation from this limiting behaviour has been quantified, introducing a residual contribution (subscript R) according to:

$$\Delta \overline{\overline{G}} = \Delta \overline{\overline{G}}^{\text{comb}} + \Delta \overline{\overline{G}}^R = -T \Delta \overline{\overline{S}}^{\text{comb}} + \Delta \overline{\overline{G}}^R \quad (12)$$

where

$$\Delta G^{\text{==}R} = RTg\varphi_1\varphi_2 \quad (13)$$

This expression takes into account enthalpic and also entropic contributions, and the parameter g is dependent of composition which is called the the integral Flory-Huggins interaction parameter.

Finally in terms of one mole of segments as the basis, the integral Gibbs energy $\overline{\Delta G}$ reads:

$$\frac{\overline{\Delta G}}{RT} = \frac{\varphi_1}{N_1} \ln \varphi_1 + \frac{\varphi_2}{N_2} \ln \varphi_2 + g\varphi_1\varphi_2 \quad (14)$$

For polymer/solvent mixtures (subscripts 2 and 1, respectively), in many cases the molar volume of the solvent is set equal to the molar volume of the segment, thus $N_1 = 1$ and N_2 is redefined as N , so expression (14) is transformed into (15):

$$\frac{\overline{\Delta G}}{RT} = (1 - \varphi_2) \ln(1 - \varphi_2) + \frac{\varphi_2}{N} \ln \varphi_2 + g\varphi_2(1 - \varphi_2) \quad (15)$$

The integral interaction parameter g , can be related to the original Flory–Huggins interaction parameter χ [5], by the following equation [11]:

$$\chi = g - (1 - \varphi_2) \frac{\partial g}{\partial \varphi_2} \quad (16)$$

Only if g does not depend on composition, this parameter becomes identical to the experimentally measurable Flory–Huggins interaction parameter χ . In the early days, this parameter χ was incorrectly considered to depend only on state variables, but not on the composition of the polymer in the mixture. Nowadays it is clear that is composition dependant. A lot of efforts were done by different authors to find reasonable expressions for the concentration dependence of the χ parameter [11, 12, 13, 14].

On the other hand, the partial segment molar Gibbs energy in a polymer/solvent mixture, expressed in terms of the “solvent” chemical potential μ_1 , is:

$$\frac{\Delta \mu_1}{RT} = \frac{\overline{\Delta G}_1}{RT} = \ln(1 - \varphi) + \frac{1 - 1/N}{\varphi} \varphi + \chi \varphi^2 = \ln a_1 \quad (17)$$

Where a_1 , the solvent activity can be approximated (enough low volatility of the solvent) to the ratio of the solvent vapour pressure in the mixture to the pure solvent vapour pressure:

$$a_1 \approx \frac{P_1}{P_{1,o}} \quad (18)$$

Equations (17) and (18) allow the estimation of a sorption point for a solvent vapor in a polymer (P₁ “vs” polymer composition), previously knowing the Flory Huggins parameter.

Moreover, Hildebrand and Scout [15] developed a regular solution model defining the Hildebrand solubility parameter (HSP) of a compound (δ_i) as the square root of its cohesive energy (c_i). The HSP of a solvent (δ_1) can be calculated by the expression:

$$\delta_1 = \sqrt{c_1} = \left[\frac{\Delta_{vap}H_1 - RT}{V_1} \right]^{0.5} \quad (19)$$

where $\Delta_{vap}H_1$ is the enthalpy of vaporization of the solvent and V_1 is the molar volume of solvent.

In addition the Flory Huggins theory modified by Blanks and Prausnitz [16] allows establishing a relationship between the Flory Huggins parameter (χ) and the solubility parameters of polymer (δ_2) and solvent (δ_1), according to the expression:

$$\chi = \chi_s + \chi_H = \chi_s + \frac{V_1}{RT} (\delta_1 - \delta_2)^2 \quad (20)$$

where χ_s is the entropic contribution and χ_H is the enthalpic contribution to χ .

However the Hildebrand solubility parameter definition only takes into account dispersive interactions, but no dipole – dipole interactions or hydrogen bonding interactions [17]. So, with the aim of overcoming this difficulty, Hansen [17] proposed to divide the solubility parameter of a compound into three different contributions: one due to non-polar or dispersion forces, another due to polar forces, and a last one which takes into account hydrogen-bonding effects; according to the expression:

$$\delta_i^2 = \delta_{d,i}^2 + \delta_{p,i}^2 + \delta_{h,i}^2 \quad (21)$$

And considering the works of Petterson [18] the Flory Huggins parameter can be defined as:

$$\chi = \frac{V \left[(\delta_{d,2} - \delta_{d,1})^2 + 0.25(\delta_{p,2} - \delta_{p,1})^2 + 0.25(\delta_{h,2} - \delta_{h,1})^2 \right]}{RT} \quad (22)$$

On the other hand, the partial segment molar Gibbs energy in a polymer/solvent mixture, expressed in terms of the “polymer” chemical potential μ_2 , can be determined by means of an expression analogous to (17) by:

$$\frac{\Delta\mu_2}{RT} = \frac{N\Delta\bar{G}_2}{RT} = \ln \phi + (1-N) \left(\frac{1-\phi}{N} + \xi \frac{1-\phi}{N} \right)^2 \quad (23)$$

This previous equation defines the interaction parameter ξ , in terms of the chemical potential of the polymer. This interaction parameter can be calculated from the integral value g by means of [11]:

$$\xi = g + \phi \frac{\partial g}{\partial \phi} \quad (24)$$

However, the integral interaction g parameter is practically inaccessible, and the parameter ξ , referring to the polymer, suffers from the difficulties associated with the formation of perfect polymer crystals, because it is based on their equilibrium with saturated polymer solutions.

1.2.2.1.2 Bernard Wolf Model

Recent works of Bernard Wolf, in order to develop a molecular relationship between the integral interaction parameter g , and the Flory–Huggins interaction parameter χ , considered two features initially neglected by the original Flory–Huggins theory, subdividing the solution dilution process (expressed in terms of the Flory Huggins parameter at infinite dilution of solvent χ_o) into two separate steps [11]:

$$\chi_o = \chi_o^{fc} + \chi_o^{cr} \quad (25)$$

The first term (the superscript “ fc ” stands for fixed conformation) quantifies the effect of separating two contacting polymer segments belonging to different macromolecules by inserting a solvent molecule between them, without changing their conformation. The second term (the superscript “ cr ” stands for conformational relaxation) is required to bring the system into its equilibrium, by rearranging the components so that the minimum of Gibbs energy is achieved.

Figure 1.2.4 illustrates these steps of dilution, where two contacting segments belonging to different macromolecules are separated by the insertion of a solvent molecule between them.

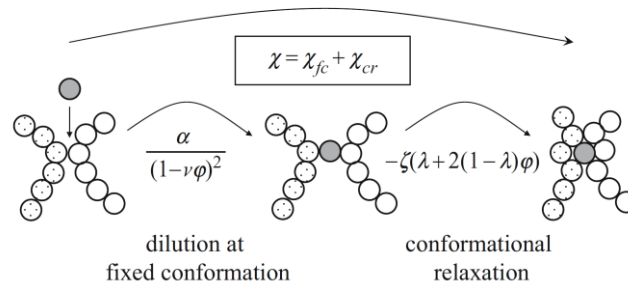


Figure 1.2.4. Individual steps of dilution considered by Bernard Wolf [11].

In order to give the second term a more specific meaning, Wolf formulated it [11], as the difference between the interaction before and after the conformational relaxation:

$$\chi_o^{cr} = \chi^{after} - \chi^{before} \quad (26)$$

where χ_o^{cr} is proportional (ξ) to the interaction between polymer segments and solvent molecules in the isolated state (λ), and χ_o^{fc} is denoted as other parameter (α), according to the expressions:

$$\chi_o^{cr} = -\zeta\lambda \quad (27)$$

$$\chi_o^{fc} = \alpha \quad (28)$$

Finally, the Flory Huggins interaction parameter at infinite dilution of solvent, can be re-written as

$$\chi_o = \alpha - \zeta\lambda \quad (29)$$

In order to generalize Equation (29) to whatever polymer composition, Wolf [11] assumed that the composition dependence of the first term can be evaluated as a function of a variable v , which take into accounts for the differences between the molecular surfaces of solvent and polymer. For the second term, Wolf assumed a linear dependence of the integral interaction parameter g on polymer volumetric fraction ϕ . The result of this generalization is shown in (30).

$$\chi = \frac{\alpha}{(1-v\phi)^2} - \zeta(\lambda + 2(1-\lambda)\phi) \quad (30)$$

The Flory–Huggins interaction parameter χ of Equation (30) yields the following expression for the integral interaction parameter g , which is required for instance to calculate phase equilibrium using the method of the direct minimization of the Gibbs energy [19] of a system:

$$g = \frac{\alpha}{(1-v)(1-v\phi)} - \zeta(1 + (1-\lambda)\phi) \quad (31)$$

Moreover, Wolf [11] consider that the second term of Equation (29) is almost always negligible (with respect to 1/2) for polymers of enough molar mass, thus the parameters ξ and λ can be merged into their product $\xi\lambda$, and the isolated λ can be replaced by 1/2. Thus Equation (29) is transformed into the more simple Equation (32), while the analogous expression for the integral parameter is Equation (33).

$$\chi \approx \frac{\alpha}{(1-v\phi)^2} - \zeta\lambda(1+2\phi) \quad (32)$$

$$g = \frac{\alpha}{(1-\nu)(1-\nu\phi)} - \xi\lambda(2+\phi) \quad (33)$$

With these assumptions, the number of adjustable parameter is reduced to three (α , ν , $\xi\lambda$). Figure 1.2.5 shows a typical breakdown of the composition dependence of the overall Flory Huggins parameter, as well as its contributions resulted from the two steps of dilution, for the system Polyvinylmethylether (PVME)/Cyclohexane (CH), predicted by the mentioned three parameters.

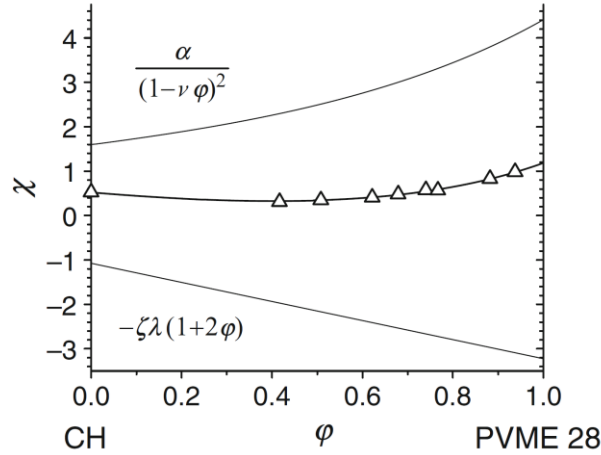


Figure 1.2.5. Polymer composition dependence of χ for PVME/CH at 35 °C [11]
($\alpha = 1.599$, $\nu = 0.398$, and $\xi\lambda = 1.074$)

To analyse the temperature dependence of the three parameters (α , ν , $\xi\lambda$), the relationship shown in Equation (34) has proved to be very versatile to model $\pi_{(T)}$, where π is whatever of the three above mentioned parameters, and π_1 or π_2 can be set to zero in most cases [11].

$$\pi = \pi_o + \pi_1 / T + \pi_2 T \quad (34)$$

All the previously described considerations are applicable to organic solvents/homopolymers solutions. The different molecular architectures of branched polymers do not require additional modifications on this theory. On the other hand, to apply the approach described above to solutions of random copolymers (containing type A and type B monomers), the different parameters π (α , ν , $\xi\lambda$) must be a function of f , the weight fraction of B-monomers contained in the A-ran-B copolymer. For this purpose, the approach of Equation (35) has been proposed [20].

$$\pi_{AB} = \pi_A(1-f) + \pi_B f + \pi_E f(1-f) \quad (35)$$

According to this equation, the different parameters π_{AB} , referred to a copolymer of composition f , are calculated with the corresponding homopolymer parameters, π_A and π_B , plus an excess term π_E , which quantify the extra effects resulting from the presence of two types of monomeric units in the copolymer chain.

1.2.2.2 Equations of state

Gibbs energy models in general can only be used to describe the activity coefficients of incompressible fluids. They do not take into account density changes of a system and thus they cannot be applied to describe non-idealities of the vapor phase at elevated and high pressures. Moreover, they cannot predict LCST demixing of a polymer/solvent system. These drawbacks can be avoided by using an equation of state. This type of model consequently considers the relation between temperature, pressure, concentration and density of a system and can be applied to calculate fugacity coefficients, formulating the two phases in equilibrium conditions for polymer and solvent as [1]:

$$x_i^I \phi_i^I = x_i^{II} \phi_i^{II} \quad (36)$$

There are different approaches for the development of an equation of state described in literature. One early-considered possibility is to extend the lattice theory previously described by introducing holes. Therewith, the number of holes in the lattice is a measure for the density of the system. Density changes in the system are considered via a variation of the hole number. Equations of state based on this idea are for example the Lattice-Fluid Theory [21] and the Mean-Field Lattice-Gas Theory [22].

Another approach to obtain an equation of state is based on the partition function of a system derived from statistical mechanics. [23, 24, 25]. An alternative way is the application of so-called perturbation theories [26,27]. The main assumption here is applied to the Helmholtz energy of a system (A), based on the residual part A^{res} (the difference between the Helmholtz energy of a system, and the Helmholtz energy of an ideal gas state A^{ideal}) can be written as the sum of different contributions: the Helmholtz energy of a chosen reference system A^{ref} , and the Helmholtz energy due to perturbations A^{pert} . [1].

$$A^{res} = A - A^{ideal} = A^{ref} + A^{pert} \quad (37)$$

This concept is also applicable to the system pressure.

An appropriate reference system (at least for small solvent molecules) is the hard-sphere (hs) system. Here, the molecules are assumed to be spheres of a fixed diameter and do not have any attractive interactions. Such a reference system covers the repulsive interactions of the molecules. Deviations of real molecules from the reference system may occur due to attractive interactions (dispersion), formation of hydrogen bondings (association), chain formation and dipolar interactions. These contributions can be accounted for by using different perturbation terms [1].

The first model in this category was the Statistical-Associating-Fluid Theory (SAFT) [28, 29, 30]. Here a chain-like molecule (solvent molecule or polymer) is assumed to be a chain of m identical spherical segments. Starting from a reference system of m hard spheres (A^{hs}), this model considers three perturbation independent contributions: dispersion, association and chain formation. The hard-chain system is obtained as the sum of the hard-sphere and chain-formation contributions A^{hs} and A^{chain}

$$A^{res} = \underbrace{mA^{hs} + A^{chain}}_{A^{hard-chain}} + mA^{disp} + A^{assoc} \quad (38)$$

1.2.2.2.1 PC- SAFT model

The recently proposed Perturbed-Chain SAFT (PC-SAFT) model [31] is a modification of SAFT which was developed especially to improve the description of polymer systems. Here the reference system of hard chains is used instead of the hard-sphere system. Therefore, the dispersion term now considers the attraction of chain-molecules instead of unbonded spheres, as a function of the chain length m . In addition to dispersive interactions, the phase behaviour of pure fluids and mixtures is also strongly affected by specific intermolecular interactions like association (hydrogen bonding) plus the dipolar interactions:

$$A^{res} = A^{hc} + mA^{disp} + A^{assoc} + A^{dipole} \quad (39)$$

Figure 1.2.6 illustrates the segment – segment interaction contributions which are taking into account in the PC-SAFT model, that allow modelling most of the binary systems: low molecularweight systems (including mixtures of strongly polar and non-polar fluids, mixtures of polar and associating fluids, and mixtures with carboxylic acids), solid–liquid equilibria, polymer/solvents systems (including copolymers), polymers blends and ionic liquid systems [31].

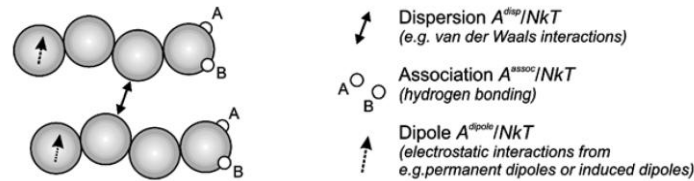


Figure 1.2.6. PC-SAFT perturbation contributions to account for dispersion, association and dipolar interactions

According to Equation (39), the different contributions to the Helmholtz energy which are considered in PC-SAFT, are resumed as follows:

- **Hard-Chain Contribution A^{hc} :** This contribution considers the hard-chain reference fluid as spherical segments that do not show any attractive interactions. It is defined by two parameters, named the number of segments m and the diameter of segments σ . The Helmholtz energy of this reference system is described by an expression developed by Chapman [32], which is based on Wertheim's first-order thermodynamic perturbation theory [33].
- **Dispersion Contribution A^{disp} :** To determine the contribution of dispersive attractions to the Helmholtz energy of a system, PC-SAFT applies the perturbation theory of

Barker and Henderson [34], to the hard-chain reference system. One additional parameter is required for describing the segment – segment interaction: the dispersion energy parameter ε/k . All three parameters (m , σ and ε/k) are determined by simultaneously fitting to liquid density and vapour - pressure data of a pure component. To model mixtures, conventional Berthelot–Lorentz combining rules are applied:

$$\sigma_{ij} = 0.5(\sigma_i + \sigma_j) \quad (40)$$

$$\varepsilon_{ij} = \sqrt{\varepsilon_i \varepsilon_j} (1 - k_{ij}) \quad (41)$$

Equation (35) contains one adjustable binary interaction parameter k_{ij} (usually independent of temperature) which is used to correct the dispersion energy in the mixture. This is determined from fitting the phase-equilibrium data of the binary mixture.

- *Association Contribution A^{assoc}* : The contribution due to short-range association interactions (hydrogen bonding) is considered by an association model that also was proposed by Chapman [32], based on Wertheim's first-order thermodynamic perturbation theory [33]. Within this theory, a molecule is assumed to have one or more association sites that can form hydrogen bonds. This is shown exemplarily also in Figure 1.2.6 for molecules with two association sites A and B. The association between two association sites is characterized by two additional parameters: the association energy ε^{AiBi}/k and the effective volume of an association interaction κ^{AiBi} . Therefore, an associating compound is characterized by five pure-component parameters. The strength of cross-association interactions between two different associating compounds can be determined using simple combining rules of the pure-component parameters, as suggested by Wolbach and Sandler [35], without introducing binary parameters.

$$\varepsilon^{AiBj} = 0.5(\varepsilon^{AiBi} + \varepsilon^{AjBj}) \quad (42)$$

$$\kappa^{AiBj} = \sqrt{\kappa^{AiBi} \kappa^{AjBj}} \left(\frac{\sqrt{\sigma_{ii} \sigma_{jj}}}{0.5(\sigma_{ii} + \sigma_{jj})} \right)^3 \quad (43)$$

- *Dipole/Polarizability Contribution A^{dipole}* : The long-range electrostatic interactions of dipolar and polarizable fluids A^{dipole} are taken into account by the expression of Kleiner and Gross (PCIP-SAFT) [36]. It is based on the renormalized perturbation theory for polarizable polar fluids of Wertheim, which was applied to the dipole contribution for non-spherical molecules of Gross and Vrabec [37]. Since tabulated values for the dipole moments and average molecular polarizabilities are available, no additional adjustable parameters are required.

Specifically in polymer/solvent systems, where large differences in molecular size of polymers and solvents are present, and the molar-mass distribution of a polymer is significant, the modelling of these systems is always challenging. As PC-SAFT model is based on the hard-chain reference system and thus explicitly considers the attractive interactions of chain molecules instead of those of the unbonded segments, is particularly suitable for describing polymer/solvent systems. Compared to low molecular weight substances, the determination of pure-component parameters for polymers is more difficult because polymer vapour-pressure data are not accessible. A methodology for the identification of pure-component parameters for polymers and the binary interaction parameter k_{ij} , is the simultaneous fitting of liquid densities and phase equilibrium data of the polymer/solvent system [38].

For example, the pure-component parameters and the binary interaction parameter k_{ij} for the system low - density polyethylene (LDPE)/ethene, shown in figure 1.2.7, were determined by fitting the liquid densities of LDPE and the experimental binary data of LDPE/ethene. The same pure-component parameters of LDPE were then subsequently used to model the cloud points of LDPE in different solvents (ethane, propane, propene, 1-butene, and n-butane) using one k_{ij} for each respective binary system [39]. The modelling results and the comparison with the experimental data show a good agreement.

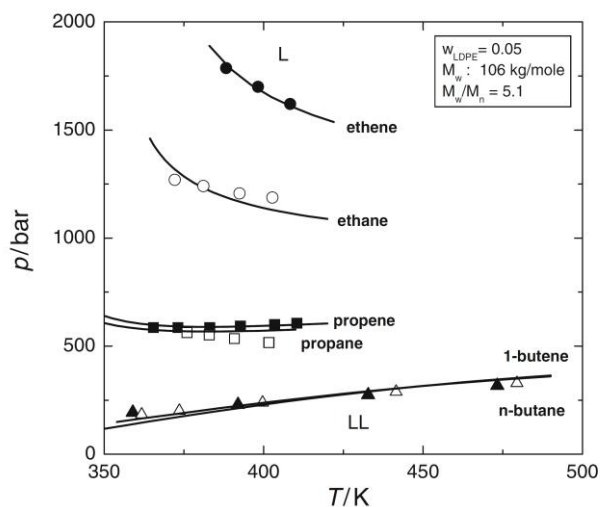


Figure 1.2.7 PC-SAFT cloud-point predictions for LDPE/solvent systems [39].

Furthermore, the influence of molecular weight on phase behaviour can be taken into account when applying PC-SAFT. By only varying the segment number proportional to the molecular weight, the solubility of the polymer/solvent mixtures can be predicted by PC-SAFT [40].

Finally, the modelling of a copolymer (consisting of α -segments and β -segments)/solvent mixture requires the appropriate pure-component parameters of the respective homopolymer segments and of the solvent. This system is illustrated in Figure 1.2.8. The binary parameters of the homopolymer/solvent systems ($k_{\alpha-S}$, $k_{\beta-S}$) can be determined from fitting the phase equilibrium data of the respective homopolymers/solvent systems. To describe the copolymer system, if necessary, one additional binary interaction parameter can be fitted to binary copolymer data, which accounts for the dispersive interactions between the homopolymer segments ($k_{\alpha-\beta}$) in the copolymer solution [40].

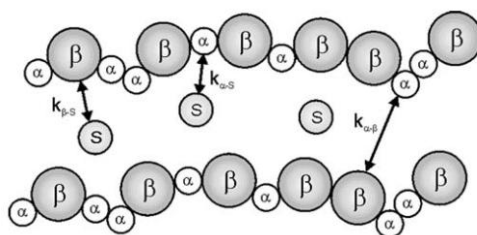


Figure 1.2.8 PC-SAFT Molecular model for a copolymer of type poly(α -co- β), composed of segments α and β in interaction with a solvent S

1.2.3 References

1. Sadowski, G. (2004, February). Thermodynamics of polymer systems. In *Macromolecular Symposia* (Vol. 206, No. 1, pp. 333-346). WILEY-VCH Verlag.
2. Enders, S., & de Loos, T. W. (1997). Pressure dependence of the phase behaviour of polystyrene in methylcyclohexane. *Fluid phase equilibria*, 139(1), 335-347.
3. Behme, S., Sadowski, G., Song, Y., & Chen, C. C. (2003). Multicomponent flash algorithm for mixtures containing polydisperse polymers. *AIChE journal*, 49(1), 258-268.
4. Sadowski, G., Mokrushina, L. V., & Arlt, W. (1997). Finite and infinite dilution activity coefficients in polycarbonate systems. *Fluid phase equilibria*, 139(1), 391-403.
5. Flory P.J., J. Chem. Phys. 1942, 10, 51
6. Fredenslund, A. A. (1977). Vapor-Liquid equilibrium using UNIFAC a group-contribution method.
7. Oishi, T., & Prausnitz, J. M. (1978). Estimation of solvent activities in polymer solutions using a group-contribution method. *Industrial & Engineering Chemistry Process Design and Development*, 17(3), 333-339.
8. Elbro, H. S., Fredenslund, A., & Rasmussen, P. (1990). A new simple equation for the prediction of solvent activities in polymer solutions. *Macromolecules*, 23(21), 4707-4714.
9. Kontogeorgis, G. M., Fredenslund, A., & Tassios, D. P. (1993). Simple activity coefficient model for the prediction of solvent activities in polymer solutions. *Industrial & engineering chemistry research*, 32(2), 362-372.
10. R. Horst and B.A. Wolf. Thermodynamics of polymer solutions. (Thermodynamik von Polymerlösungen) <http://wolf.chemie.uni-mainz.de/Internet/Students/Makro.htm>
11. Wolf, B. A. (2011). Making Flory–Huggins Practical: Thermodynamics of Polymer-Containing Mixtures. In *Polymer Thermodynamics* (pp. 1-66). Springer Berlin Heidelberg.
12. Kleintjens, L. A. L. (1979). Effects of chain branching and pressure on thermodynamic properties of polymer solutions (Doctoral dissertation, University of Essex).
13. Qian, C., Mumby, S. J., & Eichinger, B. E. (1991). Existence of two critical concentrations in binary phase diagrams. *Journal of Polymer Science Part B: Polymer Physics*, 29(5), 635-637.

14. Hu, Y., Lambert, S. M., Soane, D. S., & Prausnitz, J. M. (1991). Double-lattice model for binary polymer solutions. *Macromolecules*, 24(15), 4356-4363.
15. Hildebrand, J. H., & Scott, R. L. (1962). *Regular solutions*. Prentice-Hall.
16. Blanks, R. F., & Prausnitz, J. M. *Ind Eng Chem Fund* 1964, 3, 1. CrossRef, CAS, Web of Science® Times Cited, 219.
17. Hansen, C. M. (2007). *Hansen solubility parameters: a user's handbook*. CRCps.
18. Biroa, J., Zeman, L., & Patterson, D. (1971). Prediction of the X Parameter by the solubility parameter and corresponding states theories. *Macromolecules*, 4(1), 30-35.
19. Qian, C., Mumby, S. J., & Eichinger, B. E. (1991). Phase diagrams of binary polymer solutions and blends. *Macromolecules*, 24(7), 1655-1661.
20. Bercea, M., Eckelt, J., & Wolf, B. A. (2008). Random copolymers: their solution thermodynamics as compared with that of the corresponding homopolymers. *Industrial & Engineering Chemistry Research*, 47(7), 2434-2441.
21. Sanchez, I. C., & Lacombe, R. H. (1976). An elementary molecular theory of classical fluids. Pure fluids. *The Journal of Physical Chemistry*, 80(21), 2352-2362.
22. Kleintjens, L. A., & Koningsveld, R. (1980). Liquid-liquid phase separation in multicomponent polymer systems. *Colloid and Polymer Science*, 258(6), 711-718.
23. Beret, S., & Prausnitz, J. M. (1975). Perturbed hard-chain theory: An equation of state for fluids containing small or large molecules. *AIChE Journal*, 21(6), 1123-1132.
24. Cotterman, R. L., Schwarz, B. J., & Prausnitz, J. M. (1986). Molecular thermodynamics for fluids at low and high densities. Part I: Pure fluids containing small or large molecules. *AIChE journal*, 32(11), 1787-1798.
25. Morris, W. O., Vimalchand, P., & Donohue, M. D. (1987). The perturbed-soft-chain theory: An equation of state based on the Lennard-Jones potential. *Fluid Phase Equilibria*, 32(2), 103-115.
26. Barker, J. A., & Henderson, D. (1967). Perturbation theory and equation of state for fluids. II. A successful theory of liquids. *The Journal of Chemical Physics*, 47(11), 4714-4721.
27. Weeks, J. D., Chandler, D., & Andersen, H. C. (1971). Role of repulsive forces in determining the equilibrium structure of simple liquids. *The Journal of Chemical Physics*, 54(12), 5237-5247.

28. Chapman, W. G., Gubbins, K. E., Jackson, G., & Radosz, M. (1989). SAFT: Equation-of-state solution model for associating fluids. *Fluid Phase Equilibria*, 52, 31-38.
29. Huang, S. H., & Radosz, M. (1990). Equation of state for small, large, polydisperse, and associating molecules. *Industrial & Engineering Chemistry Research*, 29(11), 2284-2294.
30. Huang, S. H., & Radosz, M. (1991). Equation of state for small, large, polydisperse, and associating molecules: extension to fluid mixtures. *Industrial & Engineering Chemistry Research*, 30(8), 1994-2005.
31. Gross, J., & Sadowski, G. (2001). Perturbed-chain SAFT: An equation of state based on a perturbation theory for chain molecules. *Industrial & engineering chemistry research*, 40(4), 1244-1260.
32. Chapman, W. G., Jackson, G., & Gubbins, K. E. (1988). Phase equilibria of associating fluids: chain molecules with multiple bonding sites. *Molecular Physics*, 65(5), 1057-1079.
33. Wertheim, M. S. (1984). Fluids with highly directional attractive forces. II. Thermodynamic perturbation theory and integral equations. *Journal of statistical physics*, 35(1-2), 35-47.
34. Barker, J. A., & Henderson, D. (1967). Perturbation Theory and Equation of State for Fluids: The Square-Well Potential. *The Journal of Chemical Physics*, 47(8), 2856-2861.
35. Wolbach, J. P., & Sandler, S. I. (1998). Using molecular orbital calculations to describe the phase behavior of cross-associating mixtures. *Industrial & engineering chemistry research*, 37(8), 2917-2928.
36. Kleiner, M., & Gross, J. (2006). An equation of state contribution for polar components: Polarizable dipoles. *AIChE journal*, 52(5), 1951-1961.
37. Gross, J., & Vrabec, J. (2006). An equation of state contribution for polar components: Dipolar molecules. *AIChE journal*, 52(3), 1194-1204.
38. Gross, J., & Sadowski, G. (2002). Modeling polymer systems using the perturbed-chain statistical associating fluid theory equation of state. *Industrial & engineering chemistry research*, 41(5), 1084-1093.
39. Tumakaka, F., Gross, J., & Sadowski, G. (2002). Modeling of polymer phase equilibria using Perturbed-Chain SAFT. *Fluid phase equilibria*, 194, 541-551.
40. Gross, J., Spuhl, O., Tumakaka, F., & Sadowski, G. (2003). Modeling copolymer systems using the perturbed-chain SAFT equation of state. *Industrial & engineering chemistry research*, 42(6), 1266-1274.

1.3 Thermodynamic Characterization

1.3.1 Solvent/Solvent mixtures

The direct experimental determination of the vapor/liquid equilibrium of a solvent-solvent mixture means the samples separation of the liquid and vapor which are in true equilibrium and the determination of the concentrations of both phases analytically. The equilibrium curves can be carried out either at constant temperature or at constant pressure. The methods for the direct determination of equilibrium data can be classified into the following groups: (1) Distillation method. (2) Circulation method. (3) Static method. (4) Dew and Bubble point method [1].

1.3.1.1 Glass Ebullometer

This is a circulation method, where the experiments carried out with this apparatus entirely glass-made, have been successfully employed with several systems [2]. In this equipment, the vapor and liquid phases are constantly being recirculated as it is observed in Figure 3.1, with the purpose of obtaining an accurate mixing of the phases and also to guarantee that the equilibrium has been reached. To keep pressure constant and under control, the vapor condenser is attached to a constant-pressure system. The measurement of the equilibrium temperatures is performed with two thermocouples. The analysis of both liquid and condensed vapor analyses can be made by means of gas chromatography technique, which is described below.

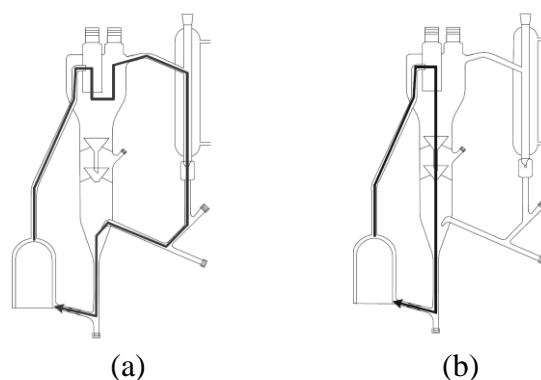


Figure 1.3.1. Glass Ebullometer: (a) Vapor phase circulation (b) Liquid phase circulation

1.3.1.2 Gas Chromatography (CG)

Chromatography is the separation of molecular mixtures by distribution between two or more phases, one phase being essentially two-dimensional (a surface) and the remaining phase, or being a bulk phase brought into contact in a counter-current fashion with the two dimensional phase. The sequence of chromatographic separation is as follows: A sample is placed at the top of a column where its components are sorbed and desorbed by a carrier. This partitioning process occurs repeatedly as the sample moves towards the outlet of the column. Each solute travels at its own rate through the column, consequently, a band representing each solute will form on the column. A detector attached to the column's outlet responds to each band. The output of detector response versus time is called a chromatogram. The time of emergence identifies the component, and the peak area defines its concentration, based on calibration with known compounds. Various types of physical states of chromatography are possible, depending on the phases involved. One branch is gas chromatography, the other is liquid chromatography. If the moving phase is a gas, then the technique is called gas chromatography (GC). In gas chromatography the sample is usually injected at high temperature to ensure vaporization. Obviously, only materials volatile at this temperature can be analyzed. [3].

If the stationary phase is a solid, the technique is referred to as gas-solid chromatography. The separation mechanism is principally adsorption. Those components more strongly adsorbed are held up longer than those which are not. If the stationary phase is a liquid, the technique is referred to as gas/liquid chromatography and the separation mechanisms are principally one of partition (solubilization of the liquid phase). Gas chromatography has developed into one of the most powerful analytical tools available to the organic chemist. The technique allows separation of extremely small quantities of material (10^{-6} gr). The technique is applicable over a wide range of temperatures ($-40 - 350$ °C). The laboratory uses packed columns along with megabore and capillary. The detector used to sense and quantify the effluent provides the specificity and sensitivity for the analytical procedure [3]. Table 3.1 summarizes significant detector characteristics.

Table 1.3.1. Summary of CG detectors characteristics [3].

Detector	Principle of operation	Selectivity	Sensitivity
Thermal Conductivity	Measures thermal conductivity of gas	Universal	6×10^{-10}
Flame Ionization	$H_2 - O_2$ Flame	Responds to organic compounds, not to H_2O or fixed gases	9×10^{-3} for alkane
Electron capture	$N_2 + B \rightarrow e^-$ $e^- + \text{sample} \rightarrow$	Responds to electron adsorbing compounds, e.g., halogen	2×10^{-14} for CCl_4
Hall Electrolytic Conductivity Detector	---	In halogen mode responds to halogens	---

1.3.2 Polymer/Solvent mixtures

As was explained in the previous chapter, the Flory Huggins interaction parameter χ is accessible from the measured activity of the solvent at certain polymer composition. In order to get the information for the entire range of compositions, a combination of several methods is necessary. Table 1.3.2 shows the concentration range for the applicability of the most common used methods [4].

Table 1.3.2. Methods for determining χ depending on the polymer compositions [4].

Range of polymer composition	Methods	Abbreviation	Ref.
$\varphi_2 \rightarrow 0$	Scattering methods	LS	[5]
	Intrinsic viscosity	IV	[6]
$0 \ll \varphi_2 \ll 0.3$	Osmosis	OS	[7]
$0.3 \ll \varphi_2 \ll 0.8$	Vapor-pressure methods	VP	[8]
$\varphi_2 \rightarrow 1$	Inverse Gas Chromatography	IGC	[9]

1.3.2.1 Intrinsic Viscosity (IV)

If η is the viscosity of a dilute polymer solution (concentration of polymer not more than about 1 g/dL) and η_o that of the solvent, the increment of viscosity due to the polymer may be represented by the specific viscosity η_{sp} which is equal to $(\eta - \eta_o)/\eta_o$. The ratio η_{sp}/c , where c is the concentration of polymer, is called the reduced viscosity. The value of η_{sp}/c at zero c is the limiting viscosity number more usually called the intrinsic viscosity and denoted by the symbol $[\eta]$. The intrinsic viscosity is a measure of the contribution of individual polymer molecules to the viscosity [10]. The relationship between the dilute solution viscosity and a polymer concentration c has been described by various functions, all of which have been used to obtain $[\eta]$ by extrapolation to zero c . The commonest is that due to Huggins [11]:

$$\eta_{sp}/c = \eta + k_H \eta^2 c \quad (1)$$

where k_H , called the Huggins slope constant, is said to be a constant for a given polymer-solvent system; its value is usually between 0.3 and 0.5. The prediction of a rectilinear plot of η_{sp}/c against c is generally correct for flexible chain polymers and extrapolation to zero c is simple. An alternative expression [12] is:

$$\ln(\eta/\eta_o)/c = \eta - k_K \eta^2 c \quad (2)$$

where k_K is called the Kramer slope constant. The quotient (η/η_o) is called the relative viscosity η_r .

The last two equations can be plotted and combined on a single diagram, as shown in Fig. 1.3.2, facilitating extrapolation since both lines have the same ordinate intercept. The constants k_H and k_K are related by $k_H + k_K \approx 0.5$.

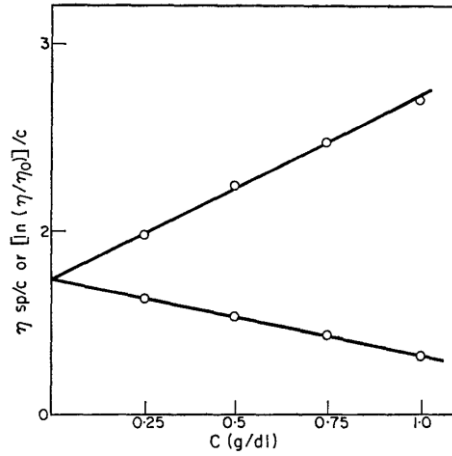


Figure 1.3.2. Huggins and Kramer procedure for the calculus of $[\eta]$ [10].

Each relative viscosity can be experimentally obtained by the relation (3), between the flow time of a solution at certain composition of polymer, through a capillary Ubbelohde viscometer (Figure 1.3.3) of known diameter and length (t) and the flow time of the pure solvent through the same capillary tube (t_o). Specific viscosity is obtained from relative viscosity according to (4).

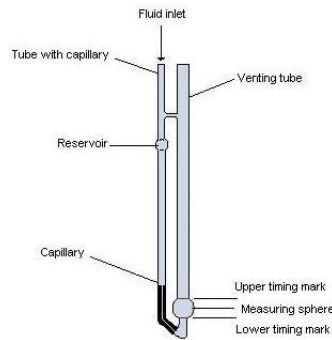


Figure 1.3.3. Ubbelohde viscometer

$$\eta_r = \frac{t}{t_o} \quad (3)$$

$$\eta_{sp} = \eta_r - 1 = \frac{t - t_o}{t_o} \quad (4)$$

On the other hand, the intrinsic viscosity values of a polymer/solvent are related to the dilution perturbation variables, by a theoretical treatment from Fox and Flory [13], based on the effects of the intramolecular interactions of polymer chains in infinitely

dilute solutions. The main results of this treatment are summarized in the following equations:

$$\eta = KM^{1/2}\alpha_n^3 \quad (5)$$

$$K = \Phi(r_o^2/M)^{3/2} \quad (6)$$

where α represents the ratio $(r^2)^{1/2}/(r_o^2)^{1/2}$ where (r^2) is the mean square end-to-end chain distance and (r_o^2) its value at the theta temperature θ , at which the net thermodynamic interaction between solvent and polymer is zero and the chains adopt their unperturbed conformation; Φ is said to be a universal constant equal to 2.1×10^{21} for flexible chains. M is the polymer molecular weight, thus (r_o^2/M) is a constant for a given polymer. Therefore K is a constant characteristic of the polymer at a given temperature.

At theta temperature, α_n^3 is equal to unity, so the intrinsic viscosity at this temperature will therefore be given by:

$$\eta_\theta = KM^{1/2} \quad (7)$$

Moreover, Stockmayer and Fixman [14] have proposed a simple expression, which relates the intrinsic viscosity with the Flory Huggins parameter:

$$\eta / M^{1/2} = K + 0.51\Phi BM^{1/2} \quad (8)$$

where according Kurata and Stockmayer [15]:

$$B = \frac{v_2(1-2\chi)}{V_1 N_A} \quad (9)$$

In this relationship V_1 is the solvent molar volume at temperature T for a flexible polymer chain of partial specific volume v_2 .

Rearranging equations (8) and (9), the Flory Huggins parameter for a polymer/solvent mixture at infinite dilution of polymer can be determined from:

$$\chi = 0.5 - \frac{\eta - \eta_\theta}{1.02\Phi M v_2 V_1^{-1} N_A^{-1}} \quad (10)$$

where $[\eta]_\theta$ is intrinsic viscosity at theta conditions. This last variable can be determined by the turbidimetric technique according the Elias method [16] or by the Stockmayer method [14].

1.3.2.2 Inverse Gas Chromatography (IGC)

Inverse gas chromatography technique (IGC) is based on the distribution (partition) of a volatile solute between a mobile gas phase and a stationary liquid or solid probe [17]. When the probe is a solid, this may be in the form of thin coating on an inert substrate, a finely divided solid, strands of fibre, or a thin polymeric coating on the column wall. To carry out the analysis, a volatile probe of known physicochemical property is passed through the column via an inert mobile gas phase, and the output is monitored. The retention time of the probe and the shape of the chromatogram give the physicochemical characteristics of the stationary phase

IGC has been especially useful for characterizing polymeric species. Measurements such as degree of crystallinity, glass and melting transition temperatures, solubility parameters, diffusion properties, interactions parameter with polymer blends, and interfacial and surface properties have been carry out on a variety of systems. Figure 1.3.4 gives the possible physicochemical studies that can be developed by inverse gas chromatography, from the general gas chromatography [18].

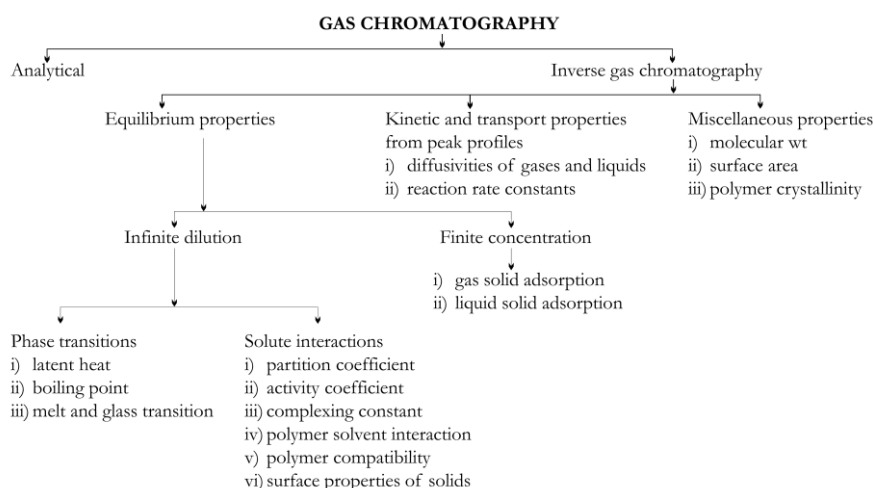


Figure 1.3.4. Physicochemical studies by Inverse Gas Chromatography [18].

The values directly measured by IGC are the retention times of solutes t_R . The mass of the stationary phase m_w , the temperature of column T and the flow rate F , are known. From these values the specific retention volume, V_g can be determined [19] from:

$$V_g^0 = \frac{t'_R F 273.15 j}{m_w T} \quad (11)$$

where $t'_R = t_R - t_M$, t_M is the gas hold-up time and j is the James–Martin coefficient, which is defined as the following relationship between the outlet (P_0) and the inlet pressure (P_i) in the column:

$$j = \frac{3}{2} \frac{P_i / P_0^2 - 1}{P_i / P_0^3 - 1} \quad (12)$$

The plot of the specific retention volume vs temperature is called retention diagram.

Finally according to several authors [19, 20, 21], at infinite dilution of the probe and for high molecular weight of the stationary phase, the Flory–Huggins interaction parameter can be determined from:

$$\chi^\infty = \ln \left(\frac{273.15 R v_2}{p_1^0 V_g^0 V_1} \right) - \frac{(B_{11} - V_1) p_1^0}{RT} - 1 \quad (13)$$

Where 1 denotes the solute and 2 denotes examined polymer material, M_1 is the molecular weight of the solute, p_1^0 is the saturated vapor pressure of the solute, B_{11} is the second virial coefficient of the solute, V_1 is the solvent molar volume, R is the gas constant and v_2 is the specific volume of the polymer.

On the other hand, a typical IGC retention diagram for a semicrystalline polymer and its melt temperature (T_m) is shown in Figure 1.3.5. Guillet and Stein [22] showed that these diagrams through the melting transitions can be analyzed quantitatively to obtain the crystallinity of the polymer. It was found that above T_m the polymer is completely amorphous and a linear retention diagram is obtained.

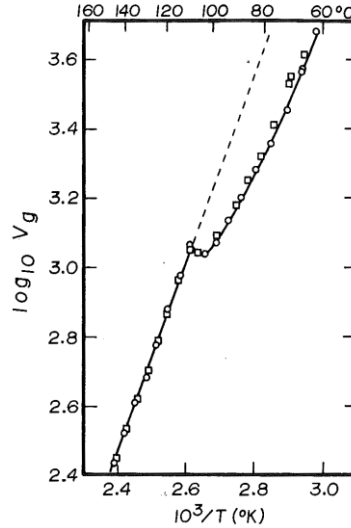


Figure 1.3.5. Retention diagram for n-dodecane on LDPE [22]

By extrapolating this straight line to lower temperatures, the retention volumes for the theoretically amorphous polymer can be computed, and then the polymer percentage of crystallinity can be determined, by the relationship:

$$X_C = \left(1 - \frac{V_{g, sample}}{V_{g, amorphous}} \right) \cdot 100 \quad (14)$$

1.3.3 References

1. Hála, E., Pick, J., Fried, V., Vilim, O., Standart, G., & Rice, S. (2009). Vapour-Liquid Equilibrium. *Physics Today*, 12(4), 46-46.
2. Ovejero Escudero, G., De Lucas Martinez, A., & Moreno Rodriguez, J. M. (1992). Vapor-liquid equilibria at 760 mmHg for the system vinyl acetate-n-decane. *Journal of Chemical and Engineering Data*, 37(3), 293-295.
3. Cheremisinoff, N. P. (1996). *Polymer characterization: laboratory techniques and analysis*. William Andrew.
4. Brandrup, J., Immergut, E. H., Abe, A., & Bloch, D. R. (Eds.). (1999). *Polymer handbook* (Vol. 89). New York: Wiley.
5. Huglin, M. B. (1972). *Light scattering from polymer solutions* Academic Press. London, New York.
6. Kok, C. M., & Rudin, A. (1982). Prediction of Flory–Huggins interaction parameters from intrinsic viscosities. *Journal of Applied Polymer Science*, 27(2), 353-362.
7. Flory, P. J., & Daoust, H. (1957). Osmotic pressures of moderately concentrated polymer solutions. *Journal of Polymer Science*, 25(111), 429-440.
8. Flory, P. J. (1953). *Principles of polymer chemistry*.
9. Smidsrød, O., & Guillet, J. E. (1969). Study of polymer-solute interactions by gas chromatography. *Macromolecules*, 2(3), 272-277.
10. Moore, W. R. (1967). Viscosities of dilute polymer solutions. *Progress in Polymer Science*, 1, 1-43.
11. Huggins, M. L. (1942). The viscosity of dilute solutions of long-chain molecules. IV. Dependence on concentration. *Journal of the American Chemical Society*, 64(11), 2716-2718.
12. Kraemer, E. O. *Ind Eng Chem* 1938, 30, 1200. CrossRef, CAS, Web of Science® Times Cited, 476.
13. Flory, P. J., & Fox, T. G. (1951). Treatment of intrinsic viscosities. *Journal of the American Chemical Society*, 73(5), 1904-1908.
14. Stockmayer, W. H., & Fixman, M. (1963, January). On the estimation of unperturbed dimensions from intrinsic viscosities. In *Journal of Polymer Science Part C: Polymer Symposia* (Vol. 1, No. 1, pp. 137-141). Wiley Subscription Services, Inc., A Wiley Company.

15. Kurata, M., & Stockmayer, W. H. (1963). Intrinsic viscosities and unperturbed dimensions of long chain molecules. In *Fortschritte der Hochpolymeren-Forschung* (pp. 196-312). Springer Berlin Heidelberg.
16. H.G. Elias. In *Polymer Handbook* 4th edition, 1999
17. Braun, J. M., & Guillet, J. E. (1976). Study of polymers by inverse gas chromatography. In *Mechanisms of Polyreactions-Polymer Characterization* (pp. 107-145). Springer Berlin Heidelberg.
18. Sen, A. K. (2005). *Inverse Gas Chromatography*. Defence Scientific Information & Documentation Centre, Defence Research & Development Organisation, Ministry of Defence.
19. Voelkel, A., Strzemiecka, B., Adamska, K., & Milczewska, K. (2009). Inverse gas chromatography as a source of physiochemical data. *Journal of Chromatography A*, 1216(10), 1551-1566.
20. Dieckmann, F., Pospiech, D., Uhlmann, P., Böhme, F., & Kricheldorf, H. R. (1999). Inverse gas chromatographic study of some polyethers. *Polymer*, 40(4), 983-987.
21. Katsanos, N. A., & Karaiskakis, G. (2004). *Time-resolved inverse gas chromatography and its applications* (p. 70). New York: HNB Publishing.
22. Guillet, J. E., & Stein, A. N. (1970). Study of Crystallinity in Polymers by Use of "Molecular Probes". *Macromolecules*, 3(1), 102-105

1.4 Polymer Characterization

1.4.1 Gel Permeation Chromatography (GPC)

Gel Permeation Chromatography (GPC), also known as Size Exclusion Chromatography (SEC), is a technique used to determine the average molecular weight distribution of a polymer sample. This technique separates the polymer chains according to size or hydrodynamic radius. This is accomplished by injecting a small amount of (100-400 μL) of polymer solution (0.01 - 0.6 %) into a set of columns that are packed with porous beads. Smaller molecules can penetrate the pores and therefore are retained to a greater extent than the larger molecules which continue down the columns and elute faster. One or more detectors are attached to the output of the columns. For routine analysis of linear homopolymers, these detectors are most often: a Differential Refractive Index (DRI) or a UV detector. For branched or copolymers, however, it is necessary to have at least two sequential detectors to determine molecular weight accurately, e.g, DRI detector coupled with a viscometer (VIS) or a low-angle laser light scattering (LALLS) detector, for branched polymers; or a DRI detector coupled with UV or FTIR, for copolymers [1].

Figure 1.4.1 shows a typical chromatogram of a polymer molecular weight distribution results on a GPC analysis with the different molecular weight that can be calculated, and their correlative order. The number average molecular weight (M_n) is the total weight of all the polymer molecules in a sample, divided by the total number of polymer molecules in the sample. On the other hand, weight average molecular weight (M_w) is based on the fact that a bigger molecule contains more of the total mass of the polymer sample than the smaller molecules do. Molecular weight can also be calculated from the viscosity of a polymer solution. In this case, the principle is that bigger polymers molecules make a solution more viscous than small ones do. The viscous average molecular weight (M_v) is closer to the weight average than to the number average.

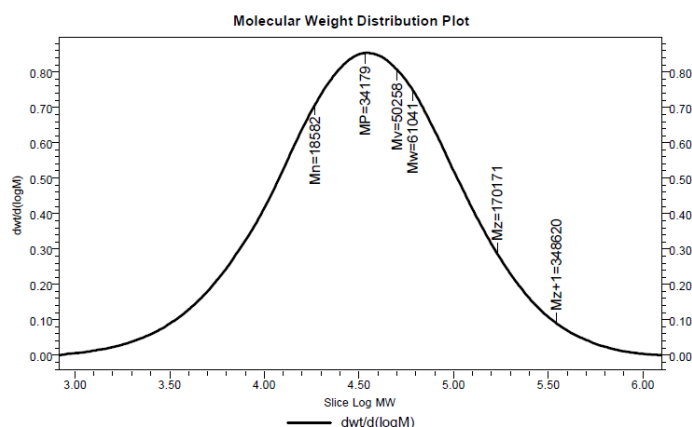


Figure 1.4.1. Typical polymer GPC chromatogram

The mathematical definitions of all the types of molecular weights of polymer are resumed in Table 1.4.1,

Table 1.4.1. Definitions of the molar mass averages [2]

Average molar mass	Symbol and definition
Number-average molar mass	$M_n = \frac{\sum_i n_i M_i}{\sum_i n_i} = \frac{\sum_i w_i}{\sum_i w_i / M_i} = \frac{W}{N}$
Weight-average molar mass	$M_w = \frac{\sum_i n_i M_i^2}{\sum_i n_i M_i} = \frac{\sum_i w_i M_i}{\sum_i w_i}$
z-Average molar mass	$M_z = \frac{\sum_i n_i M_i^3}{\sum_i n_i M_i^2} = \frac{\sum_i w_i M_i^2}{\sum_i w_i M_i}$
(z + 1)-Average molar mass	$M_{z+1} = \frac{\sum_i n_i M_i^4}{\sum_i n_i M_i^3} = \frac{\sum_i w_i M_i^3}{\sum_i w_i M_i^2}$
Viscosity-average molar mass	$M_v = \left[\frac{\sum_i n_i M_i^{1+\alpha}}{\sum_i n_i} \right]^{1/\alpha} = \left[\frac{\sum_i w_i M_i^\alpha}{\sum_i w_i} \right]^{1/\alpha}$

In this table M_i is the molar mass of the component molecules of kind i ; n_i is the number-fraction of the component molecules i ; w_i is the weight-fraction of the component molecules i ; N is total number of moles of all kinds; W is the total weight of moles of all kinds; and α is the exponent of the Mark–Houwink relationship [3], which will be discussed in secc. 1.4.5.

1.4.2 Differential Scanning Calorimetry (DSC)

The DSC measures the power (heat energy per unit time) differential between a small weighed sample of polymer (ca. 10 mg) in a sealed aluminum pan referenced to an empty pan in order to maintain a zero temperature differential between them during programmed heating and cooling temperature scans. The technique is most often used for characterizing the glass transition temperature (T_g), the melt temperature (T_m), the crystallization temperature (T_c) and heat of fusion of polymers (Figure 1.4.2). This technique can also be used for studying the kinetics of chemical reactions, e.g., oxidation and decomposition. The conversion of the measured heat of fusion can be converted to the percent of crystallinity of the polymer, if the heat of fusion for the 100% crystalline polymer is known [1].

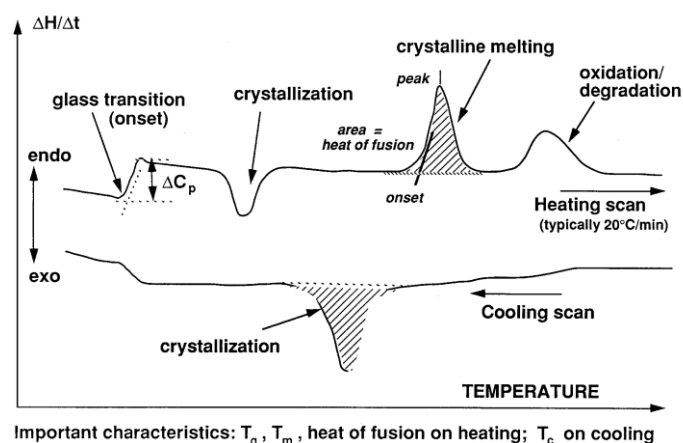


Figure 1.4.2. Typical polymer DSC thermograms [1].

1.4.3 Thermogravimetric Analysis (TGA)

TGA is based on making a continuous weighing of a small sample (ca. 10 mg) in a controlled atmosphere (e.g., air or nitrogen) while the temperature is increased at a programmed linear rate. A typical thermogram of an elastomer compound, shown in Figure 1.4.3 illustrates the weight losses due to desorption of gases (e.g., moisture) or decomposition (e.g., CO_2 from calcium carbonate filler). TGA is also a very simple technique for quantitatively analyzing for filler content of a polymer compound (e.g., carbon black decomposed in air but not nitrogen). In addition oil can be readily in the thermogram, which overlaps with the temperature range of hydrocarbon polymer degradation. [1].

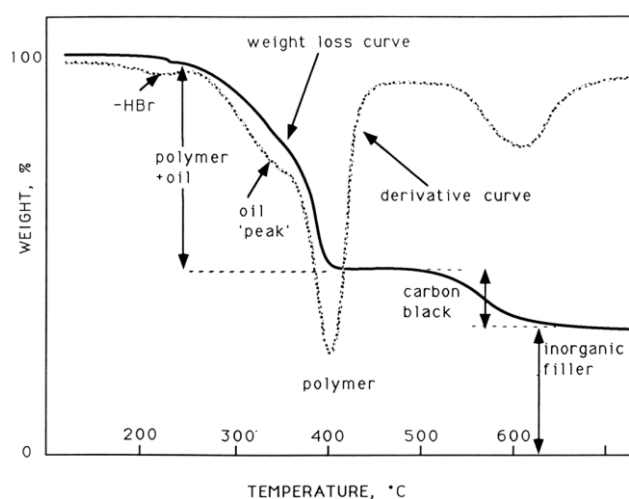


Figure 1.4.3. Typical polymer TGA thermogram

1.4.4 Scanning Electron Microscopy (SEM)

Samples in the SEM can be examined for general morphology, when the domain size is in the range of $< 1 \mu\text{m}$ to 10 nm , as freeze fractured surfaces or as microtome blocks of solid bulk samples. The image is obtained by a contrast achieved by one or combination of the methods: Solvent etching, OsO_4 staining, and RuO_4 staining, depending on the polymer/solvent solubility differences. SEM can be used to study liquids or temperature sensitive polymers on a Cryostage. SEM is also used to do semi-quantitative X-ray/elemental analysis. X-ray analysis and mapping of the particular elements present is useful for the identification of inorganic fillers and their dispersion in compounds as well as inorganic impurities in gels or on surfaces and curatives (Figure 1.4.4) [1].

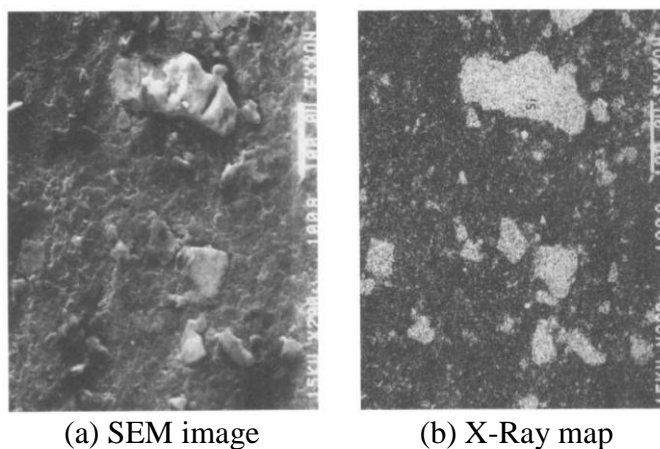


Figure 1.4.4. Mapping of polymer surface impurity

1.4.5 Intrinsic Viscosity (IV)

The intrinsic viscosity $[\eta]$ of a polymer/solvent mixture also can be related to the viscous molecular weight by the well-known Mark-Houwink or modified Staudinger equation [3]:

$$\eta = K_m M_v^\alpha$$

where K_m and the exponent α are constants for a given polymer, solvent and temperature, and M_v is the viscous average molecular weight of the polymer. The value of α generally lies between 0.5 and 1. Values of K_m and α for many polymer-solvent systems have been tabulated in reviews of viscosity molecular weight [4,5]. Therefore is relatively easy to determine the M_v of a polymer, measuring $[\eta]$ with K_m and α known.

1.4.6 References

1. Cheremisinoff, N. P. (1996). Polymer characterization: laboratory techniques and analysis. William Andrew.
2. Van Krevelen, D. W., & Te Nijenhuis, K. (2009). Properties of polymers: their correlation with chemical structure; their numerical estimation and prediction from additive group contributions. Elsevier.
3. Yang, J. T. (1960). The viscosity of macromolecules in relation to molecular conformation. *Advances in protein chemistry*, 16, 323-400.
4. Moore, W. R. (1967). Viscosities of dilute polymer solutions. *Progress in Polymer Science*, 1, 1-43.
5. Brandrup, J., Immergut, E. H., Abe, A., & Bloch, D. R. (Eds.). (1999). *Polymer handbook* (Vol. 89). New York: Wiley.

1.5 Hypothesis and objectives

1.5.1 Overview

As was mentioned previously, the knowledge of the mutual solubility of polymers and volatile organic substances is crucial for any applications in polymer chemistry and polymer engineering. Polymerizations, which should be performed in homogeneous phase, require the complete miscibility of monomer, polymer, solvent (liquid or supercritical) and other additives. Subsequently, the extraction of the polymer product from the reaction mixture requires a phase split (into two liquid phases or into a vapor and a liquid phase) to obtain a polymer product of high purity at one side as well as the unreacted monomer at the other side [1].

However, experimental binary data for polymer/solvent systems (polymer solubility or liquid-liquid equilibria, and solvent sorption in polymers or vapor-liquid equilibria) is often scarce. Considerable experimental effort is generally required, for determining these properties of polymer systems.

Nowadays, the most powerful and robust tools for modeling of experimental data and even to predict the polymer/solvent thermodynamic behavior are: molecular dynamics simulations [2] and the PC-SAFT equations of state model [3]. This last one is based on a hard-chain reference system, to take account the different perturbations over the total Helmholtz energy of the system (hard chain, dispersion, association and polarizable contributions). PC-SAFT equation of state applied to polymer systems requires these contributions parameters for the homopolymer, plus a binary interaction parameter (k_{ij}) for the polymer/solvent mixture. This last parameter can be predicted from the polymer solubility or solvent sorption data [4], and it will be the same for the further predictions of all equilibria (L - V , L - L , S - L , S - V) of the system [5]. To describe a copolymer system, one additional binary interaction parameter between the homopolymers is necessary, and can be fitted from the binary copolymer/solvent data [6].

On the other hand, also as was mentioned previously, EVA copolymers representing the largest-volume segment of ethylene copolymer market [7], are products of the radical random copolymerization of the monomers ethylene and vinyl acetate (VA) in a predetermined ratio [8], therefore they are considered to be composed on polyethylene (PE) and polyvinyl acetate (PVA) homopolymers. An important process to produce EVA copolymer is the solution production process, due the final applications of these copolymers, as rheology modifiers, adhesive binders, compounding components for thermoplasts and duroplasts, and for the production of vulcanisates [10]. In this process the solution polymerization is generally carried out with methanol (MET) as solvent [11].

The modeling of an EVA copolymer/solvent system with the PC-SAFT model will require the pure thermodynamic parameters for the perturbations of such homopolymers (m , σ , ε/k , $\varepsilon^{\text{AiBi}}/k$ and κ^{AiBi}), which are well known in literature [9], plus the binary interactions parameters (k_{ij}), which represents the crucial thermodynamic information that has to be estimated and introduced accurately in PC-SAFT modeling system.

Applying the PC-SAFT procedure to simulate the separation stage after the polymerization in a recovery column (e.g. using the module Radfrac of the Aspen Plus® Simulator) to split the EVA/MET solution for the VA co-monomer, the EVA copolymer must be subdivided into its homopolymers (PE and PVA). The following six binary interaction parameters (k_{ij}) are necessary:

- k_{ij} homopolymers/solvents (PE/MET, PE/VA, PVA/MET, PVA/VA)
- k_{ij} homopolymer/homopolymer (PVA/PE)
- k_{ij} solvent/solvent (MET/VA)

The theory described above is illustrated in Figure 1.5.1. .

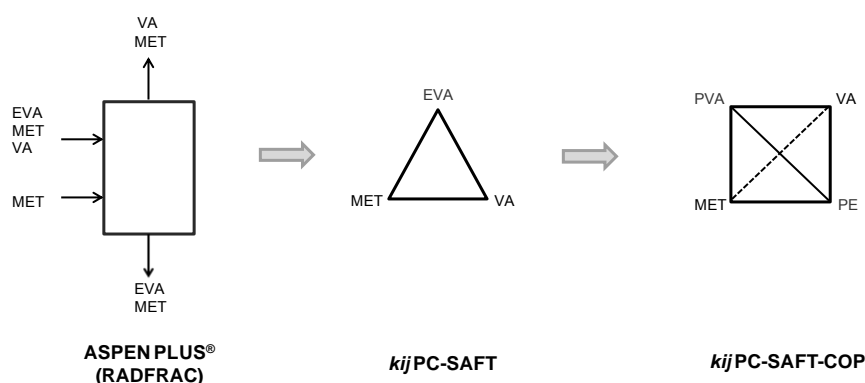


Figure 1.5.1. Illustration of the Six PC-SAFT interactions parameters (k_{ij}) necessary to model the EVA copolymer separation solution process

On the other hand, in the Catalysis and Separation Process Research Group of the UCM Department of Chemical Engineering, two of the experimental procedures more validated, well known and published [12,13,14,15], to access to the thermodynamic data of a polymer/solvent system are the inverse gas chromatography technique (IGC) [16], and the intrinsic viscosity technique (IV) [17], which allows to determine the Flory Huggins parameters at infinite dilution of solvent, and polymer, respectively. These parameters based on the primordial Gibbs energy model theory applied to polymers, allow an easily prediction of a solvent sorption point (P_i “vs” polymer composition_{*i*}) according to the relationship of the partial segment molar Gibbs energy expressed in terms of the solvent chemical potential μ_l [18].

It is also well known in literature [19] that these Flory Huggins parameters obtained by the two techniques are different; in agree with the proven dependence of such parameters with the composition of polymer [20]. Previous works of Bernard Wolf have validated a composition dependence thermodynamic model for the Flory Huggins parameters of polymers/solvents systems, based on the adjustment of three parameters (α , v , $\xi\lambda$) [20].

With the Flory Huggins parameters calculated at the extremes of the polymer composition curve (infinite dilution of polymer -IV- and solvent -IGC-) it should be possible the prediction of all the Flory Huggins parameters – polymer composition

curve, based on the Bernard Wolf model and taking account the thermodynamic information of the system. Therefore, with this curve known, the prediction of the total solvent sorption curve (Pressure - polymer composition) also should be easily. Finally, the adjustment of the solvent sorption curve to determinate the binary interaction parameter for the PC-SAFT model, will be also possible, taking into account all the variability of the perturbations over the polymer/solvent system, especially the possible association schemes [21]. The suppositions described above, are illustrated in Figure 1.5.2.

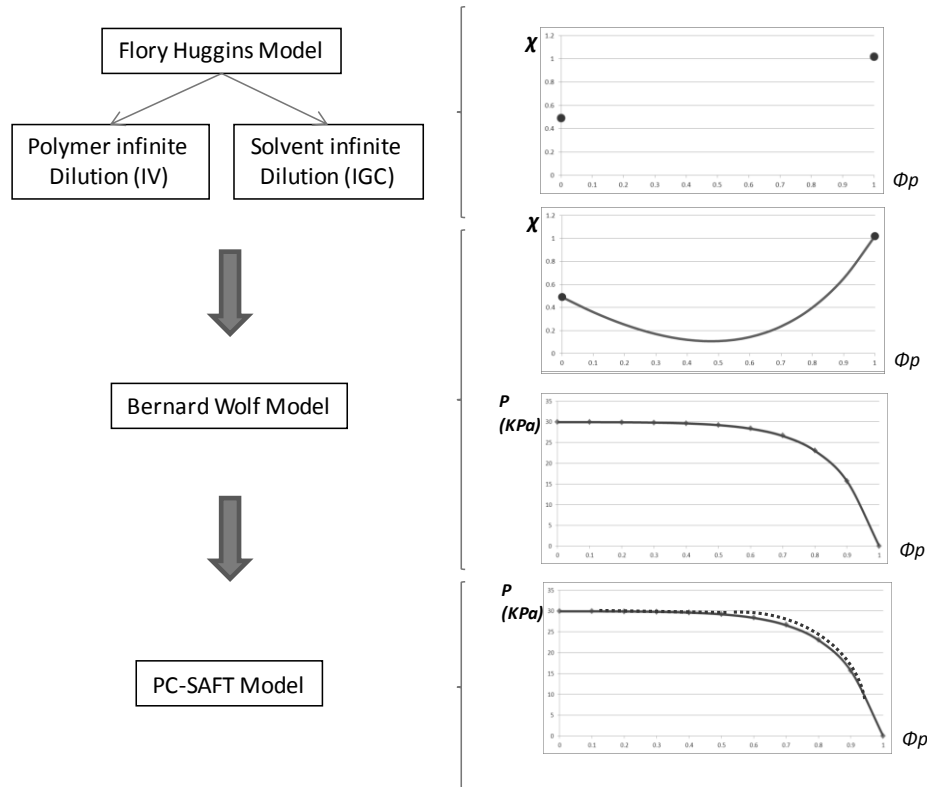


Figure 1.5.2. Strategy proposed for determining the PC-SAFT k_{ij} for a polymer/solvent system

This general hypothetical procedure which allows the estimation of the k_{ij} binary parameters of the PC-SAFT model from the sorption curves constructed from the Flory Huggins parameters determined at the extremes of the polymer compositions, could be applied to any polymer/solvent system.

Specifically for the EVA copolymer/solvents solution production process, the necessary k_{ij} described above, can be obtained from the binary data of certain sorption curves for the system, determined from the Flory Huggins parameters obtained with VI and IGC techniques. On the other hand, the MET/VA binary data can be obtained from the liquid-vapor equilibrium of these solvent, determined for example from traditional experimental techniques as the glass ebulliometer.

1.5.2 General Objective

The aim of this work is to modeling the separation stage of the Ethylene – Vinyl Acetate copolymer (EVA) solution production process carried out in methanol, with the PC-SAFT model, from a rigorous thermodynamic assessment that consider the dependence of the Flory Huggins parameters whit the copolymer composition of the system.

1.5.3 Specific Objectives

- Characterize two samples of EVA copolymer (EVA33 and EVA18, with VA content of 33% w/w and 18 % w/w, respectively), one of LDPE and one of PVA, as representative samples in this work. The characterization includes: difference scanning calorimetric (DSC), thermogravimetric analysis (TGA), gel permeation chromatography (GPC), scanning electric microscopy (SEM), and intrinsic viscosity for the Mark Houwink analysis (IV).
- Determine the overall Flory Huggins parameters at infinite dilution of solvent, with the Inverse Gas Chromatography technique (IGC), applied to the polymer/solvent mixtures: PE/MET, PE/VA, PVA/MET, PVA/VA and EVA/MET. In addition apply this technique to the same polymers with other solvents (representing dispersion, association and polar solvents) to establish a thermodynamic assessment that includes the Hildebrand solubility parameter. Compare this parameter with the predicted in molecular dynamics simulations.
- Determine the amorphous Flory Huggins parameters for the semi-crystalline polymers (PE and EVAs), from the percent of crystallinity also determined from the Inverse Gas Chromatography technique.
- Determine the overall Flory Huggins parameters at infinite dilution of polymer, with the intrinsic viscosity technique (IV), applied to the diluted systems: PE/MET, PE/VA, PVA/MET, PVA/VA and EVA/MET. In addition apply this technique for the same polymers with other solvents (representing dispersion, association and polar solvents) to establish a thermodynamic assessment at these diluted conditions. The necessary viscosity at theta conditions will be determined for the homopolymers (PE and PVA) with the Stockmayer procedure, and for EVA copolymers according the turbidimetric technique or Elias method.
- Develop and validate a mathematical relationship that considers the thermodynamics parameters defined in the Bernard Wolf thermodynamic model, to predict the Flory Huggins - polymer compositions curves, from the Flory Huggins data at the extremes of that curve at infinite dilution of solvent and polymer, previously calculated with the IGC and VI techniques, respectively.

- Predict the solvent sorption curves in polymers or vapor-liquid equilibria for the systems PE/MET, PE/VA, PVA/MET, PVA/VA and EVA/solvents.
- Determine the vapor-liquid equilibria curve for the systems VA/MET with the glass ebullometer experimental technique.
- Determine the PC-SAFT k_{ij} binary interaction parameters from these sorption curves, taking into account the accurate association scheme for each polymers/solvent system. The adjustments will be done with the commercial simulation software Aspen Plus[®], previously validating the reproducibility of the PC-SAFT module for different bibliographic polymer/solvent systems.
- Modeling the separation stage of the EVA33 solution production process with the PC-SAFT model. Compare the process predictions with the process real data shown in patents.

1.5.4 Thesis structure

This work is presented by ten scientific articles published in the framework of the global project. These articles are grouped by chapters depending on the kind of thermodynamic conditions, components and/or compositions, which were carried out, as it is shown below:

- Thermodynamics of EVA/solvents mixtures at infinite dilution of solvents.
- Thermodynamics of EVA/solvents mixtures at infinite dilution of polymer.
- Thermodynamics of solvent/solvent mixtures involved in the EVA solution process.
- Thermodynamics of EVA/solvents mixtures at finite compositions of polymer, to the final simulation of the EVA separation solution process.

Each article includes the properties of the polymers used, the characterization techniques of such polymers, the experimental procedures employed, an extensive sampling of the results and a rigorous discussion.

At the end of each chapter an inclusive summary and a discussion is presented, taking into account a general thermodynamic assessment for the EVA/solvents mixtures at the specified conditions; and a rigorous thermodynamic evaluation for the mixtures involved in the EVA separation solution process (EVA in methanol and vinyl acetate).

1.5.5 References

1. Sadowski, G. (2004, February). Thermodynamics of polymer systems. In *Macromolecular Symposia* (Vol. 206, No. 1, pp. 333-346). WILEY-VCH Verlag.
2. Rapaport, D. C. (2004). *The art of molecular dynamics simulation*. Cambridge university press.
3. Gross, J., & Sadowski, G. (2002). Modeling polymer systems using the perturbed-chain statistical associating fluid theory equation of state. *Industrial & engineering chemistry research*, 41(5), 1084-1093.
4. Tumakaka, F., Gross, J., & Sadowski, G. (2002). Modeling of polymer phase equilibria using Perturbed-Chain SAFT. *Fluid phase equilibria*, 194, 541-551.
5. Buchelli, A., Call, M. L., Brown, A. L., Bokis, C. P., Ramanathan, S., & Franjione, J. (2004). Nonequilibrium behavior in ethylene/polyethylene flash separators. *Industrial & engineering chemistry research*, 43(7), 1768-1778.
6. Gross, J., Spuhl, O., Tumakaka, F., & Sadowski, G. (2003). Modeling copolymer systems using the perturbed-chain SAFT equation of state. *Industrial & engineering chemistry research*, 42(6), 1266-1274.
7. Chanda, M., & Roy, S. K. (2008). *Industrial polymers, specialty polymers, and their applications* (Vol. 74). CRC Press.
8. Anon. (2006). PERP Program—LDPE copolymers (03/04S9). Chem systems Reports. Nexant Inc., New York, USA
9. Plus, A. (2009). DB-SEGMENT and DB-PCSAFT Database. Aspen Technology. Inc., version, 11.
10. Baade, W., Obrecht, W., & Ohm, C. (1992). U.S. Patent No. 5,093,450. Washington, DC: U.S. Patent and Trademark Office.
11. Kawahara, T., & Hikasa, T. (2005). U.S. Patent No. 6,838,517. Washington, DC: U.S. Patent and Trademark Office.
12. Ovejero, G., Pérez, P., Romero, M. D., Díaz, I., & Díez, E. (2009). SEBS triblock copolymer–solvent interaction parameters from inverse gas chromatography measurements. *European Polymer Journal*, 45(2), 590-594.
13. Díez, E., Ovejero, G., Romero, M. D., & Díaz, I. (2011). Polymer–solvent interaction parameters of SBS rubbers by inverse gas chromatography measurements. *Fluid Phase Equilibria*, 308(1), 107-113.
14. Ovejero, G., Perez, P., Romero, M. D., Guzmán, I., & Dí, E. (2007). Solubility and Flory Huggins parameters of SBES, poly (styrene-*b*-butene/ethylene-*b*-styrene) triblock copolymer, determined by intrinsic viscosity. *European polymer journal*, 43(4), 1444-1449.
15. Ovejero, G., Romero, M. D., Díez, E., & Díaz, I. (2010). Thermodynamic interactions of three SBS (styrene–butadiene–styrene) triblock copolymers with different solvents, by means of intrinsic viscosity measurements. *European Polymer Journal*, 46(12), 2261-2268.
16. Voelkel, A., Strzemiescka, B., Adamska, K., & Milczewska, K. (2009). Inverse gas chromatography as a source of physiochemical data. *Journal of Chromatography A*, 1216(10), 1551-1566.
17. Moore, W. R. (1967). Viscosities of dilute polymer solutions. *Progress in Polymer Science*, 1, 1-43.

18. R. Horst and B.A. Wolf. Thermodynamics of polymer solutions. (Thermodynamik von Polymerlösungen) <http://wolf.chemie.uni-mainz.de/Internet/Students/Makro.htm>
19. Yilmaz, F., & Cankurtaran, Ö. (1997). Comparison of the intrinsic viscosity and inverse gas chromatography techniques in determination of the exchange enthalpy and entropy parameters. *Polymer*, 38(14), 3539-3543.
20. Wolf, B. A. (2011). Making Flory–Huggins Practical: Thermodynamics of Polymer-Containing Mixtures. In *Polymer Thermodynamics* (pp. 1-66). Springer Berlin Heidelberg.
21. Kontogeorgis, G. M., & Folas, G. K. (2009). *Thermodynamic models for industrial applications: from classical and advanced mixing rules to association theories*. John Wiley & Sons.

2 Thermodynamics of EVA/solvents mixtures at infinite dilution of solvents

This chapter presents four scientific articles published in the framework of the global project, and an inclusive discussion, that are focused on the determination and evaluation of the Flory Huggins parameters of the EVA copolymers and their homopolymers (Polyethylene, PE, and Polyvinyl Acetate, PVA) at infinite dilutions of solvents ($\phi_2 \rightarrow 1$), by means of the Inverse Gas Chromatography (IGC). Additionally, several thermodynamic assessments were done at these infinite dilution conditions.

At the end of the discussion of each article, these Flory Huggins parameters for the mentioned polymers are cited in presence of the solvents participating in the EVA separation solution process (methanol and vinyl acetate), plus cyclohexane, for being a good solvent for all these polymers. In this way, the three types of solvents (association, polar and dispersion, respectively) are represented, for a suitable thermodynamic analysis.

2.1 Thermodynamic Interactions of EVA Copolymer - Solvent Systems by Inverse Gas Chromatography Measurements

Camacho, J., Díez, E., Ovejero, G., & Díaz, I. (2013). Thermodynamic Interactions of EVA Copolymer-Solvent systems by Inverse Gas Chromatography Measurements. *Journal of Applied Polymer Science*, 128(1), 481-486.

Thermodynamic Interactions of EVA Copolymer-Solvent Systems by Inverse Gas Chromatography Measurements

Javier Camacho,¹ Eduardo Díez,¹ Gabriel Ovejero,¹ Ismael Díaz²

¹Grupo de Catálisis y Procesos de Separación (CyPS), Departamento de Ingeniería Química, Facultad de C. Químicas, Universidad Complutense de Madrid, Avda. Complutense s/n, Madrid 28040, Spain

²Departamento de Ingeniería Química Industrial y del Medio Ambiente, Escuela Técnica Superior de Ingenieros Industriales, Universidad Politécnica de Madrid, C/ José Gutiérrez Abascal 2, Madrid 28006, Spain

Correspondence to: E. Díez (E-mail: ediezalc@quim.ucm.es)

ABSTRACT: The solubility parameter and the Flory–Huggins interaction parameter of two EVA (ethylene–vinyl acetate) copolymers, each one with different vinyl acetate content, are calculated by using inverse gas chromatography technique. The influence of the vinyl acetate percentage is analyzed and indicates that the polymer–solvent interactions are stronger in the case of the copolymer with the highest vinyl acetate percentage. The results also point to the fact that the most favorable solvents for the studied materials are the aromatic-type ones. Finally, from the calculated values of the polymer solubility parameter (16.3 MPa^{0.5} for EVA 460 and 15.1 MPa^{0.5} for EVA410, at 50°C), it can be noticed that the solubility parameter of the EVA copolymer with the largest vinyl acetate content is the closest to the solubility parameter of pure vinyl acetate. © 2012 Wiley Periodicals, Inc. *J. Appl. Polym. Sci.* 000: 000–000, 2012

KEYWORDS: EVA copolymer; inverse gas chromatography; solubility parameter; Flory–Huggins parameter; vinyl acetate

Received 30 March 2012; accepted 13 June 2012; published online

DOI: 10.1002/app.38193

INTRODUCTION

Nowadays, polymers are ones of the most widely used materials as a consequence of their applicability in many fields. Among these materials, the ethylene–vinyl acetate copolymer (EVA) is gaining importance, mainly due to its wide range of applications in, for example, tyres and electronic cable industries or in photovoltaic cells coatings.¹

The applicability of these EVA polymers is related to the vinyl acetate percentage, variable which also determines the way these materials are industrially obtained. Whenever the vinyl acetate content is higher than 70%, the EVA materials are manufactured by means of an emulsion process and their main applications are as adhesives. If the vinyl acetate percentage is between 30 and 40%, a dissolution process at moderate temperatures and pressures is required and, in this case, the obtained materials are mainly used as elastomers. Finally, whenever the vinyl acetate content is lower than 30%, EVA polymers are manufactured by means of high pressure processes, and their main applications are as modifiers.²

Focusing on the dissolution process, it is usually carried out with methanol as solvent, although other compounds like tetrahydrofuran (THF) could also be advisable.³ On the other hand, in this kind of processes, one of the key points to be overcome is how to achieve an accurate separation between the final ma-

terial and the solvent, with the aim of getting the EVA polymer as pure as possible. For this reason, it is crucial to thermodynamically characterize the compatibility between the EVA material and different solvents. This compatibility clearly depends on the nature of the solvent, but it might also depend on the vinyl acetate percentage of this EVA material.⁴

The analysis of the interactions between a polymer and a solvent is commonly carried out in terms of the Flory–Huggins parameter⁵ and the weight-based solvent activity coefficient,⁶ but also by comparing the solubility parameter of the solvent with the solubility parameter of the polymer.⁷

While in literature, several data showing the solubility parameter of a wide range of solvents can be easily found,^{8,9} the solubility parameter of an EVA copolymer is not a common value, so it is important to determine it experimentally. Concerning the Flory–Huggins parameter and the weight-based solvent activity coefficient, because there is no any reference reporting these values for any kind of EVA polymer, they also have to be experimentally measured.

A polymer–solvent mixture is totally different from a conventional solvent–solvent mixture because there is a large difference in the size of the molecules of both compounds. So, the measurement of thermodynamic parameters of this kind of mixtures

is carried out by using nonconventional techniques, such as intrinsic viscosity,^{10,11} swelling,^{12,13} or inverse gas chromatography.^{14,15} Among all these techniques, inverse gas chromatography (IGC) is one of the most widely used, because it gives a great deal of information with relatively simple measurements. In literature, this technique has been used with many different polymeric materials, always with good results.^{16,17} Another important point is that it has been demonstrated that the obtained values with this technique (at solvent infinite dilution conditions) can be extrapolated to the overall composition range.¹⁸

This article reports the values of the weight-based solvent activity coefficient and Flory–Huggins parameter of the mixtures of two EVA copolymers with different solvents which could be adequate in an emulsion process. It also reports the solubility parameter of the two polymeric materials, calculated from the previous values. The main purpose of this work is to analyze the influence of the vinyl acetate percentage over these parameters; this is the first stage to model the EVA-solvent separation step, which is the final aim of the project in which our group is working.

EXPERIMENTAL

IGC—Calculations

According to IGC basis,¹⁹ once the injected solvent has gone through the column, its specific retention volume (V_g) can be obtained from retention time measurements by means of eq. (1), where F is the flow rate of the carrier gas corrected to the column temperature, t_r is the retention time of the solvent, t_m is the retention time of a reference inert compound, W_s is the amount of polymer packed in the column, and j is a correction factor. Due to the carrier gas is compressible, the pressure drop along the column might cause an increase of the volume flow rate in the outlet (P_0) compared with the inlet value (P_i); therefore, a correction factor (j) is usually added [eq. (2)].¹⁹

$$V_g = \frac{j \cdot (t_r - t_m) \cdot F}{W_s} \quad (1)$$

$$j = \frac{3(P_i/P_0)^2 - 1}{2(P_i/P_0)^3 - 1} \quad (2)$$

The relation between the mass-based infinite dilution activity coefficient of the solvent, $(\Omega_i^\infty)_{\text{IGC}}$, and its retention volume (V_g), in a solvent (1)–polymer (2) mixture, is given by eq. (3),¹⁹ where T is the temperature in K, R is the ideal gas constant, M_1 is the solvent molecular weight and f_1^0 is the standard fugacity of the solvent. This last parameter can be determined with the Virial EOS truncated after the second term; so, eq. (3) is transformed into eq. (4).

$$\ln(\Omega_i^\infty)_{\text{IGC}} = \ln\left(\frac{R \cdot T}{V_g \cdot M_1 \cdot f_1^0}\right) \quad (3)$$

$$\ln(\Omega_i^\infty)_{\text{IGC}} = \ln\left(\frac{R \cdot T}{V_g M_1 p_1^0}\right) - \frac{(B_{11} - V_1)p_1^0}{RT} \quad (4)$$

In this last equation, B_{11} is the solvent second term of the Virial EOS, p_1^0 is the solvent vapor pressure, and V_1 is the solvent molar volume.

In this work, molar volumes have been calculated according to a modification of Rackett model²⁰ using the value of the Rackett parameter which appears in literature²¹; the second terms of Virial EOS have been calculated with Tsonopoulos' correlation,²² and the Antoine coefficients of the solvent vapour pressure values have been also taken from literature.²¹

From the values of infinite dilution activity coefficient, the Flory–Huggins interaction parameter (χ) can be calculated by using eq. (5),²³ where r is the ratio between molar volume of the polymer and the molar volume of the solvent, and ρ_1 and ρ_2 are the solvent and polymer densities, respectively.

$$\chi = \ln(\Omega_1^\infty)_{\text{IGC}} - \left(1 - \frac{1}{r}\right) + \ln \frac{\rho_1}{\rho_2} \quad (5)$$

Equivalent expressions have been used in literature,²⁴ because eq. (5) is directly derived from the combination of eq. (4) with the well-known Flory Equation⁵ [eq. (6)], which allows calculating the activity of a solvent, in a polymer–solvent mixture.

$$\ln(a_1) = \ln(1 - \Phi_2) + \left(1 - \frac{1}{r}\right)\Phi_2 + \chi\Phi_2^2 \quad (6)$$

On the other hand, Hildebrand and Scout,²⁵ developed a regular solution model defining the solubility parameter of one compound i as the square root of its cohesive energy, which can be calculated from heat of vaporization values [eq. (7)].

$$\delta_1 = \left[\frac{\Delta_{\text{vap}}H_1 - RT}{V_1}\right]^{0.5} \quad (7)$$

The Flory–Huggins theory, modified by Blanks and Prausnitz,⁷ allows establishing a relationship between the Flory–Huggins parameter (χ) and the solubility parameters of polymer (δ_2) and solvent (δ_1), eq. (8).

$$\chi = \chi_S + \chi_H = \chi_S + \frac{V_1}{RT}(\delta_1 - \delta_2)^2 \quad (8)$$

In this last equation, χ_S is the entropic contribution to χ and χ_H is the enthalpic contribution to χ . The value of χ_S is usually kept constant and equal to 0.34,⁷ while the enthalpic contribution is calculated from the solubility parameter values.

Rearranging terms, eq. (9) is obtained so that the polymer solubility parameter can be determined from the slope of $[(\delta_1^2/2) - (\chi RT/2V_1)]$ vs. δ_1 , by simply knowing the solubility parameter of several solvents.²⁶

$$\left(\frac{\delta_1^2}{2} - \frac{\chi RT}{2V_1}\right) = \delta_2\delta_1 - \left(\frac{\delta_2^2}{2} + \frac{\chi_S RT}{2V_1}\right) \quad (9)$$

Finally, from the activity coefficient values at different temperatures, the values of the heats of vaporization of the solvent ($\Delta_{\text{vap}}H_1$) can be obtained [eq. (10)] by calculating the heats of solution $\Delta_s H_1$ [eq. (11)] and the partial molar heats of mixing $\Delta_{\text{mix}}\bar{H}_1^\infty$ [eq. (13)].²³

$$\Delta_{\text{vap}}H_1 = \Delta_{\text{mix}}\bar{H}_1^\infty - \Delta_s H_1 \quad (10)$$

Table I. Experimental Results for EVA460 Polymer

EVA460 polymer	V_g (cm ³ /g)			$(\Omega_1^\infty)^{IGC}$			χ		
	30°C	40°C	50°C	30°C	40°C	50°C	30°C	40°C	50°C
Solvent									
Metanol (MET)	86	57	41	45.51	44.01	40.14	2.62	2.58	2.47
Ethanol (ET)	168	112	77	33.46	30.17	27.69	2.31	2.19	2.10
Butanol (BUT)	1463	906	559	18.31	15.56	14.09	1.73	1.56	1.45
n-Hexane (HEX)	139	103	76	11.55	11.14	11.13	1.07	1.01	1.00
Cyclohexane (CX)	305	224	163	6.00	5.64	5.51	0.57	0.50	0.47
Vinyl acetate (VA)	223	154	108	6.96	6.77	6.68	0.90	0.86	0.83
Toluene (TOL)	1535	1033	686	3.65	3.48	3.48	0.19	0.13	0.12
p-Xylene (XYL)	-	2763	1778	-	3.34	3.28	-	0.08	0.06
Tetrahydrofuran (THF)	293	210	153	4.51	4.35	4.27	0.42	0.37	0.34

$$\Delta_s H_1 = -R \left[\frac{\partial (\ln(V_g^\circ))}{\partial (1/T)} \right] \quad (11)$$

$$V_g^\circ = V_g \left(\frac{273.15}{T} \right) \quad (12)$$

$$\Delta_{\text{mix}} \bar{H}_1^\infty = R \left[\frac{\partial (\ln(\Omega_1^\infty))}{\partial (1/T)} \right] \quad (13)$$

These values, derived from the experimentally determined activity coefficients, can be compared with the ones estimated using the Watson model²⁷ as a kind of consistency test, to check its goodness.

Materials

The polymeric materials used in this work are two random EVA copolymers, which differ in their molecular weight and in their vinyl acetate percentage. Both of them were supplied by REPSOL-YPF Company.² While EVA-1 (EVA460) has a vinyl acetate content of 33% (w/w), EVA-2 (EVA410) has a vinyl acetate content of 18% (w/w). The weight-average molecular weight and the number-average molecular weight are 61,040 and 18,580 for EVA460, and 42,460 and 14,010 for EVA410. Finally, the densities of the two polymeric materials, given by the supplier, are 956 kg/m³ and 937 kg/m³, respectively.

On the other hand, all the used solvents (Methanol, MET; Ethanol, ET; *n*-Butanol, BUT; *n*-Hexane, HEX; Cyclohexane, CX; Vinyl Acetate, VA; Toluene, TOL; *p*-Xylene, XYL and Tetrahydrofuran, THF) were analytical grade and were purchased from Aldrich. They were used directly, without any purification step.

Experimental Procedure

The EVA stationary phases used in this work were prepared by dissolving a weighted sample of the polymer in a suitable solvent and depositing the solution on a weighted amount of support (Chromosorb W/AW-DMCS 80-100 mesh). The employed solvents were cyclohexane, in the case of EVA460 material, and tetrahydrofuran, in the case of EVA410 material.

Once dissolved, each mixture was allowed to dry by slow evaporation in a rotavapor under vacuum, while being stirred to ensure homogeneous mixture; evaporation time was at less 8 h. The final amount of each polymer deposited in the support was determined by thermogravimetric analysis on a Seiko EXSTAR 6000 TG/DTA 6200 equipment. Each analysis was performed three times, and the average value was selected in each case. The obtained percentages were 11.45% (w/w) for EVA460 and 11.28% (w/w) for EVA410.

Afterwards, each coated support was packed into a 1/4 in. nominal diameter column (1.92 m length for EVA460 and 2.00 m length for EVA410); both of them were installed in a VARIAN

Table II. Experimental Results for EVA410 Polymer

EVA410 polymer	V_g (cm ³ /g)			$(\Omega_1^\infty)^{IGC}$			χ		
	30°C	40°C	50°C	30°C	40°C	50°C	30°C	40°C	50°C
Solvent									
Metanol (MET)	47	33	23	83.54	75.43	70.23	3.25	3.13	3.05
Ethanol (ET)	93	62	43	60.83	54.44	49.18	2.93	2.81	2.69
Butanol (BUT)	765	522	328	35.01	27.03	23.97	2.40	2.13	2.00
n-Hexane (HEX)	111	85	64	14.46	13.47	13.24	1.31	1.23	1.19
Cyclohexane (CX)	241	180	135	7.59	7.00	6.60	0.83	0.74	0.67
Vinyl acetate (VA)	128	92	67	12.12	11.38	10.73	1.48	1.40	1.33
Toluene (TOL)	1056	720	493	5.31	5.00	4.85	0.59	0.51	0.47
p-Xylene (XYL)	-	1970	1286	-	4.69	4.54	-	0.44	0.40
Tetrahydrofuran (THF)	197	145	107	6.71	6.32	6.07	0.84	0.76	0.71

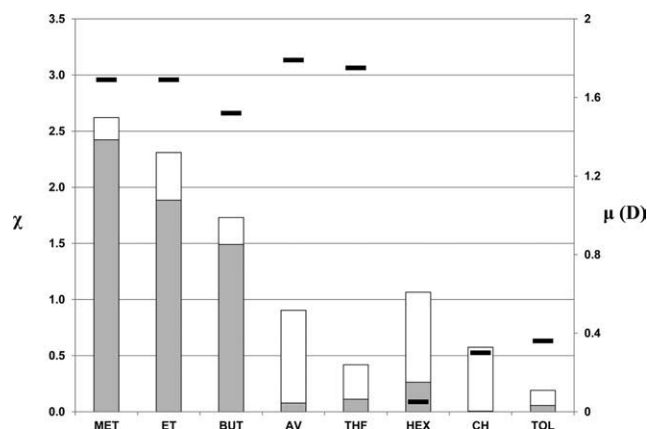


Figure 1. Flory-Huggins parameter for EVA 460—solvent pairs at 30°C (bars), related to the dipole moment of the solvent, μ (black horizontal lines). Each Flory-Huggins bar is divided into the enthalpic contribution (gray area) and entropic contribution (white area).

3800 gas chromatography, equipped with a thermal conductivity detector and an electronic flow controller.

All the measurements were carried out with a helium flow of 40 mL/min, as carrier gas, and air, as inert component, in a temperature range between 30 and 50°C.

RESULTS AND DISCUSSION

Flory-Huggins Parameter and Solvent Activity Coefficient Values

Tables I and II show the measured values of the retention volumes (V_g), along with the calculated values of the mass-based infinite dilution solvent activity coefficients, $(\Omega_i^\infty)_{IGC}$, and the Flory-Huggins interaction parameters (χ), for the binary mixtures of both EVA460 and EVA410 polymers with different solvents, in the temperature range from 30 to 50°C.

As it can be observed in these two Tables, the specific retention volumes (V_g) are higher in the case of EVA460-solvent systems, while the solvent activity coefficients and Flory-Huggins parameters are lower. Taking into account that the lower the activity coefficient and Flory-Huggins parameter the higher the compatibility between a polymer and a solvent, this could indicate that an increase of vinyl acetate content (EVA460 is the copolymer with more vinyl acetate percentage) implies higher interactions between the EVA material and the studied solvents.

As it is described in literature,²⁶ values of the Flory-Huggins parameter below 0.5 (critical χ parameter for high molecular weight polymers) indicate that the solvent is adequate for the polymer, while values higher than 0.5 indicate that the solvent is not favourable. So, according to this criterion, the most adequate solvents for both polymers should be the aromatic-type compounds, as well as tetrahydrofuran; secondly, the most adequate solvent-type should be the aliphatic, being the alcohols the less compatible solvents. Regarding the temperature dependence, it can be noticed that both solvent infinite dilution activity coefficients and Flory-Huggins parameter decrease with temperature, which is in agreement with literature.^{7,8,25}

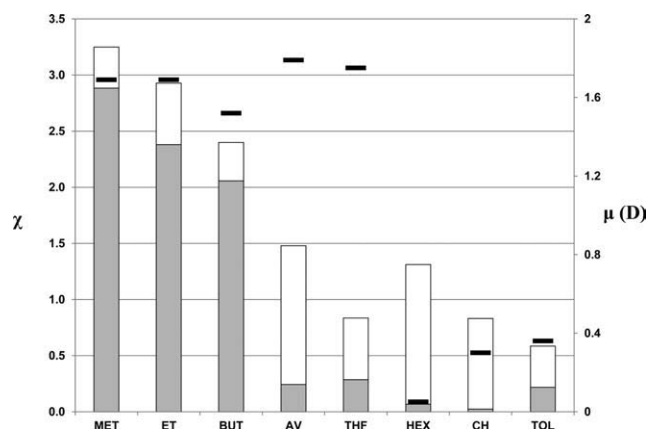


Figure 2. Flory-Huggins parameter for EVA 410—solvent pairs at 30°C (bars), related to the dipole moment of the solvent, μ (black horizontal lines). Each Flory-Huggins bar is divided into the enthalpic contribution (gray area) and entropic contribution (white area).

To further analyze the results of Tables I and II, it is important to take into consideration that the Flory-Huggins parameter includes two contributions: one entropic and one enthalpic. The entropic one is related to the free volume of the solvent, while the enthalpic one is related to the intermolecular forces between the polymer and the solvent. To investigate the relative importance of each contribution to the Flory-Huggins parameter, both of them were determined for each polymer-solvent pair. The enthalpic contribution was calculated following Blanks and Prausnitz assumption⁷ [eq. (8)], once the solubility parameter of the polymer was obtained (see next section), while the entropic contribution was determined as the difference between the overall solubility and the enthalpic contribution; the results are presented in Figures 1 and 2. Figure 1 represent the overall Flory-Huggins parameter divided in its two contributions (entropic, χ_s , and enthalpic, χ_H), related to the dipole moment of the solvents, for EVA460-solvent pairs; Figure 2 represents the same for EVA410-solvent systems.

As it can be seen, the larger contribution to the Flory-Huggins parameter of the most compatible solvents (the ones with the

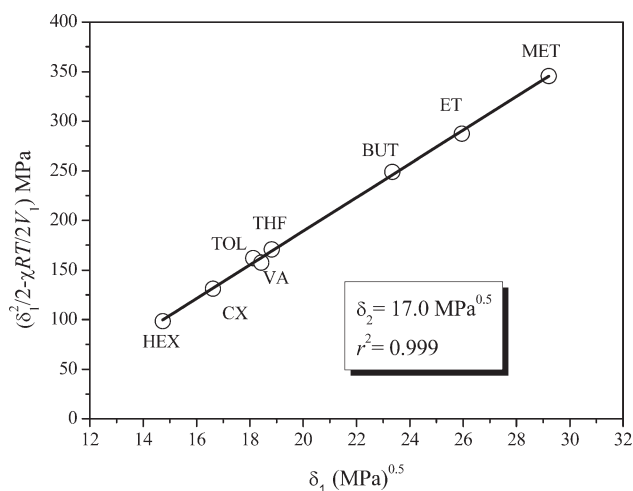


Figure 3. Plot to calculate the EVA460 solubility parameter at 30°C.

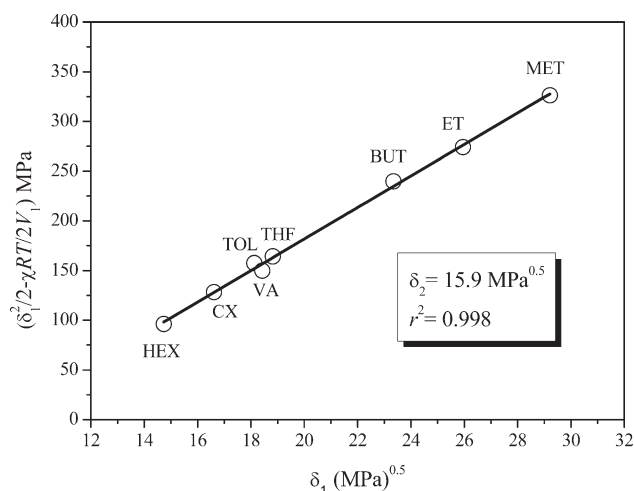


Figure 4. Plot to calculate the EVA410 solubility parameter at 30°C.

lowest values of this parameter) is the entropic one. This indicates that the interactions between the polymers and the solvents happen to be due to entropic factors, independently of the polar (THF, AV) or nonpolar (HEX, CH, TOL) character of the solvent. On the other hand, in the case of alcohol-EVA mixtures, the enthalpic contribution represents more than 80%, may be due the ability of the alcohols to form hydrogen bonds; however, because the entropic contribution is practically negligible, they are not compatible at all with neither of the two EVA materials.

Polymers Solubility Parameters

The solubility parameters of the two PVA materials were calculated from the slope of the plot of $[(\delta_1^2/2) - (\chi RT/2V_1)]$ vs. δ_1 [eq. (9)]. In both cases high regression coefficients were obtained ($r^2 > 0.995$). The values of this parameter are important due to, nowadays, they are considered to be a criterion which indicates the capacity of a polymer to be dissolved into a solvent because the closer the solubility parameters of a polymer and solvent are the better the solubility is. The above mentioned plots for EVA460 and EVA410 copolymers, respectively, at 30°C,

Table III. Solubility Parameter Values

Temperature (°C)	Solubility parameter (MPa ^{1/2})	
	EVA460	EVA 410
30	17.0	15.9
40	16.6	15.5
50	16.3	15.1

are shown in Figures 3 and 4, as an example, while all solubility parameter values are shown in Table III.

The solubility parameter is derived from the cohesion energy of a compound²⁵ so it is expected to slightly decrease with temperature, as it can be observed in Table III. It can also be noticed that the solubility parameter values of EVA460 are higher than the ones of EVA410. This can be justified by the fact that, in the case of a polymer, the cohesion energy is related to the interactions between the polymer chains and, the higher the vinyl acetate content, the stronger the interactions, due to the increasing polarity. This can be further justified by the fact that a literature value²⁶ of $\delta_2 = 17.0 \text{ MPa}^{1/2}$, obtained at 75°C, was found for an EVA with a vinyl acetate content of 40%.

On the other hand, it can also be observed that the obtained values for EVA460 material (the one with more vinyl acetate content) are closer to the solubility parameter values of pure vinyl acetate (18.4 MPa^{0.5} at 30°C, 18.1 MPa^{0.5} at 40°C and 17.8 MPa^{0.5} at 50°C)²⁰ than the obtained values for EVA410 material. As previously said, the closer the solubility parameters of polymer and solvent are, the higher the compatibility; so it is logical that the more vinyl acetate the copolymer contains, the more compatible with pure vinyl acetate is.

Heat of Vaporization of the Solvents

From the values of the activity coefficient of the solvents at several temperatures, the values of their heats of vaporization ($\Delta_{\text{vap}}H_1$) were calculated [eqs. (10)–(13)] and compared with the ones estimated with Watson model.²⁶ The results are summarized in Table IV. As it can be observed, the difference

Table IV. Experimentally Derived and Estimated Enthalpy Values

Solvent	EVA460 polymer					EVA410 polymer				
	$\Delta_s H_1$ (kJ/mol)	$\Delta_{\text{mix}} H_1^\infty$ (kJ/mol)	$\Delta_{\text{vap}} H_{1,\text{exp}}$ (kJ/mol)	$\Delta_{\text{vap}} H_{1,\text{Watson}}$ (kJ/mol)	Dev (%)	$\Delta_s H_1$ (kJ/mol)	$\Delta_{\text{mix}} H_1^\infty$ (kJ/mol)	$\Delta_{\text{vap}} H_{1,\text{exp}}$ (kJ/mol)	$\Delta_{\text{vap}} H_{1,\text{Watson}}$ (kJ/mol)	Dev (%)
MET	−32.7	5.1	37.7	36.7	2.7	−30.7	7.1	37.7	36.7	2.7
ET	−34.6	7.7	42.3	41.6	1.8	−33.7	8.7	42.3	41.6	1.8
BUT	−41.8	10.7	52.5	52.0	0.9	−37.0	15.5	52.5	52.0	0.9
HEX	−27.3	1.5	28.8	30.6	−6.0	−25.2	3.6	28.8	30.6	−6.0
CX	−28.2	3.5	31.7	32.2	−1.5	−26.0	5.7	31.7	32.2	−1.5
VA	−32.3	1.7	34.0	33.7	1.0	−29.0	5.0	34.0	33.7	1.0
TOL	−35.4	2.0	37.3	37.3	0.2	−33.6	3.7	37.3	37.3	0.2
XYL	−39.7	1.5	41.2	41.2	0.0	−38.5	2.7	41.2	41.2	0.0
THF	−29.2	2.2	31.4	31.2	0.6	−27.4	4.1	31.4	31.2	0.6

between the experimental and estimated values is always lower than 6%.

CONCLUSIONS

The mass-based infinite dilution solvent activity coefficients and Flory–Huggins interaction parameters have been experimentally determined for binary mixtures of several solvents with two EVA copolymers with different vinyl acetate content. The obtained values of these parameters are clearly lower for EVA460 mixtures (the copolymer with more vinyl acetate percentage) than for EVA410 mixtures, pointing to the fact that an increase of vinyl acetate content implies higher interactions between the EVA material and the solvent. The results also indicate that the most adequate solvents for both polymers (the ones whose mixtures with any of the polymers have the smallest Flory–Huggins parameter) are the aromatic-type compounds, as well as tetrahydrofuran.

From the calculated values of the entropic and enthalpic contributions to the Flory–Huggins parameter it can be noticed that, in the case of the most compatible solvents, the polymer–solvent interaction is mainly due to entropic effects, independently of the polar character of the solvent. On the contrary, for polymer–alcohol mixtures, the main contribution to the Flory–Huggins parameter is the enthalpic one. The influence of the temperature over this parameter shows that it tends to diminish with increasing temperature, which is in agreement with literature.

Finally, the solubility parameters of the two EVA copolymers were also determined. The obtained value for EVA460 material, the one with the most vinyl acetate percentage, is closest to the solubility parameter of the pure vinyl acetate.

ACKNOWLEDGMENTS

The authors want to acknowledge REPSOL-YPF Company for the supply of the polymer.

REFERENCES

1. Brydson, J. A. *Plastic Materials*; Elsevier: Oxford, **1999**; Chapter 1, pp 1–15.
2. REPSOL-YPF catalogue. Available at: <http://www.repsol.com/sa/herramientas/CatalogoQuimica/CatalogoQuimica.aspx>. Last accessed on: 1 November **2011**.
3. Kawahara, T.; Takai, M. (Kuraray Co.). U. S. Pat. 6,831,139 B2 (**2004**).
4. Qian, J.W.; Qi, G. R.; Cheng, R. S. *Eur. Polym. J.* **1997**, *33*, 1263.
5. Flory, P. J. *J. Chem. Phys.* **1942**, *10*, 51.
6. Radfarnia, H. R.; Kontogeorgis, G. M.; Ghotbi, C.; Taghikhani, V. *Fluid Phase Equilib.* **2007**, *257*, 63.
7. Blanks, R. F.; Prausnitz, J. M. *Ind. Eng. Chem. Fundam.* **1964**, *3*, 1.
8. Sheehan, C. J.; Bisio, A. L. *Rubber Chem. Technol.* **1966**, *39*, 149.
9. Barton, A. F. M. *Chem. Rev.* **1975**, *75*, 731.
10. Na, Y.; Zuo-Xiang, Z.; Wei-Lan, X. *J. App. Polym. Sci.* **2010**, *117*, 1883.
11. Mehrdad, A.; Talebi, I.; Akbarzadeh, R. *Fluid Phase Equilib.* **2009**, *284*, 137.
12. Eroğlu, M. S.; Baysal, B. M. *Polymer* **1997**, *38*, 1945.
13. Çaykara, T.; Özyürek, C.; Kantoğlu, O.; Güven, O. *J. Polym. Sci.* **2002**, *40*, 1995.
14. Nastasović, A. B.; Onjia, A. E. *J. Chromatogr. A* **2008**, *1195*, 1.
15. Zhang, S.; Tsuboi, A.; Nakata, H.; Ishikawa, K. *Fluid Phase Equilib.* **2002**, *194–197*, 1179.
16. Zeng, C.; Li, J.; Wang, D.; Chen, T.; Zhao, C.; Chen, C. *J. Chem. Eng. Data* **2006**, *51*, 93.
17. Krüger, K. M.; Pfohl, O.; Dohrn, R.; Sadowski, G. *Fluid Phase Equilib.* **2006**, *241*, 138.
18. Schacht, C. S.; Zubeir, L.; de Loos, T. W.; Gross, J. *Ind. Eng. Chem. Res.* **2010**, *49*, 7646.
19. Conder, J. R.; Young, C. L. *Physicochemical Measurement by Gas Chromatography*; Wiley: New York, **1979**; Chapter 5, pp 154–221.
20. Rackett, H. G. *J. Chem. Eng. Data* **1970**, *15*, 514.
21. NIST Chemistry WebBook. Available at: <http://webbook.nist.gov/chemistry/>. Last accessed on: 1 December **2011**.
22. Tsonopoulos, C. *AIChE J.* **1974**, *20*, 263.
23. Romdhane, I. H.; Plana, A.; Hwang, S.; Danner, R. P. *J. Appl. Polym. Sci.* **1992**, *45*, 2049.
24. Vrentas, J. S.; Vrentas, C. M.; Romdhane, I. H. *Macromolecules* **1993**, *26*, 6670.
25. Hildebrand, J.; Scott, R. *Regular Solutions*; Englewood Cliffs: Prentice Hall, **1962**.
26. Grulke, E. A. In *Polymer Handbook*; Brandrup, J., Immergut, E. H., Grulke, E. A., Eds.; Wiley: New York, **1999**; Chapter VII, pp 675–714.
27. Watson, K. M. *Ind. Eng. Chem.* **1943**, *35*, 398.

2.2 Inverse Gas Chromatography Study of Polyvinylacetate - Solvent and Polyethylene - Solvent Systems

Camacho J, Díez E, Ovejero G, Gomez L. (2015) Inverse Gas Chromatography study of Polyvinylacetate - Solvent and Polyethylene - Solvent Systems. Accepted for publication in Polymer Engineering and Science. (DOI 10.1002/pen.24189).

Inverse Gas Chromatography Study of Polyvinylacetate–Solvent and Polyethylene–Solvent Systems

Javier Camacho, Eduardo Díez, Lourdes Gómez, Gabriel Ovejero

Grupo De Catálisis Y Procesos De Separación (CyPS), Departamento De Ingeniería Química, Facultad De C. Químicas Universidad Complutense De Madrid Avda, Complutense S/N, Madrid 28040, Spain

In this article, the thermodynamic behavior of polyvinylacetate (PVAc)–solvent, and polyethylene (PE)–solvent mixtures have been studied by determining the thermodynamic sorption parameters (enthalpy, entropy, and free energy), the mass-based solvent activity coefficients (Ω) and the Flory Huggins parameters (χ), by means of inverse gas chromatography (IGC) measurements. According to the Flory Huggins parameters of the PE–solvent mixtures, determined between 40 and 60°C the compatibility (the ability to interact with each other) of this polymer with the different types of solvents follows this order: dispersion solvents > polar solvents > association solvents. In the case of PVAc mixtures, the thermodynamic parameters were determined between 60 and 80°C, only for polar-type and association-type solvents due to, in the studied temperature range, the retention diagrams of dispersion solvents show that there are not bulk interactions. The Hildebrand solubility parameters of both polymers were also determined, according to Guillet procedure. The higher values of PVAc material (14.1 MPa^{0.5} for PE and 19.8 MPa^{0.5} for PVAc, at 60°C) are related to the strong interactions of vinyl acetate monomer. POLYM. ENG. SCI., 00:000–000, 2015. © 2015 Society of Plastics Engineers

INTRODUCTION

Linear polyethylene (PE) is one of the most employed polymeric materials due to its wide range of applications. It is a thermoplastic crystalline material which is obtained from ethylene polymerization, and its main applications are in cable isolations, pipes, or in bottles manufacture [1].

On the other hand, polyvinyl acetate (PVAc) is also one of the most common polymeric materials. It is a thermoplastic amorphous polymer which is frequently obtained by free radical polymerization of vinyl acetate [2]. It is mainly employed as an adhesive of different porous materials such as wood or paper [3], but it also appears as a part of several copolymers, being the most important one, the ethylene–vinyl acetate copolymer (EVA) which is formed by the amorphous polyvinyl acetate plus the crystalline linear polyethylene.

In our research group, we are focusing on studying the modelling and simulation of the purification step of the EVA material [4], produced in a dissolution process (in methanol or butanol, at temperatures around 60°C), due its important applications as adhesive, elastomeric or modifier [5]. To model copolymers such as EVAs, most of the thermodynamics models are based on splitting the polymeric material into its homopolymers and determining the homopolymer–solvent binary interaction

parameters (in this case, the correspondent homopolymers of ethylene–vinyl acetate copolymer are polyethylene and polyvinyl acetate). In literature, the thermodynamic data of PE–solvent and PVAc–solvent mixtures at the temperatures of interest are scarce so, in this article we focus on obtaining these data experimentally.

One of the most well-known models for binary interaction parameters of polymer (subscript 3)–solvent (subscript 1) mixture is the Flory–Huggins theory [6, 7]. According to this theory, the solvent activity coefficient can be obtained by means of Eq. 1. In this equation, a_1 is the activity coefficient of the solvent, ϕ_3 is the polymer volumetric fraction, r is the ratio between the molar volume of the polymer and the molar volume of the solvent, and χ is the Flory–Huggins polymer–solvent interaction parameter, which is experimentally determined.

$$\ln(a_1) = \ln(1 - \phi_3) + \left(1 - \frac{1}{r}\right)\phi_3 + \chi\phi_3^2 \quad (1)$$

The Flory Huggins theory [6, 7] does not consider the free volume effect. This effect is noticeable being only at high temperatures and pressures, which is important to determine the LSCP (lower solution critical point).

This parameter has traditionally been calculated with Eq. 2, which is divided into both entropic (χ_S) and enthalpic (χ_H) contributions. While the entropic factor is normally considered, according to Blanks and Prausnitz [8] as 0.34, the enthalpic factor can be initially approximated from the molar volume of the solvent ($V_{m,1}$), the absolute temperature (T), and the Hildebrand Solubility Parameters of the polymer (δ_3) and the solvent (δ_1).

$$\chi = \chi_S + \chi_H = \chi_S + \frac{V_{m,1}}{RT}(\delta_1 - \delta_3)^2 \quad (2)$$

This division allows analyzing the temperature dependence on this parameter: The entropic term is related to the free volume of the solvent, so is expected to increase with temperature (the free volume of the solvent also increases with temperature, so this compound will be less accessible to polymer lattice); the enthalpic one is expected to decrease with temperature, due to the decreasing of intermolecular forces between polymer and solvent. For this reason, although originally [6] it was assumed a decreasing of Flory Huggins parameter with temperature, in literature it has been described that this parameter can decrease [9] but also increase [10] with temperature.

In the case of heteropolymer–solvent systems, the Flory Huggins parameter can also show a dependence on the heteropolymer composition (relative amount of the different monomers). This can be justified in terms of the relative polarity of the monomers as well as one of the solvents, although a definite pattern cannot be found in literature.

Correspondence to: E. Díez; e-mail: ediezalc@quim.ucm.es

DOI 10.1002/pen.24189

Published online in Wiley Online Library (wileyonlinelibrary.com).

© 2015 Society of Plastics Engineers

THEORY AND CALCULATIONS: IGC BASIS

Following the IGC basis [11], the retention volume ($V_{g,1}$) of a solvent (1) through a column packed with a polymer (3), once injected and gone through the column, can be calculated from retention time measurements by means of Eq. 3. In this equation, F_2 is the flow rate of the carrier gas (2) corrected to the column temperature (measured at inlet temperature and pressure conditions), t_r is the retention time of the solvent, t_m is the retention time of a reference inert compound, W_s is the amount of polymer packed in the column and j_2 is a correction factor. Because of carrier gas is compressible, the pressure drop along the column (the difference between the inlet pressure, P_i , and the outlet pressure, P_0) might cause an increase of the volume flow rate in the outlet compared with the inlet value; for this reason, a correction factor (j_2) is usually added (Eq. 4) [11].

$$V_{g,1} = \frac{j_2 \cdot (t_r - t_m) \cdot F_2}{W_s} \quad (3)$$

$$j_2 = \frac{3(P_i/P_0)^2 - 1}{2(P_i/P_0)^3 - 1} \quad (4)$$

From the retention volume, several thermodynamic properties can be determined. On one hand, the specific retention volume, $V_{g,1}^\circ$, (corrected to the reference temperature of 273.15 K) can be calculated according to Eq. 5. On the other hand, the solvent molar enthalpy of sorption and the solvent molar free energy of sorption can be calculated with Eqs. 6 and 7, respectively [11]. Besides, from the enthalpy and free energy of sorption, the solvent entropy of sorption ($\Delta_s S_1$) can be calculated by means of Eq. 8

$$V_{g,1}^\circ = V_{g,1} \left(\frac{273.15}{T} \right) = \left(\frac{j_2 \cdot (t_r - t_m) \cdot F_2}{W_s} \right) \left(\frac{273.15}{T} \right) \quad (5)$$

$$\Delta_s H_1 = -R \left[\frac{\partial (\ln(V_{g,1}^\circ))}{\partial (1/T)} \right] \quad (6)$$

$$\Delta_s G_1 = -R \cdot T \cdot \ln \left[\frac{\rho_3 j \cdot (t_r - t_m) \cdot F}{W_s} \right] \quad (7)$$

$$\Delta_s G_1 = \Delta_s H_1 - T \cdot \Delta_s S_1 \quad (8)$$

The relation between the mass-based infinite dilution activity coefficient of the solvent, (Ω_{13}^∞), and its retention volume ($V_{g,1}$), in a solvent (1)–polymer (3) mixture, is given by Eq. 9 [11], where T is the temperature in K, R is the ideal gas constant, M_1 is the solvent molecular weight and f_1° is the standard fugacity of the solvent. This last parameter is usually determined with the Virial EOS truncated after the second term; so, Eq. 9 is transformed into Eq. 10, where B_{11} is the solvent second term of the Virial EOS, p_1° is the solvent vapor pressure and V_1 is the solvent molar volume. The mass mass-based infinite dilution activity coefficient of the solvent can be expressed in terms of the retention volume ($V_{g,1}$) or the specific retention volume ($V_{g,1}^\circ$).

$$\ln(\Omega_{13}^\infty) = \ln \left(\frac{R \cdot T}{V_{g,1} \cdot M_1 \cdot f_1^\circ} \right) \quad (9)$$

$$\begin{aligned} \ln(\Omega_{13}^\infty) &= \ln \left(\frac{R \cdot T}{V_{g,1} M_1 p_1^\circ} \right) - \frac{(B_{11} - V_1) p_1^\circ}{RT} \\ &= \ln \left(\frac{273.15 \cdot R}{V_{g,1}^\circ M_1 p_1^\circ} \right) - \frac{(B_{11} - V_1) p_1^\circ}{RT} \end{aligned} \quad (10)$$

In this work, the solvent molar volumes have been calculated assuming saturated liquid at each temperature, according to a modification of Rackett model which appears in literature [12], the second terms of Virial EOS (B_{11}) have been calculated with Tsonopoulos' correlation [13], and the solvent vapor pressures have been determined from the Antoine coefficients values taken from literature [14].

From the values of infinite dilution activity coefficient, the Flory Huggins interaction parameter (χ_{13}^∞) can be calculated by using Eq. 11 [15] where r is the ratio between the molar volume of the polymer and the molar volume of the solvent, and ρ_1 and ρ_3 are the solvent and polymer densities, respectively.

$$\chi_{13}^\infty = \ln(\Omega_{13}^\infty) - \left(1 - \frac{1}{r} \right) + \ln \frac{\rho_1}{\rho_3} \quad (11)$$

Equivalent expressions have been employed in literature [16], because Eq. 11 is directly derived from the combination of Eq. 10 with the well-known Flory Equation [6] (Eq. 1), which allows calculating the activity of a solvent, in a polymer–solvent mixture.

The IGC measurements allow also determining the Hildebrand solubility parameter of a polymer by rearranging Eq. 2 into Eq. 12. This parameter can be obtained from the slope of $[(\delta_1^2/2) - (\chi RT/2V_1)]$ vs. δ_1 , by simply knowing the Hildebrand solubility parameter of several solvents [17].

$$\left(\frac{\delta_1^2}{2} - \frac{\chi_{13}^\infty RT}{2V_1} \right) = \delta_3 \delta_1 - \left(\frac{\delta_3^2}{2} + \frac{(\chi_{13}^\infty)_s RT}{2V_1} \right) \quad (12)$$

Finally, from the activity coefficient values at different temperatures, the values of the heats of vaporization of the solvent ($\Delta_{\text{vap}} H_1$) can be obtained (Eq. 13) from the solvent molar enthalpy of sorption data (Eq. 6) and the partial molar excess enthalpy at infinite dilution $\Delta H_1^{E,\infty}$ (Eq. 14) [15].

$$\Delta_{\text{vap}} H_1 = \Delta H_1^{E,\infty} - \Delta_s H_1 \quad (13)$$

$$\Delta H_{1,E}^\infty = R \left[\frac{\partial (\ln(\Omega_{13}^\infty))}{\partial (1/T)} \right] \quad (14)$$

These solvent heats of vaporization values, derived from the experimentally determined activity coefficients, can be compared with the ones estimated employing the Watson model [18] as a kind of consistency test, in order to check the goodness of the experimental data.

EXPERIMENTAL

Materials

Polyvinylacetate polymer (referred in the paper as PVAc) was purchased from Sigma–Aldrich Company. The weight-average molecular weight, the polydispersity, and the density

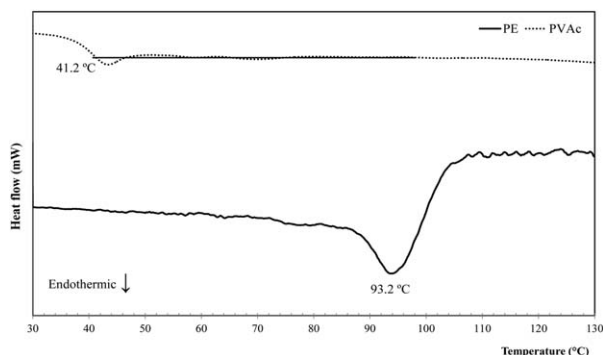


FIG. 1. DSC melting curves for PE and PVAc materials.

reported by supplier are 100 kg mol^{-1} , 2.5 and 1180 kg m^{-3} , respectively.

Low density polyethylene (LDPE, referred in the paper as PE) was also purchased from Sigma Aldrich Company. The weight-average molecular weight, the polydispersity, and the density reported by supplier are 35 kg mol^{-1} , 4.54 and 906 kg m^{-3} , respectively.

On the other hand, both employed solvents (Methanol, MET; Ethanol, ET; 1-Propanol, 1-PROP; 2-Propanol, 2-PROP; 1-Butanol, 1-BUT; 2-Butanol, 2-BUT; 1-Pentanol, 1-PENT; Vinyl Acetate, VA; Tetrahydrofuran, THF; Acetone, AC; Benzene, BZ; Toluene, TOL; Cyclohexane, CX; Methylcyclohexane, MCX; Cyclopentane, CPENT and *n*-Hexane, HEX) were analytical grade and were also purchased from Aldrich. They were used directly, without any purification step.

Polymer Thermal Characterization

The differential scanning calorimetry (DSC) analysis of both polymeric materials was performed with a Seiko EXSTAR 6000 DSC 6200 equipment. The measurements were carried out following a procedure described in literature for EVA-type materials [19]: Polymer samples were first heated up to 150°C at a rapid heating rate of $20^\circ\text{C min}^{-1}$ and kept at 150°C for 5 min. Then they were cooled down from 150 to 0°C at the rate of 5°C min^{-1} to obtain the nonisothermal crystallization curves. Finally, the re-melting was finished by second heating run from 0 to 150°C at $10^\circ\text{C min}^{-1}$.

Glass transition temperature (T_g) was determined from the onset of the corresponding jump interval of the curve. On the other hand, melting temperature (T_m) was calculated from the minimum value of the peak of the corresponding curve.

Inverse Gas Chromatography Determination

The stationary phases employed in the column were prepared by dissolving a weighted sample of the polymer (PVAc or PE) in a tetrahydrofuran solvent and depositing each solution on a weighted amount of support (Chromosorb W/AW-DMCS 80-100 mesh).

Once dissolved, each mixture was allowed to dry by slow evaporation in a rotavapor under vacuum, while being stirred to ensure homogeneous mixture; evaporation time was at <8 h. The final amount of each polymer deposited in the support was determined by thermogravimetric analysis on a Perkin Elmer

STA 6000 equipment. Each analysis was performed three times, and the average value was selected in each case. The obtained percentages were $16.54\% \pm 0.79\%$ (w/w) for PVAc and $15.78\% \pm 0.10\%$ (w/w) for PE.

Afterward, each coated support was packed into a $1/4$ in. nominal diameter and 2.00 m length column. Both of them were installed in a VARIAN 3800 gas chromatography, equipped with a thermal conductivity detector and an electronic flow controller.

All the measurements were carried out with a 40 mL min^{-1} helium flow, as a carrier gas, and air, as an inert component (to determine the necessary time just to pass through the column with interacting with the packing). The temperature ranges were from 40 to 80°C for PVAc and from 40 to 60°C for PE.

RESULTS AND DISCUSSION

Polymer Thermal Characterization

Figure 1 shows the DSC melting curves of both PE and PVAc, after the non-isothermal crystallization process. In most cases, PE is a semi-crystalline polymer. One of the main thermal characteristics of these materials is that they have both glass transition temperature (T_g) and melting temperature (T_m). From the minimum peak of the corresponding curve it can be determined that T_m is 93.2°C . However, in the studied temperature range the jump interval corresponding to the glass transition temperature was not observed for this PE. This means that this value is $<0^\circ\text{C}$, which is according to the bibliographic references [20].

On the other hand, PVAc is an amorphous material, so it has only a glass transition temperature. From the onset of the corresponding jump interval (which is not a peak as it would be in the case of a melting point) of the corresponding curve, T_g is 41.2°C .

Retention Volumes

Figures 2 and 3 show the retention diagrams (solvent specific retention volumes vs. the inverse of temperature, $\ln(V_{g,1}^0)$ vs. T^{-1} for all PE-solvent and PVAc-solvent pairs, grouped according to the nature of the solvent: association, polar or dispersion. The solvent specific retention volume ($V_{g,1}^0$) is the solvent

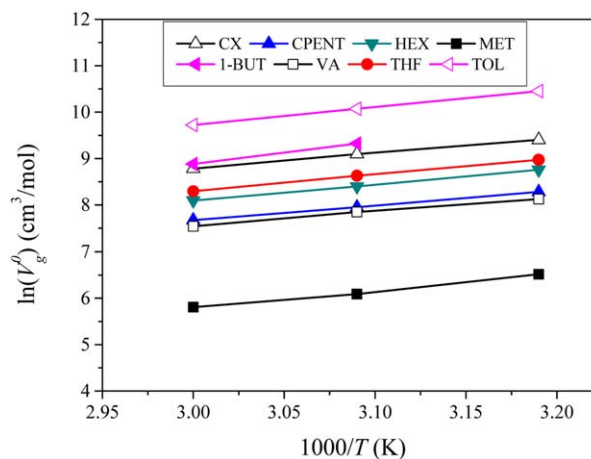


FIG. 2. $\ln(V_{g,1}^0)$ vs. T^{-1} plot for PE-solvent systems. [Color figure can be viewed in the online issue, which is available at wileyonlinelibrary.com.]

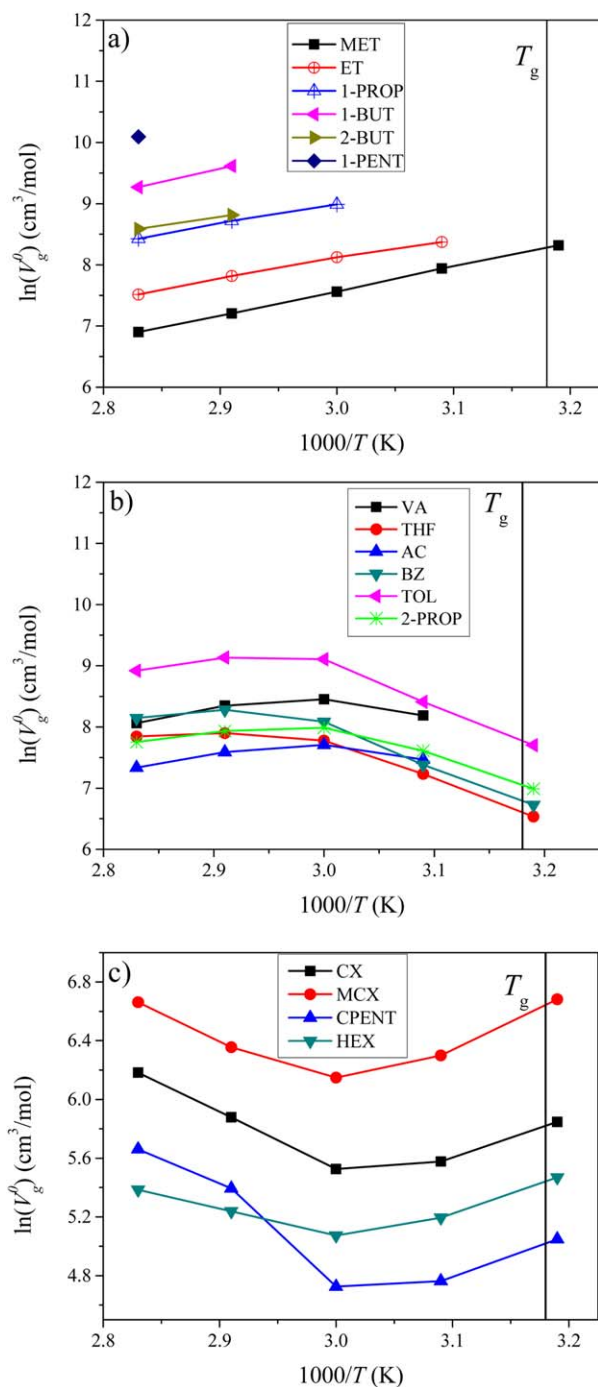


FIG. 3. $\ln(V_{g,1}^0)$ vs. T^{-1} plot for PVAc-solvent systems (a: association solvents, b: polar solvents, c: dispersion solvents). [Color figure can be viewed in the online issue, which is available at wileyonlinelibrary.com.]

retention volume ($V_{g,1}$) corrected to standard temperature (273.15 K). The temperature ranges studied were 40–60°C for PE and 40–80°C for PVAc.

In the case of PVAc-systems (Fig. 3), although the T_g of this polymer is 41.2°C, we have measured the solvent retention volumes starting from 40°C (below T_g) to analyze the intervals of temperatures with and without bulk interactions. According to literature [21], at the glassy state (below T_g), the solvent only interacts with the polymer surface because that the diffusion into the polymer is too slow to allow the bulk interaction. On the

other hand, at temperatures higher than T_g , the retention volume is a measurement of the interaction of the solvent with the bulk polymer in liquid state, where the diffusion of the solute in the polymer becomes sufficiently rapid so that the equilibrium can be established during the time of the passage of the solute peak through the column. At this point, the normal gas-chromatographic behavior can be observed (the retention volume decreases with increasing temperature). Close to the T_g , both factors can contribute to the retention volume, what causes, according to several authors [21, 22], a Z-shaped retention diagram around the glass transition temperature (T_g) of the polymer.

Regarding PE-solvent systems, as it can be observed in Fig. 2, the solvent specific retention volumes ($V_{g,1}^0$) of all PE-solvent groups tend to increase with T^{-1} ; this indicates that $V_{g,1}^0$ values decrease with temperature increasing. The more or less linear trends indicate that PE is not suffering any phase change, in the studied temperature range, which indicates that this interval is adequate to quantify the polymer-solvent bulk interactions. This seems logical because the T_g of PE is <0°C [20], while the T_m is 93.2°C.

So, it can be affirmed that the temperature range without bulk interactions corresponds to the nonlinear zone of the retention diagram and the decreasing linear zone at higher temperatures corresponds to the temperature range with bulk interactions. As it can be noticed in Fig. 3, this decreasing linear zone is observed, for association solvents and for polar solvents starting at least from 60°C, but is not observed for dispersion solvents. As a consequence, the sorption parameters and the solvent activity coefficients and the Flory Huggins parameters were calculated only in the temperature range from 60 to 80°C and for polar-type and dispersion-type solvents in whose retention diagrams this decreasing linear zone can be clearly observed. In the case of dispersion solvents, the shape of the retention diagram indicates that, in the studied temperature range, there are no bulk interactions, what makes unreliable the calculation of thermodynamic parameters.

However, to confirm this tendency, we chose one dispersion solvent, CX, one polar solvent, VA, and one association solvent, MET, and we measured their retention diagrams over an extended temperature range. The results are shown in Fig. 4. As

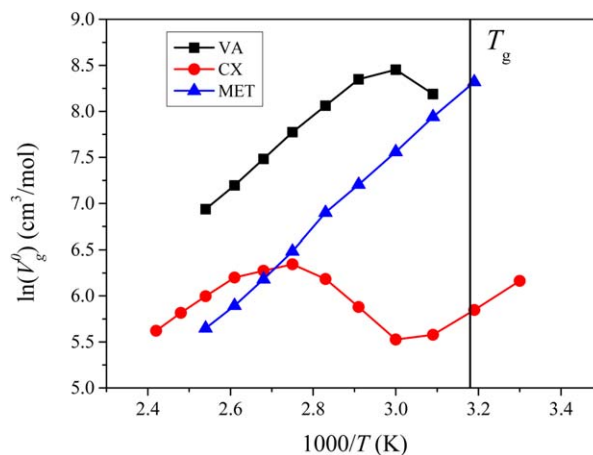


FIG. 4. $\ln(V_{g,1}^0)$ vs. T^{-1} plot for PVAc-solvent systems (CHEx, VA, MET), over an extended temperature range (30–140°C). [Color figure can be viewed in the online issue, which is available at wileyonlinelibrary.com.]

TABLE 1. Solvent molar enthalpies of sorption, $\Delta_s H_1$ (kJ mol⁻¹), of PE—solvent and PVAc—solvent mixtures.

Solvent	PVAc polymer					PE polymer				
	$\Delta_s H_1$ (kJ mol ⁻¹)	$\Delta H_1^{E,\infty}$ (kJ mol ⁻¹)	$\Delta_{\text{vap}} H_{1,\text{exp}}$ (kJ mol ⁻¹)	$\Delta_{\text{vap}} H_{1,\text{Watson}}$ (kJ mol ⁻¹)	Dev (%)	$\Delta_s H_1$ (kJ mol ⁻¹)	$\Delta H_1^{E,\infty}$ (kJ mol ⁻¹)	$\Delta_{\text{vap}} H_{1,\text{exp}}$ (kJ mol ⁻¹)	$\Delta_{\text{vap}} H_{1,\text{Watson}}$ (kJ mol ⁻¹)	Dev (%)
MET	-32.25	4.18	36.43	35.43	2.82	-30.87	6.39	37.27	36.10	3.23
ET	-29.85	10.69	40.54	40.23	0.79					
1-PROP	-27.41	17.03	44.44	45.03	-1.31					
2-PROP	-11.36	23.35	41.51	42.78	-2.96					
1-BUT	-34.69	13.55	48.24	49.81	-3.14	-43.15	7.40	50.54	50.91	-0.72
2-BUT	-18.17	21.67	44.59	45.93	-2.91					
VA	-18.97	13.33	32.30	32.39	-0.26	-25.43	7.90	33.33	33.05	0.85
THF	-5.56	24.26	29.82	30.16	-1.14	-29.41	1.55	30.96	30.70	0.84
AC	-18.10	11.27	29.38	29.33	0.18					
BZ	-13.76	17.59	31.35	31.91	-1.77					
TOL	-21.55	13.95	35.50	36.21	-1.96	-31.70	5.07	36.77	36.74	0.07
CX						-26.90	5.43	32.32	31.66	2.09
HEX						-25.62	4.76	30.39	30.01	1.27

it can be observed, in the entire studied temperature interval, a decreasing linear zone is observed for MET–PVAc pair (bulk interactions), while for VA–PVAc couple, these bulk interactions begins at ~60°C and for CX–PVAc systems this linear zone begins at 90°C (temperature out of interest as the studied process is carried out at temperatures around 60°C).

It is important to notice the anomalous of 2-propanol which, being an association solvent (as the rest of alcohols), behaves as a polar-type compound. The same way benzene, being a non-polar compound, behaves as polar one.

Thermodynamic Sorption Parameters

Table 1 shows the solvent molar enthalpies of sorption, the partial molar excess enthalpies and the polymer $\Delta H_1^{E,\infty}$, the heats of vaporization of the solvent ($\Delta_{\text{vap}} H_1$) and the ones estimated with Watson model [18]. Tables 2 and 3 show the solvent molar free energies of sorption, $\Delta_s G_1$ and solvent molar entropies of sorption, $\Delta_s S_1$ of PE-solvent and PVAc-solvent mixtures, respectively.

As previously stated, in the case of PE mixtures, the thermodynamic parameters were calculated along the overall temperature range studied (40–60°C). On the other hand, in the case of PVAc mixtures, the previously mentioned parameters were only

TABLE 2. Solvent molar free energies of sorption, $\Delta_s G_1$ (kJ mol⁻¹) and solvent molar entropies of sorption, $\Delta_s H_1$ (kJ mol⁻¹.100), of PE—solvent mixtures.

PE Solvent	$\Delta_s G_1$ (kJ mol ⁻¹)			$\Delta_s H_1$ (kJ mol ⁻¹ .100)		
	40°C	50°C	60°C	40°C	50°C	60°C
MET	-8.04	-7.23	-6.75	-7.29	-7.32	-7.24
1-BUT	-14.60	-13.66	-12.95	-9.12	-9.12	-9.07
VA	-9.65	-9.29	-8.82	-5.04	-4.99	-4.99
THF	-12.32	-11.87	-11.39	-5.46	-5.43	-5.41
TOL	-15.53	-15.09	-14.66	-5.16	-5.14	-5.11
CX	-13.03	-12.71	-12.32	-4.43	-4.39	-4.38
CPENT	-10.46	-10.12	-10.04	-2.12	-2.16	-2.06
HEX	-11.10	-10.77	-10.35	-4.64	-4.60	-4.59

determined above the glass transition temperature, from 60 to 80°C, where the plot $\ln(V_g^0)$ vs. T^{-1} follows a linear pattern.

Generally, a good linear relationship of the sorption parameters with temperature was achieved what confirms that, in the studied temperature ranges, the $V_{g,1}^0$ values are suitable for further thermodynamic calculations such as the solvent activity coefficients or the Flory Huggins parameters. This linearity can be related to the reaching of equilibrium between the stationary phase and the solvent [21].

In the above mentioned tables it can be seen that the molar enthalpies of sorption are negative (exothermic process) and the free energies of sorption are also negatives (favorable).

Solvent Activity Coefficients and Flory Huggins Parameters

Tables 4 and 5 show the calculated values of the mass-based infinite dilution solvent activity coefficients, (Ω_{13}^∞), and the Flory–Huggins interaction parameters (χ_{13}^∞), for the binary mixtures of both PE and PVAc polymers with the different solvents.

As it can be observed, in all cases both parameters decrease with the increase of temperature. Thus, and as is expected, the solubility is favored by increasing the temperature.

TABLE 3. Solvent molar free energies of sorption, $\Delta_s G_1$ (kJ mol⁻¹) and solvent molar entropies of sorption, $\Delta_s H_1$ (kJ mol⁻¹.100), of PVAc—solvent mixtures.

PVAc Solvent	$\Delta_s G_1$ (kJ mol ⁻¹)			$\Delta_s H_1$ (kJ mol ⁻¹ .100)		
	60°C	70°C	80°C	60°C	70°C	80°C
MET	-12.34	-11.78	-11.31	-5.98	-5.96	-5.93
ET	-12.90	-12.49	-12.05	-5.09	-5.06	-5.04
1-PROP	-14.55	-14.31	-13.95	-3.86	-3.82	-3.81
2-PROP	-11.78	-12.07	-11.97	-1.92	-1.78	-1.75
1-BUT		-16.26	-15.81		-5.37	-5.35
2-BUT		-13.98	-13.80		-2.61	-2.58
VA	-12.07	-12.22	-11.82	-2.07	-1.97	-2.02
THF	-10.69	-11.45	-11.71	1.54	1.72	1.74
AC	-11.10	-11.18	-10.85	-2.10	-2.02	-2.05
BZ	-11.33	-12.31	-12.35	-0.73	-0.42	-0.40
TOL	-13.70	-14.27	-14.14	-2.36	-2.12	-2.10

TABLE 4. Mass-based solvent activity coefficients and Flory Huggins parameters for PE—solvent mixtures.

PE Solvent	Ω_{13}^{∞}			χ_{13}^{∞}		
	40°C	50°C	60°C	40°C	50°C	60°C
MET	95.64	93.96	82.43	3.41	3.37	3.23
1-BUT	46.71	44.26	39.36	2.71	2.65	2.52
VA	22.65	20.11	18.88	2.12	1.99	1.91
THF	7.30	7.10	7.04	0.94	0.90	0.88
TOL	8.41	7.91	7.48	1.07	1.00	0.93
CX	8.30	7.67	7.33	0.94	0.85	0.79
CPENT	7.94	7.95	7.71	0.86	0.84	0.80
HEX	10.59	9.81	9.49	1.02	0.93	0.88

Figures 5 and 6 show the Flory Huggins diagrams (χ_{13}^{∞} vs T) for all PE—solvent and PVAc—solvent pairs, grouped again according to the solvent type: association, polar, or dispersion. It can be noticed that all the solvents follow the same linear tendency, according to the nature of the group. In addition, the linear trend shown is according to the Flory Huggins parameter–temperature [6], *Eq. 13*, where A and B are constants for a given system at a given concentration.

$$\chi = \frac{A}{T} + B \quad (13)$$

Figure 5 shows that dispersion solvents are the most compatible ones with PE, due to their Flory Huggins values are closer to 0.5. Regarding this, it is important to comment that χ values lower than 0.5 theoretically indicate complete miscibility of a polymer in a solvent. The compatibility (ability to interact with each other) order for PE—solvent mixtures tends to be: dispersion solvents > polar solvents > association solvents. This is something that could be expected, due the dispersion character of the ethylene monomer.

Figure 6 indicates that the compatibility order for PVAc—solvents mixtures tends to be: polar solvents > association solvents; this is also expected because the presence of ester groups in PVAc tends to solubilize itself with alcohols, and the vinyl acetate monomer of PVAc has a significant dipole moment.

TABLE 5. Mass-based solvent activity coefficients and Flory Huggins parameters for PVAc—solvent mixtures.

PVAc Solvent	Ω_{13}^{∞}			χ_{13}^{∞}		
	60°C	70°C	80°C	60°C	70°C	80°C
MET	14.28	13.84	13.11	1.21	1.17	1.10
ET	14.96	13.24	12.02	1.26	1.12	1.01
1-PROP	14.04	11.46	9.91	1.21	1.00	0.84
2-PROP	19.98	13.48	10.69	1.54	1.13	0.88
1-BUT		11.28	9.86		0.99	0.84
2-BUT		11.52	9.29		1.00	0.77
1-PENT			9.57			0.83
VA	7.58	5.97	5.78	0.74	0.48	0.43
THF	11.82	7.60	5.97	1.13	0.68	0.42
AC	9.06	7.48	7.20	0.75	0.54	0.48
BZ	13.75	8.08	6.79	1.28	0.73	0.55
TOL	13.82	9.21	8.02	1.28	0.86	0.71

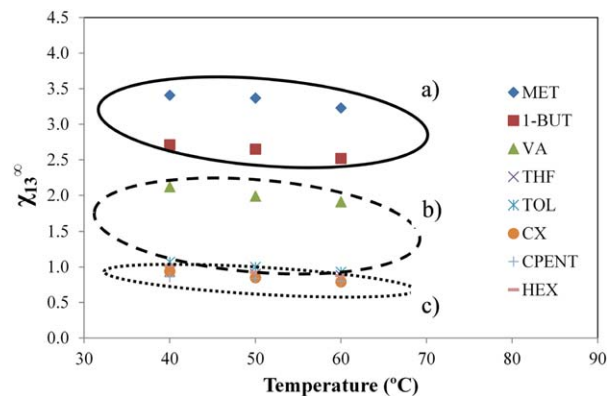


FIG. 5. Flory Huggins parameter vs. T for PE—solvent systems: (a): association solvents (—), (b): polar solvents (—), (c): dispersion solvents (---). [Color figure can be viewed in the online issue, which is available at [wileyonlinelibrary.com](http://www.interscience.wiley.com).]

Solubility Parameters Values

The Hildebrand solubility parameters of the PE and PVAc materials calculated from *Eq. 8* are presented in Table 6. These Hildebrand solubility parameters are derived from the cohesion energy of a compound, which can be related to the vaporization enthalpy. For these reasons and, as it could be expected, they slightly decrease with temperature.

An important point is that the solubility parameter values of PVAc are higher than the ones of PE. This can be justified due to the fact that the polymer cohesion energy strongly depends on the interactions between the polymer chains, so the presence of vinyl acetate groups in PVAc induces stronger interactions. Although for PVAc material the Hansen solubility parameters could be more representative we have calculated the Hildebrand solubility parameters instead to compare the obtained values with previously reported ones, with the aim of assessing the quality of the experimental data.

The importance of Hildebrand solubility parameters is that they are employed, among other criteria, to adequately select a solvent for a given polymer, because the closer the solubility parameters of a polymer and a solvent are, the more compatibility between them. To illustrate this, Table 7 shows the average values of the Hildebrand solubility parameters of the two

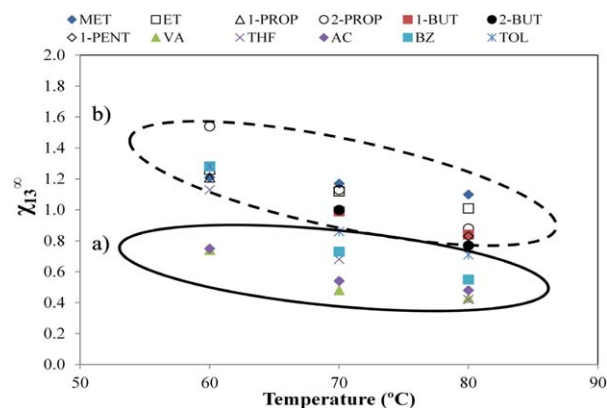


FIG. 6. Flory Huggins parameter vs. T plot for PVAc—solvent systems: (a): association solvents (—), (b): polar solvents (—). [Color figure can be viewed in the online issue, which is available at [wileyonlinelibrary.com](http://www.interscience.wiley.com).]

TABLE 6. Hildebrand solubility parameter values for PE and PVAc.

Temperature (°C)	Solubility parameter (MPa ^{1/2})	
	PE	PVAc
40	15.0	
50	14.4	
60	14.1	19.8
70		19.0
80		18.5

TABLE 7. Difference between the solubility parameter values of the PE and PVAc and the different types of solvents.

Solvent-type	δ_1 (MPa ^{1/2})	δ_3 (MPa ^{1/2})	Abs ($\delta_1 - \delta_3$)
PE			
Association	25.1	14.5	10.6
Polar	18.0		4.3
Dispersion	15.4		0.9
PVAc			
Association	25.1	19.1	6.0
Polar	18.0		1.1

polymeric materials (without considering the temperature dependence, as it is very slight), with the average values for all dispersion-type solvents, for all association-type-solvents and for all polar-type solvents (again without considering the temperature dependence). This table also includes the difference between the average solubility parameter of each polymer and the average solubility parameter of each solvent-type.

As it can be noticed, from the difference between the solubility parameter values of the polymer and the ones of the different kind of solvents, it can be confirmed what previously said: the compatibility order for PE-solvent mixtures tends to be: dispersion solvents > polar solvents > association solvents, while the compatibility order for PVAc-solvents mixtures tends to be: polar solvents > association solvents.

On the other hand, the reported Hildebrand solubility parameters, at the temperature ranges mentioned above, have not been previously published. However, some values of these parameters at high temperatures and also at 25°C can be found in literature

[23–27]. As it can be seen, when plotted together vs. temperature (Fig. 7), a linear pattern is obtained with good regression coefficients; this is logical, because the Hildebrand solubility parameter is intimately related to the enthalpy of vaporization, which is magnitude that depends inversely on temperature.

Enthalpies of Vaporization: Consistency Test

In Table 1 it can be noticed that the difference between the experimental and Watson enthalpy of vaporization values is always lower than 5%. Besides, another important matter is that the experimental solvent enthalpy values derived from PE-solvent systems are very close to the ones derived from PVAc-solvent systems. These two facts can be employed to assess the accuracy of the experimental data because, although the employed temperature range was not exactly the same in both systems and enthalpy of vaporization slightly decreases with temperature, this diminishment can be considered negligible in most of the cases.

CONCLUSIONS

In this article, the sorption parameters, as well as the mass-based solvent activity coefficients and Flory Huggins parameters of polyvinylacetate-solvent and polyethylene-solvent mixtures, have been determined from IGC measurements, to properly characterize the thermodynamic properties of these systems, and to analyze the influence of temperature and the nature of the solvent (association, polar or dispersion) over the Flory Huggins parameters.

According to the obtained values it can be concluded that, in the case of PE-solvent mixtures, the more compatible solvents with this material are dispersion solvents (lower values of solvent activity coefficients and Flory Huggins parameters), followed by polar solvents, being the less compatible the association-type solvents. On the other hand, for PVAc-solvent mixtures it can be concluded that the compatibility order is polar solvents > association solvents and that, in the studied temperature range, it was unreliable to determine thermodynamic parameters for mixtures with dispersion solvents, because no bulk interactions existed.

Regarding the temperature dependence on Flory Huggins parameter, as this parameter decrease with temperature in all cases, the solubility is favored by increasing the temperature.

Finally, from the Hildebrand solubility parameters of both polymers it can be concluded that the higher values of PVAc material are a consequence of the strong interactions of vinyl acetate monomer.

REFERENCES

1. J.A. Brydson, *Plastic Materials*, Elsevier, Oxford (1999).
2. H.Y. Erbil, *Vinyl Acetate Emulsion Polymerization and Copolymerization with Acrylic Monomers*, CRC Press, Boca Raton (2000).
3. C.A. Harper and E.M. Petrie, *Plastic Materials and Processes: A Concise Encyclopedia*, Wiley, New York (2003).
4. J. Camacho, E. Díez, G. Ovejero, and I. Díaz, *J. Appl. Polym. Sci.*, **128**, 481 (2013).
5. E. Díez, J. Camacho, I. Díaz, and G. Ovejero, *Polym. Bull.*, **71**, 193 (2014).
6. P.J. Flory, *J. Chem. Phys.*, **9**, 660 (1941).
7. M.L. Huggins, *Ann. NY Acad. Sci.*, **43**, 1 (1942).

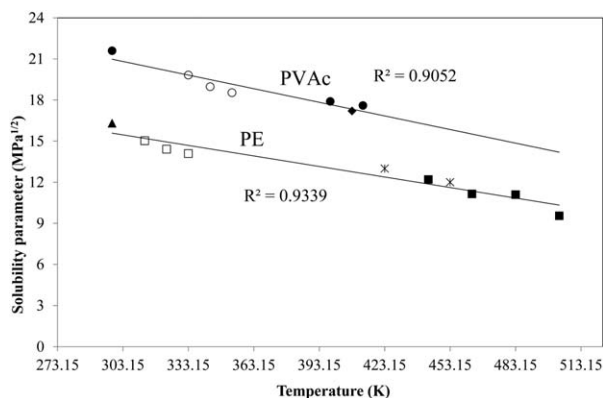


FIG. 7. Hildebrand Solubility Parameter for PE and PVAc (unfilled points: experimentally determined; filled point: literature data, ●, Ref. 23; ◆, Ref. 24; ▲, Ref. 25; *, Ref. 26, ■, Ref. 27).

8. R.F. Blanks and J.M. Prausnitz, *Ind. Eng. Chem. Fundam.*, **3**, 1 (1964).
9. E. Papadopoulou and C.E. Panayiotou, *J. Chromatogr. A*, **1229**, 230 (2012).
10. J.D. Vincent, K. Srinivas, and J.W. King, *J. Am. Oil. Chem. Soc.*, **89**, 1585 (2012).
11. J.R. Conder and C.L. Young, *Physicochemical Measurement by Gas Chromatography*, Wiley, New York (1979).
12. H.G. Rackett, *J. Chem. Eng. Data*, **15**, 514 (1970).
13. C. Tsonopoulos, *AIChE J.*, **20**, 263 (1974).
14. NIST Chemistry WebBook (accessed, December 2013). Available at: <http://webbook.nist.gov/chemistry/>
15. I.H. Romdhane, A. Plana, S. Hwang, and R.P. Danner, *J. Appl. Polym. Sci.*, **45**, 2049 (1992).
16. J.S. Vrentas, C.M. Vrentas, and I.H. Romdhane, *Macromolecules*, **26**, 6670 (1993).
17. K. Ito and J.E. Gillet, *Macromolecules*, **12**, 1163 (1979).
18. K.M. Watson, *Ind. Eng. Chem.*, **35**, 398 (1943).
19. X.M. Shi, J. Zhang, J. Jin, and S.J. Chen, *Polym. Lett.*, **2**, 623 (2008).
20. U. Gaur and B. Wunderlich, *Macromolecules*, **13**, 445 (1980).
21. A.B. Nastasović and A.E. Onjia, *J. Chromatogr. A*, **1195**, 1 (2008).
22. T.J. Hamieh, *J. Polym. Res.*, **18**, 1159 (2011).
23. W. Merk, R.N. Lichtenthaler, and J.M. Prausnitz, *J. Phys. Chem.*, **84**, 1694 (1980).
24. G. DiPaola-Baranyi, J.E. Guillet, J. Klein, and H.W. Jeberien, *J. Chromatogr.*, **166**, 349 (1978).
25. K.G. Hausler, I. Benne, and K. Jobst, *Plaste. Kautsch.*, **29**, 26 (1982).
26. U. Freytag and H.J. Radusch, *Angew. Makromol. Chem.*, **152**, 1 (1987).
27. X. Kong, M.D.L.V. Silveira, L. Zhao, and P. Choi, *Macromolecules*, **35**, 8586 (2002).

2.3 Bulk Polymer / Solvent Interactions for Polyethylene and EVA Copolymers, below their Melting Temperatures

Camacho, J., Díez, E., Ovejero, G. (2015). Bulk Polymer / Solvent Interactions for Polyethylene and EVA Copolymers, below their Melting Temperatures. Submitted for publication.

BULK POLYMER/SOLVENT INTERACTIONS FOR POLYETHYLENE AND EVA COPOLYMERS, BELOW THEIR MELTING TEMPERATURES

Javier Camacho, Eduardo Díez, Gabriel Ovejero*

Grupo de Catálisis y Procesos de Separación (CyPS), Departamento de Ingeniería Química,
Facultad de C. Químicas, Universidad Complutense de Madrid Avda. Complutense s/n, 28040
Madrid, Spain.

ABSTRACT

In this work, the Flory Huggins parameters corresponding to the polymer amorphous phase of a polyethylene (PE) and two ethylene-vinyl acetate (EVA) copolymers (with 18% and 33% vinyl acetate content, respectively) samples, with different solvents have been determined below the melting temperature of the polymers, in order to quantify the bulk interactions of these polymer/solvent systems. The employed solvents were a dispersion solvent (cyclohexane), a polar solvent (vinyl acetate) and an association solvent (methanol).

Initially, the Inverse Gas Chromatography measurements allowed obtaining the retention volumes, activity coefficients and overall Flory Huggins parameters of every polymer/solvent system. According to these parameters, in all cases, the more compatible solvent was cyclohexane, so it was selected as the probe to calculate the percentages of crystallinity at room temperature, whose results were in agreement the literature data (35% for PE, 29% for EVA18, and 12% for EVA33). The percentage of crystallinity allowed determining the amorphous Flory Huggins parameters which are the ones which take into account the bulk interactions in a polymer/solvent mixture.

The Flory Huggins parameter results show that, to accurately study the vapor-liquid equilibrium between a polymer and a solvent (bulk interactions), when the range of studied temperatures is below the melting point of the polymer, it is crucial to calculate the amorphous contribution ($\chi_{\text{amorphous}}$) on the overall Flory Huggins parameter. In the case of this study, the lower the vinyl acetate content (higher crystallinity), the higher the difference between the overall and amorphous Flory Huggins parameters is. Analyzing the interactions between the three polymeric materials and the solvents it can be noticed that, for the most compatible solvent (cyclohexane), $\chi_{\text{amorphous}}$ represents the less contribution, or the highest correction, to the overall Flory Huggins parameter (around 50% for PE and EVA18, and 79% for EVA33, the less crystalline polymer)

KEYWORDS: EVA copolymer, Polyethylene, IGC, Crystallinity, Flory Huggins, amorphous.

*Corresponding author. Tel.: +34-91-394-8509; Fax: +34-91-394-4114.

E-mail address: ediezalc@quim.ucm.es (E. Díez).

1. Introduction

Polyethylene (PE) is one of the most employed polymeric materials due to its wide range of applications. It is a thermoplastic semi-crystalline material which is obtained from ethylene polymerization, and its main applications are in wire and cable isolations, pipes and fittings, film and sheets, housewares or in bottles manufacture [1].

Ethylene-Vinyl Acetate (EVA) copolymer is another polymeric material also widely employed nowadays, due to its different possibilities depending on the vinyl acetate percentage [2], which will determine the final use of the EVA copolymer: when the vinyl acetate content is lower than 30% its main applications are as modifiers, when the vinyl acetate content is between 30% and 40% its main applications are as an elastomer (obtaining synthetic elastomers, tyres,...) and, finally, when the vinyl acetate content is higher than 70%, its main use is in adhesives.

In our research group we are focusing on studying the modelling and simulation of the purification step in a recovery column of the EVA material produced in a dissolution process (generally in methanol, at temperatures around 60 °C [3]), which is an equilibrium-based unit operation. Most of the thermodynamic models employed to analyse the equilibrium involving copolymers (such as EVA) are based on splitting the polymeric material into its homopolymers (polyethylene and polyvinylacetate in this case) to determine the homopolymer - solvent binary interaction parameters, e.g. from the vapor liquid equilibrium, in which the solvent behaves as an absorbed gas in the polymer.

To study these interaction parameters, it is crucial to consider that at temperatures below the melting point of the polymer, both amorphous and crystalline regions are observed in the polymeric sample, and thus both phases have to be taken into account. The sorption of gases in a polymer is a bulk process, as the gas molecules can usually diffuse through the amorphous parts of the polymer sample, so the terms “absorption” or “solubility” are more appropriate than the term “adsorption,” which usually refers to a surface process. On the other hand, the crystalline parts of the polymer, also called “crystallites”, behave as a barrier against the diffusion of the gas molecules in the sample. As a result, it is usually assumed that the gas molecules cannot penetrate the crystallites for steric reasons and only absorb in the amorphous regions. When the polymer is semi-crystalline, the amorphous regions present a liquid like structure and one can apply a theory for fluid phases to describe the thermodynamic properties of the amorphous phase. So, the absorption of gases in semi-crystalline polyethylene can be modeled as a vapor-liquid equilibrium between a gas phase where no polymer molecules are present, and a liquid phase consisting of gas molecules absorbing into an amorphous polymer matrix [4].

It is clear that polyethylene is a semi-crystalline polymer below the melting point, which ranges from about 60 to 140 °C depending on the polyethylene sample. When studying the solubility of gases in polyethylene above the melting point, as the polymer is in an amorphous fluid state it is enough to consider just the vapor-liquid phase equilibrium (bulk interactions). However, below the melting point of the polymer, the phase behavior becomes more complex with equilibrium between vapor, liquid (bulk interactions for amorphous polymer), and solid polymer crystallites phases (surface adsorption). In this case, the solubility of gases (bulk interactions) have been observed to be a function of crystallinity percentage [4].

One of the ways to determine this crystallinity percentage (X_C) is based on comparing the melting enthalpy of the studied polymer with the melting enthalpy of the same polymer 100% crystalline. In the case of the EVA copolymer, because it is a copolymer of polyvinylacetate (100% amorphous) and polyethylene (partially crystalline), the comparison is established between the enthalpy of the copolymer and the melting enthalpy of 100% crystalline polyethylene [5, 6]. However, this procedure must overcome an important drawback which is that in some cases it is not possible to find data of the polymer of interest 100% crystalline [7]. For this reason, a relatively new methodology, based on Inverse Gas Chromatography (IGC) measurements, is being recently employed to determine the crystallinity ratio. Although IGC measurements have been widely employed to study polymer-solvent interactions, its use to determine the crystallinity of a polymeric material is relatively new [8].

According to the IGC theory [9], the retention volume (V_g) of a solvent, once injected and gone through the column, can be calculated from retention time measurements by means of Eq. 1. In this equation, F is the flow rate of the carrier gas corrected to the column temperature (measured at inlet temperature and pressure conditions), t_r is the retention time of the solvent, t_m is the retention time of a reference inert compound, W_s is the amount of polymer packed in the column and j is a correction factor. Due to the carrier gas is compressible, the pressure drop along the column might cause an increase of the volume flow rate in the outlet (P_0) compared with the inlet value (P_i); for this reason, a correction factor (j) is usually added (Eq. 2) [9]. The retention volume data are often expressed in terms of the specific retention volume, Eq (3).

$$V_g = \frac{j \cdot (t_r - t_m) \cdot F}{W_s} \quad (1)$$

$$j = \frac{3 \left(\frac{P_i}{P_0} \right)^2 - 1}{2 \left(\frac{P_i}{P_0} \right)^3 - 1} \quad (2)$$

$$V_g^\circ = V_g \left(\frac{273.15}{T} \right) \quad (3)$$

From the retention volumes data, the percentage of crystallinity (X_C) can be determined with Eq. (4), where $V_{g,\text{sample}}$ is the retention volume of the solute along the curvature line in the crystalline region (above the melting point) and $V_{g,\text{amorphous}}$ is the retention volume of the solute along the extrapolated line of the amorphous region [10].

$$X_C = \left(1 - \frac{V_{g,\text{sample}}}{V_{g,\text{amorphous}}} \right) \cdot 100 \quad (4)$$

The relationship between the mass-based infinite dilution activity coefficient of the solvent, $(\Omega_i)_{\text{IGC}}$, and its retention volume (V_g), in a solvent (1) / polymer (2) mixture, is given by Eq. 5 [9], where T is the temperature in K, R is the ideal gas constant, M_1 is the solvent molecular weight and f_1^0 is the standard fugacity of the solvent. This last parameter is usually determined with the Virial EOS truncated after the second term; so, Eq. 5 is transformed into Eq. 6, where B_{11} is the solvent second term of the Virial EOS, p_1^0 is the solvent vapor pressure and V_1 is the solvent molar volume.

$$\ln(\Omega_1^\infty)_{\text{IGC}} = \ln \left(\frac{R \cdot T}{V_g \cdot M_1 \cdot f_1^0} \right) \quad (5)$$

$$\ln(\Omega_1^\infty)_{\text{IGC}} = \ln \left(\frac{R \cdot T}{V_g \cdot M_1 \cdot p_1^0} \right) - \frac{(B_{11} - V_1) p_1^0}{RT} \quad (6)$$

In this work, molar volumes have been calculated assuming saturated liquid at each temperature, according to a modification of Rackett model which appears in literature [11], the second terms of Virial EOS have been calculated with Tsonopoulos' correlation [12], and the Antoine coefficients of the solvent vapor pressure values have been taken from literature [13].

From the values of infinite dilution activity coefficient, the Flory Huggins interaction parameter (χ) can be calculated by using Eq. 7 [14], where r is the ratio between molar volume of the polymer and the molar volume of the solvent, and ρ_1 and ρ_2 are the solvent and polymer densities, respectively.

$$\chi = \ln(\Omega_1^\infty)_{\text{IGC}} - \left(1 - \frac{1}{r} \right) + \ln \frac{\rho_1}{\rho_2} \quad (7)$$

As discussed above, below the melting temperature, the contribution of the crystalline part of the polymer to the interaction with the solvent is not really due to the establishment of equilibrium, but due to the bulk interactions (amorphous polymer) and plus the surface adsorption (polymer crystallites) of the solvent [4]. For this reason, to properly analyze the equilibrium which is established between a semi-crystalline polymer and a solvent, it is necessary determine the Flory Huggins parameter considering only $V_{g,\text{amorphous}}$ rather than $V_{g,\text{sample}}$.

$V_{g,\text{amorphous}}$ can be calculated with Eq. 1 but employing, instead of W_s , $W_{s,\text{amorphous}}$, which is the amount of amorphous polymer packed in the column. Considering that $W_{s,\text{amorphous}}$ can be calculated with Eq.8, $V_{g,\text{amorphous}}$ corresponds to Eq. 9.

$$W_{s,\text{amorphous}} = W_s \cdot (1 - X_c) \quad (8)$$

$$V_{g,\text{amorphous}} = \frac{j \cdot (t_r - t_m) \cdot F}{W_s \cdot (1 - X_c)} \quad (9)$$

From Eq.1 and Eq.8, the following relationship can be establish between $V_{g,\text{amorphous}}$ and $V_{g,\text{sample}}$ (Eq. 10):

$$V_{g,\text{amorphous}} = \frac{V_{g,\text{sample}}}{1 - X_c} \quad (10)$$

Finally, substituting Eq.10 into Eqs.6 and 7, and considering that the density of the amorphous part of the polymer is equal to the density of the polymer itself (ρ_2), it is possible to establish a relationship between the overall Flory Huggins parameter (χ) and the Flory Huggins parameter considering only the amorphous part of the polymer ($\chi_{\text{amorphous}}$), Eq.11.

$$\chi_{amorphous} = \chi + \ln(1 - X_c) \quad (11)$$

The aim of this paper is to calculate the percentage of crystallinity at room temperature, of two EVA copolymers, and a Polyethylene sample employing the IGC procedure. From these values the Flory Huggins parameters will be evaluated, considering only the amorphous contribution of the polymer (bulk interactions). These parameters have been demonstrated to be extremely useful for further predictions related to the polymers/solvent vapor- liquid equilibrium.

2. Experimental section

2.1. Materials

Two EVA copolymers were supplied by REPSOL-YPF Company, EVA18 and EVA33 (commercially named EVA410 and EVA460, respectively). While EVA18 has a vinyl acetate content of 18% (w/w), EVA33 has a vinyl acetate content of 33% (w/w). The weight-average molecular weight and the number-average molecular weight are 42,460 and 14,008 for EVA18 and 61,041 and 18,582 for EVA33, determined by gel exclusion chromatography. The densities of the two polymeric materials are 937 kg/m³ and 956 kg/m³ respectively as reported by supplier [15].

Low density polyethylene (PE) was purchased from Sigma Aldrich Company. The weight-average molecular weight and the density reported by supplier are 35.000 and 906 kg/m³, respectively.

The employed solvents were cyclohexane (CX), methanol (MET) and vinyl acetate (VA). Every one belongs to a different solvent type: dispersion, association and polar, respectively. They were also purchased from Aldrich and used directly, without any purification step.

2.2. Polymer thermal analysis

The Differential Scanning Calorimetry (DSC) analysis of each polymeric material was performed with a Seiko EXSTAR 6000 DSC 6200 equipment. Polymer samples were first heated up to 150°C at a heating rate of 10 °C.min⁻¹ and kept at 150°C for 5 minutes. Then they were cooled down from 150 °C to 0 °C at the rate of 20 °C.min⁻¹ to obtain the non-isothermal crystallization curves. Finally, the re-melting was finished by second heating run from 0 °C to 150 °C at 10 °C.min⁻¹. Melting Temperatures (T_m) were calculated from the minimum value of the peak of the corresponding curve.

2.3. Inverse Gas Chromatography determination

The necessary stationary phases employed in this work were prepared by dissolving a weighted sample of each polymer (PE and EVA18 in hot tetrahydrofuran, and EVA33 in cyclohexane) and depositing each solution on a weighted amount of support (Chromosorb W/AW-DMCS 80-100 mesh).

Once dissolved, each mixture was allowed to dry by slow evaporation in a rotavapor under vacuum, while being stirred to ensure homogeneous mixture; evaporation time was at less 8 h. The final amount of each polymer deposited in the support was determined by thermogravimetric analysis on a Perkin Elmer STA 6000 equipment. Each analysis was performed three times, and the average value was selected in each case. The obtained coatings were 15.78 ± 0.10 % (w/w) for PE, 11.28% (w/w) for EVA18 and 11.45% (w/w) for EVA33.

Afterwards, each coated support was packed into a ¼ in. nominal diameter and 2.00 m length column. Each of them was installed in a VARIAN 3800 gas chromatography, equipped with a thermal conductivity detector and an electronic flow controller.

All the measurements were carried out with a 40 mL.min⁻¹ helium flow, as a carrier gas, and air, as an inert component. The temperature ranges were around from 40 °C to 140 °C, depending of the melting point of each polymer.

3. Results and discussion

3.1. Polymer thermal analysis

Figure 1 shows the DSC melting curves of PE and both EVA copolymers, after the non-isothermal crystallization process.

The main thermal characteristic of the semi-crystalline polymers is that they have both Glass Transition Temperature (T_g) and Melting Temperature (T_m). From the minimum peak of the corresponding curve it can be determined that T_m of PE is 93.2 °C, T_m of EVA18 is 83.4 °C and T_m of EVA33 is 63.7 °C. As it can be noticed, the lower the vinyl acetate content, the higher the melting temperature, as the material is closer to the correspondent homopolymer, polyethylene. In the studied temperature range the jump interval corresponding to the Glass Transition Temperature was not observed for any material as, in all cases, this value is less than 0 °C from the polymer samples [16, 17].

3.2. Retention Volumes

Figures 2, 3 and 4 show the retention diagrams (natural logarithmic of the specific retention volumes vs the inverse of temperature) for PE/solvents, EVA18/solvents and EVA33/solvents systems. It can be observed that the less compatible solvent was methanol (association solvent), because its overall retention volume is the lowest. This feature was expected because methanol was the fastest out solvent in the IGC experiments. Vinyl acetate (polar solvent) was medium compatible solvent, and the best solvent –the latest out- was cyclohexane (dispersion solvent). This behavior was expected as semi-crystalline polyethylene is a dispersion polymer, and both EVA copolymers are constituted by a dispersion homopolymer and a polar homopolymer.

Another important feature observed in these Figures is the higher the vinyl acetate content in the polymer (0% in polyethylene, 18% in EVA18 and 33% in EVA33) the lower the total retention volumes. This means that the more vinyl acetate content in the polymer, the more favorable the interactions with the solvents are (in this case for the EVA33).

To determine the crystallinity of the polymeric materials, cyclohexane was selected as probe according to literature (the solvent with strong interactions must be selected to measure the crystallinity [18]). Thus, for each cyclohexane/polymer system, the retention volumes below the polymer melting temperature were linearly extrapolated to temperatures above this melting point, as described in the introduction, to obtain $V_{g,amorphous}$. These linear extrapolations were carried out beginning from the highest temperature studied in each case until the interval in which the melting temperature determining by the DSC analysis is located. These intervals were 90 °C to 100 °C ($T_m = 93.2$ °C) for PE, 80 °C to 90 °C for EVA18 ($T_m = 83.4$ °C), and 60 °C to 70 °C for EVA33 ($T_m = 63.7$ °C). The linear extrapolations showed in the three cases high correlation coefficients (≈ 0.999).

From these extrapolations it can be observed that the more vinyl acetate content in the polymer, the smaller the differences between the overall retentions volumes (V_g) and the linear extrapolated amorphous retention volumes ($V_{g,amorphous}$) are. This means that when the vinyl acetate content in the copolymer is around 40%, it could be considered totally amorphous and, therefore, from this percentage to higher values, the contributions of the interactions of the crystallites will be almost negligible.

Figures 5, plots the percentages of crystallinity (calculated from Eq. 10 from the mixtures of the polymers with cyclohexane) vs temperature. As it can be observed, the three curves tend to stabilize at room temperature, in constant values, reported in Table 1. As it was expected, increasing the vinyl acetate content (lowering the content of ethylene chains, the provider of the semi-crystalline character), implies diminishing the crystallinity degree.

A value of the percentage of crystallinity of the polyethylene employed in this work can be found in literature [19, 20], where it can be seen a relationship between this percentage and the vinyl acetate content (Eq. 12) for the EVA copolymers:

$$\% X_{C_{EVA}} = -1.034(\% VA_{EVA}) + 47.638 \quad (12)$$

The percentages of crystallinity of the literature data for all the polymers, also shown in Table 1, are in agreement with the experimental values obtained in this work.

3.3. Solvent activity coefficients and Flory Huggins parameters

Tables 2, 3 and 4, show the calculated values of the mass-based infinite dilution solvent activity coefficients, $(\Omega_i^\infty)_{IGC}$, (Eq. 6) and the overall Flory Huggins interaction parameters, χ , (Eq. 7) for the binary mixtures of the three polymeric materials with the different solvents. From these overall parameters, with the experimental percentage of crystallinity reported in Table 1, and employing Eq. 11, the Flory Huggins interaction parameters corresponding to the amorphous phase ($\chi_{amorphous}$), were calculated and also reported in these Tables.

Figures 6, 7 and 8 present the trends of the overall and amorphous Flory Huggins parameters, plotted versus temperature. It can be observed the expected best interactions for the cyclohexane probe, due this solvent presents the lowest overall Flory Huggins parameters (and the mass-based infinite dilution solvent activity coefficients), following by vinyl acetate, and finally methanol. These overall and amorphous Flory Huggins parameters, are plotted together with

overall Flory Huggins parameters previously reported in literature [21, 22], showing highly satisfactory agreement.

From these Figures it can be concluded that, when the range of analysis corresponds to temperatures below the melting temperature of the polymer, it is highly important to determine the amorphous Flory Huggins parameters to achieve accurate predictions of vapor-liquid equilibrium between a polymer and a solvent (bulk interactions). In the particular case of this paper it can be observed that below the melting point of the studied polymers, the lower the vinyl acetate content of the polymer (higher crystallinity) is, the higher is the difference between the overall and amorphous Flory Huggins parameters.

Table 5 shows the percentage of the overall Flory Huggins parameter that corresponds to $\chi_{\text{amorphous}}$, at 40 °C and for all the polymer/solvent systems studied in this work. It can be noticed that for the most compatible solvent (cyclohexane) this percentage represents the less contribution or the highest correction to the overall Flory Huggins parameter (ranging from 48% to 79%), following by the medium compatible solvent (vinyl acetate, ranging from 75% to 87%) and finally by the worst solvent (methanol, around 91%).

In addition, analyzing the interactions for the best solvent (cyclohexane), it can be observed that, to determine the appropriate interactions (bulk interactions corresponding to the amorphous region of the polymer) for PE/cyclohexane and EVA18/cyclohexane systems it is necessary to consider that $\chi_{\text{amorphous}}$ represents approximately the 50% of the overall Flory Huggins parameter, while for the very low crystallinity polymer (EVA 460) $\chi_{\text{amorphous}}$ represents the 79%.

4. Conclusions

In this work, the bulk interactions of a polyethylene material and two EVA copolymers (EVA18, with 18% vinyl acetate content, and EVA33, with 33% vinyl acetate content) with different solvents (cyclohexane, vinyl acetate and methanol) have been quantified below the melting temperatures of the polymeric samples.

From the obtained results it can be concluded that, in all cases, the less compatible solvent was methanol (association solvent), following by vinyl acetate (polar solvent), and the best solvent was cyclohexane (dispersion solvent). This behavior was expected as semi-crystalline polyethylene is a dispersion polymer, and both EVA copolymers are constituted by a dispersion homopolymer and a polar homopolymer. On the other hand, it can also be concluded that the higher the vinyl acetate content in the polymer is (0% in polyethylene, 18% in EVA18 and 33% in EVA33), the more favorable the interactions with the solvents are (this implies lower retention volumes, mass-based infinite dilution solvent activity coefficients and overall Flory Huggins parameter).

The percentage of crystallinity at room temperature, determined from the interactions of the polymeric materials with the best solvent (cyclohexane) was 35% for polyethylene, 29% for EVA18 and 12% for EVA33, which are in agreement with the literature data. Increasing the vinyl acetate content in the polymer, implies diminishing the crystallinity degree.

Finally, from the Flory Huggins parameter results it can be concluded that, in order to obtain accurate predictions of vapor-liquid equilibrium between a polymer and a solvent (bulk

interactions), it is extremely important to calculate the amorphous contribution of the overall Flory Huggins parameter determined by IGC, when the range of studied temperatures is below the melting point of the polymer. In the case of this study, the lower the vinyl acetate content (higher crystallinity), the higher the difference between the overall and amorphous Flory Huggins parameters is. Analyzing the interactions between the three polymeric materials and the solvents, it can be noticed that, for the best solvent (cyclohexane) $\chi_{\text{amorphous}}$ represents the less contribution or the highest correction to the overall Flory Huggins parameter (around 50% for PE and EVA18, and 79% for EVA33, the less crystalline polymer), following by the medium compatible solvent (vinyl acetate) and finally by the worst solvent (methanol). These last two percentages were, in average, around 80% and 91%, with less dispersion among the values for the three polymers.

Literature cited

1. Chanda M, Roy SK (2008) Industrial polymers, specialty polymers, and their applications, vol 74. CRC Press, Boca Raton.
2. Harper CA, Petrie EM (2003) Plastic Materials and Processes: a concise encyclopedia. Wiley, New York.
3. Kawahara T, Hikasa T (2005) U.S. Patent No. 6,838,517. U.S. Patent and Trademark Office, Washington DC.
4. Paricaud P, Galindo A, Jackson G (2004) Modeling the cloud curves and the solubility of gases in amorphous and semicrystalline polyethylene with the SAFT-VR approach and Flory theory of crystallization. *Ind Eng Chem Res* 43(21): 6871-6889.
5. Mathot VBF, Pijpers FJ (1983) Heat capacity, enthalpy and crystallinity for a linear polyethylene obtained by DSC. *J Therm Anal Calorim* 28(1): 349-358.
6. Shi XM, Zhang J, Jin J, Chen SJ (2008) Non-isothermal crystallization and melting of ethylene-vinyl acetate copolymers with different vinyl acetate contents. *Express Polym Lett* 2(9): 623-629.
7. Brandrup J, Immergut EH, Abe A, Bloch DR (Eds.) (1999) Polymer handbook, vol. 89. Wiley, New York.
8. Yazici O, Cakar F, Cankurtaran O, Karaman F (2009) Determination of Crystallinity Ratio and Some Physicochemical Properties of Poly(4-methyl-1-pentene). *J App Polym Sci* 113: 901-906.
9. Conder JR, Young CL (1979) Physicochemical Measurement by Gas Chromatography. Wiley, New York.
10. Al-Ghamdi A, Melibari M, Al-Saigh ZY (2005) Characterization of Environmentally Friendly Polymers by Inverse Gas Chromatography: I Amylopectin. *J Polym Environ* 13(4): 319-327.
11. Rackett HG (1970) Equation of state for saturated liquids. *J Chem Eng Data* 15(4): 514-517.

12. Tsonopoulos C (1975) An empirical correlation of second virial coefficients. *AIChE J* 20(2): 263-272.
13. NIST Chemistry WebBook (accessed, July 2015) <http://webbook.nist.gov/chemistry/>
14. Romdhane IH, Plana A, Hwang S, Danner RP (1992) Thermodynamic interactions of solvents with styrene–butadiene–styrene triblock copolymers. *J Appl Polym Sci* 45(11): 2049-2056.
15. REPSOL-YPF catalogue (accessed, July 2015). <http://www.repsol.com/sa/herramientas/CatalogoQuimica/CatalogoQuimica.aspx>
16. Gaur U, Wunderlich B (1980) The glass transition temperature of polyethylene. *Macromolecules* 13(2): 445-446.
17. Sung YT, Kum CK, Lee HS, Kim JS, Yoon HG, Kim WN (2005) Effects of crystallinity and crosslinking on the thermal and rheological properties of ethylene vinyl acetate copolymer. *Polymer* 46(25): 11844-11848.
18. Chen CT, Al-Saigh ZY (1989) Characterization of semicrystalline polymers by inverse gas chromatography. 1. Poly (vinylidene fluoride). *Macromolecules* 22(7): 2974-2981.
19. Bieliński DM, Tranchida D, Lipiński P, Jagielski J, Turos A (2007) Ion bombardment of polyethylene—influence of polymer structure. *Vacuum* 81(10): 1256-1260.
20. K. Anderson, Crystallinity and its impact on ethylene vinyl acetate copolymers (accessed, July 2015) <http://www.vitaldose.com/blog/crystallinity-and-its-impact-on-ethylene-vinyl-acetate-copolymers/>. VitalDose Blog (2012).
21. Camacho J, Díez E, Ovejero G, Gómez L (2015) Inverse gas chromatography study of polyvinylacetate - solvent and polyethylene - solvent systems . *Polym. Eng. Sci.* In press DOI: 10.1002/pen.24189.
22. Camacho J, Díez E, Ovejero G, Díaz I (2013) Thermodynamic interactions of EVA copolymer solvent systems by inverse gas chromatography measurements. *J Appl Polym Sci* 128: 481-486.

Figure captions

FIGURE 1. DSC melting curves for PE and EVA materials

FIGURE 2. $\ln(V_g)$ vs T^{-1} plot for PE/solvent systems

FIGURE 3. $\ln(V_g)$ vs T^{-1} plot for EVA18/solvent systems

FIGURE 4. $\ln(V_g)$ vs T^{-1} plot for EVA33/solvent systems

FIGURE 5. %Crystallinity vs Temperature for PE and EVA materials

FIGURE 6. Overall and amorphous Flory Huggins parameters for PE/solvent systems

FIGURE 7. Overall and amorphous Flory Huggins parameters for EVA18/solvent systems

FIGURE 8. Overall and amorphous Flory Huggins parameters EVA33/solvent systems

Tables

TABLE 1. Percentage of crystallinity of the polymeric materials determined by IGC, extrapolated at room temperature, and comparison with literature values (ref 19 for PE and ref. 20 for EVA18 and EVA33)

	PE	EVA18	EVA33
% X _c (extrap.)	≈ 36	≈ 29	≈ 12
% X _c (lit.)	32.00	29.07	13.56

TABLE 2. Mass-based infinite dilution solvent activity coefficients (Ω_∞), overall (χ) and amorphous (χ_a) Flory Huggins interaction parameters, for PE/solvent mixtures

T (°C)	Ω_∞ CH	χ CH	χ_a CH	Ω_∞ MET	χ MET	χ_a MET	Ω_∞ VA	χ VA	χ_a VA
40	7.56	0.85	0.40	105.15	3.50	3.06	21.85	2.09	1.64
50	7.38	0.81	0.37	102.35	3.46	3.02	20.39	2.01	1.56
60	6.98	0.74	0.34	93.48	3.36	2.95	18.56	1.90	1.49
70	6.36	0.64	0.32	83.97	3.23	2.91	17.13	1.80	1.48
80	5.82	0.54	0.30	76.71	3.13	2.89	15.64	1.69	1.45
90	5.27	0.42	0.28	65.14	2.95	2.81	13.43	1.52	1.39
100	4.63	0.28	0.28	53.55	2.74	2.74	11.40	1.34	1.34
110	4.62	0.26	0.26	49.52	2.64	2.64	11.17	1.30	1.30
120	4.74	0.27	0.27	46.85	2.57	2.57	10.57	1.23	1.23
130	4.82	0.27	0.27	45.06	2.51	2.51	10.59	1.21	1.21

TABLE 3. Mass-based infinite dilution solvent activity coefficients (Ω_∞), overall (χ) and amorphous (χ_a) Flory Huggins interaction parameters, for EVA18/solvent mixtures

T (°C)	Ω_∞ CH	χ CH	χ_a CH	Ω_∞ MET	χ MET	χ_a MET	Ω_∞ VA	χ VA	χ_a VA
40	7.05	0.75	0.40	75.06	3.13	2.78	11.05	1.37	1.02
50	6.64	0.67	0.36	66.76	3.00	2.69	10.48	1.31	0.99
60	6.03	0.56	0.33	60.16	2.88	2.65	10.05	1.25	1.01
70	5.51	0.46	0.30	56.53	2.80	2.65	9.41	1.17	1.01
80	5.00	0.35	0.29	49.56	2.66	2.59	8.74	1.08	1.01
90	4.71	0.28	0.28	45.38	2.55	2.55	7.95	0.97	0.97
100	4.66	0.25	0.25	42.07	2.46	2.46	7.98	0.95	0.95
110	4.77	0.26	0.26	38.73	2.36	2.36	7.91	0.93	0.93

TABLE 4. Mass-based infinite dilution solvent activity coefficients (Ω_∞), overall (χ) and amorphous (χ_a) Flory Huggins interaction parameters, for EVA33/solvent mixtures

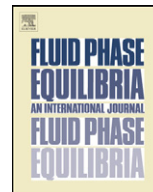
T (°C)	Ω_∞ CH	χ CH	χ_a CH	Ω_∞ MET	χ MET	χ_a MET	Ω_∞ VA	χ VA	χ_a VA
40	5.64	0.50	0.39	39.42	2.50	2.39	6.64	0.84	0.73
50	5.46	0.46	0.37	37.68	2.41	2.32	6.56	0.82	0.73
60	5.27	0.41	0.35	35.61	2.34	2.27	6.52	0.80	0.73
70	4.96	0.33	0.33	32.60	2.23	2.23	6.23	0.73	0.73
80	4.95	0.32	0.32	31.32	2.18	2.18	6.36	0.74	0.74
90	4.98	0.31	0.31	29.65	2.11	2.11	6.40	0.73	0.73
100	5.09	0.32	0.32	27.79	2.03	2.03	6.33	0.70	0.70

TABLE 5. Percentage of the overall Flory Huggins parameter that corresponds to $\chi_{\text{amorphous}}$, at 40 °C

	CH	MET	VA
PE	47.6	87.3	78.7
EVA18	53.3	88.9	74.7
EVA33	78.5	95.7	87.2

2.4 Comparison between three predictive methods for the calculation of polymer solubility parameters

Díaz, I., Díez, E., Camacho, J., León, S., & Ovejero, G. (2013). Comparison between three predictive methods for the calculation of polymer solubility parameters. *Fluid Phase Equilibria*, 337, 6-10.



Comparison between three predictive methods for the calculation of polymer solubility parameters

Ismael Díaz^{b,*}, Eduardo Díez^a, Javier Camacho^a, Salvador León^b, Gabriel Ovejero^a

^a Grupo de Catálisis y Procesos de Separación (CyPS), Departamento de Ingeniería Química, Facultad de C. Químicas, Universidad Complutense de Madrid, Avda. Complutense s/n, 28040 Madrid, Spain

^b Departamento de Ingeniería Química Industrial y del Medio Ambiente, Escuela Técnica Superior de Ingenieros Industriales, Universidad Politécnica de Madrid, C/José Gutiérrez Abascal 2, 28006 Madrid, Spain

ARTICLE INFO

Article history:

Received 20 June 2012

Received in revised form

18 September 2012

Accepted 21 September 2012

Available online 28 September 2012

Keywords:

Molecular dynamics

COSMO-SAC

Group contribution

Polymer

Bisphenol-A polycarbonate

Ethylene-co-vinyl acetate

Polyvinyl alcohol

ABSTRACT

Solubility parameters (SP) of three polymers have been estimated and compared with both experimental values. The methods employed for the estimation are: traditional group contribution procedures (Fedors and van Krevelen), molecular dynamics simulation to calculate cohesive energy density and extension of the COSMO-SAC thermodynamic model to polymer mixtures. The aim of the paper is accurately predicted polymer solubility parameters showing differences between methods. Selected polymers have been polyvinyl alcohol (PVA), ethylene-co-vinyl acetate (EVA) and bisphenol-A polycarbonate (PC).

© 2012 Elsevier B.V. All rights reserved.

1. Introduction

Polymer materials are extremely important in current way of life; adhesives, pipes, wrappings or multimedia devices are examples of items that are mainly composed of polymer materials, widely produced all around the world [1]. Therefore, polymer processing has been an important research topic in the last decades.

Many of the steps involved in polymer production processes are equilibrium staged steps, such as steam stripping or solvent devolatilization; this makes polymer–solvent compatibility a key aspect to accurately model these processes. In fact, the behaviour of the polymer is very important to be properly analyzed because, in many cases, it determines the design of the separation steps. However, polymer solution properties are quite different from conventional mixtures and they require using specific thermodynamics models. Historically, the most widely employed model has been the well-known Flory–Huggins [2,3] model, based on the determination of the so-called Flory–Huggins interaction parameter, χ_{12} , that accounts for the compatibility of component 1 (solvent) and 2 (polymer). From the regular solution theory developed by

Hildebrand [4,5] χ_{12} can be related to the solubility parameters of both components by the simple expression:

$$\chi_{12} = \frac{V_1}{RT}(\delta_1 - \delta_2)^2 \quad (1)$$

Solubility parameters can be calculated, following regular solution theory, from the values of cohesive energy density, c (energy to separate molecules in the condensed phase):

$$\delta_1 = \sqrt{c} = \sqrt{\frac{\Delta H_{1,v} - RT}{V_1}} \quad (2)$$

where $\Delta H_{1,v}$ is the vaporization energy. Later on, with Eq. (1), the value of χ_{12} can be determined from the molar volume of the solvent (V_1) and the solubility parameter of the pure components. This implies that the value of the interaction parameter χ_{12} of a polymer-containing mixture can be easily determined for a wide range of solvents if the value of the polymer solubility parameter is known.

Many efforts have been made to develop both experimental techniques and prediction methodologies. Among the first ones, the most important techniques are swelling [6], inverse gas chromatography [7,8] or intrinsic viscosity [9] measurements. Among the prediction methods, van Krevelen [10] and Fedors [11,12] developed both group contribution methods that are widely employed

* Corresponding author. Tel.: +34 91 336 5341; fax: +34 91 394 4114.
E-mail address: idadiaz@quim.ucm.es (I. Díaz).

nowadays. The main drawbacks of these methods are the lack of information regarding some contribution groups which appear in special (novel) polymers, or the fact that they predict the same solubility parameter independently of the chain structure (isomers, radial structures, branched polymers, etc.). As a consequence, other methodologies are drawing attention and interest of researchers. One of the theories which has shown very promising results in the modelling of fluid phase equilibrium is the one developed by Klamt et al. resulting in the so-called COSMO-based models [13,14]. The main models belonging to this group are the COSMO-RS model [15,16], and its re-implementations, such as the COSMO-SAC model of Lin and Sandler [17,18], and the equation-of-state derived models, such as NRCOSMO [19]. The prevailing picture in these COSMO-based models is that the solvated molecules in the solution interact with their neighbours through segment contacts. Interaction energy is then obtained by calculating the energy of all the possible contacts from the difference in charge density of both contacting segments. Although these models were not initially developed to deal with polymers, a new promising strategy has been proposed by Yang et al. [20] to use COSMO-SAC to predict polymer solution VLE (see below). The last option existing in literature to estimate polymer solubility parameters is molecular dynamics, as reported by Belmares et al. [21]. By estimating the difference of energy in the amorphous phase and the energy of the same molecules infinitely separated, cohesive energy can be determined and, with Eq. (2), solubility parameter can be calculated. Thus, the final object of the paper is to study the suitability of different modern methodologies to calculate polymer solubility parameters, as an alternative to the widely employed group contribution methods.

2. Computational details

2.1. COSMO-SAC

The implementation of COSMO-SAC model to polymer solution modelling has been developed following the work of Yang et al. [20]. The basic equations of COSMO-SAC model are:

$$\ln \gamma_i = n_i \sum_{\sigma_m} p_i(\sigma_m) [\ln \Gamma_i(\sigma_m) - \ln \Gamma_i(\sigma_m)^G] + \ln \gamma_i^{SG} \quad (3)$$

$$\ln \Gamma_i(\sigma_m) = -\ln \left\{ \sum_{\sigma_n} p_i(\sigma_n) \Gamma_i(\sigma_n) \exp \left[\frac{-\Delta W(\sigma_m, \sigma_n)}{RT} \right] \right\} \quad (4)$$

$$\ln \Gamma_s(\sigma_m) = -\ln \left\{ \sum_{\sigma_n} p_s(\sigma_n) \Gamma_s(\sigma_n) \exp \left[\frac{-\Delta W(\sigma_m, \sigma_n)}{RT} \right] \right\} \quad (5)$$

where $p_i(\sigma_n)$ and $p_s(\sigma_n)$ are the probability of finding a segment with a surface charge density σ_n in pure liquid i and in solution, respectively. The term $\ln \gamma_i^{SG}$ is the entropic contribution to the activity coefficient following Staverman–Guggenheim theory, as proposed in the original COSMO-SAC model [18]. Finally, the term $\Delta W(\sigma_m, \sigma_n) = E_{\text{pair}}(\sigma_m, \sigma_n) - E_{\text{pair}}(0, 0)$, called exchange energy, is the energy required to obtain a pair $E_{\text{pair}}(\sigma_m, \sigma_n)$ from a neutral pair. From the equations above, it can be deduced that the most important properties are the charge density and the probability of finding segments $p(\sigma)$.

To implement COSMO-SAC, the structures of both compounds are required, in order to divide them and to calculate the size, number and type of segments involved (details are described in [18]). The next stage will be to calculate the charge density of all segments and the probability of finding them. This is the most important step, which will result in the so-called sigma profile, which is the relation between σ and $p(\sigma)$ for each molecule. As $\Delta W(\sigma_m, \sigma_n) = f(\sigma_m,$

$\sigma_n)$ we will be able to solve the set of equations, with the aim of obtaining $\Gamma_i(\sigma_m)$ and $\Gamma_s(\sigma_m)$ values and, finally, $\ln \gamma_i$. So the key step is obtaining the sigma profile, and this is the sticking point to be solved in the case of polymer solutions. Conventionally, this sigma profile is determined from quantum chemical calculations, by obtaining the charge distribution in the molecule. A huge database of sigma profiles is available as well as a detailed guide to obtain them from Mullins et al. [22]. However, getting the sigma profile of polymers is not so easy because they are large molecules with a great amount of atoms and geometries that make quantum chemical software unable to work with them. To overcome this problem, Yang et al. [20], propose to characterize the sigma profile of the repeating unit, and extrapolate it to the final polymer. They suggest calculating the sigma profile of the oligomers with 2, 3, ..., 10 repeating units so that the difference of the sigma profiles of the neighbouring oligomers is assumed to be the sigma profile of the repeating unit. This is done for all the neighbouring multimers and averaged to obtain the final sigma profile of the repeating unit. Finally, it is necessary to calculate two parameters for the final polymer: the cavity surface area ($A_{\text{pol}}^{\text{COSMO}}$) and the cavity volume ($V_{\text{pol}}^{\text{COSMO}}$). They can be obtained from the values of the repeating unit along with the number of repeating units presented in the final polymer:

$$A_{\text{pol}}^{\text{COSMO}} = N_{\text{unit}} \cdot A_{\text{unit}}^{\text{COSMO}} \quad (6)$$

$$V_{\text{pol}}^{\text{COSMO}} = N_{\text{unit}} \cdot V_{\text{unit}}^{\text{COSMO}} \quad (7)$$

Obtaining sigma profiles has been made following the recommendations of Mullins et al. [22]. Calculations were made by using Dmol3 [23] package Accelrys Software Inc. with the VWN-BP functional at the DNP basis set level.

Once activity coefficients were calculated for some polymer–solvent (methanol, ethanol, 2-propanol, 1-butanol, 2-butanol, pentanol, hexanol and cyclohexanol) pairs, at very low solvent compositions, these values were fitted to the Flory–Huggins model in order to obtain the value of χ_{12} using the equation:

$$\ln(a_1) = \ln(x_1 \cdot \gamma_1) = \ln(1 - \phi_2) + \left(1 - \frac{1}{r}\right) \phi_2 + \chi_{12} \phi_2^2 \quad (8)$$

where ϕ_2 is the polymer volume fraction and r is the chain segment number (polymer volume to solvent volume ratio). Thus we could calculate χ_{12} for a set of polymer–solvent pairs with solvents of known solubility parameter. Finally, if Eq. (3) is rearranged as:

$$\chi_{12} = \frac{V_1}{RT} (\delta_1 - \delta_2)^2 \rightarrow \left(\frac{\delta_1^2}{2} - \frac{\chi_{12} RT}{2V_1} \right) = \delta_2 \delta_1 - \left(\frac{\delta_2^2}{2} \right) \quad (9)$$

The polymer solubility parameter can be determined from the slope of $((\delta_1^2/2) - (\chi_{12} RT/2V_1))$ vs δ_1 by simply knowing the solubility parameter of the solvent [24].

2.2. Molecular dynamics

Solubility parameter is defined by Eq. (4) as the root square of the cohesive energy density (CED), c . This is the energy that is required to completely remove intermolecular forces, namely infinitely separation of molecules from a condensed phase to an ideal gas state. CED can be estimated by molecular dynamics by using Forcite module contained in Materials Studio software [25].

To carry out this firstly it is necessary to build the polymer chains and to introduce some of them in a box under periodic boundary conditions (unit cell dimension are fixed attending to density values of the polymer amorphous phase). Cell equilibration is required to properly compute equilibrium energies. Finally, molecular dynamics NVT calculations were carried out at 298 K using Andersen thermostat with a time step of 1 fs. Different simulation conditions

have been compared in order to determine the optimal computational procedure. In particular, different number of monomer units per chain, number of molecules per box, simulation times, and force-fields have been considered. The specific simulation conditions employed are detailed in Sections 4.1.1–4.1.3. At the end, solubility parameters are calculated as [21]:

$$\delta_k^2 = \left(\sum_{i=1}^n \frac{\langle E_i^k - E_c^k \rangle}{N_0 \langle V_c / n \rangle} \right) \quad (10)$$

where $\langle \rangle$ indicates time average, n is the number of molecules, $k = 1, 2, 3$ for Coulomb (polar), van der Waals (dispersion) and hydrogen bond components respectively. N_0 is Avogadro's number, E_c^k is the potential energy components of the condensed phase simulation single unit cell and E_i^k is the potential energy components of individual molecules.

2.3. Group contribution

Fedors [11,12] and van Krevelen [27] calculation methods for solubility parameter were carried out by implemented on Synthia module of the Materials Studio software.

3. Experimental and bibliographic values of solubility parameters

Three different polymers were studied in order to explore diverse chemical natures: a rigid homopolymer (PC), a flexible homopolymer (PVA), and a random copolymer (EVA). The first polymer studied was bisphenol A polycarbonate (PC), with a molecular weight of 17,500 (density 1.2 g/cm³) whose solubility parameter is 20.1 MPa^{0.5} [28]. Next polymer taken into account was polyvinyl alcohol (molecular weight 130,000, fully dehydrated); the experimental value of their solubility parameter (27.9 MPa^{0.5}) and density (1.365 g/cm³) were obtained by Hg intrusion porosimetry and inverse gas chromatography measurements, carried out by our group [29]. The last studied polymer was a random copolymer of both ethylene and vinyl acetate monomers (molecular weight 61,000, 31.5% vinyl acetate content and density 0.956 g/cm³). Its solubility parameter (17.2 MPa^{0.5}) was also obtained by inverse gas chromatography measurements.

4. Results and discussion

4.1. Molecular dynamics results

4.1.1. Influence of number of repeating unit, simulation time and number of molecules in box

Preliminary PVA calculations were carried out in order to know if chain length, number of molecules in the periodic box and final time of simulation were important to determine the final value of the solubility parameter. 39 simulations were performed in the NVT ensemble with the COMPASS [30] forcefield, considering a number of monomers ranging from 5 to 20, simulation times between 20 and 200 ps, and a number of molecules per box ranging from 5 to 20. Results are shown in Table 1.

Run and Kolmogorov–Smirnov (KS) tests were performed over the previous data. Run test checks the occurrence of random or non random values. On the other hand, KS test compares data distribution function with a normal distribution showing if differences are significant or not. By using IBM SPSS software, both tests were made showing independency of the data (signification of 0.74) for the run test. Data were also assumed to follow a normal distribution from the KS test results (signification of 0.67), as shown in Fig. 1.

Non influence of these three parameters studied is assumed (maximum difference between values is about 10%), and data

Table 1

Preliminary simulations for PVA.

Number of monomers	MD time (ps)	Molecules in box	SP (MPa ^{0.5})
5	20	5	28.32
10	20	5	26.76
15	20	5	27.13
20	20	5	26.25
5	50	5	28.26
10	50	5	27.69
15	50	5	27.14
20	50	5	26.89
5	100	5	28.47
10	100	5	28.34
15	100	5	26.71
20	100	5	26.83
5	20	10	27.97
10	20	10	27.45
15	20	10	26.00
20	20	10	26.25
5	50	10	28.07
10	50	10	27.65
15	50	10	26.22
20	50	10	26.48
5	100	10	28.39
10	100	10	27.70
15	100	10	26.03
20	100	10	27.02
5	20	15	28.85
10	20	15	25.63
15	20	15	25.69
5	20	20	28.56
15	50	20	26.94
15	100	20	26.76
20	100	20	26.78
5	200	5	28.59
10	200	5	28.44
15	200	5	27.53
20	200	5	26.22
5	200	10	28.51
10	200	10	27.60
15	200	10	26.77
20	200	10	26.38

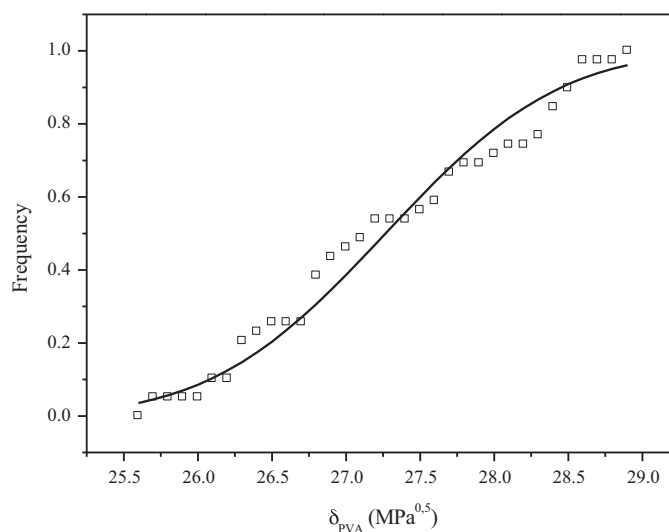


Fig. 1. Statistic distribution function of PVA solubility parameter compared with normal distribution curve. Data (□) compared with the normal distribution curve (—).

Table 2
Forcefield selection for the prediction of polymer solubility parameters.

Forcefield	Density (g/cm ³)	SP (MPa) ^{0.5}	Deviation density (%)	Deviation SP (%)
EVA				
PCFF	0.826	16.66	13.6	3.1
UNIVERSAL	0.834	19.27	12.8	12.0
COMPASS	0.851	16.72	11.0	2.8
DREIDING	0.739	13.36	22.7	22.3
PVA				
PCFF	1.096	25.86	19.7	7.3
UNIVERSAL	0.925	19.45	32.2	30.3
COMPASS	1.093	23.94	19.9	14.2
DREIDING	0.996	18.21	27.0	34.7
PC				
PCFF	1.085	17.37	9.6	13.6
UNIVERSAL	1.046	16.35	12.8	18.6
COMPASS	1.092	16.53	9.0	17.8
DREIDING	0.924	13.91	23.0	30.8

are considered to be statistically independent and normally distributed.

4.1.2. Forcefield selection

In order to choose the forcefield that best reproduces experimental data (density, solubility parameter) for each of the polymers considered in this work (PC, PVA, EVA), several molecular dynamics calculations were done considering four different forcefields: default Materials Studio Universal forcefield [26], COMPASS [30], PCFF [31,32], and Dreiding force field [33]. For each one, molecular dynamics calculations were performed in the NPT ensemble at 1 atm and 298 K for 20 ps of simulation time. Previously, annealing until 500 K in 5 cycles was done in all cases. A total of 5 chains with 10 repeating units were considered for PC and PVA, while each EVA chain had 13 ethylene and 2 vinyl acetate units in order to keep the vinyl acetate content of the copolymer. Boxes were built by using the amorphous cell module followed by a minimization energy calculation and annealing, all done with Forcite module of Materials Studio. This is the box conditioning which is made with the COMPASS [30] forcefield in Section 4.1.1. Results are shown in Table 2 and indicate that second-generation CFF based forcefield (PCFF [31,32] and COMPASS) give the lowest deviations in terms of density and SP. As a consequence, in following these two force-field will be considered.

4.1.3. Estimation of solubility parameters

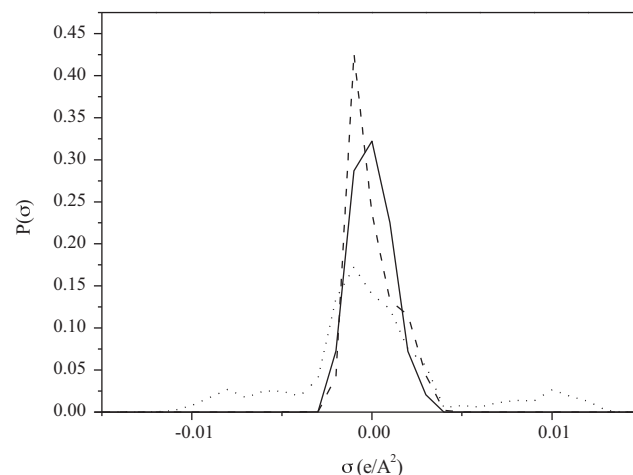
Recently, Bemares et al. [21] proposed a computational procedure for the determination of solubility parameters based on molecular dynamics calculations in the NVT ensemble. Here, we have followed such procedure for the three polymers under study, with the same systems considered in the previous section in terms of number of chains and repeat units. Molecular dynamics simulations were done until 500 ps using both PCFF and COMPASS forcefields. All the procedures were repeated with other starting geometries at least ten times in order to test the influence of different initial geometries. Results are presented in Table 3. Both force-fields provide similar results, with reasonably low standard deviations. In the following, these results will be compared with those obtained from other approaches.

4.2. COSMO-SAC results

By following the procedure of quantum mechanics optimization of increasing size oligomers proposed by Yang et al. [20] polymer sigma profiles were obtained (Fig. 2).

Table 3
SP of the polymers at 298 K.

Forcefield	SP (MPa ^{0.5})	Deviation (%)
EVA		
COMPASS	18.64	8.3
PCFF	19.42	12.9
PVA		
COMPASS	28.97	3.85
PCFF	28.96	3.78
PC		
COMPASS	17.79	11.5
PCFF	18.96	5.7

**Fig. 2.** Calculated sigma profiles of EVA (···), PVA (---) and PC (— · —) polymers.

Calculations of VLE with different solvents were carried out fitting χ_{12} parameter for each polymer–solvent pair, in the range of low solvent composition (range of inverse gas chromatography operation), i.e. EVA–Vinyl Acetate P–x diagram (Fig. 3).

By using χ_{12} parameter the solubility parameter can be obtained by fitting $((\delta_1^2/2) - (\chi_{12}RT/2V_1))$ vs δ_1 , as detailed in Section 2.1. As an example this regression for EVA copolymer is shown (Fig. 4).

Table 4 presents the results of all the calculations performed. It can be seen that group contribution methods (van Krevelen [average deviation 8.1%] and Fedors [average deviation 6.1%])

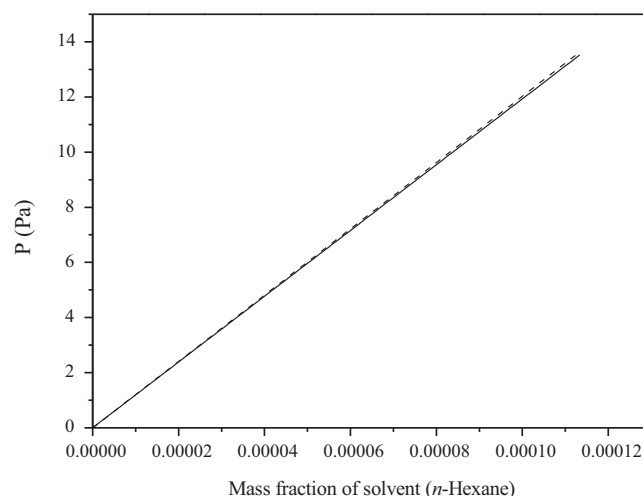
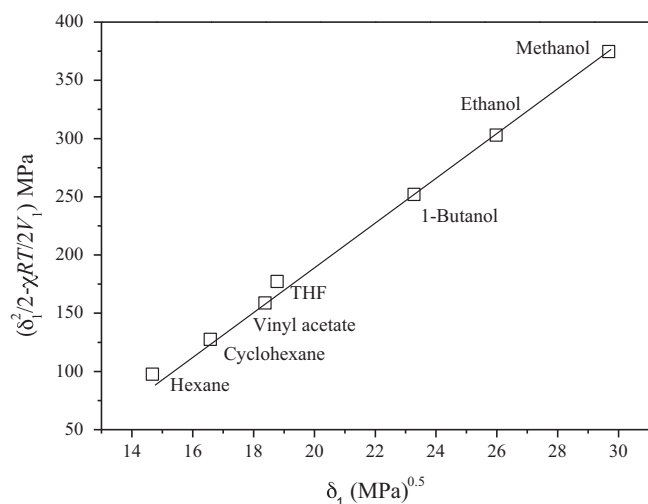
**Fig. 3.** Vapor–liquid equilibrium calculations of EVA–vinyl acetate system at 298 K (root square mean error 0.06). COSMO-SAC predictions (---), Flory–Huggins model ($\chi_{12} = 0.82$) (— · —).

Table 4

Results of SP obtained from different methodologies at 298 K.

Exp.	Bibliog.		COMPASS		PCFF		COSMO-SAC		VK		Fedors	
MPa ^{0.5}	MPa ^{0.5}	%	MPa ^{0.5}	%	MPa ^{0.5}	%	MPa ^{0.5}	%	MPa ^{0.5}	%	MPa ^{0.5}	%
EVA												
17.2	18.6	6.3	18.6	6.3	19.4	12.8	18.5	7.5	17.1	0.5	18.4	6.9
PVA												
27.9	25.8	8.1	28.97	3.7	28.96	3.7	31.2	10.6	34.3	18.7	31	10.0
PC												
n/a ^a	20.1	–	16.5	17.9	17.3	13.9	21.6	7.5	19.3	4.0	20.7	3.0

^a Not available, so the reference value for deviations is the bibliographic value.**Fig. 4.** Calculation of the EVA solubility parameter at 298 K from solvent solubility and Flory–Huggins interaction parameters ($\delta_2 = 18.5 \text{ MPa}^{0.5}$; $r^2 = 0.998$).

specifically developed to estimate polymer solubility parameters give the lowest deviation from experimental or bibliographic values. The new methodology based on the extension of COSMO-SAC model to polymers (average deviation 8.0%) proposed by Yang et al. [20] shows a great potential in the field of polymer thermodynamics, but more or less the same deviation is observed when estimating PVA solubility parameter. Finally, molecular dynamics is a very important tool for studying polymer properties such as radius of gyration and torsional effects and can be applied with good results to estimate thermodynamic properties as solubility parameters if using a proper forcefield (COMPASS [average deviation 9.35%] or PCFF [average deviation 9.29%]).

5. Conclusion

Three different methodologies have been tested in order to determine the SP values of three different polymers (EVA, PVA and PC). The results showed that the average deviation is always below 10%. In none of the cases it was observed a quantitative dependence of SP on the size of the polymers, the size of the problem or the simulation time in molecular dynamics. On the other hand, when association or high directional forces are significantly important, group contribution methods involve higher deviations in comparison with either COSMO-SAC or molecular dynamics. Finally, when dealing with common and not associated polymers conventional techniques such as van Krevelen or Fedors, are more accurate.

List of symbols

χ_{12} Flory–Huggins interaction parameter

V_i molar volume of i (cm^3/mol)
 R ideal gas constant
 δ_i solubility parameter of i ($\text{MPa}^{0.5}$)
 $\Delta H_{i,v}$ vaporization energy for i (J/mol)
 $p(\sigma_m)$ probability to find a segment of charge σ_m
 $\Gamma(\sigma_m)$ surface segment activity coefficient for a segment charged with σ_m
 $\Delta W(\sigma_m, \sigma_n)$ energy required to obtain a pair $E_{\text{pair}}(\sigma_m, \sigma_n)$ from a neutral pair (J/mol)
 γ_i activity coefficient of i
 A_i^{COSMO} cavity surface area of i (\AA^2)
 V_i^{COSMO} cavity volume of i (\AA^3)
 N_{unit} number of repeating units in the polymer
 ϕ_i volume fraction of i
 r chain segment number (polymer volume to solvent volume ratio)

References

- [1] J.A. Brydson, Plastic Materials, Elsevier, Oxford, 1999.
- [2] P.J. Flory, J. Chem. Phys. 9 (1941) 660.
- [3] P.J. Flory, Principles of Polymer Chemistry, Cornell University Press, New York, 1953.
- [4] J. Hildebrand, R. Scott, Regular Solutions, Prentice Hall, Englewood Cliffs, 1962.
- [5] J.H. Hildebrand, J. Am. Chem. Soc. 51 (1929) 66–80.
- [6] G.M. Bristow, W.F. Watson, Trans. Faraday Soc. 54 (1958) 1731–1741.
- [7] K. Ito, J.E. Guillet, Macromolecules 12 (1979) 1163–1167.
- [8] Y. Liu, B. Shi, Polym. Bull. 61 (2008) 501–509.
- [9] R. Ravindra, K.R. Krovvidi, A.A. Khan, Carbohydr. Polym. 36 (1998) 121–127.
- [10] D.W. van Krevelen, Properties of Polymers, 4 ed., Elsevier, Amsterdam, 2009.
- [11] R.F. Fedors, Polym. Eng. Sci. 14 (1974) 472.
- [12] R.F. Fedors, Polym. Eng. Sci. 14 (1974) 147–154.
- [13] A. Klamt, J. Phys. Chem. 99 (1995) 2224–2235.
- [14] A. Klamt, G. Schuurmann, J. Chem. Soc., Perkin Trans. 2 (1993) 799–805.
- [15] A. Klamt, COSMO-RS From Quantum Chemistry to Fluid Phase Thermodynamics and Drug Design, Elsevier, Amsterdam, 2004.
- [16] A. Klamt, F. Eckert, Fluid Phase Equilib. 172 (2000) 43–72.
- [17] S.-T. Lin, J. Chang, S. Wang, W.A. Goddard, S.I. Sandler, J. Phys. Chem. 108 (2004) 7429–7439.
- [18] S.-T. Lin, S.I. Sandler, Ind. Eng. Chem. Res. 41 (2001) 899–913.
- [19] C. Panayiotou, Pure Appl. Chem. 83 (2011) 1221–1242.
- [20] L. Yang, X. Xu, C. Peng, H. Liu, Y. Hu, AIChE J. 56 (2010) 2687–2698.
- [21] M. Belmares, M. Blanco, W.A. Goddard, R.B. Ross, G. Caldwell, S.H. Chou, J. Pham, P.M. Olofson, C. Thomas, J. Comput. Chem. 25 (2004) 1814–1826.
- [22] E. Mullins, R. Oldland, Y.A. Liu, S. Wang, S.I. Sandler, C.-C. Chen, M. Zwolak, K.C. Seavey, Ind. Eng. Chem. Res. 45 (2006) 4389–4415.
- [23] Dmol3 in Materials Studio Version 4.0 from Accelrys, Inc., San Diego, CA.
- [24] J. Brandrup, E.H. Immergut, E.A. Grulke, Polymer Handbook, Wiley-Interscience, 2003.
- [25] Computational Results Obtained Using Materials Studio Package from Accelrys, Inc., San Diego, CA.
- [26] A.K. Rappe, C.J. Casewit, K.S. Colwell, W.A. Goddard, W.M. Skiff, J. Am. Chem. Soc. 114 (1992) 10024–10035.
- [27] D.W. van Krevelen, P.J. Hoftyzer, Properties of Polymers Their Estimation and Correlation with Chemical Structure, Elsevier, New York, 1990.
- [28] M.S. Sulatha, U. Natarajan, J. Phys. Chem. B 115 (2011) 1579–1589.
- [29] E. Diez, G. Ovejero, M.D. Romero, I. Díaz, S. Bertholdy, Chem. Eng. Trans. 24 (2011) 553–558.
- [30] H. Sun, J. Phys. Chem. B 102 (1998) 7338–7364.
- [31] H. Sun, J. Comput. Chem. 15 (1994) 752–768.
- [32] H. Sun, S.J. Mumby, J.R. Maple, A.T. Hagler, J. Am. Chem. Soc. 116 (1994) 2978–2987.
- [33] S.L. Mayo, B.D. Olafson, W.A. Goddard, J. Phys. Chem. 94 (1990) 8897–8909.

1.1 Summary and Discussion

The previous four scientific articles, about the determination and evaluation of the Flory Huggins parameters of the EVA copolymers and their homopolymers (Polyethylene, PE, and Polyvinylacetate, PVA) at infinite dilutions of solvents ($\phi_2 \rightarrow 1$), by means of the Inverse Gas Chromatography (IGC), can be summarized and integrate, as follows:

The first article, “**Thermodynamic Interactions of EVA Copolymer/Solvent Systems by Inverse Gas Chromatography Measurements**” presents the overall Flory Huggins interaction parameter of two semicrystalline EVA copolymers samples, each one with different vinyl acetate (VA) content (EVA18, 18% and EVA 33, 33% w/w VA), determined in presence of nine different solvents at 30, 40 and 50 °C. In addition a thermodynamic assessment was done at these infinite dilutions conditions of solvents that also consider the determination and evaluation of the mass-based infinite dilution activity coefficient of the solvents, the Hildebrand solubility parameters of the EVAs samples, the heats of vaporization of the solvents, and the entropic and enthalpy contributions over the Flory Huggins parameters.

The main results indicate that the most favorable solvents for the copolymers are the aromatic-type ones, due their polar character that interacts with the vinyl acetate present on the EVA copolymers. The results also point the fact that the EVAs/solvents interactions are stronger in the case of the copolymer with the highest vinyl acetate percentage. In addition the Hildebrand solubility parameters (HSP) were determined ($15.93 \text{ MPa}^{1/2}$ for EVA33 and $14.7 \text{ MPa}^{1/2}$ for EVA18, lineally extrapolated at 60 °C), corroborating the stronger interactions of EVA33 due its HSP is the closest to the of pure vinyl acetate HSP.

Finally, from this article it is also crucial to take into account the results of those overall Flory Huggins parameters of the EVA copolymers samples in presence of methanol, vinyl acetate and cyclohexane, at 30, 40, 50 and linearly extrapolated at 60 °C. These values will be employed in the further articles and are summarized in table 2.1.

Table 2.1 Overall Flory Huggins parameters for EVA 18% VA and EVA 33% VA in methanol, vinyl acetate and cyclohexane

Solvent	χ EVA18				χ EVA33			
	30 °C	40 °C	50 °C	60 °C	30 °C	40 °C	50 °C	60 °C
Methanol (MET)	3.25	3.13	3.05	2.94	2.62	2.58	2.47	2.41
Vinyl acetate (VA)	1.48	1.4	1.33	1.25	0.57	0.5	0.47	0.41
Cyclohexane (CH)	0.83	0.74	0.67	0.59	0.9	0.86	0.83	0.79

In the second article, **“Inverse Gas Chromatography Study of Polyvinylacetate/Solvent and Polyethylene/Solvent Systems”** the overall Flory Huggins interaction parameters of a sample of a semicrystalline Polyethylene (PE) in presence of eight different solvents were determined at 40, 50 and 60 °C. In addition a thermodynamic assessment was done at these infinite dilutions conditions of solvents, that also consider the determination and evaluation of the retention volumes, the mass-based infinite dilution activity coefficient of the solvents, the Hildebrand solubility parameters of the polymer samples, the heats of vaporization of the solvents, the solvent molar enthalpies of sorption, the partial molar excess enthalpies of the polymers, and the heats of vaporization of the solvents.

According to the main results the compatibility of this polymer with the different types of solvents follows this order: dispersion solvents > polar solvents > association solvents, which was expected due the dispersion character of the ethylene monomer present in PE. Also, those overall Flory Huggins parameters were determined for an amorphous Polyvinylacetate sample (PVA) in eleven different solvents, at higher temperatures (60, 70 and 80 °C), because in an amorphous polymer there are not bulk interactions below a certain temperature that take into account the glass transition temperature (T_g (PVA) = 41.2 °C) plus a transition zone with bulk plus adsorption interactions. The compatibility order was: polar solvents > association solvents, also expected as the vinyl acetate monomer of PVA has a significant dipole moment. It was unreliable to determine thermodynamic parameters for mixtures with dispersion solvents, because despite being well above the T_g , no bulk dispersion interactions existed. In addition the Hildebrand solubility parameters of both polymers were also determined (14.1 $MPa^{1/2}$ for PE and 19.8 $MPa^{1/2}$ for PVA, at 60 °C), noting that the higher values of PVA is a consequence of the strong interactions of vinyl acetate monomer.

Although the Hildebrand solubility parameters of EVA18 and EVA33 copolymers (article 2.1), and PE and PVA polymers, were determined only to compare with literature data, because these parameters are not the more suitable for taking into account the polar and association interactions (given by the vinyl acetate monomer), the lineal correlation of the HSP at 60 °C, between the four mentioned polymers is highly satisfactory, as it is shown in figure 2.1. With increasing the content of vinyl acetate increases the solubility parameter of the polymer; which will draw ever closer to the solubility parameter of the pure vinyl acetate (17.1 $MPa^{1/2}$ at 60°C), exactly in a EVA

copolymer of a 54.3% of vinyl acetate (according the fitting equation presented in figure 2.1), which agrees the literature morphology description of the EVA copolymers, shown in Chapter 1: “Crystallization is increasingly hampered and is entirely absent from a copolymer with a vinyl acetate content of approx. 55 %”.

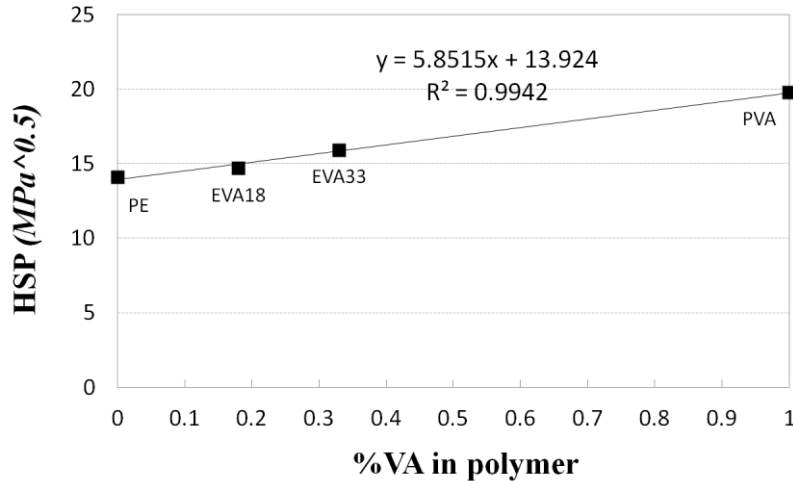


Figure 2.1 Hildebrand Solubility parameters for PE, EVA18, EVA33 and PVA, at 60°C

From this article it is also crucial to take into account the results of those overall Flory Huggins parameters of the PE and PVA samples in presence of methanol, vinyl acetate and cyclohexane, which will be employed in the further articles. They are summarized in table 2.2.

Table 2.2 Overall Flory Huggins parameters for PE and PVA in methanol, vinyl acetate and cyclohexane

Solvent	χ PE			χ PVA		
	40 °C	50 °C	60 °C	60 °C	70 °C	80 °C
Methanol (MET)	3.41	3.37	3.23	1.21	1.17	1.1
Vinyl acetate (VA)	2.12	1.99	1.91	0.74	0.48	0.43
Cyclohexane (CH)	0.94	0.85	0.79	3.78	3.09	2.46

The third article, “**Bulk polymer/solvent interactions for Polyethylene and EVA Copolymers, below their melting temperatures**” presents the amorphous Flory Huggins interaction parameter determined for the semicrystallines samples consider in the above studies (PE, EVA18 and EVA33), in presence of methanol, vinyl acetate and cyclohexane. In addition a thermodynamic assessment was done at these infinite dilutions conditions of solvents that also consider the determination and evaluation of the retention volumes and the mass-based infinite dilution activity coefficient of the solvents.

The results indicated that when the range of studied temperatures is below the melting point of a semicrystalline polymer, it is crucial to calculate the amorphous contribution ($\chi_{\text{amorphous}}$) on the overall Flory Huggins parameter determined in the last two discussed articles, according the percent of crystallinity of each polymer. The results show that the more compatible solvent was cyclohexane, and therefore it was selected as the probe to calculate the percentages of crystallinity at room temperature (35% for PE, 29% for EVA18, and 12% for EVA33), which were in agreement the literature data. Regarding the interactions between the three polymeric materials and the solvents, it can be noticed that, the lower the vinyl acetate content is in the polymer (higher crystallinity), the higher the difference between the previous published overall Flory Huggins parameters (Article 2.1), and amorphous Flory Huggins parameters is. For the best solvent (cyclohexane) $\chi_{\text{amorphous}}$ represents the less contribution or the highest correction to the overall Flory Huggins parameter (around 50% for PE and EVA18, and 79% for EVA33), following by the medium compatible solvent (vinyl acetate) and finally by the worst solvent (methanol). These last two percentages were, in average, around 80% and 91%.

These results about the amorphous Flory Huggins parameters of the semicrystalline PE and EVA polymers in presence of methanol, vinyl acetate and cyclohexane, at 40, 50 and 60 °C, which will be used in the further articles, are summarized in table 2.3.

Table 2.3 Amorphous Flory Huggins parameters for PE and EVA copolymers in methanol, vinyl acetate and cyclohexane

Solvent	$\chi_{\text{amorphous}}$ PE			$\chi_{\text{amorphous}}$ EVA18			$\chi_{\text{amorphous}}$ EVA33		
	40 °C	50 °C	60 °C	40 °C	50 °C	60 °C	40 °C	50 °C	60 °C
Methanol (MET)	3.06	3.02	2.95	2.78	2.69	2.65	2.39	2.32	2.27
Vinyl acetate (VA)	1.64	1.56	1.49	1.02	0.99	1.01	0.73	0.73	0.73
Cyclohexane (CH)	0.40	0.37	0.34	0.40	0.36	0.33	0.39	0.37	0.35

Finally in the fourth article, “**Comparison between three predictive methods for the calculation of polymer solubility parameters**”, which is presented as an annex, the Hildebrand solubility parameter (HSP) for the EVA33 has been estimated by means of molecular dynamics simulations, employing the COSMO-SAC model, in order to compare it with the experimental HSP values obtained in the first article showed in this chapter, by means of the overall Flory Huggins obtained by Inverse Gas Chromatography, and other traditional group contribution procedure (Fedors and Van Krevelen). The results showed that the average deviation for the EVA33 HSP is below to 7.5%, between the COSMO-SAC and the experimental one, determined by IGC.

This evaluation also has been done for other two kinds of polymers (Polyvinyl alcohol and Bisphenol-A polycarbonate) in order to validate a general HSP comparison assessment for the polymer engineer. The results for the HSP of all polymers, estimated from all methods showed that the average deviation is always below 10%.

3 Thermodynamics of EVA/solvents mixtures at infinite dilution of polymer

This chapter presents three scientific articles published in the framework of the global project and a final discussion, that are focused on the determination and evaluation of the Flory Huggins parameters of the EVA copolymers and their homopolymers (Polyethylene, PE, and Polyvinylacetate, PVA) at infinite dilutions of polymers ($\phi_2 \rightarrow 0$), by means of the Intrinsic Viscosity technique (IV). Additionally, several thermodynamic assessments were done at these infinite dilution conditions.

At the end of the discussion of each article, these Flory Huggins parameters are cited for the studied polymers that were soluble in presence of the solvents participating in the EVA separation solution process (methanol and vinyl acetate), plus cyclohexane.

3.1 Turbidimetric and intrinsic viscosity study of EVA copolymer/solvent systems

Díez, E., Camacho, J., Díaz, I., & Ovejero, G. (2014). Turbidimetric and intrinsic viscosity study of EVA copolymer–solvent systems. *Polymer bulletin*, 71(1), 193-206.

Turbidimetric and intrinsic viscosity study of EVA copolymer–solvent systems

Eduardo Díez · Javier Camacho · Ismael Díaz ·
Gabriel Ovejero

Received: 26 February 2013 / Revised: 19 April 2013 / Accepted: 28 August 2013 /
Published online: 4 September 2013
© Springer-Verlag Berlin Heidelberg 2013

Abstract Both Hansen solubility parameter and Flory–Huggins interaction parameter of two EVA [Poly(ethylene-co-vinyl acetate)] copolymers with different vinyl acetate content have been obtained by means of intrinsic viscosity measurements. To calculate this last parameter it was also necessary to determine the theta solvent at different temperatures of the two EVA copolymers with turbidimetric measurements. The results indicate that the vinyl acetate content is a variable which influences the composition of the theta solvent and Flory–Huggins parameter (the higher the vinyl acetate content, the lower the Flory–Huggins parameter), although its influence over the Hansen solubility parameter is almost negligible.

Keywords EVA · Intrinsic viscosity · Hansen solubility parameter · Flory–Huggins parameter

Introduction

The ethylene–vinyl acetate copolymer (EVA) is one of the most useful polymers, due to its wide range of applications in, for example, coating of photovoltaic cells, or obtaining tyres and cable, as a consequence of the different varieties of the material, depending on the vinyl acetate percentage [1].

E. Díez (✉) · J. Camacho · G. Ovejero
Grupo de Catálisis y Procesos de Separación (CyPS), Departamento de Ingeniería Química,
Facultad de C. Químicas, Universidad Complutense de Madrid,
Avda. Complutense s/n, 28040 Madrid, Spain
e-mail: ediezalc@quim.ucm.es

I. Díaz
Departamento de Ingeniería Química Industrial y del Medio Ambiente, Escuela Técnica Superior de
Ingenieros Industriales, Universidad Politécnica de Madrid, C/José Gutiérrez Abascal 2,
28006 Madrid, Spain

The way the EVA copolymer is industrially obtained is related to the vinyl acetate content. When the vinyl acetate content is lower than 40 %, this material is manufactured by means of high pressure processes, and its main applications are as modifiers [2]; when the vinyl acetate content is between 30 and 40 %, a dissolution process at moderate temperatures and pressures is carried out, and the main applications of the obtained material are as an elastomer (obtaining synthetic elastomers, tyres, ...) [2]; finally, when the vinyl acetate content is higher than 70 %, the manufacture is carried out employing an emulsion process, and the main uses of the final material are as adhesives.

Due to the most important applications of EVA-type materials as elastomers, we are focusing in studying dissolution processes [3–5]. In these processes, the main drawback is the separation step, with the aim of getting a pure EVA material; for this reason, it is advisable to accurately study the interactions between the polymer and the solvent.

A polymer–solvent mixture differs from a conventional solvent–solvent mixture, as a consequence of the great difference between the relative sizes of the molecules of both components. Two of the most important parameters of these special systems are the solubility parameter (δ) [6] and the polymer–solvent Flory–Huggins parameter (χ) [7].

Initially, the solubility parameter a compound i was defined by Hildebrand [6] as the square root of its cohesive energy according to Eq. (1), where $\Delta_{\text{vap}}H_{\text{m},i}$ is the enthalpy of vaporization of the compound i , R is the universal gases constant, T is the absolute temperature and $V_{\text{m},i}$ is the molar volume of the i compound. Cohesive energy can be derived from the enthalpy of vaporization because the intermolecular attractive forces which have to be overcome to vaporize a liquid are the same ones that have to be overcome to dissolve it.

$$\delta_i = \sqrt{c_i} = \left[\frac{\Delta_{\text{vap}}H_{\text{m},i}RT}{V_{\text{m},i}} \right]^{0.5} \quad (1)$$

The more important drawback of the traditional defined Hildebrand solubility parameter definition is that it only takes into account dispersive interactions, but no dipole–dipole interactions or hydrogen bonding interactions. This approximation is reliable with non-polar solvents, like cyclohexane, but it does not seem to be accurate with polar solvents, like tetrahydrofuran.

So, with the aim of overcoming this difficulty, Hansen proposed in 1969 [8] to divide the solubility parameter into three different contributions: one due to non-polar or dispersion forces, another due to polar forces, and a last one which takes into account hydrogen bonding effects. Thus, the overall solubility parameter of a compound is now determined with Eq. (2), where δ_i indicates the solubility parameter of a solvent i , $\delta_{d,i}$ is the apolar contribution, $\delta_{p,i}$ is the polar contribution, and $\delta_{h,i}$ is the hydrogen bonding contribution.

$$\delta_i^2 = \delta_{d,i}^2 + \delta_{p,i}^2 + \delta_{h,i}^2 \quad (2)$$

From the solubility parameter of both polymer and solvent, the Flory–Huggins interaction parameter (FH parameter) can be determined, according to Blanks and Prausnitz [9], by applying Eq. (3).

$$\chi = \chi_S + \chi_H = \chi_S + \frac{V_{m,i}}{RT} (\delta_i - \delta_2)^2 \quad (3)$$

In this last equation, χ is the Flory–Huggins parameter, χ_S is the entropic contribution of this parameter (usually 0.34, according Blanks and Prausnitz [9]), and χ_H is the enthalpic contribution, obtained from the molar volume of a solvent i ($V_{m,i}$), the absolute temperature (T), and the Hildebrand solubility parameters of the polymer (δ_2) and the solvent i (δ_i).

However, in order to take into account not only dispersion forces but also polar and hydrogen bonding forces in the calculation of the FH parameter, it is necessary to substitute in Eq. (3) the Hildebrand solubility parameters by a new term which includes the different terms of Hansen solubility parameter (HSP), Eqs. (4) and (5).

$$A_{12} = \left[(\delta_{d,i} - \delta_{d,2})^2 + 0.25 (\delta_{p,i} - \delta_{p,2})^2 + 0.25 (\delta_{h,i} - \delta_{h,2})^2 \right] \quad (4)$$

$$\chi = \chi_S + \chi_H = \chi_S + \frac{V_{m,i}}{RT} A_{12} \quad (5)$$

These parameters (HSP and FH) have been demonstrated to be extremely useful to properly model the separation steps in a polymer obtaining process [10].

In the literature, several data showing the solubility parameter of a wide range of solvents have been previously published [11, 12]; however, the solubility parameter of an EVA copolymer is not a standard value because could depend on the vinyl acetate content and on the polymer molecular weight distribution. For this reason, it is important to determine this last value experimentally. Concerning the FH parameter, there is no reference reporting this parameter for any kind of EVA. Both parameters are quite important to choose, for example, a suitable solvent for a specific polymer, so that the further purification can be efficiently carried out.

As previously mentioned, a polymer–solvent mixture is quite different from a conventional mixture because there is a great difference between both molecular sizes. For this reason, in order to determine thermodynamic parameters of these mixtures, it is necessary to use non-conventional techniques, because typical ebullometric measurements cannot be directly performed. The most well-known techniques are swelling [13], inverse gas chromatography [14, 15], intrinsic viscosity [16] and turbidimetry [17].

Among all these techniques, intrinsic viscosity (IV) is one of the most widely used because of its reliability and easy starting up. We selected intrinsic viscosity method because, for our purpose, it is very fast and simple to get accurate values indirectly from viscosity measurements of polymer dilute solutions. Since IV is related to an infinite diluted solution, a really small amount of polymer added to pure solvent will change so much its viscosity. In the literature [18, 19], this technique has been widely employed with good results.

This paper reports the results of the HSP and the FH polymer–solvent interaction parameters of two EVA copolymers, with different vinyl acetate contents. The

purpose of this study is to assess the dependence of these two parameters on the vinyl acetate content, so that the interactions between each polymer and the studied solvents are clearly defined. This is fundamental to accurately design the polymer–solvent purification steps, which are extremely important in a polymer production process. Besides, the HSP is frequently used as criteria to select the most suitable solvent for a polymer.

Experimental section

Materials

Both EVA copolymers were supplied by REPSOL-YPF Company. While EVA 1 (EVA460) has a vinyl acetate content of 33 % (w/w), EVA 2 (EVA410) has a vinyl acetate content of 18 % (w/w). The weight-average molecular weight and the number-average molecular weight are 61,041 and 18,582 for EVA 1, and 42,460 and 14,008 for EVA 2 determined by gel exclusion chromatography. Finally, the densities of the two polymeric materials are 956 and 937 kg/m³, respectively, as reported by the supplier.

On the other hand, all the employed solvents were analytical grade and were purchased from Aldrich. They were used directly, without any purification step.

Intrinsic viscosity determination

All most concentrated polymer solutions were prepared by adding 200–300 mg of polymer over approx. 60 g of pure solvent, and then shaking until the elastomer became dissolved. The rest of solutions were prepared adding pure solvent.

Viscosity measurements were carried out in a JP–Selecta Ubbelohde 0b type of capillary viscosimeter. Once prepared, each solution was transferred into the viscosimeter, which was immersed in a water bath, thermostated at $T \pm 0.01$ °C. The solutions were allowed to equilibrate at the adequate temperature before starting the measurement. The accuracy of the measurements was 10^{-2} s. Each flow time was measured 5 times and the average value was taken; from the flow times, relative and specific viscosities were determined.

The IV of a polymer–solvent mixture, $[\eta]$, is defined as the viscosity of an infinitely diluted polymer solution, and it can be calculated, from the previously described flow time measurements, with Huggins (Eq. 6) and Kraemer (Eq. 7) expressions [20, 21].

$$\frac{\eta_{sp}}{c} = [\eta] + K_H[\eta]^2c \quad (6)$$

$$\frac{\ln(\eta_r)}{c} = [\eta] + K_K[\eta]^2c \quad (7)$$

In these equations, c is the concentration of polymer solution, K_H is the Huggins coefficient, and K_K is the Kramer coefficient; relative viscosity (η_r) is the relation between the flow time of the polymer solution through the viscosimeter and the flow

time of the pure solvent through the apparatus; finally, specific viscosity (η_{sp}) is defined as relative viscosity minus one, and represents the viscosity increasing due to the polymer. So, the intrinsic viscosity ($[\eta]$) can be determined as the common intercept of the Kraemer and Huggins relationships, using η_r and η_{sp} experimentally determined.

Solubility parameter calculation

The three contributions of the HSP of the two EVA copolymers were calculated following Segarceanu and Leca [22] procedure. In this method, the intrinsic viscosities values are normalized by the intrinsic viscosity of that solvent giving the highest value, according to Eqs. (8), (9) and (10). Finally, the overall solubility parameter can be calculated using Eq. (2).

$$\delta_{d,2} = \frac{\sum_i^n \delta_{d,i} [\eta]_i}{\sum_i^n [\eta]_i} \quad (8)$$

$$\delta_{p,2} = \frac{\sum_i^n \delta_{p,i} [\eta]_i}{\sum_i^n [\eta]_i} \quad (9)$$

$$\delta_{h,2} = \frac{\sum_i^n \delta_{h,i} [\eta]_i}{\sum_i^n [\eta]_i} \quad (10)$$

In these equations, the subscript 2 refers to polymer, and the subscript i refers to each solvent from 1 to n ($n = 5$ in this case). The subscripts d , p and h refers to dispersion, polar and hydrogen bonding contributions, respectively.

FH parameter calculation

The FH parameter values were directly determined from IV values, by means of Stockmayer and Fixman [23] (Eq. 11) and Berry [24] (Eq. 12) relationships. These equations relate the intrinsic viscosity and the Flory–Huggins parameter in theta conditions, with the intrinsic viscosity and the Flory–Huggins parameter in non-theta conditions. It allows calculating the value of the Flory–Huggins parameter in any condition, taking into account that the value of this parameter at theta conditions is 0.5. These expressions have been already used in the literature [25] to obtain polymer solvent interaction parameters, with good results.

$$[\eta]/M_2^{1/2} = K_0 + 0.51B\phi_0M_2^{1/2} \quad (11)$$

$$[\eta]^{1/2}/M_2^{1/4} = K_0^{1/2} + 0.42K_0^{1/2}B\phi_0M_2[\eta]^{-1} \quad (12)$$

In these last expressions, $[\eta]$ is the IV value of the polymer–solvent couple, K_0 is the unperturbed dimension parameter, which is related to the intrinsic viscosity under theta conditions ($[\eta]_\theta$) by means of Eq. (13), Φ_0 is the universal viscosity constant, being equal to $2.5 \times 10^{-21} \text{ mol}^{-1}$ if the unit of $[\eta]$ is dl g^{-1} , M_2 is number-average polymer molecular weight, and B is the parameter for the polymer–

solvent interactions, which is related to the Flory–Huggins parameter (χ) by means of Eq. (14).

$$K_0 = [\eta]_0 / M_2^{1/2} \quad (13)$$

$$B = \frac{v_2^2(1 - 2\chi)}{V_1 N_A} \quad (14)$$

In these last equations, v_2 is the partial specific volume of the polymer, V_1 is molar volume of the solvent, and N_A is Avogadro's number.

Intrinsic viscosity under theta conditions determination

To determine the intrinsic viscosity under theta conditions, several techniques have been proposed; however, the most reliable ones are the turbidimetric-based or cloud-point techniques: cloud-point titration and cloud temperature titration [12]. The first one consists on titrating dilute polymer solutions of different compositions, with a non-solvent at constant temperature. The second one implies cooling or heating a polymer solution until the appearance of cloudiness. In the literature, these techniques have been accurately employed with a wide range of polymeric materials [26].

In this work, we have applied the cloud-point titration according to the “Elias method” [27]. Following this method, five diluted solutions (D1–D5) of both EVA copolymers (component 2) in cyclohexane (component 1) were prepared, with compositions ranging between 0.0005 and 0.003 v/v. The solutions were initially prepared in weight basis and later on, the volumetric fractions were calculated from the mass fractions, taking into account the density of both components.

In the next step, from each solution, a 5 mL aliquot was taken and put in a thermostated bath until reaching constant temperature (measured with an Hg thermometer with an accuracy of ± 0.1 °C). Finally, while magnetically stirring, the aliquot was titrated with acetone (component 3) until cloud point was achieved, employing an analogic burette whose accuracy is 0.05 mL; the cloud point was visually detected.

This experiment was repeated five times for each solution so the final acetone volume was considered to be the arithmetic mean of the five titrations. The experiments were carried out at temperature values of 30, 40 and 50 °C.

From the acetone consumption, the average volume fraction of acetone at cloud point ($\Phi_{3,cp}$) of each solution was calculated. According to the “Elias method”, this parameter is plotted, at each temperature, against the logarithm of the polymer volume fraction at cloud point ($\Phi_{2,cp}$), and the intercept of the plot is the volume fraction of the titrating agent ($\Phi_{3,\theta}$) in a solvent-titrating agent mixture (cyclohexane-acetone in this case) which behaves as “theta solvent” at the specified temperature (Eq. 15).

$$\phi_{3,cp} = \phi_{3,\theta} - B_{cp} \cdot \ln \phi_{2,cp} \quad (15)$$

Once the “theta solvent” was known at each temperature for both EVA materials, their intrinsic viscosity was measured at 30, 40 and 50 °C following the procedure already described in “[Intrinsic viscosity determination](#)” and “[Solubility parameter calculation](#)”.

Results and discussion

Intrinsic viscosity under theta conditions

Tables 1 and 2 show the acetone consumption (expressed as $\Phi_{3,cp}$, volumetric fraction of acetone at cloud point), as a function of the volumetric fraction of EVA (Φ_3) in the initial solution.

As it can be observed, the acetone consumption is clearly higher for EVA460 polymer than for EVA410 polymer. This can be related to the vinyl acetate content: the more vinyl acetate content, the more polar character of the copolymer and the more affinity towards acetone, which implies that a higher amount of acetone is needed to reach the immiscibility.

It can also be noticed that the acetone consumption increases with the temperature. Taking into account that cyclohexane and acetone are completely miscible in the whole temperature range and that both EVA copolymers are completely miscible with cyclohexane, this indicates that it is the solubility of the two polymeric materials in acetone what really increases with the temperature.

Figures 1 and 2 show the Elias plots for the two polymeric materials at the three different temperatures.

From the intercepts of Figs. 1 and 2, the acetone/cyclohexane volumetric proportion which behaves as theta solvent for each copolymer and at each temperature can be determined; the values are shown in Table 3. Finally, the IV values under theta conditions are shown in Table 4.

Flory–Huggins and solubility parameters from intrinsic viscosity measurements

In this work, the intrinsic viscosity of five different solvents (cyclopentane, cyclohexane, toluene, *p*-xylene and tetrahydrofuran) in two commercial EVA copolymers supplied by REPSOL-YPF Company and at three different temperatures

Table 1 Turbidimetric results for EVA 1 (460)

	$T = 30\text{ }^{\circ}\text{C}$		$T = 40\text{ }^{\circ}\text{C}$		$T = 50\text{ }^{\circ}\text{C}$	
	$\Phi_{2,cp}$	$\Phi_{3,cp}$	$\Phi_{2,cp}$	$\Phi_{3,cp}$	$\Phi_{2,cp}$	$\Phi_{3,cp}$
D1	2.68×10^{-3}	0.659	2.26×10^{-3}	0.704	1.90×10^{-3}	0.735
D2	2.11×10^{-3}	0.663	1.77×10^{-3}	0.708	1.49×10^{-3}	0.740
D3	1.56×10^{-3}	0.667	1.32×10^{-3}	0.712	1.07×10^{-3}	0.751
D4	1.02×10^{-3}	0.676	8.54×10^{-4}	0.720	6.78×10^{-4}	0.763
D5	4.78×10^{-4}	0.697	4.01×10^{-4}	0.737	3.28×10^{-4}	0.773

Table 2 Turbidimetric results for EVA 2 (410)

	$T = 30\text{ }^{\circ}\text{C}$		$T = 40\text{ }^{\circ}\text{C}$		$T = 50\text{ }^{\circ}\text{C}$	
	$\Phi_{2,\text{cp}}$	$\Phi_{3,\text{cp}}$	$\Phi_{2,\text{cp}}$	$\Phi_{3,\text{cp}}$	$\Phi_{2,\text{cp}}$	$\Phi_{3,\text{cp}}$
D1	4.48×10^{-3}	0.421	3.57×10^{-3}	0.516	3.00×10^{-3}	0.550
D2	3.40×10^{-3}	0.451	2.81×10^{-3}	0.524	2.35×10^{-3}	0.557
D3	2.45×10^{-3}	0.473	2.06×10^{-3}	0.532	1.73×10^{-3}	0.568
D4	1.52×10^{-3}	0.510	1.36×10^{-3}	0.540	1.14×10^{-3}	0.574
D5	7.38×10^{-4}	0.532	6.66×10^{-4}	0.554	5.57×10^{-4}	0.589

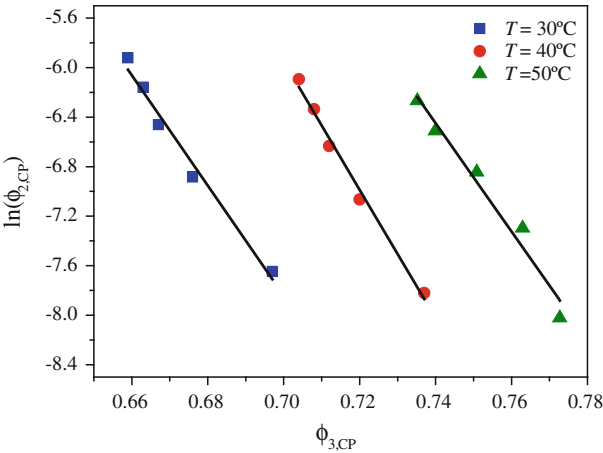


Fig. 1 Elias plot for EVA 1—cyclohexane/acetone system

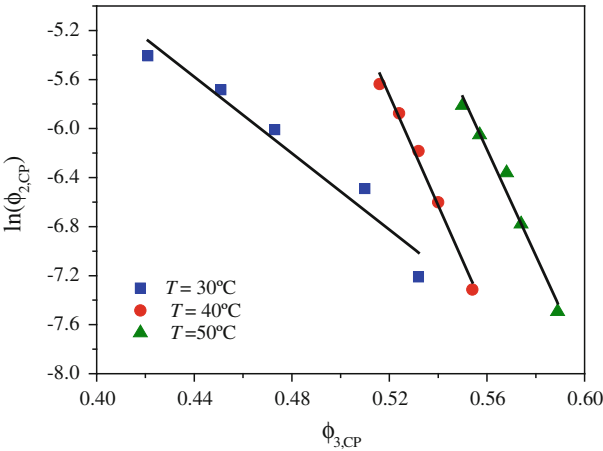


Fig. 2 Elias plot for EVA 2—cyclohexane/acetone system

Table 3 Volumetric composition of theta solvent for both EVA's copolymers

Temp. (°C)	Acetone vol. fraction ($\Phi_{3,0}$)		B_{cp}	
	EVA 1 (460)	EVA 2 (410)	EVA 1 (460)	EVA 2 (410)
30	0.526	0.101	0.022	0.061
40	0.588	0.394	0.019	0.022
50	0.597	0.419	0.022	0.028

Table 4 Intrinsic viscosity under theta conditions

Temp. (°C)	$[\eta]_0$ (dL g ⁻¹)	
	EVA 1 (460)	EVA 2 (410)
30	0.610	0.772
40	0.529	0.540
50	0.554	0.518

(30, 40, 50 °C) has been measured; all of them are potential solvents to carry out the synthesis of an EVA material following a dissolution process. The intrinsic viscosity results along with the difference between Huggins and Kraemer constants are summarized in Table 5. Moreover, as an example, the Huggins and Kraemer plots for both toluene–EVA systems at 30 °C are shown in Fig. 3.

To analyze the dependence of intrinsic viscosity upon temperature and vinyl acetate content, it is important to point out that the behavior of a polymer in solution is related mainly to its nature, but also on the kind of solvent; these two parameters will influence the dimensions of the polymer, which are related to the intrinsic viscosity.

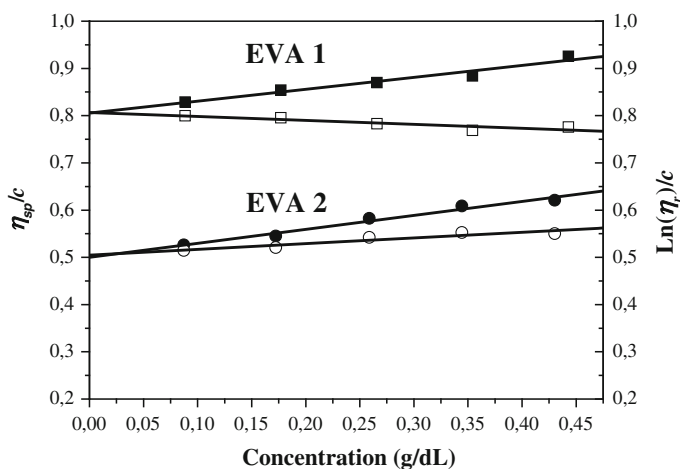
Although, the unperturbed dimension of a polymer ($\langle r^2 \rangle_0$) is supposed to be independent of the temperature (due to its own definition: the dimension of a macromolecule in solution, in absence of long-range interactions), the dimension of a macromolecule, related to the intrinsic viscosity, is clearly influenced by the interactions between the polymer chains and between the polymer and the solvent [28]. These interactions can be short-range ones, between adjacent atoms, and long-range ones, which are attractive or repulsive forces between segments of a polymer chain that are far from each other (although in some cases they can be close, due to the excluded volume effect), and between polymer segments and solvent molecules.

This way, the intrinsic viscosity rises up, whenever the molecules of the polymer are more opened, as a consequence of the polymer–solvent interactions. On the other hand, the intrinsic viscosity decreases, whenever the interactions between the segments of the polymer are stronger than the interactions between the polymer segment and the solvent and, as a result, the polymer molecules are more closed.

As it can be observed in Table 5, there is no clear dependence of intrinsic viscosity with temperature. In the case of EVA 1, there is a tendency of the intrinsic viscosity to decrease with temperature; in the case of EVA 2, the tendency is the

Table 5 Intrinsic viscosity results

Solvent	EVA 1 (460)		EVA 2 (410)	
	$[\eta]$ (dL/g)	$K_H - K_K$	$[\eta]$ (dL/g)	$K_H - K_K$
$T = 30\text{ }^{\circ}\text{C}$				
Cyclohexane	0.651	0.584	0.500	0.575
Toluene	0.806	0.518	0.503	0.691
Tetrahydrofuran	0.738	0.615	0.512	0.590
<i>p</i> -Xylene	0.846	0.487	0.584	0.417
Cyclopentane	0.745	0.451	0.679	0.425
$T = 40\text{ }^{\circ}\text{C}$				
Cyclohexane	0.710	0.497	0.553	0.446
Toluene	0.775	0.533	0.571	0.592
Tetrahydrofuran	0.720	0.609	0.589	0.725
<i>p</i> -Xylene	0.798	0.523	0.516	0.538
Cyclopentane	0.733	0.474	0.673	0.480
$T = 50\text{ }^{\circ}\text{C}$				
Cyclohexane	0.677	0.539	0.534	0.568
Toluene	0.751	0.548	0.621	0.482
Tetrahydrofuran	0.727	0.580	0.583	0.644
<i>p</i> -Xylene	0.726	0.607	0.588	0.428
Cyclopentane		—	—	—

**Fig. 3** Huggins and Kraemer plots for Toluene—EVA mixtures at $T = 30\text{ }^{\circ}\text{C}$

opposite. This means that when the vinyl acetate content is high, the interactions between the segments of the polymer and the solvent tend to diminish with temperature, and when the vinyl acetate content is lower, the interactions between

the segment of the polymer and the solvent tend to become stronger as temperature increases.

Regarding the overall dependence with vinyl acetate content, it can be observed that the intrinsic viscosity values are lower in the EVA elastomer having less vinyl acetate percentage. This means that the vinyl acetate segment is the main responsible of the interactions between the polymer and the solvents; so, when the amount of vinyl acetate segments decreases, the interactions between polymer and solvent become less important than the interaction between the segments of the polymer. As a consequence the polymer coils itself and the intrinsic viscosity goes down.

Regarding the Flory–Huggins parameter, Table 6 shows their calculated values following the Stockmayer–Fixman relationship [23], and Table 7 shows their calculated values according to Berry relationship [24]. Both Tables also show the values of the enthalpic [calculated with Eqs. 4 and 5] and entropic (calculated as the difference between the overall value and the enthalpic term) contributions to the FH parameter.

As it can be observed, the values of the FH interaction parameters calculated with both methods are very close, being the values lower in the case of the EVA material with more vinyl acetate content (the one with more polar character), although all the solvents are clearly compatible with both elastomers.

Table 6 Flory–Huggins parameter results, following the Stockmayer and Fixman method [23]

Solvent	EVA 1 (460)			EVA 2 (410)		
	χ	% χ_H	% χ_S	χ	% χ_H	% χ_S
<i>T</i> = 30 °C						
Cyclohexane	0.484	0.124	0.360	0.645	0.112	0.534
Toluene	0.426	0.043	0.383	0.641	0.045	0.596
Tetrahydrofuran	0.405	0.338	0.066	0.605	0.353	0.251
<i>p</i> -Xylene	0.294	0.015	0.279	0.614	0.016	0.598
Cyclopentane	0.354	0.062	0.292	0.543	0.052	0.491
<i>T</i> = 40 °C						
Cyclohexane	0.429	0.125	0.304	0.493	0.113	0.380
Toluene	0.406	0.044	0.362	0.484	0.046	0.438
Tetrahydrofuran	0.404	0.343	0.062	0.480	0.358	0.122
<i>p</i> -Xylene	0.313	0.015	0.299	0.514	0.017	0.498
Cyclopentane	0.360	0.063	0.298	0.437	0.053	0.384
<i>T</i> = 50 °C						
Cyclohexane	0.451	0.127	0.324	0.492	0.114	0.377
Toluene	0.424	0.044	0.380	0.445	0.046	0.398
Tetrahydrofuran	0.396	0.347	0.049	0.473	0.362	0.111
<i>p</i> -Xylene	0.352	0.015	0.337	0.457	0.017	0.440
Cyclopentane	–			–		

Table 7 Flory–Huggins parameter results, following the Berry method [24]

Solvent	EVA 1 (460)			EVA 2 (410)		
	χ	χ_H	χ_S	χ	χ_H	χ_S
<i>T</i> = 30 °C						
Cyclohexane	0.490	0.124	0.366	0.563	0.112	0.452
Toluene	0.444	0.043	0.401	0.562	0.045	0.516
Tetrahydrofuran	0.411	0.338	0.073	0.546	0.353	0.193
<i>p</i> -Xylene	0.276	0.015	0.261	0.556	0.016	0.540
Cyclopentane	0.333	0.062	0.271	0.524	0.052	0.472
<i>T</i> = 40 °C						
Cyclohexane	0.473	0.125	0.348	0.496	0.113	0.383
Toluene	0.454	0.044	0.411	0.496	0.046	0.444
Tetrahydrofuran	0.417	0.343	0.074	0.487	0.358	0.129
<i>p</i> -Xylene	0.305	0.015	0.290	0.508	0.017	0.492
Cyclopentane	0.337	0.063	0.274	0.455	0.053	0.402
<i>T</i> = 50 °C						
Cyclohexane	0.482	0.482	0.127	0.495	0.114	0.380
Toluene	0.461	0.461	0.044	0.495	0.046	0.415
Tetrahydrofuran	0.413	0.413	0.347	0.482	0.362	0.120
<i>p</i> -Xylene	0.347	0.347	0.015	0.471	0.017	0.454
Cyclopentane	–			–		

It can also be noticed that except for THF, the main contribution to the FH parameter is the entropic ones. This seems to be related to the low polar character of the solvents. In the case of THF, its high polarity makes the enthalpic contribution to be more important.

Concerning the temperature dependence in the literature has been described that the Flory–Huggins parameter can decrease [29] but also increase [19] with temperature. The Flory–Huggins parameter is obtained by adding two components, one entropic and one enthalpic [9]. The first one, mainly due to the free volume of the solvent, is expected to increase with temperature; the free volume of the solvent also increases with temperature, so this compound will be less accessible to polymer lattice. The second one is expected to decrease with temperature, due to the decreasing of intermolecular forces between polymer and solvent. Therefore, the overall dependence of χ with temperature will depend on the prevailing effect. In this case, the temperature dependence is almost negligible.

Finally, the three contributions to the Hansen solubility parameter of both elastomers were calculated according to Eqs. (2), (8), (9) and (10), from the values of the Hansen solubility parameter of the studied solvents (Table 8). The obtained results, shown in Table 9, indicate that the different vinyl acetate content, although having quite influence in the value of the FH parameter, is not a factor that affects the HSP. On the other hand, although the main contribution to the HSP in both cases

Table 8 Non-polar, polar and hydrogen bonding contributions, and overall solubility parameter of the studied solvents [12]

Solvent	$\delta_{d,i}$ (MPa ^{1/2})	$\delta_{p,i}$ (MPa ^{1/2})	$\delta_{h,i}$ (MPa ^{1/2})	δ_i (MPa ^{1/2})
Cyclohexane	16.8	0.0	0.2	16.80
Tetrahydrofuran	16.8	5.7	8.0	19.46
Toluene	18.0	1.4	2.0	18.16
Cyclopentane	16.4	0.0	1.8	16.50
Ethylbenzene	17.8	0.6	1.4	17.87

Table 9 Non-polar, polar and hydrogen bonding contributions, and overall solubility parameter of the studied copolymers, at $T = 30\text{ }^{\circ}\text{C}$

Elastomer	$\delta_{d,2}$ (MPa ^{1/2})	$\delta_{p,2}$ (MPa ^{1/2})	$\delta_{h,2}$ (MPa ^{1/2})	δ_2 (MPa ^{1/2})
EVA 1 (460)	17.2	1.6	3.1	17.5
EVA 2 (410)	17.1	1.6	3.0	17.4

is the dispersion one, the hydrogen bonding contribution is also relatively important, due to the relatively polar character of the vinyl acetate monomer.

Conclusion

The theta solvent composition, the Hansen solubility parameter and the Flory–Huggins parameter have been obtained for two EVA copolymers with different vinyl acetate content, by means of turbidimetric and intrinsic viscosity measurements.

The obtained values of the theta solvent composition indicate that the more vinyl acetate content the polymer has, the more polar the theta solvent is, as a consequence of the increasing polar character. The vinyl acetate content is a variable which has a good influence over the Flory–Huggins parameter (the higher the vinyl acetate content, the lower the Flory–Huggins parameter), although its influence over the Hansen solubility parameter is almost unnoticeable.

References

1. Brydson JA (1999) Plastic materials. Elsevier, Oxford
2. <http://www.repsol.com/sa/herramientas/CatalogoQuimica/CatalogoQuimica.aspx>. Accessed Jan 2013
3. Sato K, Yonezu K (1984) Method for continuous copolymerization of ethylene and vinyl acetate. US Pat Number 4(485):225
4. Kawahara T, Takai M (2004) Method for manufacturing ethylene-vinyl acetate copolymer and apparatus for manufacturing the same. US Pat Number 6.831.139 B2
5. Tsai JJ, Lin LS, Chang HM, Fan KH, Lin WS (2009) The process for continuously producing ethylene-vinyl acetate copolymer and reaction system. Eur Pat EP Number 1 645 574 B1
6. Hildebrand JH (1936) The solubility of non-electrolytes. Reinhold, New York

7. Sheehan CJ, Bisio AL (1966) Polymer-solvent interaction parameter. *Rubber Chem Tech* 39:149–192
8. Hansen CM (1969) The Universality of the solubility parameter. *Ind Eng Chem Res* 8:2–11
9. Blanks RF, Prausnitz JM (1964) Thermodynamics of polymer solubility in polar and nonpolar systems. *Ind Eng Chem Fund* 3(1):1–8
10. Ovejero G, Romero MD, Díez E, Díaz I, Pérez P (2009) Thermodynamic modeling and simulation of styrene–butadiene rubbers (SBR) solvent equilibrium staged processes. *Ind Eng Chem Res* 48(16):7713–7723
11. Hansen CM (2007) Hansen solubility parameters. CRC Press, Boca Ratón
12. Brandrup J, Immergut EH (2005) *Polymer Handbook*. Wiley, New York
13. Eroğlu MS, Baysal BM, Güven O (1997) Determination of solubility parameters of poly(epichlorohydrin) and poly(glycidyl azide) networks. *Polymer* 38(8):1945–1947
14. Zhao S, Zhang W, Zhang F, Li B (2008) Determination of Hansen solubility parameters for cellulose acrylate by inverse gas chromatography. *Polym Bull* 61:189–196
15. Liu Y, Shi B (2008) Determination of Flory interaction parameters between polyimide and organic solvents by HSP theory and IGC. *Polym Bull* 61:501–509
16. Cain N, Haywood A, Roberts G, Kiserow D, Carbonell R (2011) Polystyrene/decahydronaphthalene/propane phase equilibria and polymer conformation properties from intrinsic viscosities. *J Polym Sci Part B Polym Phys* 49:1093–1100
17. Schenderlein S, Lück M, Müller BW (2004) Partial solubility parameters of poly(D, L-lactide-co-glycolide). *Int J Pharm* 286:19–26
18. Bustamante P, Navarro-Lupión J, Escalera B (2005) A new method to determine the partial solubility parameters of polymers from intrinsic viscosity. *Eur J Pharm Sci* 24(2–3):229–237
19. Ovejero G, Pérez P, Romero MD, Guzmán I, Díez E (2007) Solubility and Flory Huggins parameters of SBES, poly(styrene-*b*-butene/ethylene-*b*-styrene) triblock copolymer, determined by intrinsic viscosity. *Eur Polym J* 43(4):1444–1449
20. Huggins ML (1942) The viscosity of dilute solutions of long-chain molecules. 4. Dependence on concentration. *J Am Chem Soc* 64:2716–2718
21. Kraemer EO (1938) Molecular weights of celluloses and cellulose derivatives. *Ind Eng Chem Res* 30:1200–1203
22. Segarceanu O, Leca M (1997) Improved method to calculate Hansen solubility parameters of a polymer. *Prog Org Coat* 31(4):307–310
23. Stockmayer WH, Fixman M (1963) On the estimation of unperturbed dimensions from intrinsic viscosities. *J Polym Sci Part C* 1:137–141
24. Berry GC (1967) Thermodynamic and conformational properties of polystyrene. 2. Intrinsic viscosity studies on dilute solutions of linear polystyrenes. *J Chem Phys* 46(4):1338–1352
25. Lee JS, Kim SC (2008) Intrinsic viscosity and unperturbed dimension of poly(DL-lactic acid) solution. *Macromol Res* 16(7):631–636
26. Tang S, Dong X (2012) Theta temperatures of chlorinated poly(propene) solutions. *J Chem Eng Data* 57:1499–1501
27. Elias HG (1999) Theta solvents. In: Brandrup J, Immergut EH, Grulke EA (eds) *Polymer Handbook*, 4th edn. Wiley, New York, pp VI 291–VI 236
28. Bercea M, Morariu S (2006) Interpretation of the intrinsic viscosity–temperature dependence on the basis of the excluded volume analysis. *Rev Roum Chim* 51(1):31–37
29. Flory PJ (1941) Thermodynamics of high polymer solutions. *J Chem Phys* 9:660–661

3.2 Thermodynamic study PVAc-solvent and PE-solvent diluted solutions. Chemical Engineering Transactions

Camacho, J., Díez, E., Blanco, D., Martín, E., Ovejero, G. (2015).
Thermodynamic study PVAc-solvent and PE-solvent diluted solutions.
Chemical Engineering Transactions, 43, 1717-1722.



Thermodynamic Study of PVAc – Solvent and PE – Solvent Diluted Solutions

Javier Camacho, Eduardo Díez*, Débora Blanco, Eva Martín, Gabriel Ovejero

Departamento de Ingeniería Química, Facultad de C.C. Químicas, Universidad Complutense, Avda. Complutense s/n, 28040 Madrid, Spain
ediezalc@quim.ucm.es

The objective of this work is to develop a thermodynamic study of poly-vinyl acetate (PVAc) – methanol (MET), polyethylene (PE) – cyclohexane (CX) and polyethylene – *p*-xylene (*p*-XYL) mixtures by means of Intrinsic Viscosity (IV) technique, with the aim of obtaining the Flory Huggins polymer-solvent interaction parameter. As it can be seen, the higher is the value of viscous-average molecular weight of the polymeric materials (M_w), the higher is the IV. From the Intrinsic Viscosity data, the Flory-Huggins parameters of the studied couples were calculated following the Stockmayer-Fixman procedure. The obtained parameter, at 60 °C, of both PE – CX and PVAc – MET pairs is lower than 0.5 which, according to Flory Huggins theory, implies that, at polymer infinite dilution, the polymer and the solvent are completely compatible. However, the Flory Huggins parameter PE – *p*-XYL couple is higher than 0.5 so this couple is not completely compatible.

1. Introduction

Polyvinyl acetate (PVAc) is a highly employed thermoplastic amorphous polymer, which is commonly obtained by free radical polymerization of vinyl acetate. Additionally, polyethylene (PE) is a thermoplastic crystalline polymer which is typically obtained from ethylene polymerization.

The main applications of PVAc are as an adhesive for several porous materials like paper of wood (Harper and Petrie, 2003), while PE is basically employed in cable isolations, pipe structures or recipients manufacture (Brydson, 1999) and, recently, it residues have been used in hydrogen production (Moghadam, 2013). Additionally, the monomers of these two homopolymers can also constitute a copolymer, named ethylene – vinyl acetate copolymer, which is widely applied in tyres manufacture or as photovoltaic cells coverage (Brydson, 1999).

Among other procedures, this copolymer is industrially produced in a solution process, at temperatures around 60°C and with methanol as solvent, although other impurities, such as cyclohexane or *p*-xylene, can be present in the media after the reaction has taken place (Brydson, 1999). For this reason, it is crucial to thermodynamically characterize the polymer-solvent mixtures.

A frequent approximation to model these copolymer (such as EVA) – solvent systems is to split the polymeric material into its correspondent homopolymers and to determine the homopolymer - solvent binary interaction parameters. Because in literature the thermodynamic data of PE – solvent and PVAc – solvent systems at the temperatures of interest are seldom found, in this article we have experimentally obtained them.

One of the widely used theories to determine the polymer solvent interaction parameters is the Flory Huggins theory (Flory, 1941). As stated by this theory, in a polymer (subscript 2) – solvent (subscript 1) mixture, the solvent activity can be calculated by means of Eq(1). In this equation, a_1 is the activity of the solvent, ϕ_2 is the polymer volumetric fraction, and χ is the Flory-Huggins polymer-solvent interaction parameter.

Although originally this parameter was assumed to be composition independent, nowadays it is well established that its value changes with the relative amount of solvent in the mixture (Wolf, 2003). So, it is important to determine its value both at solvent infinite dilution and polymer infinite dilution. In this study we are focusing on

determining the Flory Huggins parameter at polymer infinite dilution as we have previously obtained the values at solvent infinite dilution.

At polymer infinite dilution, this parameter can be experimentally determined by means of Intrinsic Viscosity (IV) measurements. The Intrinsic Viscosity (IV) of a polymer – solvent mixture (denoted as $[\eta]$) is defined as the viscosity of an infinite diluted solution and its value is related to the Flory-Huggins parameter by plotting the Stockmayer-Fixman (Stockmayer and Fixman, 1963) relationship ($[\eta]/M_w^{1/2}$ vs $M_w^{1/2}$), Eq(2)), where M_w is the viscous-average polymer molecular weight, r is the ratio between the molar volume of the polymer and the molar volume of the solvent, ϕ_2 is the polymer volumetric fraction, $[\eta]_\theta$ is the IV under theta conditions V_1 is the solvent molar volume, v_2 is the polymer specific volume, ϕ_0 is the Flory universal constant (equal to 2.8E23 if the IV units are mL.g⁻¹), N_A is the Avogadro number and K_0 is the unperturbed dimension of the polymer in the studied solvent.

$$\ln(a_1) = \ln(1 - \phi_2) + \left(1 - \frac{1}{r}\right)\phi_2 + \chi\phi_2^2 \quad (1)$$

$$\frac{[\eta]}{M_w^{1/2}} = K_0 + 0,51B\phi_0 M_w^{1/2} \quad (2)$$

$$K_0 = \frac{[\eta]_\theta}{M_w^{1/2}} \quad B = \frac{v_2^2(1-2\chi)}{V_1 N_A}$$

The viscous-average polymer molecular weight, M_w , can be directly determined from Intrinsic Viscosity values with the well-known Mark-Hawking relationship (Brandrup and Immergut, 2005), Eq(3). In this equation, a and K are constants that can be taken from literature for determined polymer-solvent system.

$$[\eta] = K \cdot M_w^a \quad (3)$$

This technique has only one drawback to be overcome: the polymer and the solvent must be miscible each other in the composition range studied. For this reason, the selected pairs to study in this work are PE – cyclohexane, PE – *p*-xylene and PVAc – methanol.

2. Experimental section

2.1 Materials

All the polymeric materials were purchased from Aldrich in pellet-type form. The density values of the three PE materials are 920 kg.m⁻³ (PE1), 906 kg.m⁻³ (PE2) and 925 kg.m⁻³ (PE3). The average density of the three PVAc materials is 1180 kg.m⁻³. On the other hand, all the employed solvents (cyclohexane, CX, *p*-xylene, p-XYL, and methanol, MET) were analytical grade and were also obtained from Aldrich. They were used directly, without any purification step.

2.2 Intrinsic Viscosity Determination

The IV of each polymer-solvent mixture was determined by measuring the flow time through a capillary viscosimeter of five solutions. The most concentrated solution of each series was prepared by adding 200-300 mg of polymer over approx. 60 g of pure solvent, and then shaking until the polymer completely dissolved. The rest of solutions were prepared from the first one by adding pure solvent. Flow time measurements were carried out in a JP – Selecta Ubbelohde 0b type of capillary viscosimeter. Once prepared, each solution of the series was transferred into the viscosimeter, which was immersed in a water bath, thermo-stated at $T \pm 0.01^\circ\text{C}$. The solutions were allowed to equilibrate at the adequate temperature before starting the measurement. The accuracy of the measurements was 10⁻² s. Each flow time was measured 5 times and the average value was taken; from the flow times, relative and specific viscosities were determined.

The IV of a polymer-solvent mixture, $[\eta]$, can be calculated, from the previously described flow time measurements, with Huggins, Eq(4) and Kraemer, Eq(5) expressions (Huggins, 1942 and Kraemer, 1938).

$$\frac{\eta_{sp}}{c_2} = [\eta] + K_H [\eta]^2 c_2 \quad (4)$$

$$\frac{\ln(\eta_r)}{c_2} = [\eta] + K_K [\eta]^2 c_2 \quad (5)$$

In these equations, c_2 is the concentration of polymer solution, K_H is the Huggins coefficient, and K_K is the Kramer coefficient; relative viscosity (η_r) is the ratio between the flow time of the polymer solution through the viscosimeter, and the flow time of the pure solvent through the apparatus; finally, specific viscosity (η_{sp}) is defined as relative viscosity minus one, and represents the viscosity increasing due to the polymer. So, the Intrinsic Viscosity ($[\eta]$) can be determined as the common intercept of the Kraemer and Huggins relationships, using η_r and η_{sp} experimentally measured.

3. Results and discussion

3.1 Viscous-average molecular weight

To determine the viscous-average molecular weight of the polymeric materials (three PE samples with different molecular weight and three PVAc samples also with different molecular weight), Intrinsic Viscosity measurements of the systems PE – *p*-xylene at 75 °C and PVAc – methanol at 53 °C were carried out. Under these conditions, the Mark Hawking constants are $a = 0.63$ and $K = 0.135$ for PE – *p*-xylene system and $a = 0.59$ and $K = 0.0366$ for PVAc – methanol system (Brandrup and Immergut, 2005).

These IV (Huggins and Kraemer equations) plots are shown in Figure 1. On the other hand, the Intrinsic Viscosity values, as well as the M_w data, are summarized in Table 1. In all cases, good regression coefficients were obtained; this indicates the validity of the obtained values.

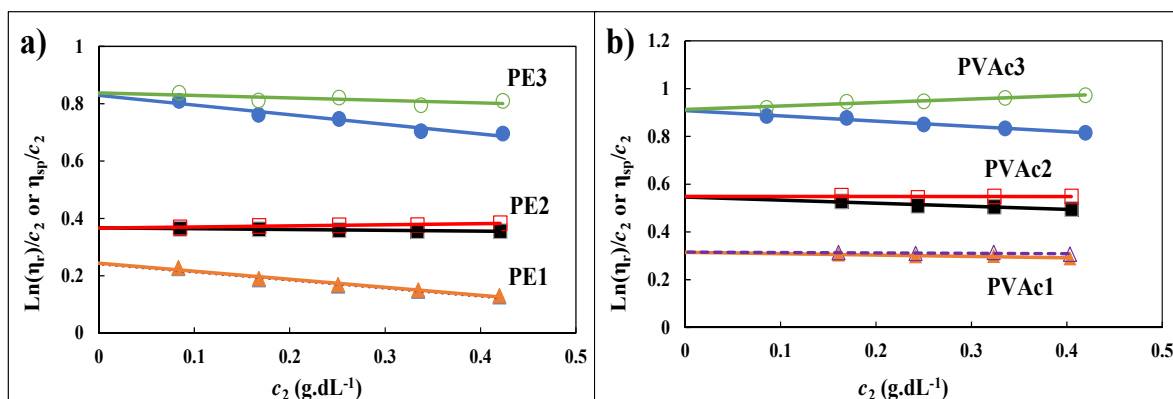


Figure 1. Huggins and Kraemer plots of PE – *p*-xylene systems at 75 °C (a) and PVAc – methanol systems at 53 °C (b)

Table 1. M_w determination of the polymeric materials

Parameter	Polymer					
	PE-1	PE-2	PE-3	PVAc-1	PVAc-2	PVAc-3
IV (dL.g ⁻¹)	0.243	0.367	0.833	0.315	0.547	0.910
Mw (kg.kmol ⁻¹)	3800	7300	26900	94400	240500	569200

3.2 Intrinsic Viscosity values at 60 °C

The Intrinsic Viscosity values, as well as the Huggins and Kraemer constants of the studied systems at 60 °C are summarized in Table 2.

Figures 2, 3 and 4 show the Huggins and Kraemer plots for the studied systems. In all cases, good regression coefficients were reached, except for the system PE3 – CX. This can be related to the fact that experimentally was quite difficult to completely dissolve this couple.

As it could be expected, the higher the molecular weight is, the higher the Intrinsic Viscosity values are, The systems where the lower influence of molecular weight on IV is less noticeable is PE – p-XYL because, as seen in Figure 3, the IV of PE2 ($M_w = 7300 \text{ g.mol}^{-1}$) with this solvent is practically equal to the IV of p-XYL with PE3 ($M_w = 26900 \text{ g.mol}^{-1}$).

Apart from the Intrinsic Viscosity value, a good criterion to ascertain if a solvent will be suitable for a determined polymer is the difference between Huggins and Kraemer constants. The closer this difference to 0.5, the more compatible the polymer and the solvent are. According to this criterion, all couples are compatible (at low polymer compositions) except PE3 – CX and PE1 – p-XYL and PE2 – p-XYL. This is in agreement with what was experimentally observed as these systems were the most difficult to completely dissolve.

Table 2. Intrinsic Viscosity values

System	IV (dL.g^{-1})	K_H	K_K	$K_H - K_K$
PE-1 - CHX	0.138	-1.248	-1.663	0.415
PE-2 - CHX	0.423	0.650	0.100	0.550
PE-3 - CHX	0.848	-0.591	-0.962	0.371
PE-1 - p-XYL	0.201	-3.203	-3.414	0.211
PE-2 - p-XYL	0.465	-0.604	-0.932	0.328
PE-3 - p-XYL	0.415	-0.196	-0.606	0.410
PVAc-1 - MET	0.327	-0.287	-0.686	0.399
PVAc-2 - MET	0.510	0.360	-0.145	0.505
PVAc-3 - MET	0.938	0.168	-0.266	0.434

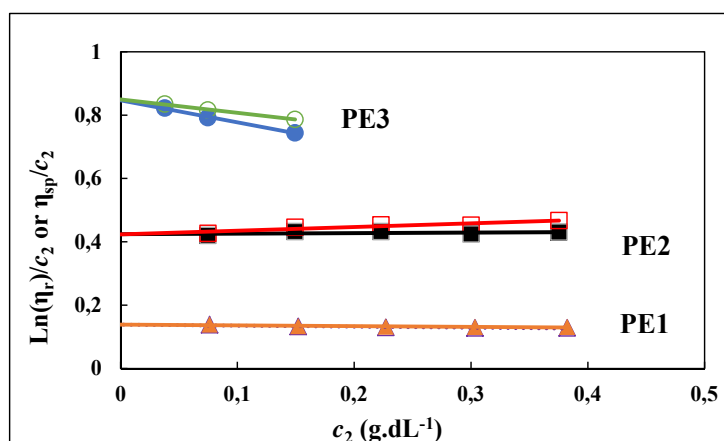


Figure 2. Huggins and Kraemer plots for polyethylene – cyclohexane systems

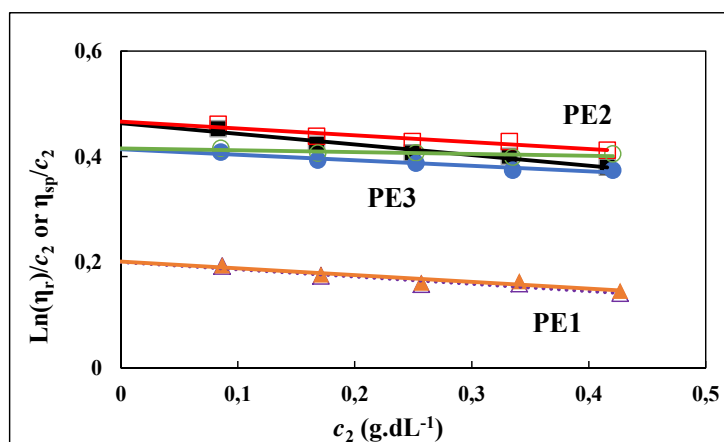


Figure 3. Huggins and Kraemer plots for polyethylene - p-xylene systems

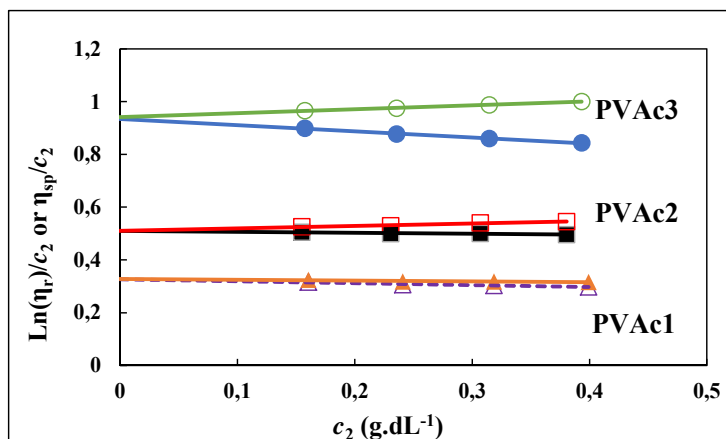


Figure 4. Huggins and Kraemer plots for polyvinyl acetate - methanol systems

3.3 Flory Huggins parameters

Having obtained the viscous-average molecular weight of the materials, the Stockmayer-Fixman plots ($[\eta]/M_w^{1/2}$ vs $M_w^{1/2}$) were carried out, as it can be seen in Figure 5, for each polymer – solvent pair. The plots were done at 60 °C for the three mixtures but also at 75 °C for PE – CX mixture and at 53 °C for PVAc – MET mixture. From the slopes, it could possible to obtain the Flory Huggins parameter (χ) for each couple, while the K_0 values were calculated from the intercepts. These data are summarized in Table 3.

To obtain the Flory Huggins parameter, it was necessary to calculate the specific volumes (v_2) of the polymers and the molar volumes of the solvents (V_1). The first data were determined from the densities of the polymeric materials (906 kg.m⁻³ for PE and 1180 kg.m⁻³ for PVAc), while the second data were calculated from the solvent densities at different temperatures (NIST, 2014).

Table 3. Flory Huggins parameter and K_0 value for the studied pairs at 60°C

Couple	K_0 (mL.g ⁻¹)	χ
PE – CX at $T = 60$ °C	0.183	0.065
PE – <i>p</i> -XYL at $T = 60$ °C	0.526	0.825
PE – <i>p</i> -XYL at $T = 75$ °C	0.331	0.281
PVAc – MET at $T = 53$ °C	0.091	0.495
PVAc – MET at $T = 60$ °C	0.090	0.495

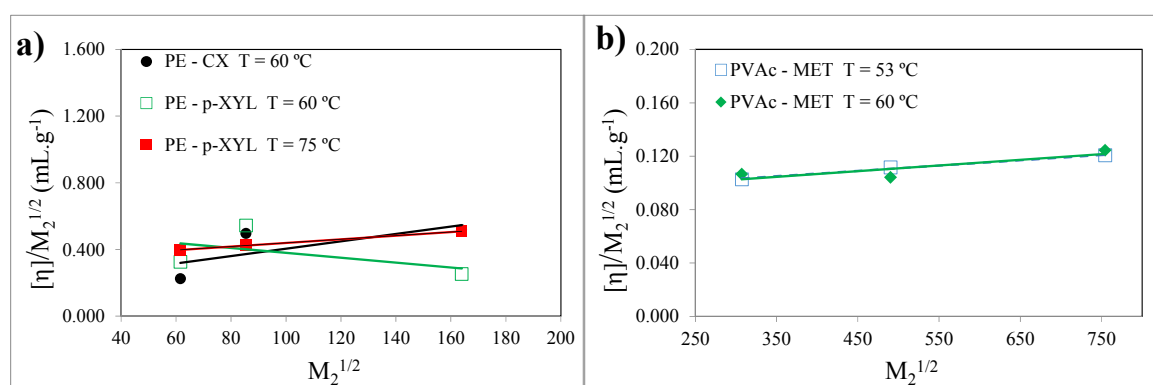


Figure 5. Stockmayer-Fixman plots of PE – *p*-xylene and PE – cyclohexane mixtures (a) and PVAc – methanol mixture (b)

As it can be noticed in Table 3, the Flory Huggins parameter for PE – CX and PVAc – MET pairs is lower than 0.5. According to Flory Huggins model, this implies that, in the studied composition interval, the polymer and the solvent are completely compatible. On the other hand, the Flory Huggins parameter PE – *p*-XYL couple is

higher than 0.5 so this couple is not completely compatible. This is in agreement with what experimentally was observed and has previously commented.

Regarding the K_0 values, it can be also noticed that the higher value correspond to PE – p-XYL couple. This parameter is known as unperturbed dimension and is a measurement of the dimensions of the polymer random coil in a solvent media and in theta estate (an estate in which polymer-solvent interactions and balanced with polymer-polymer interactions). The higher this value, the less importance of polymer-solvent interactions compared with polymer-polymer interactions.

In Figure 2 it can be noticed that the Stockmayer-Fixman plot is quite accurate for PVAc – Methanol couple, although it is not for the other two pairs. However, the Flory Huggins parameters obtained for PE- CX and PE – p-XYL pairs at 60 °C, are in between the expected interval, as they are in agreement with the values of this parameter at lower temperatures (Brandrup and Immergut, 2005).

4. Conclusions

Intrinsic Viscosity measurements have been carried out for polyethylene – cyclohexane, polyethylene – p-xylene and polyvinyl acetate – methanol systems have been carried out with the aim of obtaining the Flory Huggins parameters by means of the Stockmayer – Fixman procedure. To perform this it was previously necessary to determine the viscous-average molecular weight of the employed polymer, what was done by means of Mark Hawking relationship with Mark Hawking parameters taken from literature. These molecular weights were accurately obtained as, in all cases, good adjustment parameters were achieved.

The Flory Huggins results indicate that, in the studied composition interval, the most compatible pairs are polyethylene – cyclohexane and polyvinyl acetate – methanol, as the Flory Huggins parameter is below 0.5. This is supported by means of the Intrinsic Viscosity and K_0 obtained values.

References

- Brandrup J., Immergut E.H., Eds., 2005, Polymer Handbook. John Wiley & Sons, New York, United States.
- Brydson J.A., 1999, Plastic Materials. Elsevier, Oxford, United Kingdom.
- Flory P.J., 1941, Thermodynamic of high polymer solutions, J. Chem. Phys. 9, 660-661.
- Harper C.A., Petrie E.M., 2003, Plastic Materials and Processes: a concise enciclopedia. John Wiley & Sons, New York, United States.
- Huggins M.L., 1942, The viscosity of dilute solutions of long-chain molecules. 4. Dependence on concentration, J. Am. Chem. Soc. 64, 2716-2718.
- Kraemer E.O., 1938, Molecular weights of celluloses and cellulose derivatives, Ind. Eng. Chem. Res. 30, 1200-1203.
- Moghadam R.A., Yusup S., Lam H.L., Al Shoaibi A., Ahmad M.M., 2013, Hydrogen production from mixture of biomass and polyethylene waste in fluidized bed catalytic steam co-gasification process, Chemical Engineering and Transactions, 35, 565-570, DOI: 10.3303/CET1335094.
- NIST (National Institute of Standards and Technology), 2014, < <http://webbook.nist.gov/chemistry/>> accessed 15.09.2014.
- Stockmayer W.H., Fixman M., 1963, On the estimation of unperturbed dimensions from Intrinsic Viscosities, J. Polym. Sci. Part. C 1, 137-141.
- Wolf B.A., 2003, Chain connectivity and conformational variability of polymers: clues to an adequate thermodynamic description of their solutions, 2 - Composition dependence of Flory-Huggins interaction parameters, Macromol. Chem. Phys. 204(11), 1381-1390.

3.3 Generalization of a Double-Point Method to determine the Intrinsic Viscosity in a Polymer-Solvent Mixture

Díez, E., Díaz, I., Camacho, J., Ovejero, G., & Romero, M. (2013). Generalization of a Double-Point Method to determine the Intrinsic Viscosity in a Polymer-Solvent Mixture. 11th International Conference on Chemical and Process Engineering.



Generalization of a Double-Point Method to Determine the Intrinsic Viscosity in a Polymer-Solvent Mixture

Eduardo Díez^{a,*}, Ismael Díaz^b, Javier Camacho^a, Gabriel Ovejero^a, María D. Romero^a

^aDepartamento de Ingeniería Química, Facultad de C.C. Químicas, Universidad Complutense, Avda. Complutense s/n, 28040 Madrid, Spain

^bDepartamento de Ingeniería Química Industrial y del Medio Ambiente, Universidad Politécnica de Madrid, C/José Gutiérrez Abascal 2, 28006 Madrid, Spain
ediezalc@quim.ucm.es

A double-point method proposed in literature for the determination of the Intrinsic Viscosity of a polymer-solvent solution and based on the Ram-Moham-Rao single point equation, have been extended to all single-point expressions available in literature. To assess the validity of the method, Intrinsic Viscosity values of several rubber-solvent mixtures, calculated following the classical procedure of looking for the common intercept of Huggins and Kraemer plots, have been compared with the ones calculated by means of the double-point methods. The deviations between the results obtained by both methodologies allows assuring that double-point equations are a reliable alternative of Huggins and Kraemer plots to determine Intrinsic Viscosity values.

1. Introduction

In the last decades, the importance of polymer-type materials is growing exponentially, as a consequence of their almost infinite range of applications. Because most of them are obtained by means of dissolution processes (Miller-Chou and Koenig, 2003), the rheology of the polymer-solvent systems is really important (Kraguljac et al., 2009). Besides, the intrinsic viscosity technique is one of the most employed methodologies with the aim of obtaining thermodynamic parameters of such mixtures (Mehrdad et al., 2011), such as Infinite Dilution coefficients.

The Intrinsic Viscosity ($[\eta]$) is the viscosity of an infinite diluted polymer solution. It is usually calculated from flow time measurements which are extrapolated to infinite dilution by means of Huggins (1942), Kraemer (1938) or Schulz-Blaschke (1941) expressions (Eqs 1, 2 and 3).

$$\frac{\eta_{sp}}{c} = [\eta] + K_H [\eta]^2 c \quad (1)$$

$$\frac{\ln(\eta_r)}{c} = [\eta] + K_K [\eta]^2 c \quad (2)$$

$$\frac{\eta_{sp}}{c} = [\eta] + K_{SB} [\eta] \eta_i \quad (3)$$

In these equations, c is the concentration of polymer solution, K_H is the Huggins constant, K_K is the Kramer constant and K_{SB} is the Schulz-Blaschke constant. Relative viscosity (η_r) is obtained as the relation between the flow time of the polymer solution through a capillary tube of known diameter and length and the flow time of the pure solvent through the same capillary tube. Specific viscosity (η_{sp}) is defined as relative viscosity minus one, and represents the viscosity increasing due to the polymer. The intrinsic

viscosity ($[\eta]$) is usually obtained from intercept of the Kraemer, Huggins or Schulz-Blaschke relationships, using η_r and η_{sp} experimentally determined for different polymer solutions; theoretically, $K_K + K_H = 0.5$.

However, single-point equations have been proposed with the aim of determining the intrinsic viscosity by a single flow-time measurement. The most important expressions are the Solomon-Ciuta (1963) one, Eq 4 the Deb-Chatterjee (1968) one, Eq 5, the Ram-Mohan-Rao (1986) one, Eq 6, the Kuwahara (1963) one, Eq 7 and the Palit and Kar (1967) one, Eq 8.

$$[\eta] = \frac{1}{c} \sqrt{2\eta_{sp} - 2\ln(\eta_r)} \quad (4)$$

$$[\eta] = \frac{1}{2c} \sqrt{3\ln(\eta_r) + \frac{3}{2}(\eta_{sp})^2 - 3\eta_{sp}} \quad (5)$$

$$[\eta] = \frac{1}{2c} [\eta_{sp} + \ln(\eta_r)] \quad (6)$$

$$[\eta] = \frac{1}{4c} [\eta_{sp} + 3\ln(\eta_r)] \quad (7)$$

$$[\eta] = \frac{1}{c} \sqrt{4\eta_{sp} - 2\eta_{sp}^2 + \frac{4}{3}\eta_{sp}^3 - 4\ln(\eta_r)} \quad (8)$$

The former expressions are based on assuming $K_K + K_H = 0.5$ and have the advantage of being capable of extrapolating to infinite dilution by means of a single experimental measurement, while for applying Huggins or Kraemer plots, at least five measurements should be desirable. However, the main drawback of employing these expressions is that the final Intrinsic Viscosity result can be different depending on the polymer concentration in the solution employed to perform the single-point measurement.

So, for all the reasons stated above, recently Curvale and Cesco (2009) proposed an intermediate strategy named as double-point equation, based on the Ram-Mohan-Rao expression, which is represented in Equation 9. In this equation, c_1 and c_2 are concentrations of the two polymer solutions (being $c_2 > c_1$), $\eta_{r,1}$ and $\eta_{r,2}$ are the relative viscosities, and $\eta_{sp,1}$ and $\eta_{sp,2}$ are the specific viscosities.

$$[\eta] = \frac{1}{2} \frac{c_2}{c_2 - c_1} \left[\frac{\eta_{sp,1}}{c_1} + \frac{\ln(\eta_{r,1})}{c_1} \right] - \frac{1}{2} \frac{c_1}{c_2 - c_1} \left[\frac{\eta_{sp,2}}{c_2} + \frac{\ln(\eta_{r,2})}{c_2} \right] \quad (9)$$

So the final aim of this paper is to generalize the double-point method by extending it not only to Ram-Mohan-Rao expression but also to any single-point equation, and analysing its validity by comparing the obtained results with previously calculated ones by means of the classical procedure of seeking the common intercept of Huggins and Kraemer equations.

2. Theoretical background

Assuming two polymer-solvent solutions of compositions c_1 and c_2 (being $c_2 > c_1$), their Intrinsic Viscosities determined by any of the single-point equations will be $[\eta]_1$ and $[\eta]_2$, respectively. These values should be equal because the Intrinsic Viscosity is defined as an extrapolation of the viscosity to infinite dilution conditions; however, due to all single point methods make this extrapolation from only one concentration point, the final Intrinsic Viscosity value is not the same in both cases. So, a reasonable approximation could be considering that the true Intrinsic Viscosity value is in between the points $(c_1, [\eta]_1)$ and $(c_2, [\eta]_2)$. Assuming a linear relationship, the slope (m) of the straight line joining the points $(c_1, [\eta]_1)$ and $(c_2, [\eta]_2)$ will be (Eq 10):

$$m = \frac{[\eta]_2 - [\eta]_1}{c_2 - c_1} \quad (10)$$

If we now consider a generic point i (whose concentration is c_i) belonging to the previous straight line, its Intrinsic Viscosity ($[\eta]_i$) will be able to be calculated with Eq (11), taking into account that the slope of the line is described by means of Eq 10.

$$[\eta]_i = m(c_i - c_1) + [\eta]_1 = \left(\frac{[\eta]_2 - [\eta]_1}{c_2 - c_1} \right) (c_i - c_1) + [\eta]_1 \quad (11)$$

If we now consider the case when c_i tends to 0 (because the Intrinsic Viscosity is the viscosity of an infinite polymer solution), the Eq 11 is transformed into Eq 12.

$$[\eta]_{c \rightarrow 0} = \left(\frac{c_2}{c_2 - c_1} \right) [\eta]_1 - \left(\frac{c_1}{c_2 - c_1} \right) [\eta]_2 \quad (12)$$

In this last expression, the terms $[\eta]_1$ and $[\eta]_2$ can be replaced by any of the Eqs 4 to 8.

The final result is that the Intrinsic Viscosity of whatever polymer-solvent mixture can be determined with Eq 12, by simply two flow-time measurements at two different compositions, c_1 and c_2 , and calculating the relative and specific viscosities (which appear in $[\eta]_1$ and $[\eta]_2$ terms) by any Eq from 4 to 8.

3. Results and discussion

To assess the reliability of the generalized double-point proposed here, we have compared the results that we have previously determined for different poly (styrene-butadiene) rubber-cyclohexane mixtures at 30 °C, following the classical procedure of finding the common intercept of Huggins and Kraemer plots, with the obtained values with the Eq 12 combined with all the Eqs 4 to 8.

The studied polymers employed as examples were, on one hand a poly (styrene-*b*-butene/ethylene-*b*-styrene) triblock copolymer (SEBS) (Ovejero et al., 2007) and, on the other hand, three poly (styrene – butadiene – styrene) triblock copolymers (SBSs) with different structure and styrene content, named C411, C500 and C501 respectively (Ovejero et al., 2010). The main characteristics of these materials are summarized in Table 1. The Table also shows the Intrinsic Viscosity values ($[\eta]$) of each cyclohexane-polymer mixtures, obtained from the common intercept of Huggins and Kraemer plots (values named as $[\eta]_{real}$).

Table 1. Main characteristics of the employed polymers

POLYMER	Mw (kg/kmol)	ρ (kg/m ³)	$[\eta]_{real}$ at 30 °C
SEBS	86000	960	0.938
C411	237000	908	1.250
C500	78000	931	0.709
C501	113000	929	0.952

On the other hand, Tables 2 to 5 show the Intrinsic Viscosity values determined for each cyclohexane-polymer-binary mixture at different compositions with any single-point (subscript 1) or double point (subscript 2) method (values named as $[\eta]_{calc}$).

As it can be observed, the double-point methods perform, in many cases, better estimations than the single-point methods, especially when working with the most diluted compositions; this is especially noticeable in the case of the mixtures with C411 and C500 rubbers. To further reinforce what previously said, Figures 1 and 2 show the deviations of the $[\eta]_{calc}$ values with respect to the $[\eta]_{real}$ values. The deviations have been calculated according to Eq 13.

$$\text{Deviation} = \text{abs} \left(\frac{[\eta]_{real} - [\eta]_{calc}}{[\eta]_{real}} 100 \right) \quad (13)$$

Table 2. $[\eta]$ Values obtained by single and double point methods when comparing with Table 1 values, for cyclohexane – SEBS mixtures

PROCEDURE	COMPOSITIONS (g/dL)				
	0.401	0.322	0.233	0.128	0.078
	$[\eta]_{\text{calc}}$ at 30 °C				
(Solomon-Ciuta) ₁	0.924	0.901	0.944	0.938	0.935
(Deb-Chatterjee) ₁	0.952	0.923	0.961	0.947	0.941
(Ram-Mohan-Rao) ₁	0.955	0.925	0.963	0.948	0.941
(Kuwahara) ₁	0.913	0.892	0.937	0.934	0.932
(Palit and Kar) ₁	0.969	0.936	0.972	0.953	0.944
(Solomon-Ciuta) ₂		0.810	1.056	0.930	0.931
(Deb-Chatterjee) ₂		0.804	1.062	0.930	0.930
(Ram-Mohan-Rao) ₂		0.801	1.061	0.929	0.930
(Kuwahara) ₂		0.809	1.053	0.930	0.930
(Palit and Kar) ₂		0.801	1.065	0.930	0.930

Table 3. $[\eta]$ Values obtained by single and double point method when comparing with Table 1 values, for cyclohexane – C411 mixtures

PROCEDURE	COMPOSITIONS (g/dL)				
	0.416	0.333	0.249	0.167	0.083
	$[\eta]_{\text{calc}}$ at 30 °C				
(Solomon-Ciuta) ₁	1.292	1.296	1.286	1.267	1.261
(Deb-Chatterjee) ₁	1.350	1.342	1.320	1.289	1.273
(Ram-Mohan-Rao) ₁	1.360	1.348	1.324	1.291	1.273
(Kuwahara) ₁	1.273	1.279	1.273	1.258	1.256
(Palit and Kar) ₁	1.385	1.370	1.341	1.303	1.279
(Solomon-Ciuta) ₂		1.308	1.259	1.229	1.256
(Deb-Chatterjee) ₂		1.309	1.257	1.227	1.256
(Ram-Mohan-Rao) ₂		1.302	1.252	1.224	1.255
(Kuwahara) ₂		1.300	1.255	1.227	1.255
(Palit and Kar) ₂		1.309	1.255	1.225	1.255

Table 4. $[\eta]$ Values obtained by single and double point method when comparing with Table 1 values, for cyclohexane – C500 mixtures

PROCEDURE	COMPOSITIONS (g/dL)				
	0.392	0.313	0.235	0.157	0.078
	$[\eta]_{\text{calc}}$ at 30 °C				
(Solomon-Ciuta) ₁	0.719	0.723	0.715	0.712	0.713
(Deb-Chatterjee) ₁	0.736	0.736	0.725	0.719	0.717
(Ram-Mohan-Rao) ₁	0.738	0.737	0.726	0.719	0.717
(Kuwahara) ₁	0.713	0.717	0.711	0.709	0.712
(Palit and Kar) ₁	0.747	0.745	0.731	0.723	0.719
(Solomon-Ciuta) ₂		0.736	0.692	0.706	0.714
(Deb-Chatterjee) ₂		0.737	0.691	0.706	0.714
(Ram-Mohan-Rao) ₂		0.736	0.690	0.706	0.714
(Kuwahara) ₂		0.735	0.691	0.706	0.714
(Palit and Kar) ₂		0.737	0.690	0.706	0.714

Table 5. $[\eta]$ Values obtained by single and double point method when comparing with Table 1 values, for cyclohexane – C501 mixtures

PROCEDURE	COMPOSITIONS (g/dL)				
	0.395	0.316	0.237	0.158	0.079
	$[\eta]_{\text{calc}}$ at 30 °C				
(Solomon-Ciuta) ₁	0.939	0.932	0.941	0.957	0.944
(Deb-Chatterjee) ₁	0.968	0.955	0.958	0.969	0.950
(Ram-Mohan-Rao) ₁	0.971	0.957	0.960	0.969	0.950
(Kuwahara) ₁	0.928	0.923	0.933	0.951	0.941
(Palit and Kar) ₁	0.986	0.969	0.969	0.976	0.953
(Solomon-Ciuta) ₂		0.905	0.966	0.989	0.931
(Deb-Chatterjee) ₂		0.904	0.967	0.990	0.931
(Ram-Mohan-Rao) ₂		0.901	0.966	0.989	0.930
(Kuwahara) ₂		0.903	0.964	0.988	0.931
(Palit and Kar) ₂		0.903	0.968	0.991	0.931

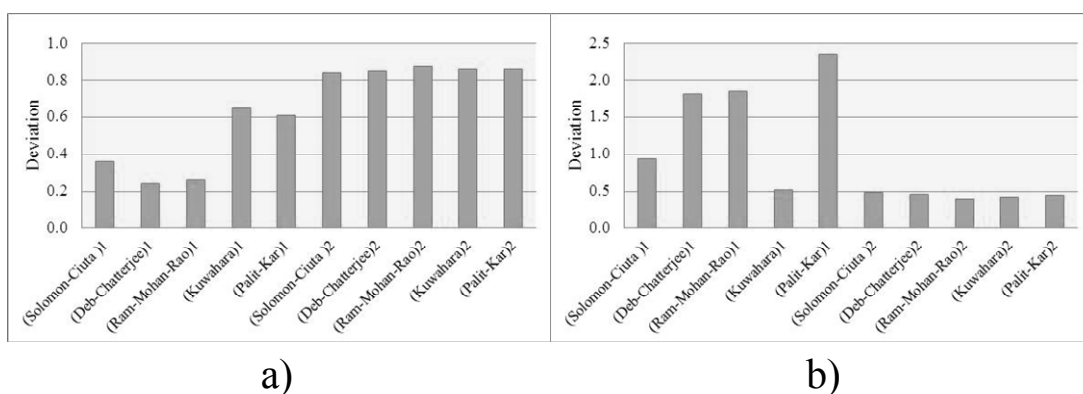


Figure 1. Deviations of the $[\eta]_{\text{calc}}$ values with respect to the $[\eta]_{\text{real}}$ values, for a) cyclohexane – SEBS mixture and b) cyclohexane – C411 mixture

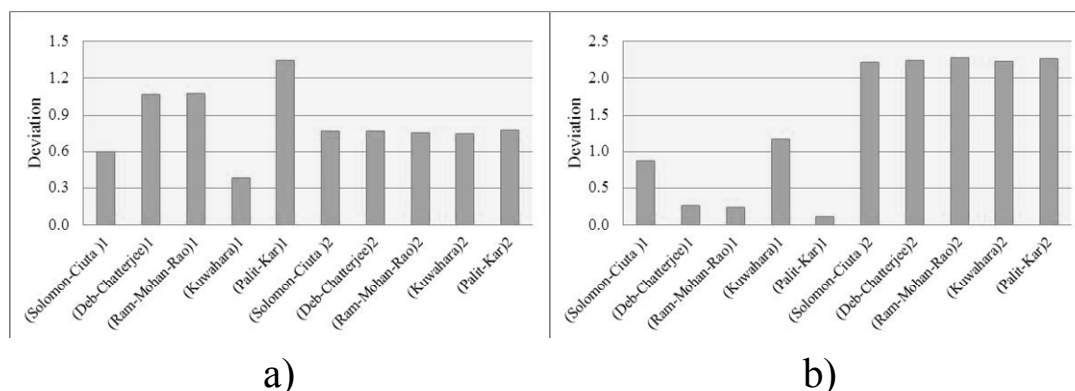


Figure 2. Deviations of the $[\eta]_{\text{calc}}$ values with respect to the $[\eta]_{\text{real}}$ values, for a) cyclohexane – C500 mixture and b) cyclohexane – C501 mixture

Another important point is that both single-point and double-point methods approximate better to the “real” Intrinsic Viscosity value (being the “real” value the one obtained by getting the common slope of Huggins and Kraemer plots) whenever the compositions are as low as possible. This seems to be logical, taking into account that Intrinsic Viscosity is defined as the viscosity of an infinite diluted polymer-solvent solution. As a final remark simply comment that double-point methods have demonstrated to be a reliable alternative to obtain accurate values on Intrinsic Viscosity. With them, it is possible to achieve a reasonable time saving because one two experimental points are needed, while to draw a proper straight line are necessary at least five points.

4. Conclusion

A generalized double-point method to determine the Intrinsic Viscosity of a polymer-solvent mixture is proposed here. The assessment of this method was done by comparing the Intrinsic Viscosity values obtained by this method, with the ones obtained following the traditional procedure (common intercept of Huggins and Kraemer plots). In all cases a good agreement between both methodologies was reached, especially when applying the low composition values to the double-point method.

References

- Curvale R.A., Cesco J.C., 2009, Intrinsic viscosity determination by "single point" and "double point equations". *Appl. Rheol.* 19, 53347-53352.
- Deb P.C., Chatterjee S.R., 1968, Unperturbed dimension of polymer molecules from viscosity measurements, *Die Makromolekulare Chemie* 120, 49-57.
- Huggins M.L., 1942, The viscosity of dilute solutions of long-chain molecules. 4. Dependence on concentration, *J. Am. Chem. Soc.* 64, 2716-2718.
- Kraemer E.O., 1938, Molecular weights of celluloses and cellulose derivatives, *Ind. Eng. Chem. Res.* 30, 1200-1203.
- Kragulac K., Soljic I., Vidovic E., Jukic A., 2009, Miscibility and interactions of rheology improvers based on functional polymethacrylate in toluene solutions, *Chemical Engineering Transactions*, 17, 1741-1746, DOI: 10.3303/CET17291.
- Kuwahara N., 1963, On the polymer-solvent interaction in polymer solutions. *J. Polym. Sci. A* 1, 2395-2406.
- Mehrdad A., Saghatforoush L.A., Marzi G., 2011 Effect of temperature on the intrinsic viscosity of poly(ethylene glycol) in water/dimethyl sulfoxide solutions, *J. Molec. Liquids* 161, 153-157.
- Miller-Chou B.A., Koenig J.L., 2003, A review of polymer dissolution, *Prog. Polym. Sci.* 28, 1223:1270.
- Ovejero G., Perez P., Romero M.D., Guzman I., Díez E., 2007, Determination of solubility parameters of polymers by using intrinsic viscosity method, *Proceedings of European Congress of Chemical Engineering (ECCE-7)* 2, 69-70 Copenhagen.
- Ovejero G., Romero M.D., Díez E., Díaz I., 2010 Thermodynamic interactions of three SBS (styrene-butadiene-styrene) triblock copolymers with different solvents, by means of intrinsic viscosity measurements, *Eur. Polym. J.* 46, 2261-2268.
- Palit S.R., Kar I., 1967, Polynomial expansion of log relative viscosity and its application to polymer solutions, *J. Polym. Sci.* 5, 2629-2632.
- Ram-Mohan-Rao M.V., Yassen M., 1986, Determination of intrinsic viscosity measurement, *J. Appl. Polym. Sci.* 31, 2501-2508.
- Schulz G.V., Blaschke F., 1941, An equation for calculating the viscosity number for very small compositions, *J. Prakt. Chem.* 158, 130-138.
- Solomon O.F., Ciuta I.Z., 1962, Determination de la viscosité intrinsèque de solutions de polymères par una simple détermination de la viscosité, *J. Appl. Polym. Sci.* 6, 683-685.

3.4 Summary and Discussion

The previous three scientific articles about the determination and evaluation of the Flory Huggins parameters of the EVA copolymers and/or their homopolymers (Polyethylene, PE, and Polyvinylacetate, PVA) at infinite dilutions of polymers ($\phi_p \rightarrow 0$), by means of the Intrinsic Viscosity technique (IV), can be summarized and integrate as follows:

The first article “**Turbidimetric and intrinsic viscosity study of EVA copolymer/solvent systems**” presents the Flory Huggins interaction parameters of the two semicrystalline EVA copolymers samples, with different vinyl acetate content (18% and 33% w/w), determined in presence of five different diluent solvents at 30, 40 and 50 °C. These Flory Huggins parameters were calculated according the Stockmayer and Berry relationships, which takes into account the overall and the theta intrinsic viscosities, for each polymer solvent mixture. The first viscosity one was determined from the Huggins-Kramer plot, and the second one from the turbidimetric Elias method. In addition a thermodynamic assessment was done at these infinite dilutions conditions of polymer, that also consider the evaluation of the intrinsic viscosities under theta conditions, the Hansen solubility parameters of the EVAs samples, and the entropic and enthalpy contributions over the Flory Huggins parameters.

The main results indicate that all the solvents are clearly compatible with the copolymers ($\chi \leq 0.6$), which is expected due the diluent character of the solvents. Also it was found that the EVAs/solvents interactions are quite stronger ($\Delta\chi \approx 0.1$) in the case of the copolymer with the highest vinyl acetate percentage. In addition the Hansen solubility parameters were determined, obtaining almost the same value ($17.5 \text{ MPa}^{1/2}$ for EVA33 and $17.4 \text{ MPa}^{1/2}$ for EVA18, at 30 °C), highlighting the presence of the triple contribution for dispersion, polar an association interactions, of these copolymers.

Finally, from this article it is also crucial to take into account the results of the Flory Huggins parameters of the EVA copolymers samples in presence of cyclohexane, which will be employed in the further articles. They are summarized in table 3.1.

Table 3.1 Flory Huggins parameters for EVA18 and EVA33 in cyclohexane

Solvent	χ EVA 18% VA			χ EVA 33% VA		
	30 °C	40 °C	50 °C	30 °C	40 °C	50 °C
Cyclohexane (CH)	0.563	0.496	0.495	0.490	0.473	0.482

In the second article, “**Thermodynamic Study of PVAc/Solvent and PE/Solvent Diluted Solutions**” the Flory Huggins interaction parameters of two mixtures, Polyethylene (PE) in presence on cyclohexane, and Polyvinylacetate in methanol, were determined at 60 °C, by means of intrinsic viscosity measurements, following the Stockmayer-Fixman procedure that need at least two more samples for PE and PVA. Previously the viscous average molecular weights of all the polymers employed were obtained through the Mark-Houwink procedure. In addition a thermodynamic assessment was done at these infinite dilutions conditions of polymer, that also consider the evaluation of the viscous-average molecular weight and the intrinsic viscosities of the entire polymers employed. Additionally the system PE/p-xylene was studied.

According to the main results the obtained Flory Huggins parameter were lower than 0.5, which implies that at infinite dilution of polymer, the mentioned systems are completely compatible, being the more favorable miscible interactions for the PE/cyclohexane mixture.

From this article it is also crucial to take into account the results the Flory Huggins parameters of such PE/cyclohexane and PVA/methanol systems. They are summarized in table 3.2.

Table 3.2 Flory Huggins parameters for PE/cyclohexane and PVA/methanol

Solvent	χ PE	χ PVA
	60 °C	60 °C
Metanol (MET)	-	0.495
Cyclohexane (CH)	0.065	-

Finally the third article, “**Generalization of a Double-Point Method to determine the Intrinsic Viscosity in a Polymer-Solvent Mixture**”, is presented as an annex, in order to propose an easier method to determine the experimental intrinsic viscosity, from the experience in the previous works, in the determination of the Huggins-Kraemer (HK) plots, which need at least five measurements and therefore five mixtures at infinite dilution of polymer, which can be tedious and over-timed. Moreover, although single-point methods to determine the intrinsic viscosity exist, generally these final results can be different depending on the polymer concentration in the solution employed. In this work an intermediate strategy named as double-point equation, based on the Ram-Mohan-Rao expression was generalized to any single-point equation, and was validated for several rubber-solvent mixtures, obtaining %AAD respect to HK values below to 2.5%.

4 Thermodynamics of solvent/solvent mixtures involved in the EVA solution process

This chapter presents one scientific article published in the framework of the project global, and a final discussion, which are focused on the determination of the thermodynamic interaction parameters between the solvents implicated in the EVA solution process (methanol/vinyl acetate and butanol/vinyl acetate).

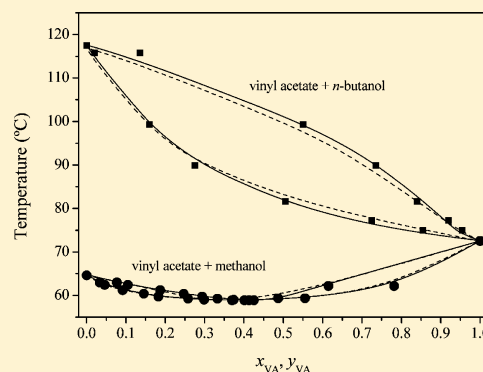
At the end of the discussion of the article, the PC-SAFT model parameters are cited, for the system methanol/vinyl acetate. In this project, methanol has been selected as the solvent sample on the EVA solution process.

4.1 Vapor–Liquid Equilibrium at p/kPa = 101.3 of the Binary Mixtures of Ethenyl Acetate with Methanol and Butan-1-ol

Camacho, J., Díez, E., Díaz, I., & Ovejero, G. (2012). Vapor–Liquid Equilibrium at p/kPa= 101.3 of the Binary Mixtures of Ethenyl Acetate with Methanol and Butan-1-ol. *Journal of Chemical & Engineering Data*, 57(11), 3198-3202.

Vapor–Liquid Equilibrium at $p/\text{kPa} = 101.3$ of the Binary Mixtures of Ethenyl Acetate with Methanol and Butan-1-olJavier Camacho,[†] Eduardo Díez,^{*,†} Ismael Díaz,[‡] and Gabriel Ovejero[†][†]Grupo de Catálisis y Procesos de Separación (CyPS), Departamento de Ingeniería Química, Facultad de C. Químicas, Universidad Complutense de Madrid, Avda. Complutense s/n, 28040 Madrid, Spain[‡]Departamento de Ingeniería Química Industrial y del Medio Ambiente, Escuela Técnica Superior de Ingenieros Industriales, Universidad Politécnica de Madrid, C/José Gutiérrez Abascal 2, 28006 Madrid, Spain

ABSTRACT: The vapor–liquid equilibrium (VLE) at the constant pressure of $p/\text{kPa} = 101.3$ has been determined for the binary mixtures of ethenyl acetate with both methanol and butan-1-ol. The consistency of the data was checked with the Wisniak L–W test, and the data were found to be consistent. The experimental data were also satisfactorily adjusted to nonrandom two-liquid (NRTL) and universal quasichemical (UNIQUAC) activity coefficient models, as well as to Peng–Robinson and perturbed-chain statistical associating fluid theory (PC-SAFT) equations of state, with the aim of obtaining the binary interaction parameters of both mixtures. With these parameters, the VLE of both mixtures can be accurately predicted, which includes the azeotropic point of the ethenyl acetate + methanol pair. The PC-SAFT and Peng–Robinson equations of state were also employed as purely predictive.



1. INTRODUCTION

Recently, distillation-based processes are gaining importance as a reliable alternative to separate a wide variety of binary and also multicomponent systems. As a consequence, the importance of accurately knowing the vapor–liquid equilibrium (VLE) data of these systems is extremely high, if wanting to calculate the dimensions of the equipment which is necessary to carry out the separation.

In many polymer production processes, after the polymerization step, there are VLE-based stages, such as distillation or devolatilization, with the aim of purifying the desired product as well as the unreacted monomers; such is the case of the ethylene–ethenyl acetate copolymer (EVA). This copolymer is becoming one of the most important polymeric materials due to its wide range of applications (coatings of photovoltaic cells, tires, cables, etc.), depending on the ethenyl acetate content.^{1,2}

When the ethenyl acetate content of the final product is between 40 % and 70 %, the copolymer is usually obtained by a solution process, the most common solvents being methanol and butan-1-ol.³ In these processes, although the polymerization reaction is clearly the core of the overall process, both purification and separation steps are equally important, to obtain a final product with the required specifications, but also to recover as much unreacted monomers as possible and to purify the solvent, so that the process is economically feasible.⁴ The importance of recovering the ethenyl acetate is due to this compound is one of the two monomers which constitute the EVA copolymer.

In the EVA solution process, the separation between ethenyl acetate and solvents is usually carried out by employing a series of flashes and distillation columns.⁵ This implies that, to model

these stages, is indubitably essential to accurately know the VLE; for this reason, we have decided to obtain these data as a previous stage before modeling the separation columns.

The paper shows the results of the VLE measurements that were performed for the binary systems of ethenyl acetate with methanol and butan-1-ol at $p/\text{kPa} = 1.013$. All of the obtained data were initially fitted to nonrandom two-liquid (NRTL)⁶ and universal quasichemical (UNIQUAC)⁷ activity coefficient models, but also to Peng–Robinson⁸ and perturbed-chain statistical associating fluid theory (PC-SAFT)^{9,10} equations of state (EoS). The great potential of recently developed EoS such as PC-SAFT is that they allow extrapolating from low pressure VLE to high pressures; for this reason, they are suitable to be employed for simulation purposes. All of the adjustments were carried out by employing ASPEN PLUS commercial software.¹¹

2. EXPERIMENTAL SECTION

2.1. Materials. All of the analytical grade materials employed in this work were purchased directly from Aldrich. Their purities, expressed in mass fraction, are shown in Table 1.

Table 1. Mass Fraction Purities of the Employed Reagents

chemical name	source	mass fraction purity
methanol	Aldrich	0.999
butan-1-ol	Aldrich	0.998
ethenyl acetate	Aldrich	0.990

Received: July 16, 2012

Accepted: October 1, 2012

Published: October 10, 2012

2.2. Apparatus and Procedure. The experiments were carried out with an apparatus entirely glass-made that had been successfully employed with other systems.^{12,13} In this equipment, the vapor and liquid phases are constantly being recirculated with the purpose of obtaining an accurate mixing of the phases and also to guarantee that the equilibrium has been reached. To keep pressure constant and under control, the vapor condenser is attached to a constant-pressure system controlled by a Cartesian manostat, with an accuracy in the measurement of pressure of $\Delta p/\text{Pa} = \pm 133$. The measurement of the equilibrium temperatures was performed with two certified type J thermocouples, with an accuracy of $T/\text{K} \pm 0.1$.

The analysis of both liquid and condensed vapor analyses was made by means of gas chromatography technique. For ethenyl acetate + methanol mixture, a Perkin-Elmer A/S chromatograph with a flame ionization detector and a J&W DB-23 capillary column were employed. For ethenyl acetate + butan-1-ol mixture, an Agilent A/S gas chromatograph with a mass spectrometer detector and also a J&W DB-23 capillary column was employed. In this last case, pentan-1-ol was used as a solvent to prepare the samples, and hexan-1-ol was employed as an internal standard.

3. RESULTS AND DISCUSSION

The VLE data (x_1, y_1, T) and the calculated activity coefficients of components in the liquid phase are shown in Tables 2 and 3. As it

Table 2. Ethenyl Acetate (1) + Methanol (2) VLE Data (Mole Fraction) at $p/\text{kPa} = 101.3$

x_1	y_1	T_b/K	γ_1	γ_2
0.000	0.000	64.6		1.000
0.033	0.077	63.0	3.160	1.084
0.046	0.105	62.5	3.169	1.088
0.092	0.187	61.2	2.964	1.089
0.145	0.247	60.4	2.550	1.109
0.183	0.294	59.8	2.470	1.114
0.258	0.333	59.3	2.018	1.183
0.299	0.374	59.0	1.972	1.187
0.367	0.401	58.9	1.717	1.268
0.413	0.425	58.9	1.630	1.306
0.555	0.487	59.4	1.367	1.510
0.782	0.615	62.2	1.107	2.069
1.000	1.000	72.6	1.000	

$$^a u(T) = 0.1 \text{ K}, u(x_1) = 0.005, u(y_1) = 0.001.$$

Table 3. Ethenyl Acetate (1) + Butan-1-ol (2) VLE Data (Mole Fraction) at $p/\text{kPa} = 101.3$

x_1	y_1	T_b/K	γ_1	γ_2
0.000	0.000	117.5		1.000
0.020	0.135	115.8	1.924	0.946
0.160	0.550	99.4	1.537	1.044
0.275	0.735	89.9	1.507	1.045
0.505	0.840	81.7	1.227	1.314
0.725	0.920	77.2	1.077	1.447
0.855	0.955	75.0	1.018	1.709
1.000	1.000	72.6	1.000	

$$^a u(T) = 0.1 \text{ K}, u(x_1) = 0.007, u(y_1) = 0.007.$$

can be noticed, the ethenyl acetate + methanol mixture presents an azeotrope; for this reason, the majority of the experimental data points are distributed around this value, due to this area of

the T - xy curve is going to be the critical one to obtain a reliable set of interaction parameters.

To calculate the activity coefficients, an excel algorithm with eqs 1 and 2 was employed. According to these equations the nonideality of the vapor phase is considered by determining the vapor-phase fugacity with the virial equation, truncated after second term.

$$\gamma_i = \frac{y_i \cdot P}{x_i \cdot P_i^0} \cdot \exp \left[\frac{(B_{ij} - v_i) \cdot (P - P_i^0) + (1 - y_i) \cdot P \cdot \delta_{ij}}{R \cdot T} \right] \quad (1)$$

$$\delta_{ij} = 2B_{ij} - B_{ii} - B_{jj} \quad (2)$$

In these eqs 1 and 2, γ_i represents the liquid phase activity coefficient of component i , and x_1 and y_1 are the mole fractions of component i in liquid and vapor phases, respectively, P is the total pressure, P_i^0 is the vapor pressure of the pure components, v_i is the liquid molar volume of component i , and R and T are the universal gas constant and the absolute temperature, respectively. The terms B_{ii} and B_{ij} are the second virial coefficient of the pure gas and the cross second virial coefficient, respectively; both coefficients were obtained following Tsonopoulos correlation.¹⁴ Finally, the calculation of the pure component vapor pressure was performed by means of Antoine equation (the Antoine constants taken from NIST database¹⁵ are shown in Table 4). According to the activity coefficient values, it can be seen in Tables 1 and 2 that both the two binary systems have a positive deviation of ideality.

Table 4. Pure Component Antoine Equation Parameters^a

compound	A	B	C	temperature range/K
ethenyl acetate	5.22841	1807.332	0.7	280–380
metanol	5.15853	1569.613	−34.846	245–370
butan-1-ol	4.54607	1351.555	−93.34	310–411

^a

$$\log P_i^0(\text{Pa}) = A - \frac{B}{[T(\text{K}) + C]}$$

The thermodynamic consistency of the experimental data was assessed with the L–W method of Wisniak.¹⁶ Following this method, the obtained $D = 100(L - W)/(L + W)$ values were less than 5 in both cases (2.8 for ethenyl acetate + methanol and 4.1 for ethenyl acetate + butan-1-ol), which indicates that the data are thermodynamically consistent (this value has to be lower than 5 whenever the values of the enthalpy of vaporization are estimated).

Later on, the equilibrium data were adjusted to the NRTL⁶ and UNIQUAC⁷ activity coefficient models, as well as with Peng–Robinson⁸ and PC-SAFT^{9,10} equations of state, by means of ASPEN PLUS commercial software.¹¹ In all cases the fitting was carried out using an objective function called “maximum likelihood”;¹⁷ this function is characterized by simultaneously minimizing the difference between the experimental and the adjusted values of all of the variables that can be manipulated (in this study, liquid and vapor composition of both components pressure and temperature).

As recommended in literature,¹¹ the NRTL and UNIQUAC binary interaction parameters were assumed to be temperature dependent, according to eqs 3 and 4, respectively.

$$G_{ij} = \exp(-\alpha_{ij}\tau_{ij})\tau_{ij} = a_{ij} + \frac{b_{ij}}{T} \quad (3)$$

In this last expression, τ_{ij} , τ_{ji} and α_{ij} are the binary interaction parameters of the NRTL equation.

$$\tau_{ij} = \exp\left(a_{ij} + \frac{b_{ij}}{T} + c_{ij} \ln T + d_{ij}T\right) \quad (4)$$

In this last expression, τ_{ij} and τ_{ji} are the binary interaction parameters of the UNIQUAC equation.

With both NRTL and UNIQUAC models, we only adjusted the b_{ij} and b_{ji} terms of the binary interaction parameters. On the other hand, the NRTL equation nonrandomness α factor was kept constant at 0.3, for the two studied binary systems.

Concerning the Peng–Robinson EoS, the pure component parameters (critical pressure, critical temperature, critical volume, and acentric factor) which are required for this model, were taken from NIST database,¹⁵ and the employed mixing rules were the classical ones⁸ defined in the original Peng–Robinson article. The binary interaction parameter (k_{ij}^{PR}) was determined by adjusting the experimental data of each mixture; besides, this model was also employed in a purely predictive way, by evaluating the VLE assuming a value of the binary interaction parameter equal to zero.

In relation to PC-SAFT EoS, the pure component parameters (segment diameter, σ ; segment number, m ; segment energy parameter, ε/k ; association energy, ε^{ABi}/k , and effective association volume, κ^{ABi}) were taken from ASPEN PLUS database¹⁸ and are summarized in Table 5; the binary interaction

Table 5. PC-SAFT Pure Component Parameters

parameter	ethenyl acetate	methanol	butan-1-ol
σ	3.2570	3.2300	3.6139
m	3.4442	1.5255	2.7515
$\varepsilon/k/K$	232.25	188.90	259.59
$\varepsilon^{ABi}/k/K$	0.0	2899.5	2544.6
κ^{ABi}	0.035176/6.692·10 ⁻³	0.035176	6.692·10 ⁻³

parameter ($k_{ij}^{PC-SAFT}$) was obtained by fitting the experimental data. It has to be considered that, according to literature,¹⁹ when dealing with a binary mixture of a polar compound (ethenyl acetate) and an associating compound (methanol or butan-1-ol), the association-energy parameter, ε^{ABi}/k , of the nonself-associating (polar) component ought to be set to zero, while the association volume parameter, κ^{ABi} , of the nonself-associating component must be assumed to be equal to the value of the associating component in the mixture. The PC-SAFT model was also employed as a purely predictive one, like it had been previously done with the Peng–Robinson equation (assuming a zero-value for the binary interaction parameter).

Figure 1 shows the experimental T - xy data of both mixtures, as well, as the regressed values with NRTL and UNIQUAC models. Figure 2 shows the same experimental data along with the regressed values with Peng–Robinson and PC-SAFT equations of state. Finally, Figure 3 shows the experimental data compared with the predictions made by Peng–Robinson and PC-SAFT equations of state (by fixing the binary interaction parameter at zero).

As it can be observed, both NRTL and UNIQUAC models (Figure 1) are perfectly capable of fitting the VLE data by adjusting only the b_{ij} terms of the binary interaction parameters; as a consequence no more than these two terms were considered.

Regarding the EoS models (Figure 2), it can be noticed that PC-SAFT is perfectly capable of adjusting the experimental data; nevertheless, the fitting to Peng–Robinson EoS is not so accurate, maybe because the studied mixtures are a combination of a relatively high polar compound (ethenyl acetate) with an associating compound (methanol or butan-1-ol), and this EoS was first developed for nonpolar systems.

For the two mixtures involved in this work, PC-SAFT EoS presents a clear advantage over the other models, such as NRTL or UNIQUAC because, to accurately describe the equilibrium, it is only necessary a temperature-independent binary interaction parameter.

When the two EoS models act in a purely predictive way (Figure 3), it can be noticed that, despite the incapability of the Peng–Robinson EoS to accurately predict the equilibrium of

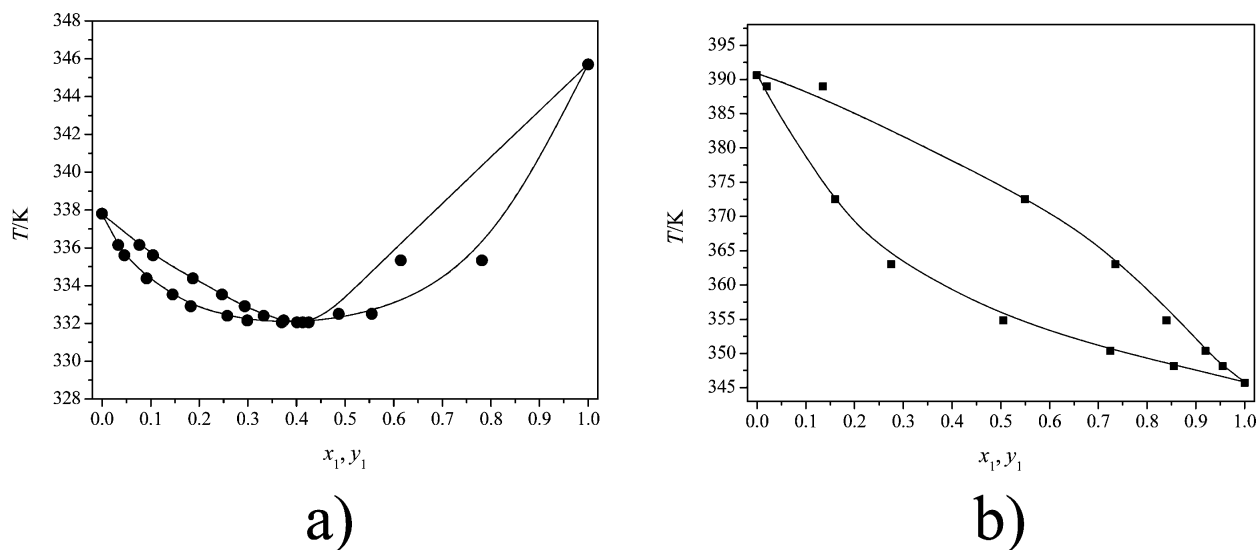


Figure 1. VLE of ethenyl acetate (1) + methanol (2) and ethenyl acetate (1) + butan-1-ol (2) mixtures. (a) ●, experimental T - xy data of the ethenyl acetate + methanol mixture. (b) ■, experimental T - xy data of the ethenyl acetate + butan-1-ol mixture. Solid lines (—), NRTL regressed values; dashed lines (---), UNIQUAC regressed values.

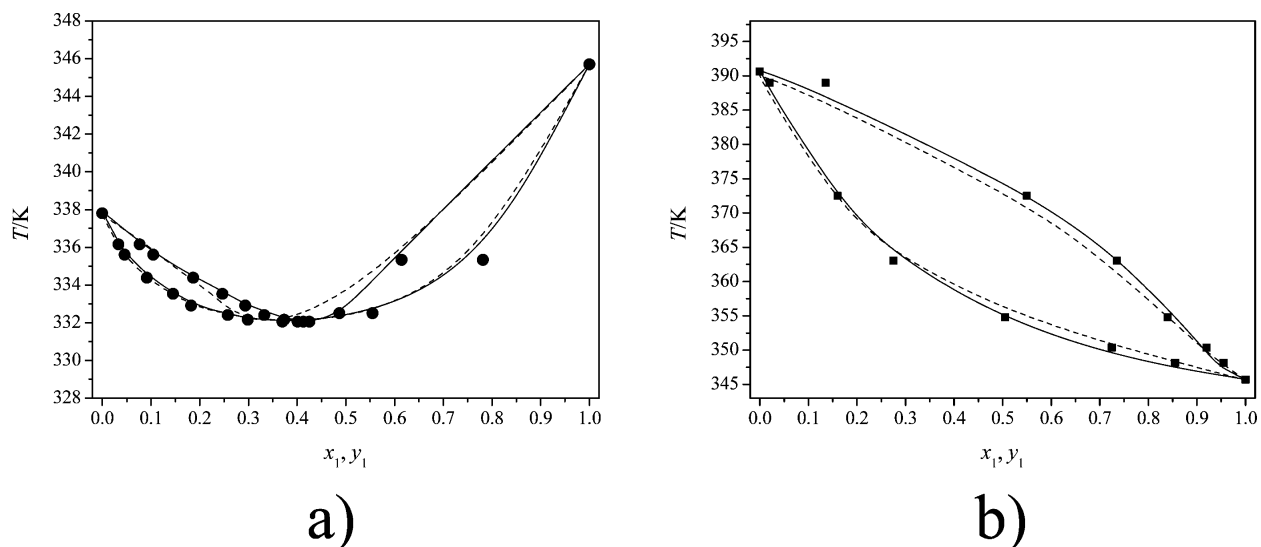


Figure 2. VLE of ethenyl acetate (1) + methanol (2) and ethenyl acetate (1) + butan-1-ol (2) mixtures. (a) ●, experimental T - xy data of the ethenyl acetate + methanol mixture. (b) ■, experimental T - xy data of the ethenyl acetate + butan-1-ol mixture. Solid lines (—), PC-SAFT regressed values; dashed lines (---), Peng–Robinson regressed values.

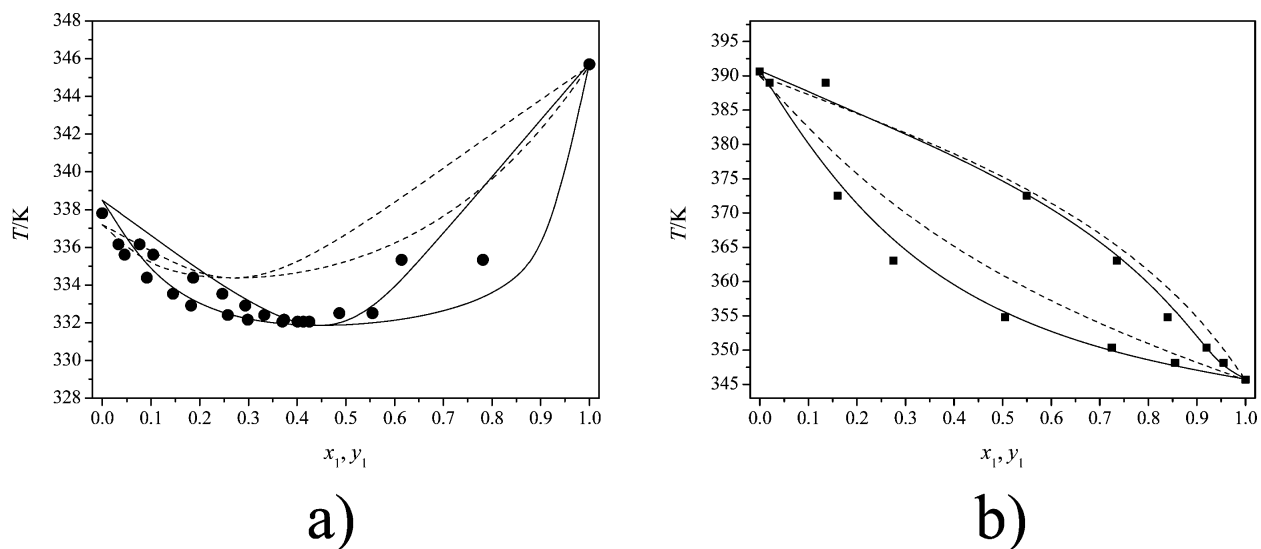


Figure 3. VLE of ethenyl acetate (1) + methanol (2) and ethenyl acetate (1) + butan-1-ol (2) mixtures. (a) ●, experimental T - xy data of the ethenyl acetate + methanol mixture. (b) ■, experimental T - xy data of the ethenyl acetate + butan-1-ol mixture. Solid lines (—), PC-SAFT predicted values; dashed lines (---), Peng–Robinson predicted values.

both mixtures, the PC-SAFT equation is clearly able to give a good approximation to the equilibrium data.

Analyzing more in detail the ethenyl acetate + methanol mixture, as it was previously indicated, this mixture presents an azeotrope at a value of ethenyl acetate mole fraction of 0.41. According to Figure 1, both NRTL and UNIQUAC models are perfectly capable of adjusting the equilibrium data of this mixture around the azeotropic point; this allows drawing the conclusion that the binary interaction parameters of both models can be employed to accurately predict the azeotropic point; the same comment can be applied to the PC-SAFT equation (Figure 2, continuous line). However, the Peng–Robinson equation (Figure 2, dotted line), despite performing a reasonable good overall adjustment, is not able to provide an accurate value of the azeotropic value. When these last two equations are employed as purely predictive (Figure 3), it can be observed that, by

employing the PC-SAFT equation, a reasonable value of the azeotropic point can be obtained.

Tables 6, 7, 8, and 9 show the binary interaction parameters determined from fitting the experimental data of both mixtures

Table 6. NRTL Binary Interaction Parameters

	ethenyl acetate (1) + methanol (2)	ethenyl acetate (1) + butan-1-ol (2)
b_{ij}	336.8	351.6
b_{ji}	171.4	−17.7

Table 7. UNIQUAC Binary Interaction Parameters

	ethenyl acetate (1) + methanol (2)	ethenyl acetate (1) + butan-1-ol (2)
b_{ij}	−464.0	−149.6
b_{ji}	65.8	37.7

Table 8. PC-SAFT k_{ij} Binary Interaction Parameter

	ethenyl acetate (1) + methanol (2)	ethenyl acetate (1) + butan-1-ol (2)
k_{ij}	-0.0059	0.0060

Table 9. Peng–Robinson k_{ij} Binary Interaction Parameter

	ethenyl acetate (1) + methanol (2)	ethenyl acetate (1) + butan-1-ol (2)
k_{ij}	0.017	0.044

to the four studied models. The main point to be emphasized is that the k_{ij} values of PC-SAFT EoS are close to zero. This confirms the ability of this model of acting as purely predictive.

With the aim of assessing the quality of the adjustments, in Table 10, the average absolute deviations, in percentage, of

Table 10. Temperature, $\sigma(T) = 1/k \sum (T_{\text{calc}} - T_{\text{exp}})/T_{\text{exp}}$, and Ethenyl Acetate Vapor Mole Fraction, $\sigma(y_1) = 1/k \sum (y_{1,\text{calc}} - y_{1,\text{exp}})/y_{1,\text{exp}}$, Root-Mean-Square Deviations for the Methods Tested

ethenyl acetate (1) + methanol (2)			ethenyl acetate (1) + butan-1-ol (2)		
method	$\sigma(T)$	$\sigma(y_1)$	method	$\sigma(T)$	$\sigma(y_1)$
NRTL	0.072	2.12	NRTL	0.54	2.60
UNIQUAC	0.074	2.10	UNIQUAC	0.54	2.60
Peng–Robinson	0.142	10.26	Peng–Robinson	0.79	4.16
PC-SAFT	0.148	1.83	PC-SAFT	0.62	4.00

temperature (eq 5) and ethenyl acetate vapor mole fraction (eq 6) are presented.

$$\sigma(T) = \frac{1}{k} \left| \sum_k \frac{T_{\text{calc}} - T_{\text{exp}}}{T_{\text{exp}}} \right| \quad (5)$$

$$\sigma(y) = \frac{1}{k} \left| \sum_k \frac{y_{1,\text{calc}} - y_{1,\text{exp}}}{y_{1,\text{exp}}} \right| \quad (6)$$

In both eqs 5 and 6, T indicates the temperature, y_1 the ethenyl acetate vapor mole fraction, and k the number of data points; the subscript exp represents experimental data and the subscript calc represents regressed data. As it can be observed, except for Peng–Robinson EoS, all the values are lower than 5 % and also similar among them. This reaffirms the previously made comments indicating that NRTL, UNIQUAC and PC-SAFT equations are suitable to adjust the experimental data of the two studied binary systems.

4. CONCLUSION

In this work, experimental and consistent VLE data of the binary systems methanol + ethenyl acetate and butan-1-ol + ethenyl acetate have been determined at $p/kPa = 101.3$; their consistency was evaluated with the Wisniak L–W method.

The NRTL and UNIQUAC activity coefficient models and PC-SAFT EoS are capable of accurately fitting the experimental data, while a much higher deviation is obtained when the Peng–Robinson EoS is employed.

PC-SAFT and Peng–Robinson EoS were also employed in a predictive way (by assuming a zero value for the binary interaction parameter), and it was found that the PC-SAFT equation is able to give a good approximation to the equilibrium data.

The regressed interaction parameters of NRTL, UNIQUAC, and PC-SAFT models can be employed to obtain an accurate value of the azeotropic point of the ethenyl acetate + methanol mixture.

AUTHOR INFORMATION

Corresponding Author

*Tel.: +34-91-394-8509. Fax: +34-91-394-4114. E-mail address: ediezalc@quim.ucm.es (E.D.).

Notes

The authors declare no competing financial interest.

REFERENCES

- (1) Chieng, I. L.; Wei Kan, T.; Chen, B. S. Dynamic simulation and operation of a high pressure ethylene-ethenyl acetate (EVA) copolymerization autoclave reactor. *Comput. Chem. Eng.* **2007**, *31*, 233–245.
- (2) REPSOL-YPF catalogue. <http://www.repsol.com/sa/herramientas/CatalogoQuimica/CatalogoQuimica.aspx> (accessed May 2012).
- (3) Junsuke Tanaka, I.; Kenji Matsumoto, O. Process for continuous production of ethylene-ethenyl acetate copolymer. U.S. Patent 4.657.994, 1987.
- (4) Kawahara, T.; Takai, M. Method for manufacturing ethylene-ethenyl acetate copolymer and apparatus for manufacturing the same. U.S. Patent 6.831.139 B2, 2004.
- (5) Tsai, J. J.; Lin, L. S.; Chang, H. M.; Fan, K. M.; Lin, W. S. Process for continuously producing ethylene-ethenyl acetate copolymer and reaction system. European Patent 1.645.574 B1, 2009.
- (6) Renon, H.; Prausnitz, J. M. Local compositions in thermodynamic excess functions for liquid mixtures. *AIChE J.* **1968**, *14*, 135–144.
- (7) Abrams, D. S.; Prausnitz, J. M. Statistical thermodynamics of liquid mixtures: a new expression for the partial excess Gibbs energy of partly or completely miscible systems. *AIChE J.* **1975**, *21*, 116–128.
- (8) Peng, D. Y.; Robinson, D. B. A new two-constant equation of state. *Ind. Eng. Chem. Fundam.* **1976**, *15* (1), 59–64.
- (9) Gross, J.; Sadowski, G. Perturbed-chain SAFT: an equation of state based on a perturbation theory for chain molecules. *Ind. Eng. Chem. Res.* **2001**, *40*, 1244–1260.
- (10) Gross, J.; Sadowski, G. Application of the perturbed-chain SAFT equation of state to associate systems. *Ind. Eng. Chem. Res.* **2002**, *41*, 5510–5515.
- (11) ASPENTECH webpage. <http://www.aspentech.com> (accessed May 2012).
- (12) Ovejero, G.; Romero, M. D.; Díez, E.; Lopes, T.; Díaz, I. Isobaric vapor-liquid equilibrium for the binary systems 1-pentanol + cyclohexane and 1-pentanol + *n*-hexane at low alcohol compositions. *J. Chem. Eng. Data* **2007**, *52*, 1984–1987.
- (13) Ovejero, G.; Romero, M. D.; Díez, E.; Lopes, T.; Díaz, I. Evaluation of (vapor + liquid) equilibria for the binary systems (1-octanol + cyclohexane) and (1-octanol + *n*-hexane) at low alcohol compositions. *J. Chem. Thermodyn.* **2008**, *40*, 1617–1620.
- (14) Tsionopoulos, C. An empirical correlation of second virial coefficients. *AIChE J.* **1974**, *20*, 263–272.
- (15) DECHEMA database. <http://i-systems.dechema.de/index.php> (accessed May 2012).
- (16) Wisniak, J. A new test for the thermodynamic consistency of vapor-liquid equilibrium. *Ind. Eng. Chem. Res.* **1993**, *32*, 1531–1533.
- (17) Ashour, I.; Aly, G. Effect of computation techniques for equation of state binary interaction parameters on the prediction of binary VLE data. *Comput. Chem. Eng.* **1996**, *20* (1), 79–91.
- (18) ASPEN PLUS database. <http://www.aspentech.com> (accessed May 2012).
- (19) Kleiner, M.; Tumakaka, F.; Sadowski, G. Thermodynamic modeling of complex systems. *Struct. Bonding (Berlin)* **2009**, *131*, 75–108.

1.1 Summary and Discussion

The article shown above, “**Vapor–Liquid Equilibrium at $p/\text{kPa} = 101.3$ of the Binary Mixtures of Ethenyl Acetate with Methanol and Butan-1-ol**” presents the binary interaction parameters estimated for several thermodynamic models (NRTL and UNIQUAC activity coefficient models, and Peng-Robinson and PC-SAFT equations of state), adjusted from the liquid-vapor equilibrium curve (T - x_i , y_i) obtained for the mixtures of vinyl acetate/methanol and vinyl acetate/butanol at atmospheric pressure, by means of the glass ebullometer experimental technique. The experimental data consistency was evaluated favorably with the Wisniak L–W method.

The main results show that the NRTL, UNIQUAC and PC-SAFT models are capable of accurately fitting the experimental data of the two systems ($\%AAD_{y_i} \leq 4\%$) while a much higher deviation is obtained when the Peng Robinson model is employed ($\%AAD_{y_i} \approx 10\%$). The fittings were done with Aspen Plus[®] data regression model.

From this article it is crucial to take into account the results of the PC-SAFT adjustment to the vapor-liquid equilibrium experimental data of vinyl acetate/methanol ($\%AAD_{y_i} = 1.83\%$), taking into account the best interactions association scheme. This adjustment is plotted together with the experimental data of such system, in Figure 4.1.

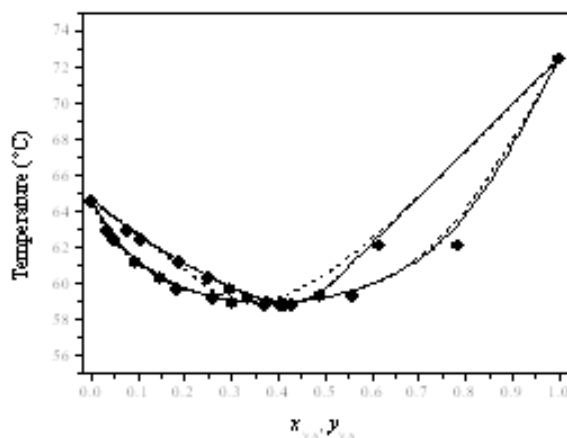


Figure 4.1. Vapor-liquid equilibrium for vinyl acetate/methanol system, at 1 atm.
(Points: experimental data / Solid Line: PC-SAFT adjustment)

The resulting PC-SAFT parameters are summarized in table 4.1. The pure component parameters (m , σ , ε/k , $\varepsilon^{\text{AiBi}}/k$ and κ^{AiBi}) were taken from the ASPEN PLUS database, and the binary interaction parameter (k_{ij}) was obtained by fitting the experimental data, considering the association scheme when a binary mixture of a polar compound (vinyl acetate) and an associating compound (methanol), the association-energy parameter, $\varepsilon^{\text{AiBi}}/k$, of the non-self-associating (polar) component ought to be set to zero, while the association volume parameter, κ^{AiBi} , of the non-self-associating component must be assumed to be equal to the value of the associating component in the mixture

Table 4.1 PC-SAFT parameters for Vinyl Acetate/Methanol system

Parameter	Vinyl acetate	Methanol
σ	3.2570	3.2300
m	3.4442	1.5255
ε/k (K)	232.25	188.90
$\varepsilon^{\text{AiBi}}/k$ (K)	0.0	2899.5
κ^{AiBi}	0.035176	

5 Thermodynamics of EVA/solvents mixtures at finite compositions of polymer

This chapter presents two scientific articles published in the framework of the global project, and a final discussion, that are focused on the determination and evaluation of Flory Huggins – polymer composition curves, and the subsequent sorption curves for the EVA copolymers and their homopolymers (Polyethylene, PE, and Polyvinylacetate, PVA) in equilibrium with methanol, vinyl acetate and cyclohexane; by means of the extrapolation of the previous thermodynamic data of infinite dilution of solvent and polymer, to finite compositions of polymer. Additionally, several thermodynamic assessments were done at these finite conditions.

Then a thermodynamic adjusting of these sorption curves to the PC-SAFT model is presented, to the final goal of the simulation of the recovery column of the EVA separation solution process (choosing the EVA33 as a sample, for being an EVA copolymer with a typical vinyl acetate content for the mentioned process), in order to reproduce the rigorous thermodynamics assessment presented in this project.

5.1 Prediction of sorption curves from Flory Huggins parameters determined at solvent and polymer infinite dilution

Camacho, J., Díez, E., Díaz & Ovejero, G. (2015). Prediction of sorption curves from Flory Huggins parameters determined at solvent and polymer infinite dilution. Submitted for publication.

*Corresponding Author: Eduardo Díez

E-mail: ediezalc@quim.ucm.es

Tel: (+) 34-91-394-8509

Fax: (+)34-91-394-4114

Address: Grupo de Catálisis y Procesos de Separación (CyPS), Departamento de Ingeniería Química, Facultad de C. Químicas, Universidad Complutense de Madrid, Avda. Complutense s/n, 28040 Madrid, Spain.

Prediction of sorption curves from Flory Huggins parameters determined at solvent and polymer infinite dilution

Javier Camacho, Eduardo Díez*, Gabriel Ovejero

Grupo de Catálisis y Procesos de Separación (CyPS), Departamento de Ingeniería Química, Facultad de C. Químicas, Universidad Complutense de Madrid, Avda. Complutense s/n, 28040 Madrid, Spain.

Received Month Xth, 20XX; Revised Month Xth, 20XX; Accepted Month Xth, 20XX

Running Head: From Flory Huggins parameters to P - x curves

Abstract: In this work, a new methodology to determine the solvent sorption curve (pressure-composition curves for the vapor-liquid equilibrium) of a polymer/solvent mixture, from the Flory Huggins data measured at the composition extremes of the binary mixture (infinite dilution of polymer, and infinite dilution of solvent) has been proposed. This methodology is based on the works of Bernard Wolf about the dependence of the Flory Huggins parameter, χ , on the polymer composition. The methodology was validated for ten different polymer/solvent systems, with an overall value of the Average Absolute Deviation (%AAD) between the literature and estimated pressure values around 1%. Once validated, the procedure was employed to obtain the sorption curves of several systems of interest for our research group: the binary mixtures of ethylene/vinyl acetate copolymer (EVA), the ones of its correspondent homopolymers, polyethylene (PE) and polyvinyl acetate (PVA), with cyclohexane, and the binary system polyvinyl acetate/methanol. For these systems, the Flory Huggins parameter values at infinite dilution of solvent and polymer were taken from our previous works (studies of inverse gas chromatography and intrinsic viscosity, respectively). Finally from the previously obtained values, the dependence of the Wolf parameters on the vinyl acetate percentage was analyzed taking into account the excess properties.

Keywords: *Polymer, Sorption curve, vapour-liquid equilibrium, Flory Huggins, ethylene vinyl acetate, polyethylene, polyvinyl acetate*

1. Introduction

In our research group we are currently focusing on studying how to model and simulate the separation stage of the EVA copolymer (ethylene and vinyl acetate copolymer) solution process (usually carried out at 60 °C and 1 atm),¹ which is a thermodynamic-based operation. So, to accurately model the thermodynamic polymer/solvent equilibrium is crucial to determine the correct thermodynamic parameters, of the mixtures involving the EVA copolymer and its corresponding homopolymers: polyethylene (PE) and polyvinyl acetate (PVA).

The basis for a better understanding of the particularities of polymer/solvent mixtures was laid more than half a century ago in the form of the well-known Flory Huggins interaction equation.² Since then, numerous attempts have subsequently been made to extend and to modify the Flory Huggins theory. Some of the more widely employed approaches are the different varieties of both lattice fluid and hole theories,³ the lattice gas model,⁴ the Sanchez–Lacombe theory,⁵ the cell theory,⁶ different perturbation theories,⁷ the Statistical-Associating-Fluid-Theory (SAFT),⁸ the Perturbed-Hard-Sphere Chain Theory (PCSAFT),^{9,10} the UNIFAC model¹¹ and the UNIQUAC model.¹²

The Flory Huggins relationship is usually stated in terms of the segment molar Gibbs free energy, $\bar{\Delta G}$, with one mole of segments as the basis. For polymer-solvent mixtures, where the molar volume of the solvent normally defines the size of a segment, this relationship is written as:¹³

$$\frac{\bar{\Delta G}}{RT} = (1 - \phi) \ln(1 - \phi) + \frac{\phi}{N} \ln \phi + g\phi(1 - \phi) \quad (1)$$

The number of segments that constitute the polymer (N), is calculated by dividing the molar volume of the macromolecule by the molar volume of the solvent. The composition variable (ϕ) representing the segment molar fraction of the polymer, is in most cases approximated to its volume fraction (neglecting nonzero volumes of mixing), and g is the integral Flory–Huggins interaction parameter.

The integral interaction parameter g , can be related to the original Flory–Huggins interaction parameter χ by the following equation:¹⁴

$$\chi = g - (1 - \phi) \frac{\partial g}{\partial \phi} \quad (2)$$

Only if g does not depend on composition, this parameter becomes identical to the experimentally measurable Flory–Huggins interaction parameter χ . In the early days, this parameter χ was incorrectly considered to depend only on state variables, but not on the composition of the polymer in the mixture. Nowadays it is clear that is composition dependant.

A simple mathematical approach to describe Flory–Huggins interaction parameter χ temperature dependence consists on the following series expansion:¹³

$$\chi = \chi_o + \chi_1\phi + \chi_2\phi^2 \dots \quad (3)$$

A more sophisticated approach¹⁵ is formulated in Equation (4), with B as parameter, which take into account for the differences in the molecular surfaces of solvent molecules and polymer segments, while A and C are considered to be constants for a given system and fixed variables of state.

$$\chi = \frac{A}{(1 - B\phi)^2} + C \quad (4)$$

Another important variable is the partial segment molar Gibbs energy, which, in a solvent (subscript 1) / polymer (subscript 2) mixture expressed in terms of the solvent chemical potential μ_1 , according to Equation (5):

$$\frac{\Delta \mu_1}{RT} = \frac{\bar{\Delta G}_1}{RT} = \ln(1 - \phi) + (1 - 1/N)\phi + \chi\phi^2 = \ln a_1 \quad (5)$$

Where a_1 , the solvent activity can be approximated (enough low volatility of the solvent) to the ratio of the solvent vapour pressure in the mixture to the pure solvent vapour pressure:

$$a_1 \approx \frac{P_1}{P_{1,0}} \quad (6)$$

Equations (5) and (6) allow the construction of the sorption curves for a solvent vapor in a polymer (P_1 “vs” polymer composition).¹⁵

Regarding, the polymer chemical potential, this magnitude can be determined by means of an expression analogous to (5) applied to the polymer:

$$\frac{\Delta\mu_2}{RT} = \frac{N\Delta\bar{G}_2}{RT} = \ln \phi + (1-N)(1-\phi) + \xi N(1-\phi)^2 \quad (7)$$

This previous equation defines the interaction parameter ξ , in terms of the chemical potential of the polymer. This interaction parameter can be calculated from the integral value g by means of:¹³

$$\xi = g + \phi \frac{\partial g}{\partial \phi} \quad (8)$$

However, the integral interaction g parameter is practically inaccessible, and the parameter ξ , referring to the polymer, suffers from the difficulties associated with the formation of perfect polymer crystals, because it is based on their equilibrium with saturated polymer solutions.¹³

Bernard Wolf, in order to develop a molecular relationship between the integral interaction parameter g , and the Flory–Huggins interaction parameter χ , considered two features initially neglected by the original Flory–Huggins theory, by subdividing the solution dilution process (in terms of Flory Huggins at infinite dilution of solvent χ_o) into two separate steps:¹³

$$\chi_o = \chi_o^{fc} + \chi_o^{cr} \quad (9)$$

The first term (the superscript “ fc ” stands for fixed conformation) quantifies the effect of separating two contacting polymer segments belonging to different macromolecules by inserting a solvent molecule between them, without changing their conformation. The second term (the superscript “ cr ” stands for conformational relaxation) is required to bring the system into its equilibrium, by rearranging the components so that the minimum of Gibbs energy is achieved. In order to give the second term a more specific meaning, Wolf formulated it, as the difference between the interaction before and after the conformational relaxation as:

$$\chi_o^{cr} = \chi^{after} - \chi^{before} \quad (10)$$

Naming λ to the interaction between polymer segments and solvent molecules in the isolated state, the parameter χ_o^{cr} should be proportional to this interaction. This proportionality was established by Wolf in terms of the interaction parameter ξ :

$$\chi_o^{cr} = -\xi\lambda \quad (11)$$

where the negative sign in the above expression has been chosen to obtain positive values for this parameter χ_o^{cr} in the great majority of cases. If χ_o^{cr} is denoted according to Equation (12), then, Equation (9), representing the Flory Huggins interaction parameter at infinite dilution of solvent can be re-written as Equation (13).

$$\chi_o^{fc} = \alpha \quad (12)$$

$$\chi_o = \alpha - \zeta\lambda \quad (13)$$

In order to generalize Equation (13) to whatever polymer composition, Wolf assumed that the composition dependence of the first term could be evaluated by an expression analogous to Equation (4), where the term v accounts for the differences between the molecular surfaces of solvent and polymer. For the second term, Wolf assumed a linear dependence of the integral interaction parameter g on polymer volumetric fraction ϕ .¹³ The result of this generalization is Equation (14).

$$\chi = \frac{\alpha}{(1-v\phi)^2} - \zeta(\lambda + 2(1-\lambda)\phi) \quad (14)$$

The Flory–Huggins interaction parameter χ of Equation (14) yields the following expression for the integral interaction parameter g with four molecularly adjustable parameters, and which is required for instance to calculate phase equilibrium using the method of the direct minimization of the Gibbs energy¹³ of a system:

$$g = \frac{\alpha}{(1-v)(1-v\phi)} - \zeta(1 + (1-\lambda)\phi) \quad (15)$$

Considering that the second term of Equation (14) is almost always negligible (with respect to $1/2$) for polymers of enough molar mass, the parameters ξ and λ can be merged into their product $\xi\lambda$, and the isolated λ can be replaced by $1/2$.¹³ Thus Equation (14) is transformed into the more simple Equation (16), while the analogous expression for the integral parameter is Equation (17).

$$\chi \approx \frac{\alpha}{(1-v\phi)^2} - \zeta\lambda(1 + 2\phi) \quad (16)$$

$$g = \frac{\alpha}{(1-v)(1-v\phi)} - \zeta\lambda(2 + \phi) \quad (17)$$

With these assumptions, the number of adjustable parameter is reduced to three (α , v , $\xi\lambda$). Moreover, if χ_o (Flory Huggins at infinite dilution of solvent) is known, with the use of Equation (13), α is defined, and the adjustable parameters are reduced to two (v , $\xi\lambda$).

To analyse the temperature dependence of the three parameters (α , v , $\xi\lambda$), the relationship shown in Equation (18) has proved to be very versatile to model $\pi_{(T)}$, where π is whatever of the three above mentioned parameters, and π_1 or π_2 can be set to zero in most cases.¹³

$$\pi = \pi_o + \pi_1 / T + \pi_2 T \quad (18)$$

All the previously described considerations are applicable to organic solvents/ homopolymers solutions. The different molecular architectures of branched polymers do not require additional modifications on this theory.¹³ To apply the current approach to solutions of random copolymers (containing type A and type B monomers), the different parameters π (α , v , $\xi\lambda$) must be a function of f , the weight fraction of B-monomers contained in the A-ran-B copolymer. For this purpose, the approach of Equation (19) has been proposed.¹⁶

$$\pi_{AB} = \pi_A(1-f) + \pi_B f + \pi_E f(1-f) \quad (19)$$

According to this equation, the different parameters π_{AB} , referred to a copolymer of composition f , are calculated with the corresponding homopolymer parameters, π_A and π_B , plus an excess term π_E , which quantify the extra effects resulting from the presence of two types of monomeric units in the copolymer chain.

Considering all the above theory, the aim of this work is to calculate the Wolf parameters and from these parameters develop the solvent sorption curves in a polymer/solvent mixture (P - x for the vapor-liquid equilibria). This calculation will have as a starting the two values of Flory Huggins interaction parameters measured at the compositions extremes of the polymer/solvent mixture (infinite dilution of polymer, and infinite dilution of solvent), considering the dependence of this parameter on the polymer composition.

2. Methodology proposed and validation

To give such compliance to the goal of this work, we have proposed a simple mathematical approach, based on the phenomenological study of the Flory Huggins and Wolf parameters found in the literature for various polymer/solvent systems, shown in Table 1.

In this table it can be observed that the values of v parameter (which account for the differences between the molecular surfaces of solvent and polymer) do not show a wide range of variation (an average value of 0.318, with a coefficient of variation below 12%). On the other hand, the $\xi\lambda$ parameter does exhibit a high coefficient of variation (around 72%), with values ranging from 0 to 1.2. The mathematical study can be summarized as follows:

The starting point are the Flory Huggins parameters at solvent infinite dilution (χ_o , $\phi_o = 0$) and the Flory Huggins parameter at polymer infinite dilution (χ_f , $\phi_f = 1$). The first values were directly taken from the literature references. The second values were calculated, combining equations (13) and (16) into Equation (20), considering $\phi_f = 1$, from v and $\xi\lambda$ literature values. If both χ_o and χ_f values were directly available, it would not be necessary to perform the previously described calculation.

$$\chi_f = \frac{\chi_o + \xi\lambda}{(1-v)^2} - 3\xi\lambda \quad (20)$$

Once χ_o and χ_f are known, the following procedure was followed to determine $\xi\lambda$ and v , and with these values the Flory Huggins interaction parameters, and the sorption curves:

- 1) Initially, different values of $\xi\lambda$, ranging from 0 to 2 with a fixed step of 0.5, were assumed.
- 2) For every $\xi\lambda$ value, Equation (20) was solved to obtain a value of v by means of a non-linear regression.
- 3) For each solvent/polymer mixture and for each ($\xi\lambda$, v) regressed pair, a Flory Huggins-composition curve and a sorption curve was obtained, with Equations (16) and (5) respectively. Is important to notice that, for every solvent/polymer mixture, more than one Flory Huggins-composition curve and sorption curve is displayed.
- 4) To illustrate this, the above mentioned curves are shown in Figure 1 for polystyrene/cyclohexane, polystyrene/toluene and polystyrene/tetrahydrofuran systems.
For every binary system, the Flory Huggins-composition curves and the sorption curves obtained with all ($\xi\lambda$, v) combinations are displayed. Besides, for each system, the Flory Huggins-composition curve and the sorption curve obtained with ($\xi\lambda$, v) literature values (from Table 1) is also included.

The agreement between the obtained curves with ($\xi\lambda$, v) regressed values and the ones obtained with ($\xi\lambda$, v) literature values was analyzed with the percentage average value of absolute deviation for the pressure (%AADP). This magnitude is defined in Equation 21, where P is the pressure of the system, NP is the number of data points used for the analysis, and the subscripts are referred to literature (biblio) and regressed (calc) values, respectively.

$$\%AADP = \frac{1}{NP} \sum_{i=1}^{NP} ABS \left(\frac{P_{biblio,i} - P_{calc,i}}{P_{biblio,i}} \right) \cdot 100 \quad (21)$$

- 5) Once the above study was conducted for all the polymer /solvents systems shown in Table 1, it was possible to establish a methodology to determine the ($\xi\lambda$, v) regressed values which allowed obtaining the sorption curve whose values are the closest to the ones of the sorption curve obtained from ($\xi\lambda$, v) literature

parameters. This methodology is explained in Figure 2 for polystyrene/cyclohexane, polystyrene/toluene and polystyrene/tetrahydrofuran systems.

The figure represents the assumed $\xi\lambda$ values (0; 0.5; 1; 1.5; 2) vs its corresponding v values, determined by non-linear regression of equation (20). Calculating the %AADP of the sorption curves obtained with each combination of ($\xi\lambda$, v) parameters (values appearing in figure 2 next to each point), it can be noticed that the combination which gives a lower %AADP is the one in which the parameter v begins to stabilize. This is when $\Delta v = |(v_{sol+i} - v_{sol})| \rightarrow 0.1^- (\rightarrow 0.1^+ \text{ means that tends to } 0.1 \text{ by left})$.

- 6) The determination of the best solution for the ($\xi\lambda$, v) values, is the final step of the proposed methodology as it allows constructing the Flory Huggins-composition curve and a sorption curve of every binary solvent/polymer mixture.

The obtained %AADP values for the tested systems are shown in Table 2. As it can be observed in all cases the deviation is lower than 2.8%, with an overall average error of 1.02% -standard deviation (STD) of 1.126. This represents a highly satisfactory result as it implies that it is possible to accurately determine the entire sorption curve (P - xy) of a solvent/polymer mixture by only knowing the Flory Huggins parameters measured at the extremes of the composition curve (infinite dilution of the solvent and infinite dilution of the polymer).

3. Prediction of sorption curves for polymer/solvent systems of interest

The previously proposed methodology has been applied to several systems of interest for the current research of our group. These systems are: polyvinyl acetate/methanol (PVA/MET), polyethylene/cyclohexane (PE/CX), ethylene vinyl acetate copolymer/cyclohexane (EVA/CX), and polyvinyl acetate/cyclohexane (PVA/CX). Table 3 summarizes the physical data of the involved polymers.

For each mixture, the Flory Huggins parameters at infinite dilution of polymer χ_0 ($\phi_0 = 0$) were previously determined by means of intrinsic viscosity (IV) procedure.^{23,24} The Flory Huggins parameters at infinite dilution of solvent χ_1 ($\phi_1 = 1$) were also previously determined by means of Inverse Gas Chromatography (IGC) procedure.^{25,26} It is important to notice that for the semicrystalline polymers studied (polyethylene and EVAs) the Flory Huggins parameters at infinite dilution of solvent have been obtained from the amorphous bulk interactions of these polymer/solvent systems.²⁷ All the Flory Huggins parameters cited are summarized in Table 4.

3.1. Polyvinylacetate/methanol

Figure 3 shows several sorption curves for this system: two predicted curves and a literature one for a PVA/MET system, with a polymer with a molecular weight (M_w) of 167,000 kg/kmol,²⁸ at 60 °C. The dot curve was predicted following the procedure described in this work, with final values of $\xi\lambda = 0$ and $v = 0.360$. The dash curve was predicted employing a constant Flory Huggins parameter, equal to the value obtained by IGC.

This figure is an example that shows the most outgoing and important result of this study: it is drastically demonstrated that the assumption of considering the Flory Huggins parameter as a constant (independent of composition) cannot be done, as vapour pressures above the vapour pressure of the pure solvent, are obtained. Meanwhile, the curve that considers the dependence of the concentration of the Flory Huggins parameter is much closer to the bibliographic points. The small differences can be explained in terms of the differences in the molecular weights of the PVA polymer.

3.2. Polyethylene/cyclohexane

Figure 4 shows the sorption curve, estimated for the polyethylene/cyclohexane system at 60 °C (punctuated line). For this system the best solution to the Wolf parameters are: $\xi\lambda = 0.5$ and $v = 0.445$. As polyethylene is a semicrystalline polymer, it is importance to emphasize the importance of the use of the amorphous Flory Huggins parameters at infinite dilution of solvent for this prediction ($\chi_{\text{amorphous}} = 0.34$),²⁷ in order to take account only the bulk interactions, instead the use of the overall Flory Huggins parameter ($\chi = 0.79$)²⁵ which considers both bulk and adsorption interactions.

Despite, literature data are very scarce for this system, Figure 4 also shows the data published²⁹ for highest temperatures, together with the vapour pressures for pure cyclohexane. The trend predicted at 60 °C is according to literature.

3.3. Ethylene vinyl acetate copolymer/cyclohexane

The methodology proposed in this work was also employed to estimate the $\xi\lambda$ and v parameters of two ethylene vinyl acetate copolymer/cyclohexane mixtures (EVA18/CX and EVA33/CX) at 30 °C, 40 °C and 50 °C. As EVA is also a semicrystalline polymer, the amorphous Flory Huggins parameters at infinite dilution of solvent were employed.²⁷

Besides, in order to compare the results with the literature data of other EVA copolymers with different vinyl acetate content, at 80 °C,³⁰ the obtained Wolf parameters were extrapolated to 80°C with equation (18) setting $\pi_1 = 0$. From these values the correspondent sorption curves were calculated. The parameter α was also included, because χ_o is unknown at 80 °C. All these Wolf parameters are presented in table 5. In addition the values extrapolated at 60 °C were also reported.

In table 5 can be observed that in all cases, the $\xi\lambda$ parameters was always set equal to 0.5 according to the methodology described in this work. Moreover, the v and α parameters are almost constants.

Figure 5 shows the sorption curves estimated for the mixtures of cyclohexane with the two EVA copolymers studied (EVA18, 18% vinyl acetate content and EVA33, 33% vinyl acetate content), plus the literature sorption curves reported for the mixtures of cyclohexane with 25%, 50% and 75% EVA copolymers, at 80 °C. As it can be observed, the lines of EVA18/CX and EVA33/CX mixtures perfectly keep the correlativity order, regarding vapour pressure: 18% < 25% < 33% < 50% < 75%.

3.4. Polyvinylacetate/cyclohexane

This is a particular thermodynamic system, in which several assumptions have been done because as it is reported in table 4, this system doesn't show values at infinite dilutions conditions. Thus χ_o is also unknown, and it would be approximated to a proper theoretical value.

The first consideration for this system is the fact that one phase solution at 60 °C, was not observed in the entire of the polymer compositions range (even at infinite dilution of polymer). This represents, a restriction to the methodology proposed in this work. If at certain polymer composition (ϕ_i) in a polymer/solvent mixture a liquid/solid phase separation is appreciated or the polymer is not dissolved, χ_i should be greater than 0.5; if the polymer were found to convert to thermos-reversible gels, χ_i should be around 0.5, and if the polymer/solvent system, show one phase solution, χ_i should be below than 0.5.³¹ As above, all χ_i values for this system, must be at least greater than 0.5.

Another consideration was the value employed of χ_f (IGC) = 1.75, shown in table 4. This value was linearly extrapolated to 60 °C from data obtained in our previous work²⁶ at 110 °C – 140 °C interval (range in which the cyclohexane presents bulk interactions with the polymer in the retention diagram).

In addition, another very useful restriction is the inequality which implies that in the sorption curve, the vapour pressure should decrease with polymer composition (at a certain polymer fractions i and w with $i < w$, $P_{(w)} \leq P_{(w-i)}$).¹⁵ These restrictions must be considered to the non-linear regression of Equation (20).

With these assumptions, it was observed that, from values of $\xi\lambda = 0.5$, the v and χ_o values begin to stabilize ($v = 0.43$ and $\chi_o = 0.55$). Figure 6, presents the sorption curve for this approach, which is in agreement with the literature data published for this system.³²

4. Prediction of sorption curves for polymer/solvent systems of interest

It is important to compare the thermodynamic performance of solutions of EVA copolymers, with the behaviour of their corresponding homopolymers (PE and PVA). This has been done in their mixtures with cyclohexane at 60 °C.

To establish this comparison, the previously determined Wolf parameters of PE/CX, EVA 18/CX, EVA 33/CX, PVA/CX at 60 °C mixtures, were employed. Figure 7 presents the variability of the Wolf parameters for the studied system. It can be observed that the v and α values (it is well known that the $\xi\lambda$ parameters are around 0.5), exhibit a typical second grade polynomial variation, as expected, based on previous publications.¹⁶

From these parameters, the Flory Huggins composition curves were obtained with Equation (16). They are plotted together in Figure 8.

As it was expected, the presence of the PE homopolymer, allows reducing the solubility of the PVA homopolymer in cyclohexane. Figure 10 also shows that EVA 18 is more soluble than EVA 33 (χ_i -EVA 18 \leq χ_i -EVA 33). This is reasonable due the less content of vinyl acetate monomer.

On the other hand, the excess properties between PVA and PE (that quantify the extra effects resulting from the presence of two types of monomeric units in the copolymer chain), generate soluble EVA copolymers with mixed physicochemical properties of their homopolymers. These excess parameters (EXC) can be calculated, with $f = 0.18$ and 0.33 , in Equation (19). The Wolf parameters, including the excess values of each parameter, are summarized in Table 6.

In Table 6 it can be observed, the more soluble copolymer (EVA 18), presents lower v , $\xi\lambda$ and α excess parameters. In addition, is important to point out that these values of the excess parameters determined from Equation (19) are the responsible of the non-correlative values of Flory Huggins parameter in Figure 8 at volume compositions greater than 0.85 to EVA 18 copolymer. It is demonstrated, that the Flory Huggins parameter of a copolymer with certain vinyl acetate content cannot be obtained by weighting the Flory Huggins parameters of the homopolymers with their volume fraction, neglecting the excess contribution.

5. Conclusions

A methodology to estimate the sorption curves for solvent/polymer systems, from the values of Flory Huggins determined at the extreme dilution conditions (of solvent and polymer) has been proposed and validated for ten different systems, with an overall value of percentage average absolute deviation (%AAD) between bibliographic and estimated pressure around 1%. The polymers validated are in a range of molecular weights from 10 to 250 kg/mol. This methodology takes into account the dependence of the Flory Huggins parameters on composition, according to the equations and parameters (v and $\xi\lambda$) proposed by Bernard Wolf.

The proposed methodology was also applied to solvent/polymer mixtures which are interesting for our research group: the sorption curves for the systems polyvinyl acetate/methanol, polyethylene/cyclohexane, ethylene-vinyl-acetate/cyclohexane, and polyvinyl acetate/cyclohexane, were determined, with also high agreement with the trends shown in literature. It was drastically demonstrated that the assumption of considering the Flory Huggins parameter as a constant (e.g. equal to the Flory Huggins value determined by IGC) in the entire range of the polymer/solvent composition cannot be done.

Finally, the thermodynamic behavior of the two studied EVA copolymers was compared with the thermodynamic behavior of the corresponding homopolymers (polyethylene and polyvinylacetate), in their mixtures with cyclohexane at 60°C. From this study it can be concluded that the Flory Huggins parameter of a copolymer with certain vinyl acetate content cannot be obtained by weighting the Flory Huggins parameters of the homopolymers with their volume fraction, neglecting the excess contribution.

6. References

- (1) O. Takaharu and O. Tetsuya, Kuraray Co, US Patent 6838517 B2 (2005).
- (2) P.J. Flory, *J. Chem. Phys.*, **10**(1), 51 (1942).
- (3) R. Simha and T. Somcynsky, *Macromolecules*, **2**(4), 342 (1969).
- (4) N.J. Trappeniers, J.A. Schouten and C.A. Ten Seldam, *Chem. Phys. Lett.*, **5**(9), 541 (1970).
- (5) I.C. Sanchez and R.H. Lacombe, *J. Phys. Chem.*, **80**(21), 2352 (1976).
- (6) G.T. Dee and D.J. Walsh, *Macromolecules*, **21**(3), 815 (1988).
- (7) S. Beret and J.M. Prausnitz, *AIChE J.*, **21**(6), 1123 (1975).
- (8) W.G. Chapman, K.E. Gubbins, G. Jackson and M. Radosz, *Fluid Phase Equilib.*, **52**, 31 (1989).
- (9) J. Gross and G. Sadowski, *Ind. Eng. Chem. Res.*, **40**(4), 1244 (2001).
- (10) J. Gross and G. Sadowski, *Ind. Eng. Chem. Res.*, **41**(5), 1084 (2002).
- (11) A. Fredenslund, R.L. Jones and J.M. Prausnitz, *AIChE J.*, **21**(6), 1086 (1975).
- (12) J.F. Heil and J.M. Prausnitz, *AIChE J.*, **12**(4), 678 (1966).
- (13) B.A. Wolf, *Adv. Poly. Sci.*, **238**, 1 (2011).
- (14) R. Horst, *Macromol. Theor. Simul.*, **5**(5), 789 (1996).
- (15) R. Koningsveld, W.H. Stockmayer and E. Nies, *Polymer phase diagrams*, Oxford Univ. Press, Oxford, 2001.
- (16) M. Bercea, J. Eckelt and B.A. Wolf, *Ind. Eng. Chem. Res.*, **47**(7), 2434 (2008).
- (17) N. Schuld and B.A. Wolf in *Polymer handbook*, J. Brandrup, E.H. Immergut, A Abe and D.R. Bloch, Eds., Wiley, New York, 1999, Vol.7, p 247.
- (18) M. Bercea, J. Eckelt, and B.A. Wolf, *Ind. Eng. Chem. Res.*, **48**(9), 4603 (2009).
- (19) J. Eckelt, F. Samadi, F. Wurm, H. Frey and B.A. Wolf, *Macromol. Chem. Phys.*, **210**(17), 1433 (2009).
- (20) B.A. Wolf, *Macromol. Chem. Phys.*, **204**(11), 1381 (2003).
- (21) A. Schneider, N. Schuld, M. Bercea and B.A. Wolf, *J. Poly. Sci. Pol. Phys.*, **42**(9), 1601 (2004).
- (22) B.A. Wolf, *Macromolecules*, **38**(4), 1378 (2005).
- (23) E. Díez, J. Camacho, I. Díaz and G. Ovejero, *Polym. Bull.*, **71**(1), 193 (2014).
- (24) J. Camacho, E. Díez, D. Blanco, E. Martín and G. Ovejero, *Chem. Eng. Trans.*, **43**, 1717 (2015).
- (25) J. Camacho, E. Díez, G. Ovejero and I. Díaz, *J. Appl. Polym. Sci.*, **128**(1), 481 (2013).
- (26) J. Camacho, E. Díez, L. Gómez and G. Ovejero, *Polym. Eng. Sci.*, DOI: 10.1002/pen.24189 (2015).
- (27) J. Camacho, E. Díez and G. Ovejero, *Polym. Bull.*, submitted for publication (2015).
- (28) G. Wibawa, R. Hatano, Y. Sato, S. Takishima and H. Masuoka, *J. Chem. Eng. Data*, **47**(4), 1022 (2002).
- (29) J.L. Rausch, *Study of the Diffusion and Solubility for a Polyethylene-cyclohexane System Using Gravimetric Sorption Analysis*, Doctoral dissertation, The Pennsylvania State Univ., 2009.
- (30) R.B. Gupta and J.M. Prausnitz, *J. Chem. Eng. Data*, **40**(4), 784 (1995).
- (31) M. Okabe, R. Wada, M. Tazaki and T. Homma, *Polym. J.*, **35**(10), 798 (2003).
- (32) G. Wibawa, M. Takahashi, Y. Sato, S. Takishima and H. Masuoka, *J. Chem. Eng. Data*, **47**(3), 518 (2002).

Tables

Table I. Flory Huggins and Wolf parameters for the literature data

Polymer /Solvent	Mw (kg/mol)	T (°C)	χ_o	ν	$\xi\lambda$	χ_f (eq.20)	Reference
PS / CH	233	45	0.490	0.313	0.023	1.02	17
PS / THF	30	20	0.416	0.295	1.110	-0.25	18
PVME / THF	50	20	0.474	0.257	0.660	0.07	18
PS / TOL	180	20	0.452	0.305	0.480	0.49	18
PI / CH	23	45	0.373	0.352	0.468	0.60	19
PVME / CH	81	65	0.446	0.339	0.810	0.44	20
PDMS / OCT	87	40	0.395	0.332	0.500	0.50	21
PDMS / MEK	87	40	0.496	0.385	0.136	1.26	21
PDMS / TOL	9	40	0.454	0.294	0.155	0.76	21
PIB / BZ	90	25	0.500	0.307	0.000	1.04	22

Where the polymers are: PS (polystyrene), PVME (Polyvinyl methyl ether), PI (Polyisoprene), PVME (Polyvinyl methyl ether), PDMS (Polydimethylsiloxane), PIB (polyisobutylene). And the solvents are: CH (Cyclohexane), THF (tetrahydrofuran), TOL (Toluene), OCT (Octanol), MEK (Methyl ethyl ketone), BZ (Benzene)

Table II. Percentage Average absolute deviation between bibliographic and estimated pressure (%AADP)

Polymer / Solvent	%AADP	Polymer / Solvent	%AADP
PS / CH	0.176	PVME / CH	2.534
PS / THF	0.748	PDMS / OCT	0.000
PVME / THF	2.448	PDMS / MEK	1.191
PI / CH	0.269	PDMS / TOL	2.714
PS / TOL	0.155	PIB / BZ	0.000

Table III. Physical properties of the studied polymers

Polymer	Supplier	% Vinyl Acetate	Molecular weight (g/mol)	Density at 25°C (gr/mL)	T_g (°C)	T_m (°C)
Polyethylene (PE)	Aldrich	0	35,000	0.906	-	93.2
Ethylene vinyl acetate (EVA 18)	Repsol	18.21	42,460	0.937	-	83.4
Ethylene vinyl acetate (EVA 33)	Repsol	31.51	61,041	0.956	-	63.7
Polyvinylacetate (PVAc)	Aldrich	100	100,000	1.18	42.7	N/A

Table IV. Flory Huggins parameters for the polymer/solvent systems of interest

T (°C)	System	χ_o (IV)	χ_f (IGC)	References
60	PVA / MET	0.495	1.21	24,26
50	EVA 18 / CX	0.495	0.36	23,27
40	EVA 18 / CX	0.496	0.4	23,27
30	EVA 18 / CX	0.563	0.47(*)	23,27
50	EVA 33 / CX	0.482	0.37	23,27
40	EVA 33 / CX	0.473	0.39	23,27
30	EVA 33 / CX	0.49	0.44(*)	23,27
60	PE / CX	0.051	0.34	24,27
60	PVA / CX	-	1.75(**)	26

Table V. Wolf parameters for EVA/CX mixtures between 30 °C and 80 °C

EVA 18	30 °C	40 °C	50 °C	60 °C	80 °C	EVA 33	30 °C	40 °C	50 °C	60 °C	80 °C
v	0.265	0.275	0.267	0.270	0.272	v	0.286	0.282	0.275	0.271	0.261
$\xi\lambda$	0.500	0.500	0.500	0.500	0.500	$\xi\lambda$	0.5	0.5	0.5	0.5	0.5
α	1.063	0.996	---	0.862	0.728	α	0.990	0.973	0.982	0.974	0.966

Table VI. Wolf excess parameters for EVA/CX and its homopolymers at 60°C

	EXC EVA18	EXC EVA33
v	-2.284	-1.222
$\xi\lambda$	-2.368	-1.180
α	-2.466	-1.086

Schemes and Figures

Figure 1. Thermodynamics for the systems PS/CH (a), PS/THF (b) and PS/TOL (c) (1), Flory Huggins-composition curves; (2) Sorption curves
Literature (a); ref. 17 / Literature (b, c); ref. 18.

Figure 2. Variation of $\xi\lambda$ supposed “vs” v calculated
Each point present the %AADP / Points in circles are the best solution for $\xi\lambda, v$ pair

Figure 3. Sorption curve for PVA/MET at 60 °C / Literature: ref. 28.

Figure 4. Sorption curve for PE/CX at 60°C / Literature: ref. 29.

Figure 5. Sorption curves for EVA/CX at 80°C / Literature: ref. 30.

Figure 6. Sorption curves for PVA/CX at 60°C / Literature: ref. 32.

Figure 7. α and v parameters for EVA/CX and its homopolymers at 60°C

Figure 8. Flory Huggins-composition curves for EVA/CX and its homopolymers at 60°C

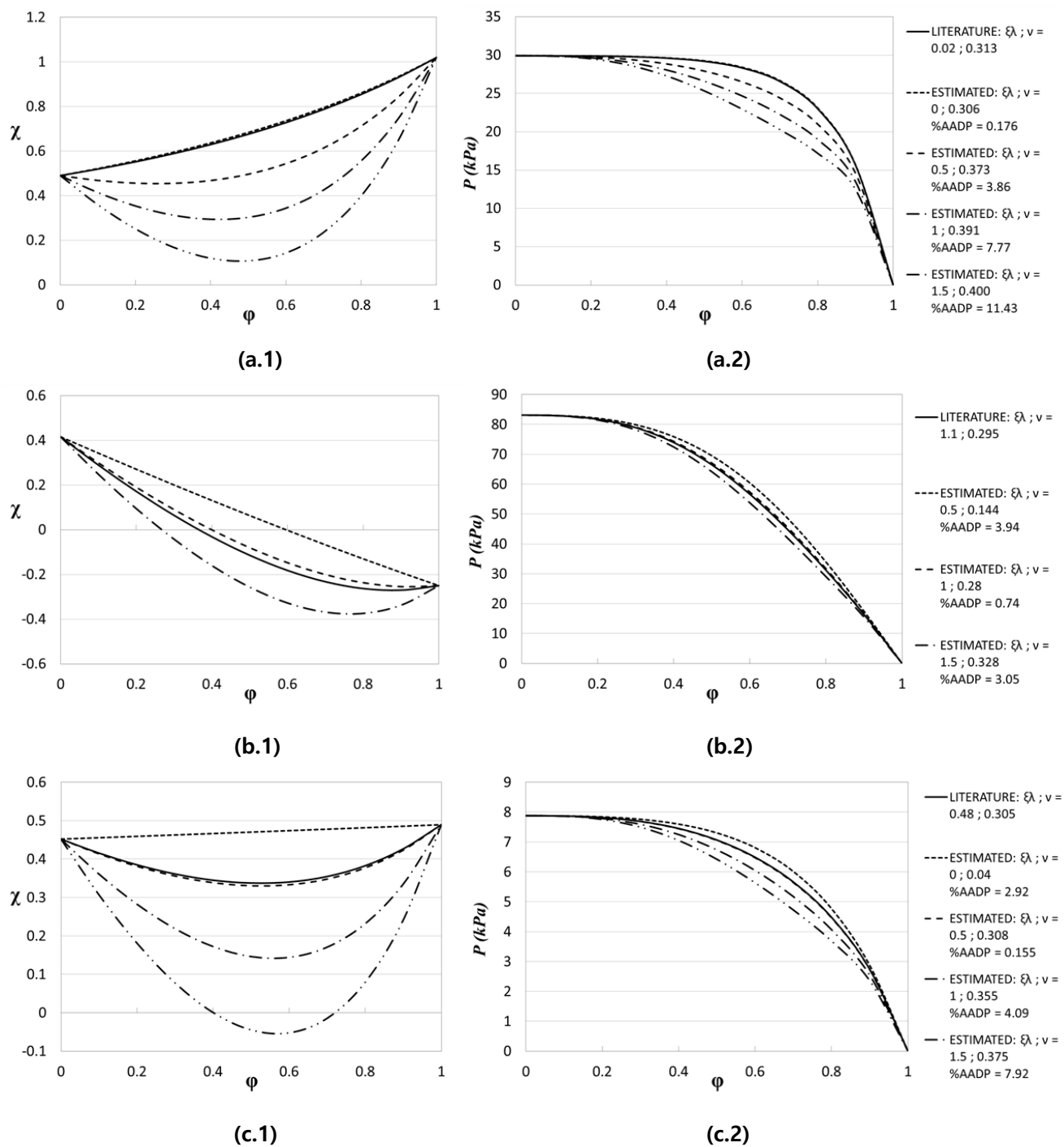


Figure 1

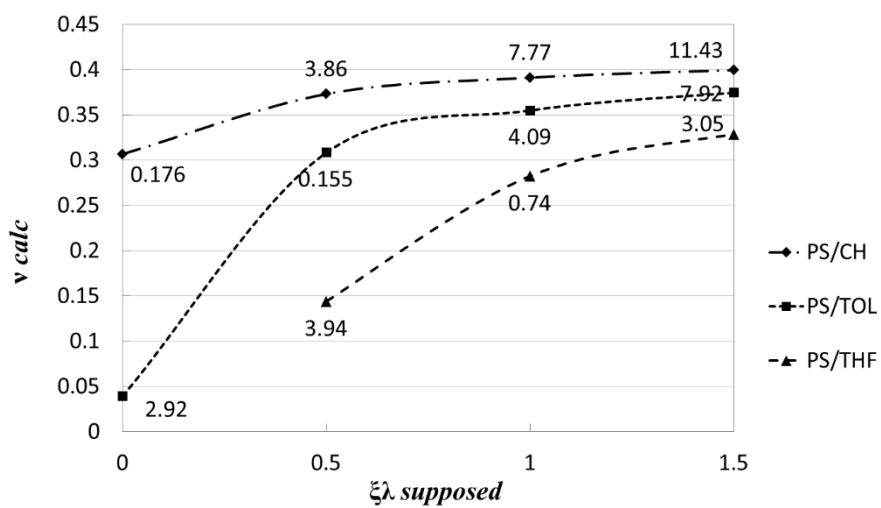


Figure 2

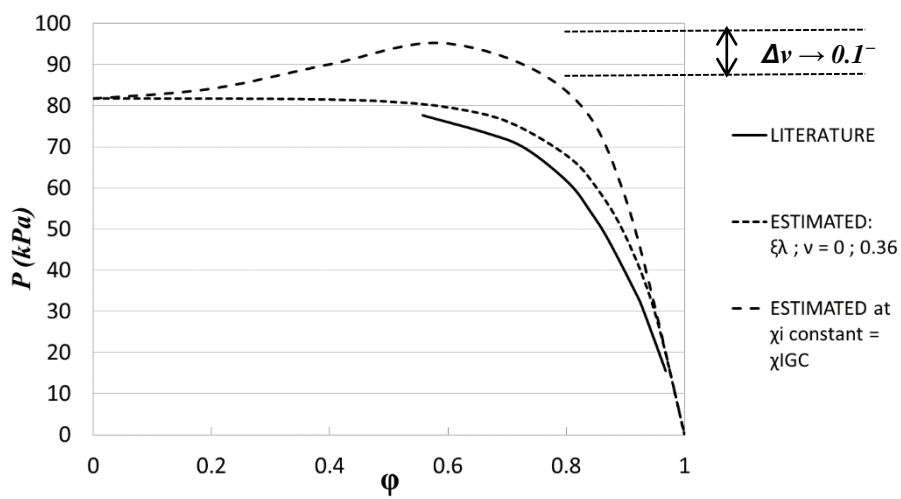


Figure 3

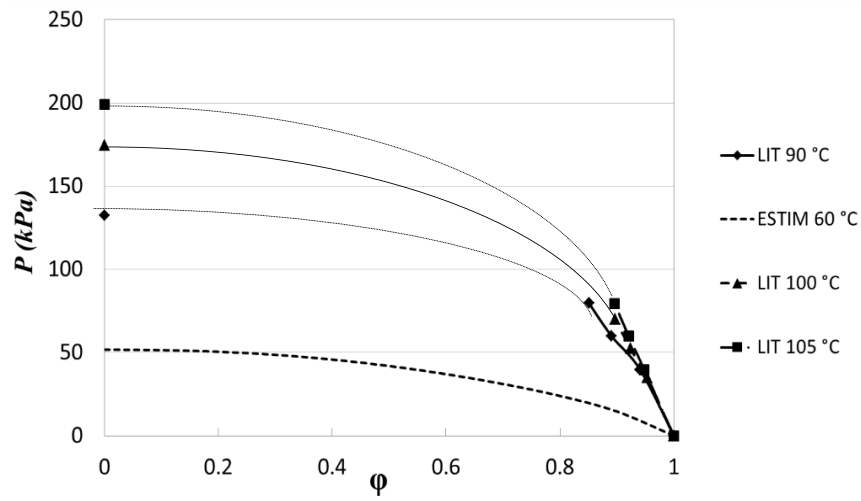


Figure 4

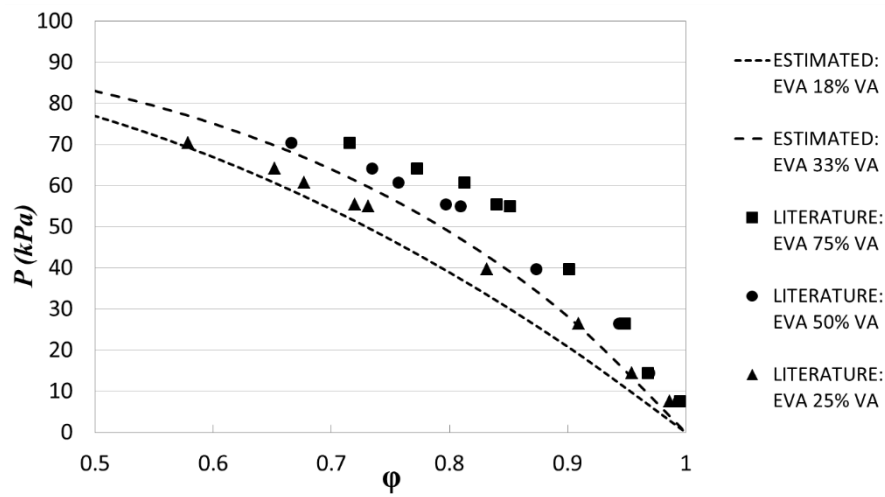


Figure 5

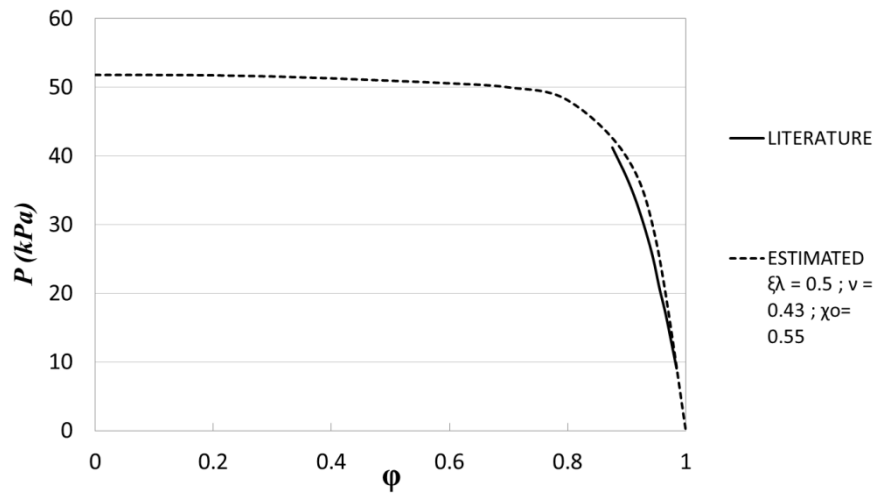


Figure 6

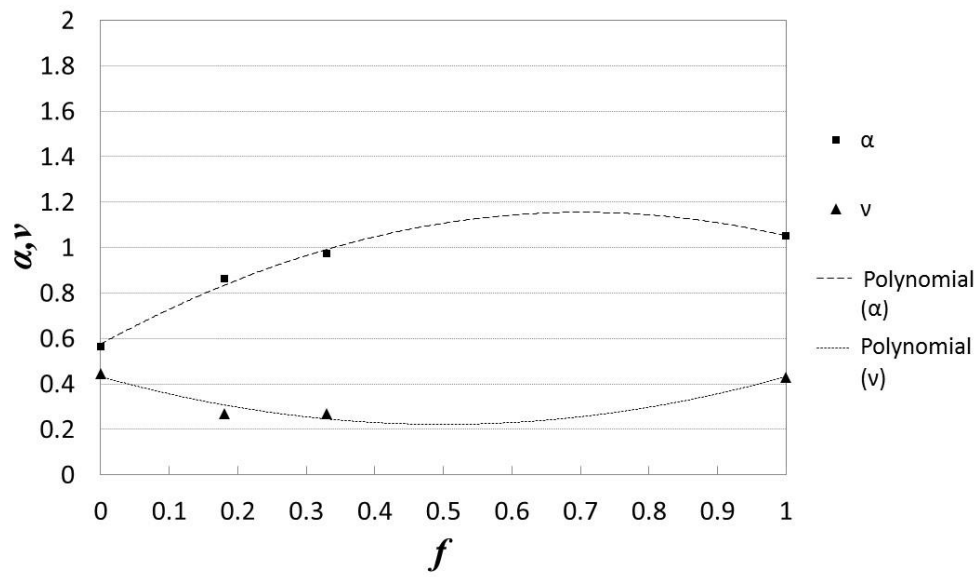


Figure 7

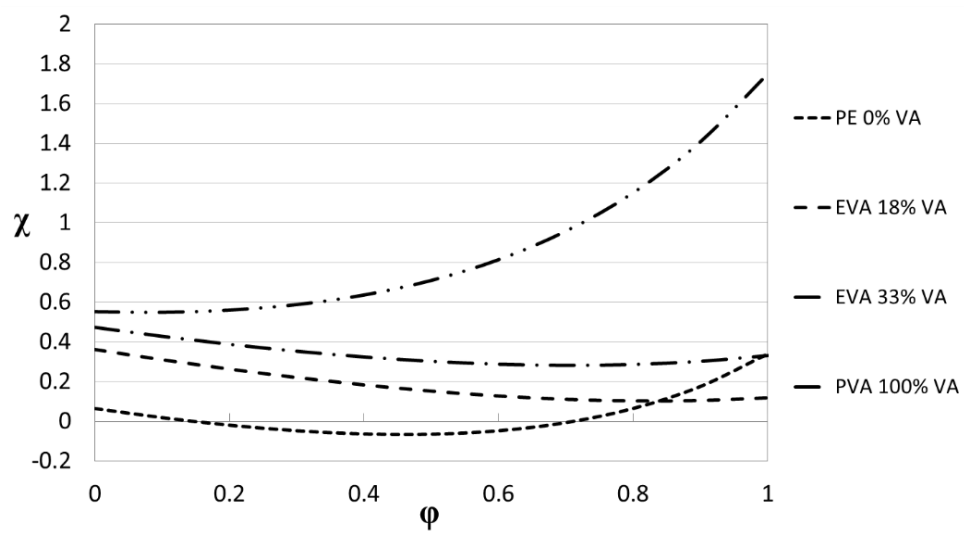


Figure 8

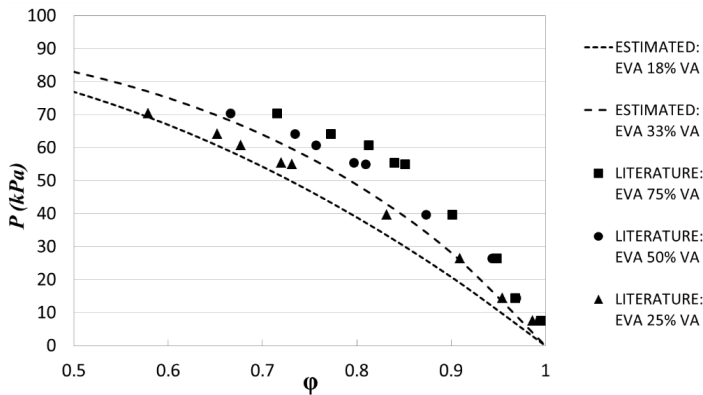
Table of Contents

Prediction of sorption curves from Flory Huggins parameters determined at solvent and polymer infinite dilution

Javier Camacho, Eduardo Díez* and Gabriel Ovejero

Macromol. Res., XX, XXX (20XX)

This work includes a new methodology to determine the solvent sorption curve) of a polymer/solvent mixture, taking as starting points the Flory Huggins parameters data measured at the composition extremes of the binary mixture. The methodology has been validated with several literature systems and has been applied to systems of interest for our research group.



5.2 PC-SAFT thermodynamics of EVA copolymer / solvents in the EVA separation solution process

Camacho, Camacho, J., Díez, E., Díaz & Ovejero, G. (2015). PC-SAFT thermodynamics of EVA copolymer / solvents in the EVA separation solution process. Submitted for publication.

PC-SAFT THERMODYNAMICS OF EVA COPOLYMER/SOLVENTS IN THE EVA SEPARATION SOLUTION PROCESS

Javier Camacho, Eduardo Díez*, Gabriel Ovejero

Grupo de Catálisis y Procesos de Separación (CyPS), Departamento de Ingeniería Química, Facultad de C. Químicas, Universidad Complutense de Madrid
Avda. Complutense s/n, 28040 Madrid, Spain.

Abstract

In this work a rigorous thermodynamic simulation for the separation stage of the Ethylene Vinyl Acetate copolymer (EVA) solution production process carry out in methanol (MET) to separate the unreacted vinyl acetate monomer (VA), is presented, employing the PC-SAFT equation of state model.

This rigorous thermodynamic simulation includes the splitting of the EVA copolymer in its correspondent homopolymers, Polyethylene (PE) and Polyvinylacetate (PVA), and the determination of the PC-SAFT binary interaction parameters (k_{ij}), that take into account all the possible interactions (six parameters) between the components participating in the mentioned process (PE, PVA, MET and VA). Also, the best association scheme for the interactions for these compounds was defined, and the pure PC-SAFT parameters were taken from literature.

The homopolymers/solvents k_{ij} was determined from the adjustment of the solvent sorption curves in polymers, which were constructed from the Flory Huggins data at infinite dilution of polymer and solvent, following a methodology published in one of our previous works that considers the Bernard Wolf theories, about the dependence of the Flory Huggins parameters with the polymer composition. The solvent/solvent k_{ij} was obtained from the liquid-vapour equilibrium curve reported for MET/VA. Additionally, the homopolymer/ homopolymer k_{ij} was determined from the sorption curves for the EVA copolymer and its homopolymers in cyclohexane (CH). In all cases, a good agreement between the theoretical equilibrium curves and the PC-SAFT predictions was observed.

Finally, with all the PC-SAFT binary interaction parameters known, a global process simulation was done, obtaining an average of %AAD for the mass flows of each component participating in the EVA solution separation production process below to 1%, regarding the literature data shown in patents.

Keywords: PC-SAFT, EVA copolymer, binary interaction parameter, sorption curve

*Corresponding author. Tel.: +34-91-394-8509; Fax: +34-91-394-4114.

E-mail address: ediezalc@quim.ucm.es (E. Díez).

1. Introduction

EVA copolymers representing the largest-volume segment of ethylene copolymer market [1], are products of the radical random copolymerization of the monomers ethylene and vinyl acetate (VA) in a predetermined ratio [2], therefore they are considered to be composed on polyethylene (PE) and polyvinyl acetate (PVA) homopolymers.

An important process to produce EVA copolymer is the solution production process, due the final applications of these copolymers, as rheology modifiers, adhesive binders, compounding components for thermoplasts and duroplasts, and for the production of vulcanisates [3]. In this process the solution polymerization is generally carried out with methanol (MET) as solvent [4].

Nowadays, in our the Catalysis and Separation Processes Research Group of the Chemical Engineering Department of the Complutense University of Madrid, one of the goals is to simulate the separation stage after the polymerization of the EVA copolymers, in order to propose a model tool for the prediction and optimization of the EVA copolymer production process an industrial scale. At the present time, the most powerful and robust tools for modeling of experimental data and even to predict the polymer/solvent thermodynamic behavior are: molecular dynamics simulations [5] and the PC-SAFT equations of state model [6], being this last one, the model considered in our studies for the thermodynamics assessments.

Besides, in our mentioned research group, two of the experimental procedures more validated, well known and published [7,8,9,10], to access to the thermodynamic data of a polymer/solvent system are the inverse gas chromatography technique (IGC) [11], and the intrinsic viscosity technique (IV) [12], which allows to determine the Flory Huggins parameters at infinite dilution of solvent, and polymer, respectively. These parameters based on the primordial Gibbs energy model theory applied to polymers, allow an easily prediction of a solvent sorption point (P_i “vs” polymer composition_{*i*}) according to the relationship of the partial segment molar Gibbs energy expressed in terms of the solvent chemical potential μ_I [13].

It is also well known in literature [14] that these Flory Huggins parameters obtained by the two techniques are different; in agree with the proven dependence of such parameters with the composition of polymer [15]. Previous works of Bernard Wolf have validated a composition dependence thermodynamic model for the Flory Huggins parameters of polymers/solvents systems, based on the adjustment of three parameters (α , v , $\xi\lambda$) [15]. In one of our previous work [16] a new methodology to determine the solvent sorption curve (Pressure – polymer composition) of a polymer/solvent mixture, from the Flory Huggins data measured at the composition extremes of the binary mixture (infinite dilution of polymer, and infinite dilution of solvent) has been proposed. This methodology is based on the works of Bernard Wolf mentioned above, and it was validated for ten different polymer/solvent systems, with an overall value of the average absolute deviation (%AAD) between the literature and estimated pressure values around 1%.

Finally, the adjustment of the solvent sorption curves to determinate the binary interaction parameter for the PC-SAFT model, will be also possible, taking into account

all the variability of the perturbations over the polymer/solvent system, especially the possible association schemes [17]. The theory described above, is illustrated in Fig. 1.

2. Theoretical Background

2.1 Thermodynamics of Solvent Sorption in Polymers (Vapor-Liquid Equilibria)

At low pressures (below the vapor pressure of the pure solvent), the solvent starts to evaporate from the polymer solution. On the other hand, solvent vapor of a given partial pressure may dissolve in the polymer. In these cases a liquid polymer/solvent mixture is in equilibrium with pure solvent vapor. The amount of solvent sorbed in the liquid polymer solution is a strong function of solvent partial pressure and temperature [18].

The mainly thermodynamics models considered in this work, for the modeling of the vapor-liquid phase equilibria are:

2.1.1 Gibbs energy models

The sorption of a solvent vapor in a polymer can be described using [18]:

$$p = x_1 \gamma_1 p_{1,o} \quad (1)$$

$$p = x_1 \Omega_1 p_{1,o} \quad (2)$$

where p is the pressure, x_1 is the solvent mole fraction and γ_1 the solvent activity coefficient, respectively. $p_{1,o}$ is the pure-component vapor pressure of the solvent at system temperature. Very often, instead of mole fraction x_1 , the weight fraction w_1 is used in (1), and Ω_1 , is the solvent weight-fraction activity coefficient.

The activity coefficients γ_1 and Ω_1 , in (1) and (2) can be easily calculated from Gibbs energy models using classical thermodynamic relationships.

The first Gibbs energy model developed for polymer solutions is the well-known expression from Flory and Huggins [19], which was developed based on a lattice theory, from which in terms of one mole of segments as the basis, the integral Gibbs energy \bar{G} , for polymer/solvent mixtures, can be expressed as:

$$\frac{\Delta \bar{G}}{RT} = (1 - \phi_2) \ln(1 - \phi_2) + \frac{\phi}{N} \ln \phi_2 + g \phi_2 (1 - \phi_2) \quad (3)$$

where R is the universal gas constant, ϕ_2 is the volume fraction of the polymer, g is the integral Flory-Huggins interaction parameter, and N is the number of polymer segments that is calculated by dividing the molar volume of the macromolecule by the molar volume of the solvent. Only if g does not depend on composition, this parameter becomes identical to the experimentally measurable Flory-Huggins interaction parameter χ .

Moreover, the partial segment molar Gibbs energy in a polymer/solvent mixture, expressed in terms of the “solvent” chemical potential μ_1 , is [15]:

$$\frac{\Delta\mu_1}{RT} = \frac{\Delta\bar{G}_1}{RT} = \ln(1-\phi) + \frac{1-\phi}{N} + \chi\phi^2 = \ln a_1 \quad (4)$$

Where a_1 , the solvent activity can be approximated (enough low volatility of the solvent) to the ratio of the solvent vapour pressure in the mixture to the pure solvent vapour pressure:

$$a_1 \approx \frac{P_1}{P_{1,o}} \quad (5)$$

Equations (4) and (5) allow the estimation of a sorption point for a solvent vapor in a polymer (P_1 “vs” polymer composition), previously knowing the Flory Huggins parameter.

On the other hand, a lot of efforts were done by different authors to find reasonable expressions for the concentration dependence of the χ parameter [20,21,22]. Recents works, of Bernard Wolf [15], have shown the accuracy of a composition dependant relationship, to predict g and χ , based on subdividing the polymer-solvent dilution process into two separate steps neglected by the original Flory–Huggins: the fixed conformation and the conformational relaxation, from wich $\chi_o = \alpha - \xi\lambda$ (α stands the fixed conformation step, λ the conformational relaxation step, ξ is a proporcional constant). Then arranging a complex analysis (where v accounts for the differences between the molecular surfaces of solvent and polymer), χ have been rewritten as:

$$\chi \approx \frac{\alpha}{(1-v\phi)^2} - \xi\lambda(1+2\phi) \quad (6)$$

In addition, the dependence $\pi = \pi_o + \pi_1/T + \pi_2T$, has proved to be very versatile to model $\pi(T)$, where π is whatever of the above mentioned parameters [15].

To apply the approach described above to solutions of random copolymers (containing type A and type B monomers), the different parameters π (α , v , ξ λ) must be a function of f , the weight fraction of B-monomers contained in the A-ran-B copolymer, taking into account excess parameters. For this purpose, the following approach has been proposed [23].

$$\pi_{AB} = \pi_A(1-f) + \pi_B f + \pi_E f(1-f) \quad (7)$$

2.1.2 Equations of state

Gibbs energy models in general can only be used to describe the activity coefficients of incompressible fluids. They do not take into account density changes of a system and thus they cannot be applied to describe non-idealities of the vapor phase at elevated and high pressures. These drawbacks can be avoided by using an equation of state.

There are different approaches for the development of an equation of state described in literature: extending the lattice theory previously described by introducing holes (Lattice-Fluid Theory [24] and the Mean-Field Lattice-Gas Theory [25]), partitioning a system derived from statistical mechanics. [26,27,28], and applying the so-called perturbation theories [29,30]. The main assumption here is applied to the Helmholtz energy of a system (A), based on the residual part A^{res} (the difference between the Helmholtz energy of a system, and the Helmholtz energy of an ideal gas state A^{ideal}) can be written as the sum of different contributions: the Helmholtz energy of a chosen reference system A^{ref} , and the Helmholtz energy due to perturbations A^{pert} . [18].

$$A^{res} = A - A^{ideal} = A^{ref} + A^{pert} \quad (8)$$

An appropriate reference system (at least for small solvent molecules) is the hard-sphere (hs) system. Here, the molecules are assumed to be spheres of a fixed diameter and do not have any attractive interactions. Such a reference system covers the repulsive interactions of the molecules. Deviations of real molecules from the reference system may occur due to attractive interactions (dispersion), formation of hydrogen bondings (association), chain formation and dipolar interactions. These contributions can be accounted for by using different perturbation terms [18].

The first model in this category was the Statistical-Associating-Fluid Theory (SAFT) [31,32,33]. Here a chain-like molecule (solvent molecule or polymer) is assumed to be a chain of m identical spherical segments. Starting from a reference system of m hard spheres (A^{hs}), this model considers three perturbation independent contributions: dispersion, association and chain formation. The recently proposed Perturbed-Chain SAFT (PC-SAFT) model [34] is a modification of SAFT which was developed especially to improve the description of polymer systems. Here the reference system of hard chains is used instead of the hard-sphere system. Therefore, the dispersion term now considers the attraction of chain-molecules instead of unbonded spheres, as a function of the chain length m . In addition to dispersive interactions, the phase behaviour of pure fluids and mixtures is also strongly affected by specific intermolecular interactions like association (hydrogen bonding) plus the dipolar interactions:

$$A^{res} = A^{hc} + mA^{disp} + A^{assoc} + A^{dipole} \quad (9)$$

According to Equation (9), the different contributions to the Helmholtz energy which are considered in PC-SAFT, are resumed as follows:

- *Hard-Chain Contribution A^{hc}* : This contribution considers the hard-chain reference fluid as spherical segments that do not show any attractive interactions. It is defined by two parameters, named the number of segments m and the diameter of segments σ . The Helmholtz energy of this reference system is described by an expression developed by Chapman [35], which is based on Wertheim's first-order thermodynamic perturbation theory [36].

- *Dispersion Contribution A^{disp}* : To determine the contribution of dispersive attractions to the Helmholtz energy of a system, PC-SAFT applies the perturbation theory of Barker and Henderson [37], to the hard-chain reference system. One additional

parameter is required for describing the segment – segment interaction: the dispersion energy parameter ε/k . All three parameters (m , σ and ε/k) are determined by simultaneously fitting to liquid density and vapour - pressure data of a pure component. To model mixtures, conventional Berthelot–Lorentz combining rules are applied.

- *Association Contribution A^{assoc}* : The contribution due to short-range association interactions (hydrogen bonding) is considered by an association model that also was proposed by Chapman [35], based on Wertheim's first-order thermodynamic perturbation theory [36]. Within this theory, a molecule is assumed to have one or more association sites that can form hydrogen bonds. Therefore, the association between two association sites is characterized by two additional parameters: the association energy ε^{AiBi}/k and the effective volume of an association interaction κ^{AiBi} . The strength of cross-association interactions between two different associating compounds can be determined using simple combining rules of the pure-component parameters, as suggested by Wolbach and Sandler [38], without introducing binary parameters.

- *Dipole/Polarizability Contribution A^{dipole}* : The long-range electrostatic interactions of dipolar and polarizable fluids A^{dipole} are taken into account by the expression of Kleiner and Gross (PCIP-SAFT) [39]. It is based on the renormalized perturbation theory for polarizable polar fluids of Wertheim, which was applied to the dipole contribution for non-spherical molecules of Gross and Vrabec [40]. Since tabulated values for the dipole moments and average molecular polarizabilities are available, no additional adjustable parameters are required.

In a polymer/solvent system, where large differences in molecular size of polymers and solvents are present, and the molar-mass distribution of a polymer is significant, the modelling of these systems with the PC-SAFT model is very suitable. PC-SAFT model is based on the hard-chain reference system and thus explicitly considers the attractive interactions of chain molecules instead of those of the unbonded segments [41].

Specifically, to modelling a copolymer (consisting of α -segments and β -segments)/solvent mixture with the PC-SAFT model, the pure-component parameters of the respective homopolymer segments and of the solvent are required. The binary parameters of the homopolymer/solvent systems ($k_{\alpha-s}$, $k_{\beta-s}$) can be determined from fitting the phase equilibrium data of the respective homopolymers/solvent systems. To describe the copolymer system, if necessary, one additional binary interaction parameter can be fitted to binary copolymer data, which accounts for the dispersive interactions between the homopolymer segments ($k_{\alpha-\beta}$) in the copolymer solution [42].

2.2 EVA copolymer solution production process

The following section describes a typical solution process for producing an ethylene-vinyl acetate copolymer based on the patents assigned to Kuraray Company [4]. This process comprises two main steps: copolymerizing ethylene and vinyl acetate in an alcohol based solvent and recovering unreacted vinyl acetate from a solution after copolymerizing.

A stream containing ethylene, vinyl acetate and methanol is introduced in the polymerization vessel (R1), with methanol used as a solvent. In the reactor, polymerization temperature is between 50 °C and 80 °C, and the pressure of the gaseous

phase (ethylene pressure) is from 20 to 80 bar. Finally, the radical polymerization produces ethylene vinyl acetate (EVA) copolymers with a degree of polymerization about 30 to 80%, based on vinyl acetate.

Next, the unreacted ethylene gas is evaporated from the copolymer solution in a flash tank (S1), and removed through the upper portion thereof.

The polymerization reaction solution (copolymer solution) drawn continuously from the polymerization vessel through its bottom portion, is fed into a recovery bubble-cap tower column (C1) filled with Rasching ring (e.g. 20 steps and diameter of 0.85 m), through the upper portion thereof, in order to extract the unreacted vinyl acetate from the copolymer solution. A vapor of the alcohol-based solvent (methanol) is continuously blown into the recovery column through the lower portion. Then, the unreacted vinyl acetate is taken out of the tower through the top portion thereof with part of the methanol, while the copolymer solution (EVA copolymer plus methanol) is taken out of the column through its bottom portion.

Next, the mixture solution taken out of the recovery column through the top portion is introduced into another treatment column (C2), where vinyl acetate is separated from the mixture solution by extractive distillation with water. Furthermore, by separating and purifying this water/alcohol mixture solution in (C3), an alcohol-based solvent can be recovered. On the other hand, the ethylene-vinyl acetate copolymer contained in the methanol solution from which vinyl acetate had been separated can be separated in another column, or it is saponified to produce EVOH copolymers.

The EVA copolymer solution production process described above is shown in Figure 2 and an industrial mass balance for the main separation column (C1), which is the control volume of the simulation of this work, is presented in Table 1.

3. PC-SAFT modeling of the EVA copolymer separation solution process

3.1. PC-SAFT configuration of the EVA copolymer and the binary interactions

As was previously mentioned, PC-SAFT equations of state model, based on a hard-chain reference system, take into account the different perturbations over the total Helmholtz energy of the system (hard chain, dispersion, association and polarizable contributions). PC-SAFT equation of state applied to polymer systems requires these contributions parameters for the homopolymer, plus a binary interaction parameter (k_{ij}) for the polymer/solvent mixture. This last parameter can be predicted from the polymer solubility or solvent sorption data [4], and it will be the same for the further predictions of all equilibria ($L-V$, $L-L$, $S-L$, $S-V$) of the system [44]. To describe a copolymer system, one additional binary interaction parameter between the homopolymers is necessary, and can be fitted from the binary copolymer/solvent data [42].

Therefore, applying the PC-SAFT procedure to simulate the separation stage after the polymerization in a recovery column (e.g., using the module Radfrac of the Aspen Plus[®] software) to split the EVA/MET solution for the VA co-monomer, the EVA copolymer must be subdivided into its homopolymers (PE and PVA). Then, the following six binary interaction parameters (k_{ij}) are necessary:

- k_{ij} homopolymers/solvents (PE/MET, PE/VA, PVA/MET, PVA/VA)
- k_{ij} homopolymer/homopolymer (PVA/PE)
- k_{ij} solvent/solvent (MET/VA)

The theory described above is illustrated in Figure 3.

The necessities k_{ij} for each homopolymer/solvent mixture described above can be obtained by regression of fitting of the binary data of certain sorption curves for the systems (e.g., using the mode Regression of Aspen Plus[®] software). As was previously mentioned, the sorption curves can be determined from the Flory Huggins parameters, obtained with VI and IGC techniques, following the methodology described in [16]. Table 2 summarizes the physical data of the polymers selected from this last study, for the modeling of the EVA separation solution process.

Besides, in this previous work [16] it was also shown, that cyclohexane (CH) was a favorable solvent ($\chi \leq 0.5$) for the EVA copolymer and its correspondent homopolymers (PE and PVA) at all conditions of infinite dilution (of polymer and solvent). For this reason, although cyclohexane it is not present in the EVA solution separation process, this is a system whit all the sorption curves known, which represent extra important thermodynamic information between EVA/solvents, that will be used for the determination of the binary parameters between the PE and PVA homopolymers.

On the other hand, the solvent/solvent binary data can be obtained from the liquid-vapor equilibrium, determined for example from traditional experimental techniques as the glass ebullometer, published in [46].

3.2. PC-SAFT pure parameters and association's interactions scheme

In this work, the five pure-component parameters (m , σ , ε/k , $\varepsilon^{\text{AiBi}}/k$, and κ^{AiBi}) for the EVA homopolymers (PE and PVA) and solvents (MET and VA) were taken directly from the Aspen Plus[®] DB-SEGMENT and DB-PCSAFT databases [45], respectively. It is important to notice that DB-SEGMENT database for polymers is defined for each one of their segments (SEG), which are determined as the number of moles of each homopolymer respect to the number molecular weight average of the copolymer, defining the parameter r , instead m , as a characteristic segment ratio parameter for each homopolymer.

Regarding the association scheme, it is important to note that the majority of the applications of SAFT models variants are found in the field of non-associating mixtures. Although the number of applications for associating mixtures has increased substantially, the nature of association schemes and the combining rules for solvating/cross-associating mixtures are worthy of investigation [17]. Next, the major conclusions considered for the associating compound (MET) and its interactions with the other compounds that determined changes in the initial values of $\varepsilon^{\text{AiBi}}/k$ and κ^{AiBi} in the mentioned databases, are:

- For the binary solvent mixture of a polar compound (VA) and an associating compound (MET), the association-energy parameter, ϵ^{AiBi}/k , of the non-self-associating (polar) component ought to be set to zero, while the association volume parameter, κ^{AiBi} , of the non-self-associating component must be assumed to be equal to the value of the associating component in the mixture [17]. This association scheme was previously employed in [46] with good predictions.
- For the polymer/solvent interactions the induced associations was considered, and the cross-association energy, ϵ^{AiBi}/k , of the polar homopolymer (SEG-PVA) was set equal to half the value of the association energy of the self-associating or the hydrogen bonding compound (MET). Moreover, κ^{AiBi} was set equal to the value of the self-associating compound [17]. This approach was previously validated for the literature data reported for the system PVA/MET [47], with good agreements.
- For the dispersion solvent (CH) and dispersion homopolymer (SEG-PE), the ϵ^{AiBi}/k and κ^{AiBi} was maintained to zero.

The final data for the five pure-component parameters employed for the PC-SAFT model is summarized in Table 3. Henceforth, whenever the PC-SAFT model is used, this configuration for the pure parameters of solvent and the homopolymers is considered.

3.3. Determination of PC-SAFT binary interactions parameters (k_{ij})

3.3.1. k_{ij} homopolymer/homopolymer (PVA/PE)

The determination of the PC-SAFT binary interactions parameters between the homopolymers presents in the EVA copolymer, PE and PVA, is based on the adjustment of the sorption curves for the system EVA/CH, as was mentioned above, for being a system with all the equilibriums known.

Initially each sorption curves for the systems PVA/CH, PE/CH and EVA33/CH were constructed with (7) and (4) from the Wolf parameters estimated at 60 °C in [16]. These parameters are summarized in Table 4.

Next, the PC-SAFT k_{ij} for the systems PVA/CH and PE/CH were determined, by the thermodynamic regression of the estimated data of the respective sorption curve. Finally, introducing these last k_{ij} parameters in the regression of the EVA33/CH sorption curve, the k_{ij} between the homopolymers segments, PE and PVA, was determined. These binary interactions parameters are summarized in Table 5.

Figure 4, shows the sorption curves for the mentioned systems, and the results of the liquid-vapor equilibria data regression with the PC-SAFT model.

3.3.2. k_{ij} homopolymer/solvent (PVA/MET)

The sorption curve for the system PVA/MET was constructed from the Wolf parameters reported for this system, at 60 °C in [16]. They are shown in Table 4.

Then, the PC-SAFT k_{ij} for the system PVA/MET was determined by a thermodynamic regression. This binary interaction parameter is shown in Table 5, and the adjustment is shown graphically in Figure 5.

3.3.3. k_{ij} homopolymer/solvent (PE/MET)

Due the weak interactions for the PE/MET system [48], the PC-SAFT binary interaction parameter for this mixture was determined from the thermodynamics of the EVA33/MET system.

The sorption curve for the system EVA33/MET was constructed from the amorphous Flory Huggins parameter reported at infinite dilution of solvent for this system at 60 °C in [48] ($\chi_{IGC} = 2.27$) and applying the specific procedure described in [16, section 3.4] for the estimation of the Wolf parameters of this system. These Wolf parameters determined for the EVA33/MET are shown in Table 4.

Then, introducing the PC-SAFT k_{ij} for the systems PVA/MET and PVA/PE previously determined, the PC-SAFT k_{ij} for the system PE/MET, was determined by means of a thermodynamic regression. This binary interaction parameter is shown in Table 5, and the adjustment is shown graphically in Figure 5.

3.3.4. k_{ij} homopolymer/solvent (PVA/VA)

The sorption curve for the system PVA/VA was constructed from the amorphous Flory Huggins parameter reported at infinite dilution of solvent for this system at 60 °C in [48] ($\chi_{IGC} = 0.40$). In addition, the Flory Huggins parameter at infinite dilution of polymer was experimentally determined, by means of intrinsic viscosity measurements following the Stockmayer procedure described in [49] and employed the same PVA polymer samples reported in this last cited work. The resulting Flory Huggins parameter was $\chi_{IV} = 0.461$. The respective plots for this determination are shown in Figure 6 and 7.

Next, the sorption curve for the system PVA/VA was constructed following the general procedure described in [16] for the estimation of the Wolf parameters. These Wolf parameters determined for this system are shown in Table 4.

Then, the PC-SAFT k_{ij} for the system PVA/VA was determined by a thermodynamic regression. This binary interaction parameter is shown in Table 5, and the adjustment is shown graphically in Figure 8.

3.3.5. k_{ij} homopolymer/solvent (PE/VA)

Here, again due the weak interactions for the PE/VA system [48], the PC-SAFT binary interaction parameter for this mixture was determined from the thermodynamics of the EVA33/VA system

The sorption curve for the system PE/VA was constructed from the amorphous Flory Huggins parameter reported at infinite dilution of solvent for the system EVA33/VA at 60 °C in [48] ($\chi_{IGC} = 0.73$) and applying the specific procedure described in [16, section 3.4] for the estimation of the Wolf parameters. These Wolf parameters determined for EVA33/VA are shown in Table 4.

Then, introducing the PC-SAFT k_{ij} for the systems PVA/VA and PVA/PE previously determined, the PC-SAFT k_{ij} for the system PE/VA, was determined by means of a thermodynamic regression. This binary interaction parameter is shown in Table 5, and the adjustment is shown graphically in Figure 8.

3.3.6. k_{ij} solvent/solvent (MET/VA)

This parameter was taken directly from [46] and it is shown in Table 5. In the cited study the PC-SAFT thermodynamic assessment was done employing the same association scheme for the solvents involved in the EVA copolymer solution production process (MET and VA).

Also, the experimental liquid vapor equilibrium data obtained for this system by means of the glass ebullometer technique, and analyzing the liquid and vapor samples employing the Gas Chromatography apparatus, was adjusted with the run mode “Regression” of Aspen Plus[®].

The vapor-liquid equilibrium curve for this system, and the PC-SAFT fitting, is shown in Figure 9.

3.4. EVA separation solution process simulation.

The final simulation of the EVA copolymer separation solution process was done by means of Aspen Plus[®] software, introducing the previous six PC-SAFT k_{ij} binary parameters estimated for PVA/PE, PVA/MET, PE/MET, PVA/VA, PVA/PE and VA/MET, and the patent mass balance [4] reported for this production process (Table 1).

Initially, a “DSTW” column module was employed to estimate initial values of the reflux ratio, number of stages and feed stage, obtained an average %AAD for the mass flows of the components participating in the EVA solution separation stage below to 1%. Next, a “RADFRACC” column module was used to optimize these variables. Finally the column diameter was determined, considering a fractional approaching to flooding 80%. The diameter result ($D = 0.8$ m) was in good agreement with the theoretical diameter shown in the patents [4].

4. Conclusions

A rigorous thermodynamic simulation for the separation stage of the Ethylene Vinyl Acetate copolymer (EVA) solution production process carry out in methanol (MET) to separate the unreacted vinyl acetate monomer (VA), was presented; employing the PC-SAFT equation of state model, splitting the EVA copolymer in its correspondent homopolymers, Polyethylene (PE) and Polyvinylacetate (PVA), and determining the six PC-SAFT binary interaction parameters (k_{ij}), that take into account all the possible interactions between the components participating in the mentioned process (PE, PVA, MET and VA). These k_{ij} for homopolymers, were determined from the solvent sorption curves constructed from the Flory Huggins data at infinite dilution of polymer and solvent, following a methodology described in literature that considers the Bernard Wolf thermodynamic theories. The k_{ij} between the solvents was determined from the vapour liquid equilibrium data reported in literature. Also, the best association scheme for the interactions for these compounds was defined, and the pure PC-SAFT parameters were taken from literature.

A good agreement between each sorption curves for polymer/solvent estimated theoretically and predicted with the PC-SAFT model, was obtained.

Finally, a global process simulation was done, obtaining an average of %AAD for the mass flows of each component participating in the EVA solution separation production process below to 1%, regarding the literature data shown in patents.

Literature

1. Chanda, M., & Roy, S. K. (2008). Industrial polymers, specialty polymers, and their applications (Vol. 74). CRC Press.
2. Anon. (2006). PERP Program—LDPE copolymers (03/04S9). Chem systems Reports. Nexant Inc., New York, USA
3. Baade, W., Obrecht, W., & Ohm, C. (1992). U.S. Patent No. 5,093,450. Washington, DC: U.S. Patent and Trademark Office
4. Kawahara, T., & Hikasa, T. (2005). U.S. Patent No. 6,838,517. Washington, DC: U.S. Patent and Trademark Office.
5. Rapaport, D. C. (2004). *The art of molecular dynamics simulation*. Cambridge university press.
6. Gross, J., & Sadowski, G. (2002). Modeling polymer systems using the perturbed-chain statistical associating fluid theory equation of state. *Industrial & engineering chemistry research*, 41(5), 1084-1093.
7. Ovejero, G., Pérez, P., Romero, M. D., Díaz, I., & Díez, E. (2009). SEBS triblock copolymer–solvent interaction parameters from inverse gas chromatography measurements. *European Polymer Journal*, 45(2), 590-594.
8. Díez, E., Ovejero, G., Romero, M. D., & Díaz, I. (2011). Polymer–solvent interaction parameters of SBS rubbers by inverse gas chromatography measurements. *Fluid Phase Equilibria*, 308(1), 107-113.
9. Ovejero, G., Perez, P., Romero, M. D., Guzmán, I., & Díez, E. (2007). Solubility and Flory Huggins parameters of SBES, poly (styrene-*b*-butene/ethylene-*b*-styrene) triblock copolymer, determined by intrinsic viscosity. *European polymer journal*, 43(4), 1444-1449.
10. Ovejero, G., Romero, M. D., Díez, E., & Díaz, I. (2010). Thermodynamic interactions of three SBS (styrene–butadiene–styrene) triblock copolymers with different solvents, by means of intrinsic viscosity measurements. *European Polymer Journal*, 46(12), 2261-2268
11. Voelkel, A., Strzemieska, B., Adamska, K., & Milczewska, K. (2009). Inverse gas chromatography as a source of physiochemical data. *Journal of Chromatography A*, 1216(10), 1551-1566.
12. Moore, W. R. (1967). Viscosities of dilute polymer solutions. *Progress in Polymer Science*, 1, 1-43.
13. R. Horst and B.A. Wolf. Thermodynamics of polymer solutions (Thermodyn. von Polymer) <http://wolf.chemie.uni-mainz.de/Internet/Students/Makro.htm>

14. Yilmaz, F., & Cankurtaran, Ö. (1997). Comparison of the intrinsic viscosity and inverse gas chromatography techniques in determination of the exchange enthalpy and entropy parameters. *Polymer*, 38(14), 3539-3543.
15. Wolf, B. A. (2011). Making Flory–Huggins Practical: Thermodynamics of Polymer-Containing Mixtures. In *Polymer Thermodynamics* (pp. 1-66). Springer Berlin Heidelberg.
16. Camacho, J., Díez, E., Díaz & Ovejero, G. (2015). Prediction of sorption curves from Flory Huggins parameters determined at solvent and polymer infinite dilution. Submitted for publication.
17. Kontogeorgis, G. M., & Folas, G. K. (2009). *Thermodynamic models for industrial applications: from classical and advanced mixing rules to association theories*. John Wiley & Sons.
18. Sadowski, G. (2004, February). Thermodynamics of polymer systems. In *Macromolecular Symposia* (Vol. 206, No. 1, pp. 333-346). WILEY-VCH Verlag.
19. Flory P.J., *J. Chem. Phys.* 1942, 10, 51
20. Kleintjens, L. A. L. (1979). Effects of chain branching and pressure on thermodynamic properties of polymer solutions (Doctoral dissertation, University of Essex).
21. Qian, C., Mumby, S. J., & Eichinger, B. E. (1991). Existence of two critical concentrations in binary phase diagrams. *Journal of Polymer Science Part B: Polymer Physics*, 29(5), 635-637.
22. Hu, Y., Lambert, S. M., Soane, D. S., & Prausnitz, J. M. (1991). Double-lattice model for binary polymer solutions. *Macromolecules*, 24(15), 4356-4363.
23. Bercea, M., Eckelt, J., & Wolf, B. A. (2008). Random copolymers: their solution thermodynamics as compared with that of the corresponding homopolymers. *Industrial & Engineering Chemistry Research*, 47(7), 2434-2441.
24. Sanchez, I. C., & Lacombe, R. H. (1976). An elementary molecular theory of classical fluids. Pure fluids. *The Journal of Physical Chemistry*, 80(21), 2352-2362.
25. Kleintjens, L. A., & Koningsveld, R. (1980). Liquid-liquid phase separation in multicomponent polymer systems. *Colloid and Polymer Science*, 258(6), 711-718.
26. Beret, S., & Prausnitz, J. M. (1975). Perturbed hard-chain theory: An equation of state for fluids containing small or large molecules. *AIChE Journal*, 21(6), 1123-1132.

27. Cotterman, R. L., Schwarz, B. J., & Prausnitz, J. M. (1986). Molecular thermodynamics for fluids at low and high densities. Part I: Pure fluids containing small or large molecules. *AIChE journal*, 32(11), 1787-1798.
28. Morris, W. O., Vimalchand, P., & Donohue, M. D. (1987). The perturbed-soft-chain theory: An equation of state based on the Lennard-Jones potential. *Fluid Phase Equilibria*, 32(2), 103-115.
29. Barker, J. A., & Henderson, D. (1967). Perturbation theory and equation of state for fluids. II. A successful theory of liquids. *The Journal of Chemical Physics*, 47(11), 4714-4721.
30. Weeks, J. D., Chandler, D., & Andersen, H. C. (1971). Role of repulsive forces in determining the equilibrium structure of simple liquids. *The Journal of Chemical Physics*, 54(12), 5237-5247.
31. Chapman, W. G., Gubbins, K. E., Jackson, G., & Radosz, M. (1989). SAFT: Equation-of-state solution model for associating fluids. *Fluid Phase Equilibria*, 52, 31-38.
32. Huang, S. H., & Radosz, M. (1990). Equation of state for small, large, polydisperse, and associating molecules. *Industrial & Engineering Chemistry Research*, 29(11), 2284-2294.
33. Huang, S. H., & Radosz, M. (1991). Equation of state for small, large, polydisperse, and associating molecules: extension to fluid mixtures. *Industrial & Engineering Chemistry Research*, 30(8), 1994-2005
34. Gross, J., & Sadowski, G. (2001). Perturbed-chain SAFT: An equation of state based on a perturbation theory for chain molecules. *Industrial & engineering chemistry research*, 40(4), 1244-1260.
35. Chapman, W. G., Jackson, G., & Gubbins, K. E. (1988). Phase equilibria of associating fluids: chain molecules with multiple bonding sites. *Molecular Physics*, 65(5), 1057-1079.
36. Wertheim, M. S. (1984). Fluids with highly directional attractive forces. II. Thermodynamic perturbation theory and integral equations. *Journal of statistical physics*, 35(1-2), 35-47.
37. Barker, J. A., & Henderson, D. (1967). Perturbation Theory and Equation of State for Fluids: The Square-Well Potential. *The Journal of Chemical Physics*, 47(8), 2856-2861.
38. Wolbach, J. P., & Sandler, S. I. (1998). Using molecular orbital calculations to describe the phase behavior of cross-associating mixtures. *Industrial & engineering chemistry research*, 37(8), 2917-2928.
39. Kleiner, M., & Gross, J. (2006). An equation of state contribution for polar components: Polarizable dipoles. *AIChE journal*, 52(5), 1951-1961.

40. Gross, J., & Vrabec, J. (2006). An equation of state contribution for polar components: Dipolar molecules. *AIChE journal*, 52(3), 1194-1204.
41. Gross, J., & Sadowski, G. (2002). Modeling polymer systems using the perturbed-chain statistical associating fluid theory equation of state. *Industrial & engineering chemistry research*, 41(5), 1084-1093.
42. Gross, J., Spuhl, O., Tumakaka, F., & Sadowski, G. (2003). Modeling copolymer systems using the perturbed-chain SAFT equation of state. *Industrial & engineering chemistry research*, 42(6), 1266-1274.
43. Tumakaka, F., Gross, J., & Sadowski, G. (2002). Modeling of polymer phase equilibria using Perturbed-Chain SAFT. *Fluid phase equilibria*, 194, 541-551.
44. Buchelli, A., Call, M. L., Brown, A. L., Bokis, C. P., Ramanathan, S., & Franjione, J. (2004). Nonequilibrium behavior in ethylene/polyethylene flash separators. *Industrial & engineering chemistry research*, 43(7), 1768-1778
45. Plus, A. (2009). DB-SEGMENT and DB-PCSAFT Database. Aspen Technology. Inc., version, 11.
46. Camacho, J., Díez, E., Díaz, I., & Ovejero, G. (2012). Vapor–Liquid Equilibrium at p/kPa= 101.3 of the Binary Mixtures of Ethenyl Acetate with Methanol and Butan-1-ol. *Journal of Chemical & Engineering Data*, 57(11), 3198-3202.
47. Wibawa, G., Hatano, R., Sato, Y., Takishima, S., & Masuoka, H. (2002). Solubilities of 11 polar organic solvents in four polymers using the piezoelectric-quartz sorption method. *Journal of Chemical & Engineering Data*, 47(4), 1022-1029.
48. Camacho, J., Díez, E., Ovejero, G. (2015). Bulk interactions for polyethylene and EVA copolymers below their melting temperatures. Submitted to publication.
49. Camacho, J., Díez, E., Blanco, D., Martín, E., Ovejero, G. (2015). Thermodynamic study PVAc-solvent and PE-solvent diluted solutions. *Chemical Engineering Transactions*, 43, 1717-1722.

Table 1. Mass Balance of an EVA copolymers solution production process [4]

Stream	4	5	6	7
Temperature (°C)	60	60	60	60
Pressure (bar)	1.00	1.00	1.00	1.00
Mass Flow (kg/h)	1,200	474.0	927.3	746.7
% w/w Vinyl acet.	0.464	0.00	0.600	0.00
% w/w Methanol	0.256	1.00	0.400	0.550
% w/w Ethylene	0.00	0.00	0.00	0.00
% w/w EVA	0.280	0.00	0.000	0.450
% w/w Water	0.280	0.00	0.000	0.450

Table 2. Properties of the studied polymers

Polymer	Supplier	% VA	Mol. weight (g/mol)	Density at 25°C (gr/ml)	Tg (°C)	Tm (°C)
Polyethylene (PE)	Aldrich	0.00	35,000	0.906	-	93.2
EVA copolymer (EVA33)	Repsol	31.51	61,041	0.956	-	63.7
Polyvinylacetate (PVA)	Aldrich	100.00	100,000	1.18	42.7	N/A

Table 3. PC-SAFT parameters for EVA copolymer / solvents

Parameters	MET	VA	CH	SEG-PVA	SEG-PE
ϵ^{AiBi}/k	2899.5	0	0	1449.75	0
κ^{AiBi}	0.035176	0.035176	0	0.035176	0
m	1.5255	3.4442	2.5303	-	-
r	-	-	-	0.04224	0.04132
ϵ/k	188.9	232.25	278.11	243.9829	267.1854
σ	3.23	3.257	3.8499	3.0617	3.4751

Table 4. Wolf parameters for polymers studied / solvents 60 °C.

Parameter	PVA/CH	PE/CH	EVA 33/CH	PVA/MET	EVA33/MET	PVA/VA	EVA33/VA
ν	0.430	0.455	0.271	0.360	0.436	0.289	0.297
$\xi\lambda$	0.500	0.500	0.500	0.00	1.069	0.500	0.500
α	1.050	0.551	0.974	0.495	1.669	0.960	1.100

Table 5. PC-SAFT k_{ij} binary parameters for polymers studied / solvents

Parameter	SEG PVA/CH	SEG PE/CH	SEG PVA/SEG PE	SEG PVA/MET	SEG PE/MET	SEG PVA/VA	SEG PE/VA	MET/VA
k_{ij}	0.0082	-0.0098	0.0247	-0.0136	-0.0267	-0.0286	0.0228	0.0352

Figures captions

Figure 1. Determination of the PC-SAFT k_{ij} for a polymer/solvent system

Figure 2. Process Diagram of an EVA copolymers solution production process [4]

Figure 3. Illustration of the Six PC-SAFT interactions parameters (k_{ij}) necessary to model the EVA copolymer separation solution process

Figure 4. Sorption curves PVA, PE and EVA33 in cyclohexane at 60 °C. Lit: [16]

Figure 5. Sorption curves PVA and EVA33 in methanol at 60 °C. Lit: [16]

Figure 6. Intrinsic viscosity determination for PVA/VA at 60 °C.

Figure 7. Stockmayer procedure for the determination of the Flory Huggins parameter for the PVA/VA system at 60 °C.

Figure 8. Sorption curves PVA and EVA33 in vinyl acetate at 60 °C. Lit: [16]

Figure 9. Vapor-liquid equilibrium for vinyl acetate/methanol system, at 1 atm. (Points: experimental data / Solid Line: PC-SAFT adjustment) [46]

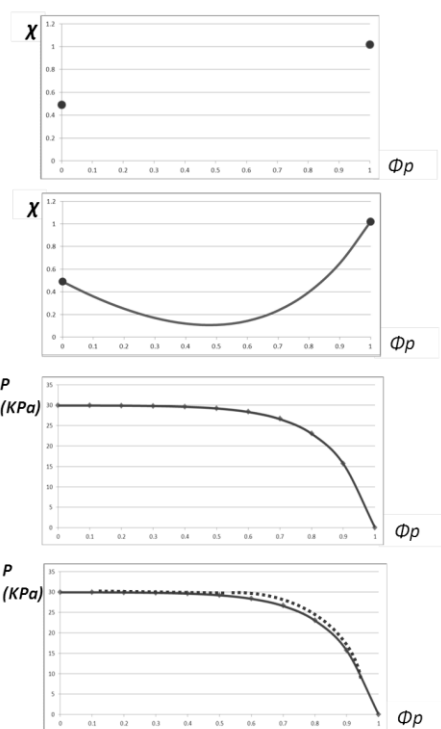
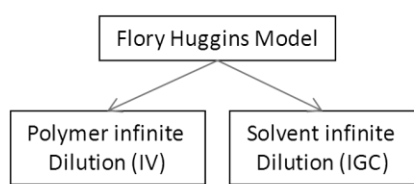


Figure 1

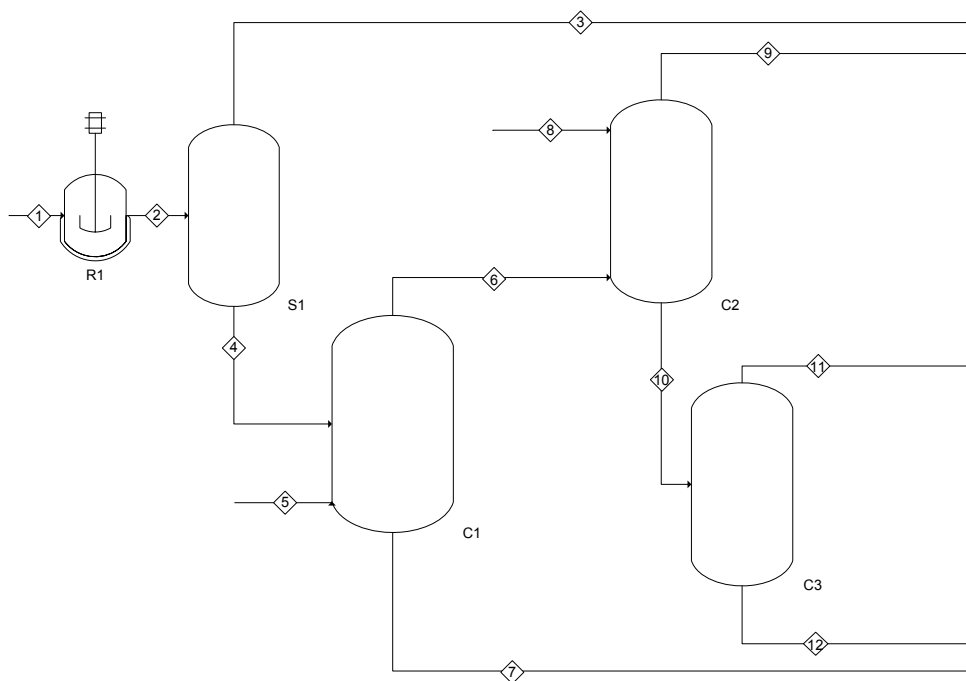


Figure 2

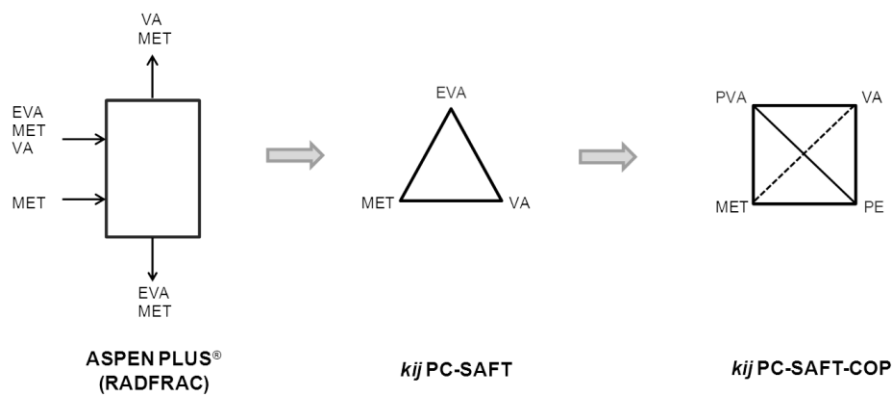


Figure 3

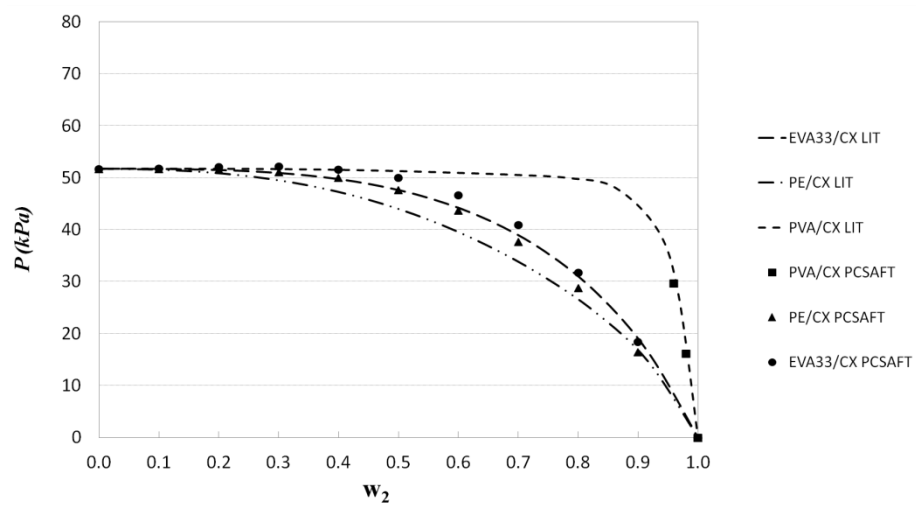


Figure 4

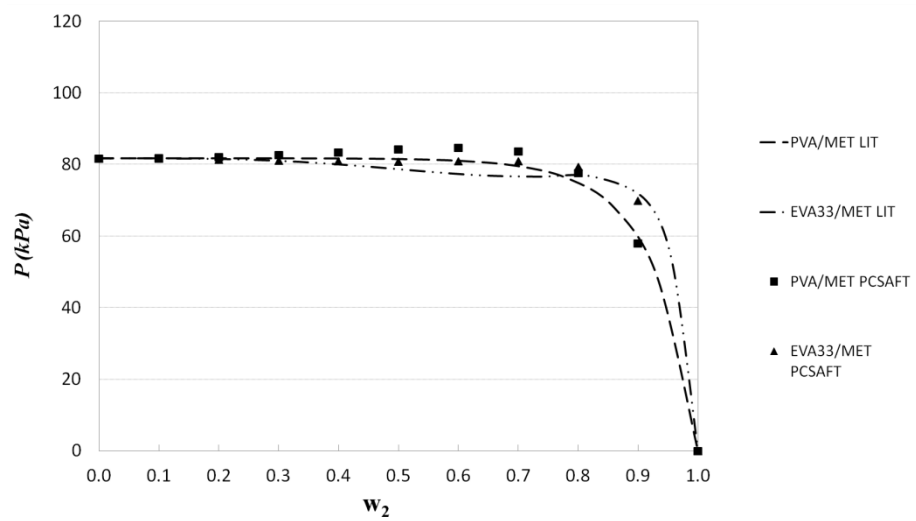


Figure 5

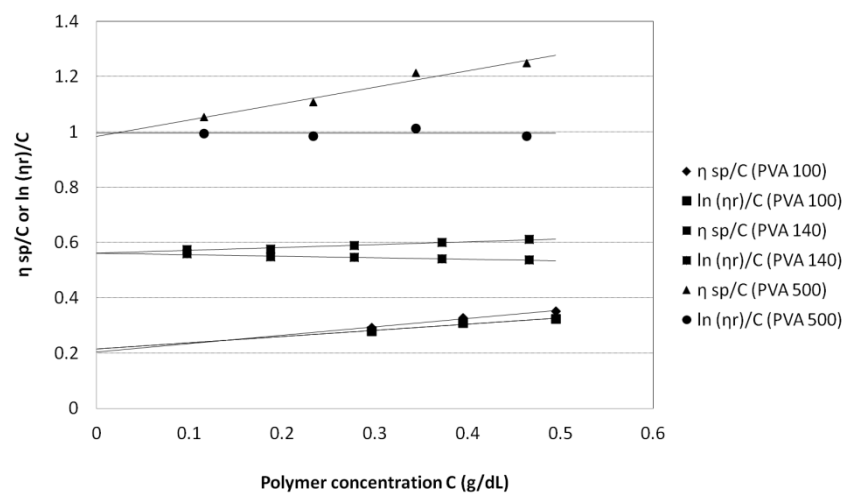


Figure 6

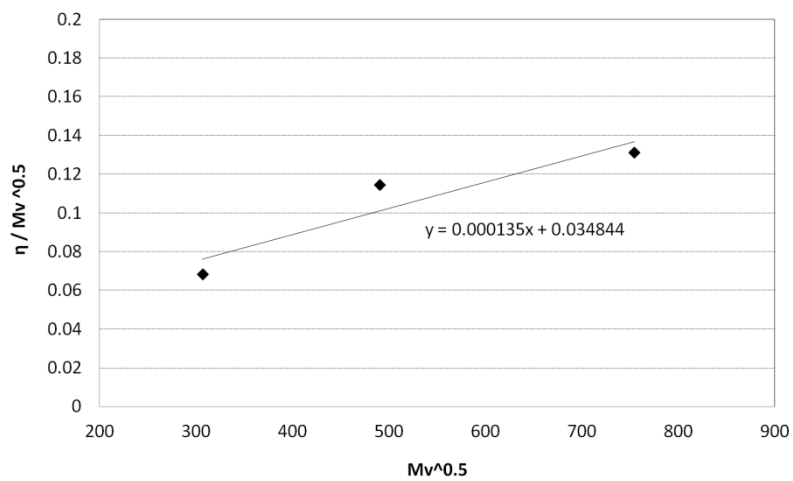


Figure 7

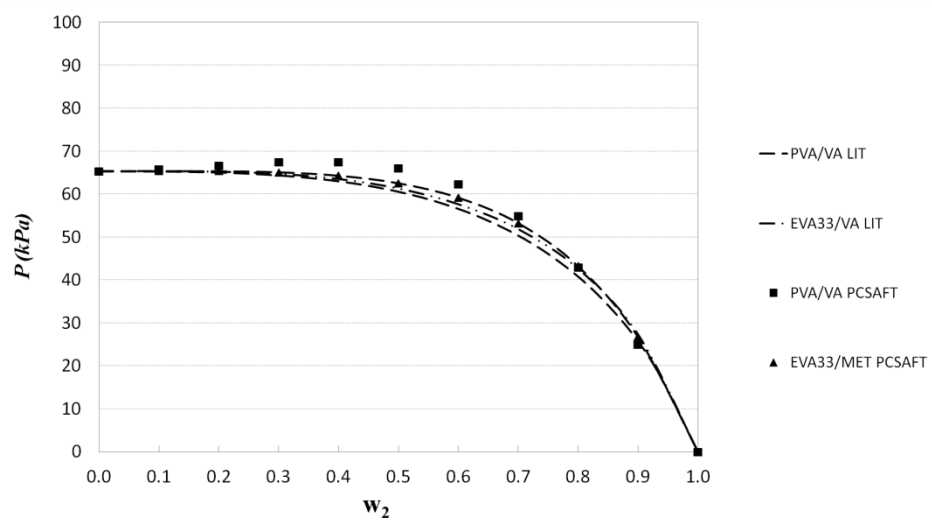


Figure 8

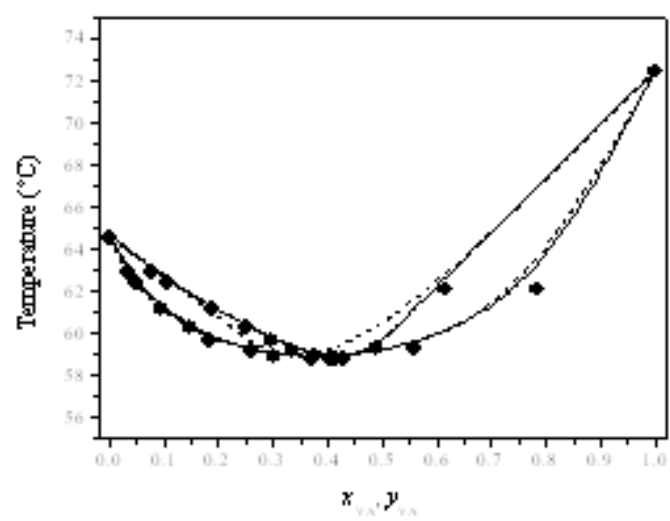


Figure 9

5.3 Summary and discussion

The above two scientific articles, about the determination and evaluation of the Flory Huggins – polymer composition curves, and the subsequent sorption curves and PC-SAFT fittings, of the EVA copolymers and their homopolymers (PE and PVA) in equilibrium with methanol, vinyl acetate and cyclohexane; by the extrapolation of the previous thermodynamic data for infinite dilution of solvent and polymer, to finite compositions of polymer, by means of the novel methodology proposed; can be summarized and integrate, as follows:

The first article “**Prediction of sorption curves from Flory Huggins parameters determined at solvent and polymer infinite dilution**” presents a new methodology to determine the solvent sorption curve (pressure-composition curves for the vapor-liquid equilibrium) of a polymer/solvent mixture, from the Flory Huggins data measured at the composition extremes of the binary mixture (infinite dilution of polymer, and infinite dilution of solvent). This methodology is based on the works of Bernard Wolf about the dependence of the Flory Huggins parameter, χ , on the polymer composition. The methodology was validated for ten different polymer/solvent systems in a range of molecular weights from 10 to 250 kg/mol, with an overall value of the average absolute deviation (%AAD) between the literature and estimated pressure values around 1%.

From this article it is crucial to take into account the results for the Flory Huggins – polymer compositions curves, constructed with the Wolf parameters (v , $\xi\lambda$ and α) estimated from the Flory Huggins parameter values at infinite dilution of solvent and polymer, taken from the values reported in the previous chapters (studies of inverse gas chromatography and intrinsic viscosity, respectively) for the binary mixtures: EVA33/cyclohexane, and the ones of its correspondent homopolymers, PE/cyclohexane and PVA/cyclohexane, at 60 °C. In addition to the PVA/methanol mixture, at the same temperature. These Wolf parameters estimated are summarized in table 5.1.

Table 5.1 Wolf parameters for EVA33/cyclohexane, PE/cyclohexane, PVA/cyclohexane, and PVA/methanol at 60 °C.

Parameter	PVA/CH	PE/CH	EVA 33/CH	PVA/MET
v	0.430	0.455	0.271	0.360
$\xi\lambda$	0.500	0.500	0.500	0.000
α	1.050	0.551	0.974	0.495

With the constructed Flory Huggins – polymer composition curves (Figure 5.1), the subsequent estimation of the pressure – polymer compositions curves (Figure 5.2 and 5.3) was possible with the well-known thermodynamics relationships between the Flory Huggins parameters and the activity of the solvent, and this last one with the vapor pressure of the solvent and the pressure of the system.

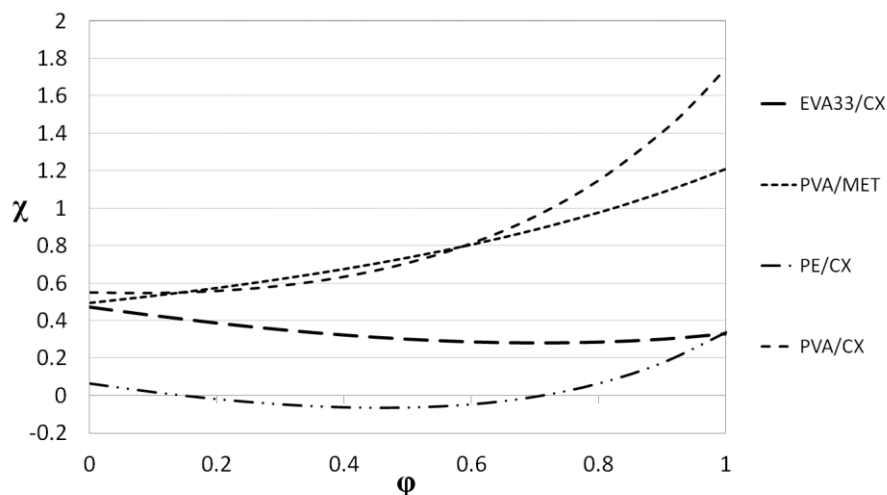


Figure 5.1. Flory Huggins – polymer composition curves for EVA33/cyclohexane, PE/cyclohexane, PVA/cyclohexane, and PVA/methanol at 60 °C.

In Figure 5.1, it is clearly observed the more favorable interactions for the PE/CH system (polymer/solvent dispersion characters), following with the EVA33/CH system (the dispersion character of this system decreases with the presence of vinyl acetate). Finally the PVA/MET and PVA/CH systems are not compatible systems for polymer diluted conditions. The first system is based on weak association interactions between the vinyl acetate monomer and methanol, meanwhile the second one is the most incompatible system, due to the association/polar character of the PVA in a dispersion solvent (CH).

In the last article of this work, “**PC-SAFT thermodynamics of ethylene vinyl acetate copolymer in a solution separation process**” a rigorous thermodynamic simulation for the separation stage of the Ethylene Vinyl Acetate copolymer (EVA) solution production process carry out in methanol (MET) to separate the unreacted vinyl acetate monomer (VA), is presented, employing the PC-SAFT equation of state model.

Initially, other polymer/solvent sorption curves strategically considered for the multi-equilibrium of the separation stage were determined, following the methodology validated in the previous article that uses the Bernard Wolf theories. Here, it is important to emphasize also the consideration of the system EVA/cyclohexane. Although this system is not present in the EVA solution separation process, it is a system with all sorption curves known, as it is shown in Figure 5.2, which represent an extra important thermodynamic information between the EVA copolymer and its correspondents homopolymers (PE and PVA). The Wolf parameters determined for the remaining systems are presented in Table 5.2, and their sorption curves are shown in Figures 5.2, 5.3 and 5.4.

Table 5.2 Wolf parameters for EVA33/methanol, PVA/vinyl acetate and EVA33/vinyl acetate at 60 °C.

Parameter	EVA33/MET	PVA/VA	EVA33/VA
ν	0.436	0.289	0.297
$\xi\lambda$	1.069	0.500	0.500
α	1.669	0.960	1.100

Then, the pure components PC-SAFT parameters were taken from literature (Aspen Plus[®] database), and the best association interactions scheme was specified for all the interactions of the considered compounds, also taking into account the association scheme previously defined between methanol and vinyl acetate solvents (Chapter 4). These resulting parameters are presented in Table 5.3.

Table 5.3 PC-SAFT parameters for EVA copolymer / solvents

Parameters	MET	VA	CH	SEG-PVA	SEG-PE
$\varepsilon^{\text{AiBi}}/k$	2899.5	0	0	1449.75	0
κ^{AiBi}	0.035176	0.035176	0	0.035176	0
m	1.5255	3.4442	2.5303	-	-
r	-	-	-	0.04224	0.04132
ε/k	188.9	232.25	278.11	243.9829	267.1854
σ	3.23	3.257	3.8499	3.0617	3.4751

Finally, the PC-SAFT binary interactions parameters (k_{ij}) were determined, adjusting strategically the polymer/solvent sorption curves constructed, by means of the Aspen Plus[®] regression simulation tool. These resulting k_{ij} parameters are summarized in Table 5.4. In all cases, a good agreement between the theoretical equilibrium curves and the PC-SAFT predictions was observed (Figures 5.2, 5.3, 5.4).

Table 5.4. PC-SAFT k_{ij} binary parameters for PVA/CH, PE/CH and PVA/PE

Parameter	SEG PVA/CH	SEG PE/CH	SEG PVA/ SEG PE	SEG PVA/MET	SEG PE/MET	SEG PVA/VA	SEG PE/VA	MET/VA
k_{ij}	0.0082	-0.0098	0.0247	-0.0136	-0.0267	-0.0286	0.0228	0.0352

Whit all the PC-SAFT parameters known, the global EVA separation production stage was simulated in a recovery column, by means of the Aspen Plus[®] flowsheet simulation tool, obtaining an average of %AAD for the mass flows of each component participating in the process, below to 1%, regarding the literature data shown in patents.

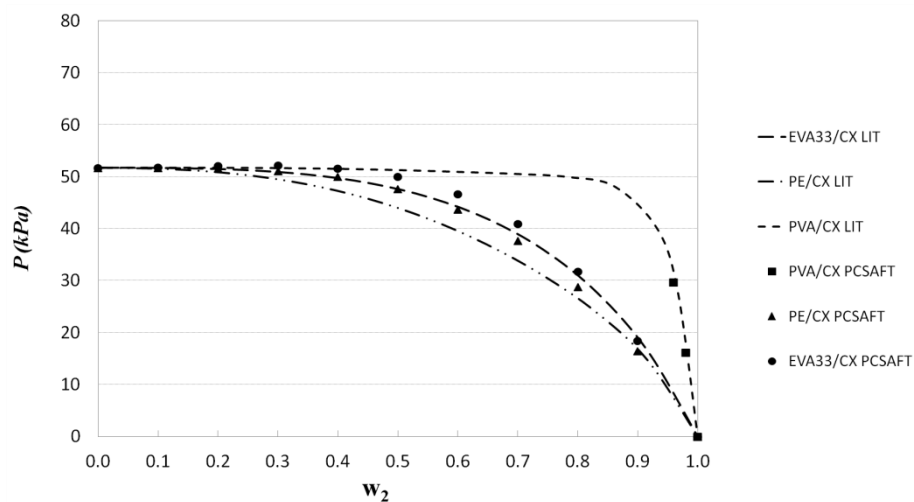


Figure 5.2 Sorption curves PVA, PE and EVA33 in cyclohexane at 60 °C

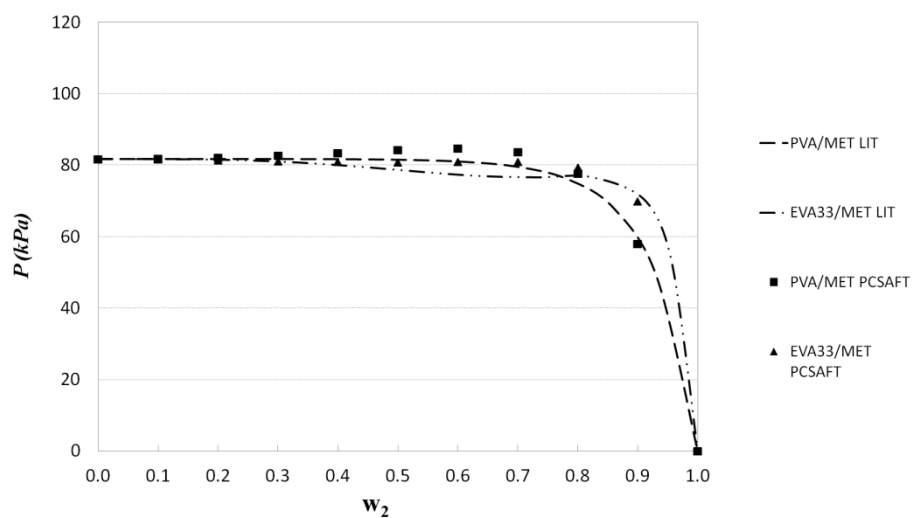


Figure 5.3 Sorption curves PVA and EVA33 in methanol at 60 °C

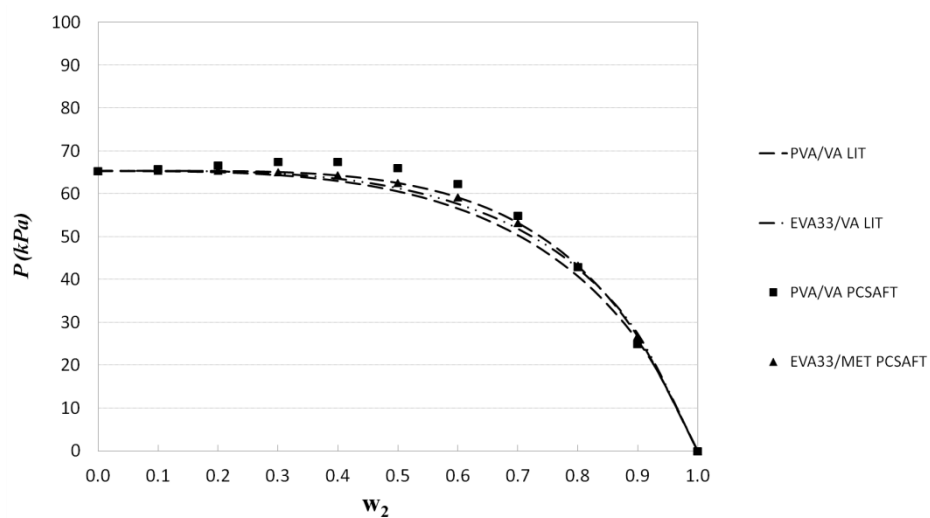


Figure 5.4 Sorption curves PVA and EVA33 in vinyl acetate at 60 °C

6 Conclusions

This work has presented a rigorous thermodynamic study for interactions between the Ethylene Vinyl Acetate (EVA) copolymer and the solvents involved in the separation stage of the EVA solution production process. To achieve this goal, the EVA copolymer was splitted into its correspondent homopolymers, Polyethylene (PE) and Polyvinylacetate (PVA). The solvents participating in this process are methanol and vinyl acetate, plus the strategic consideration of cyclohexane. In addition, the interaction between these polymers and other solvents (representing dispersion, association and polar solvents) were determined. The results of the global project include the following conclusions:

- The overall Flory Huggins interactions parameters of the two semicrystallines EVA copolymers samples, each one with different vinyl acetate (VA) content (EVA18, 18% and EVA33, 33% w/w VA), were determined in presence of nine different solvents at 30, 40 and 50 °C, by means of the Gas Inverse Chromatography technique. In addition a thermodynamic assessment was done at these infinite dilutions conditions of solvents. The main results indicate that the most favorable solvents for the EVA copolymers are the aromatic-type ones, due their polar character that interacts with the vinyl acetate present on the copolymers. The results also point the fact that the EVAs/solvents interactions are stronger in the case of the copolymer with the highest vinyl acetate percentage. In addition the Hildebrand solubility parameters (HSP) were determined ($15.93 \text{ MPa}^{1/2}$ for EVA33 and $14.7 \text{ MPa}^{1/2}$ for EVA18, lineally extrapolated at 60 °C).
- The overall Flory Huggins interaction parameters of a sample of a semicrystalline Polyethylene (PE) in presence of eight different solvents were determined at 40, 50 and 60 °C, by means of the Gas Inverse Chromatography technique. In addition a thermodynamic assessment was done at these infinite dilutions conditions of solvents. According to the main results the compatibility of the PE with the different types of solvents follows this order: dispersion solvents > polar solvents > association solvents, which was expected due the dispersion character of the ethylene monomer present in PE.

- The overall Flory Huggins parameters for an amorphous sample of Polyvinylacetate (PVA) in presence of eleven different solvents, were determined by means of the Gas Inverse Chromatography technique at 60, 70 and 80 °C, because in this amorphous polymer there are not bulk interactions below a certain temperature that take into account the glass transition temperature ($T_{g(PVA)} = 41.2$ °C) plus a transition zone with bulk plus adsorption interactions. The compatibility PVA/solvents follows this order was: polar solvents > association solvents, which is expected as the vinyl acetate monomer of PVA has a significant dipole moment. It was unreliable to determine thermodynamic parameters for mixtures with dispersion solvents, because despite being well above the T_g , no bulk dispersion interactions existed. In addition the Hildebrand solubility parameters of both polymers were also determined (14.1 $MPa^{1/2}$ for PE and 19.8 $MPa^{1/2}$ for PVA, at 60 °C), noting that the higher values of PVA is a consequence of the strong interactions of vinyl acetate monomer.
- Although the Hildebrand solubility parameters of EVA18 and EVA33 copolymers and PE and PVA polymers, were determined only to compare with literature data, because theoretically these parameters are not the more suitable for taking into account the polar and association interactions (given by the vinyl acetate monomer), the lineal correlation of the HSP at 60 °C, between the four mentioned polymers was highly satisfactory. With increasing the content of vinyl acetate increases the solubility parameter of the polymer; which will draw ever closer to the solubility parameter of the pure vinyl acetate (17.1 $MPa^{1/2}$ at 60°C), exactly in an EVA copolymer of a 54.3% of vinyl acetate, which agrees the literature morphology description of the EVA copolymers.
- The amorphous Flory Huggins interaction parameter for the semicrystallines samples consider above (PE, EVA18 and EVA33), were determined in presence of methanol, vinyl acetate and cyclohexane by means of the Gas Inverse Chromatography technique. In addition a thermodynamic assessment was done at these infinite dilutions conditions of solvents. The results indicated that when the range of studied temperatures is below the melting point of a semicrystalline polymer, it is crucial to calculate the amorphous contribution ($\chi_{amorphous}$) on the overall Flory Huggins parameters previously determined, according the percent of crystallinity of each polymer. The results show that the more compatible solvent was cyclohexane, and therefore it was selected as the probe to calculate the percentages of crystallinity at room temperature (35% for PE, 29% for EVA18, and 12% for EVA33), which were in agreement the literature data. Regarding the interactions between the three polymeric materials and the solvents, it can be noticed that, the lower the vinyl acetate content is in the polymer (higher crystallinity), the higher the difference between the previous published overall Flory Huggins parameters, and amorphous Flory Huggins parameters is. For the best solvent (cyclohexane) $\chi_{amorphous}$ represents the less contribution or the highest correction to the overall Flory Huggins parameter (around 50% for PE and EVA18, and 79% for EVA33), following by the medium compatible solvent (vinyl acetate) and finally by the worst solvent (methanol). These last two percentages were, in average, around 80% and 91%.

- The Hildebrand solubility parameter (HSP) for the EVA33 has been estimated by means of molecular dynamics simulations, employing the COSMO-SAC model, in order to compare it with the experimental HSP values obtained by means of the overall Flory Huggins obtained by Inverse Gas Chromatography. The results showed that the average deviation for the EVA33 HSP is below to 7.5%, between the COSMO-SAC and the experimental one, determined by IGC.
- The Flory Huggins interaction parameters of the two semicrystallines EVA copolymers samples, with different vinyl acetate content (18% and 33% w/w), were determined in presence of five different diluent solvents at 30, 40 and 50 °C, by means of the Intrinsic Viscosity technique . These Flory Huggins parameters were calculated according the Stockmayer and Berry relationships, which takes into account the overall and the theta intrinsic viscosities, for each polymer solvent mixture. The first viscosity one was determined from the Huggins-Kramer plot, and the second one from the turbidimetric Elias method. In addition a thermodynamic assessment was done at these infinite dilutions conditions of polymer. The main results indicate that all the solvents are clearly compatible with the copolymers ($\chi \leq 0.6$), which is expected due the diluent character of the solvents. Also it was found that the EVAs/solvents interactions are quite stronger ($\Delta\chi \approx 0.1$) in the case of the copolymer with the highest vinyl acetate percentage. In addition the Hansen solubility parameters were determined, obtaining almost the same value ($17.5 \text{ MPa}^{1/2}$ for EVA33 and $17.4 \text{ MPa}^{1/2}$ for EVA18, at 30 °C), highlighting the presence of the triple contribution for dispersion, polar an association interactions, of these copolymers.
- The Flory Huggins interaction parameters of two mixtures, Polyethylene (PE) in presence on cyclohexane, and Polyvinylacetate in methanol, were determined at 60 °C, by means of intrinsic viscosity measurements, following the Stockmayer-Fixman procedure. Previously, the viscous average molecular weights of all the polymers employed were obtained through the Mark-Houwink procedure. In addition a thermodynamic assessment was done at these infinite dilutions conditions of polymer..According to the main results the obtained Flory Huggins parameter were lower than 0.5, which implies that at infinite dilution of polymer, the mentioned systems are completely compatible, being the more favorable miscible interactions for the PE/cyclohexane mixture.
- The binary interaction parameters were estimated for several thermodynamic models (NRTL and UNIQUAC activity coefficient models, and Peng-Robinson and PC-SAFT equations of state), adjusted from the liquid-vapor equilibrium curve ($T-x_i, y_i$) obtained experimentally for the mixtures of vinyl acetate/methanol and vinyl acetate/butanol at atmospheric pressure, by means of the glass ebullometer experimental technique. The experimental data consistency was evaluated favorably with the Wisniak L–W method. The main results show that the NRTL, UNIQUAC and PC-SAFT models are capable of accurately fitting the experimental data of the two systems ($\%AAD_{y_1} \leq 4\%$) while a much higher deviation is obtained when the Peng Robinson model is employed ($\%AAD_{y_1} \approx 10\%$).

- A new methodology to determine the solvent sorption curve (pressure-polymer composition) of a polymer/solvent mixture, from the Flory Huggins data measured at the composition extremes of the binary mixture (infinite dilution of polymer, and infinite dilution of solvent), were development. This methodology is based on the works of Bernard Wolf about the dependence of the Flory Huggins parameter, χ , on the polymer composition. The methodology was validated for ten different polymer/solvent systems in a range of molecular weights from 10 to 250 kg/mol, with an overall value of the average absolute deviation (%AAD) between the literature and estimated pressure values of 1%.
- A rigorous thermodynamic simulation for the separation stage of the Ethylene Vinyl Acetate copolymer (EVA) solution production process carry out in methanol (MET) to separate the unreacted vinyl acetate monomer (VA), was presented; employing the PC-SAFT equation of state model, splitting the EVA copolymer in its correspondent homopolymers, Polyethylene (PE) and Polyvinylacetate (PVA), and determining the six PC-SAFT binary interaction parameters (k_{ij}), that take into account all the possible interactions between the components participating in the mentioned process (PE, PVA, MET and VA). These k_{ij} for homopolymers, were determined from the solvent sorption curves constructed from the Flory Huggins data at infinite dilution of polymer and solvent, following a methodology described in literature that considers the Bernard Wolf thermodynamic theories. The k_{ij} between the solvents was determined from the vapour liquid equilibrium data reported in literature. Also, the best association scheme for the interactions for these compounds was defined, and the pure PC-SAFT parameters were taken from literature. A good agreement between each sorption curves for polymer/solvent estimated theoretically and predicted with the PC-SAFT model, was obtained. Finally, a global process simulation was done, obtaining an average of %AAD for the mass flows of each component participating in the EVA solution separation production process below to 1%, regarding the literature data shown in patents.

7 Appendix

This chapter presents the polymer characterization results for the other techniques discussed in the introduction chapter, that were employed in the framework of this study, and don't were included in the previously articles shown.

These techniques includes the results for the Gas Permeation Gel Chromatography (GPC) of the EVA33 and EVA18 copolymers, the Thermogravimetric Analysis (TGA) for an a sample of EVA33 copolymer, and images taken by Scanning Electronic Microscopy (SEM), for several samples of EVA and its homopolymers, Polyethylene and Polyvinylacetate, pure and impregnated in Chromosorb for packing of the Inverse Gas Chromatography columns.

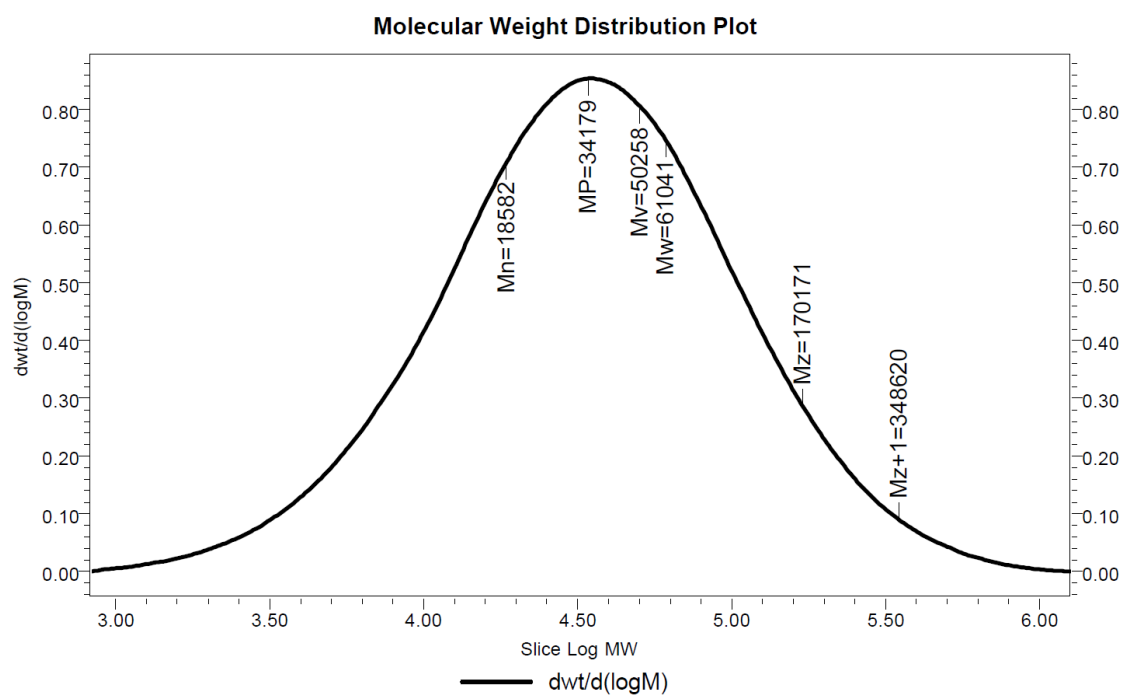


Figure 7.1. GPC analysis for EVA33 copolymer

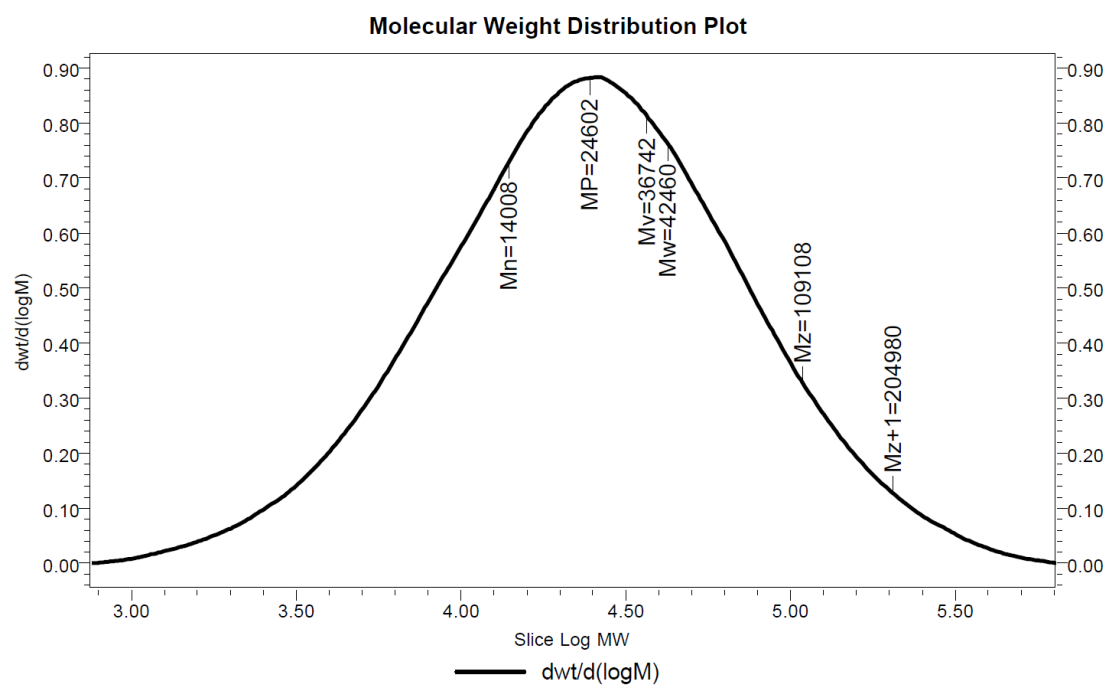


Figure 7.2. GPC analysis for EVA18 copolymer

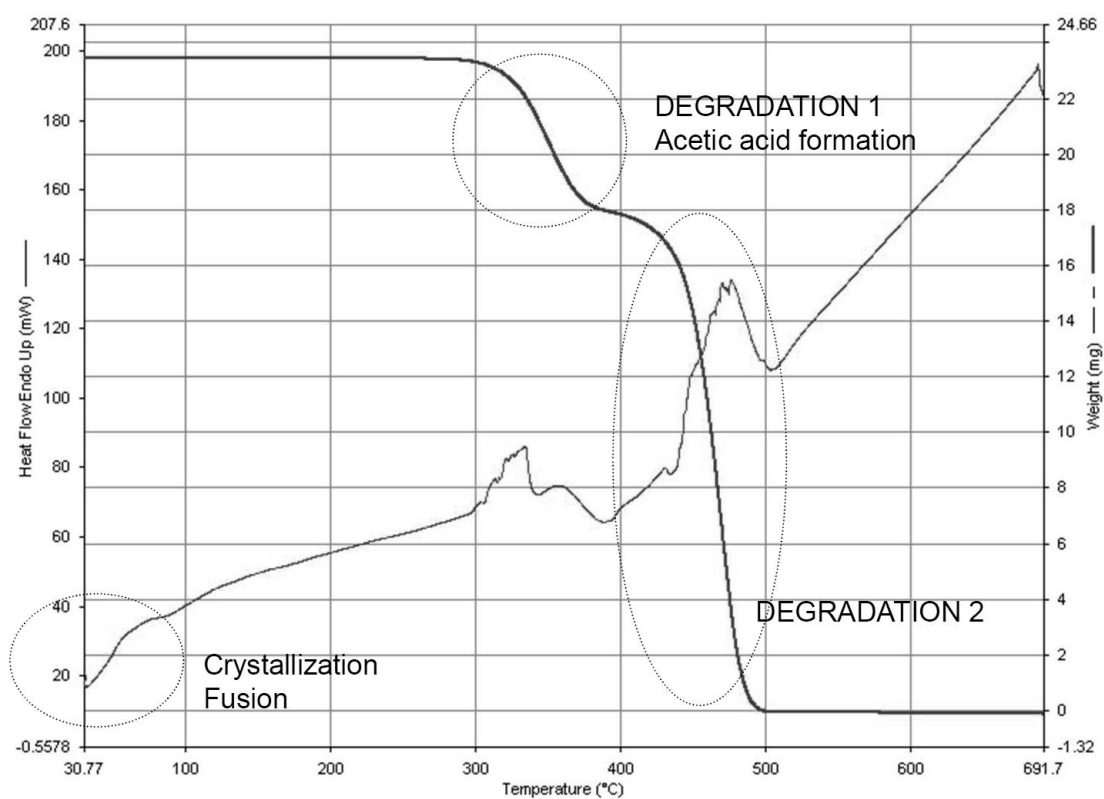


Figure 7.3. TGA analysis for EVA33 copolymer

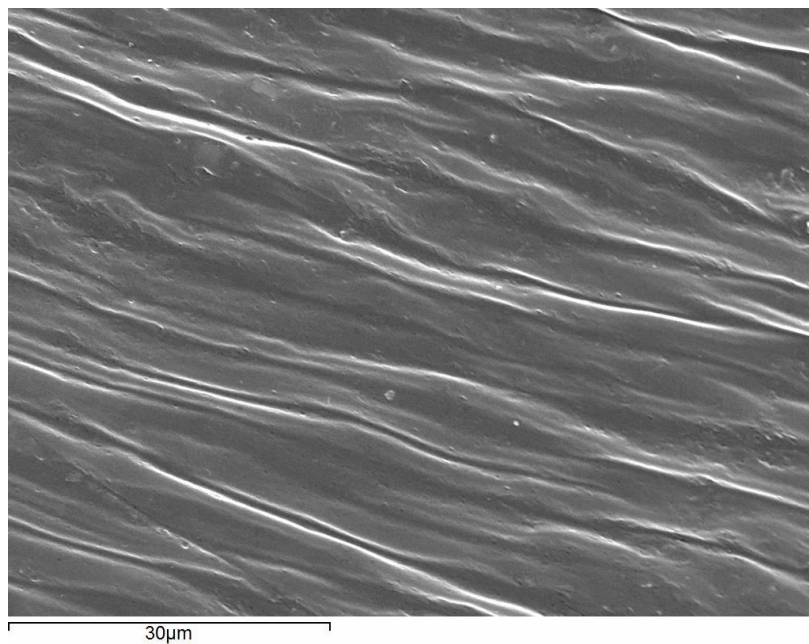


Figure 7.4. SEM analysis for EVA33 copolymer, 30 μm



Figure 7.5. SEM analysis for EVA33 copolymer impregnated in Chromosorb, 50 μm

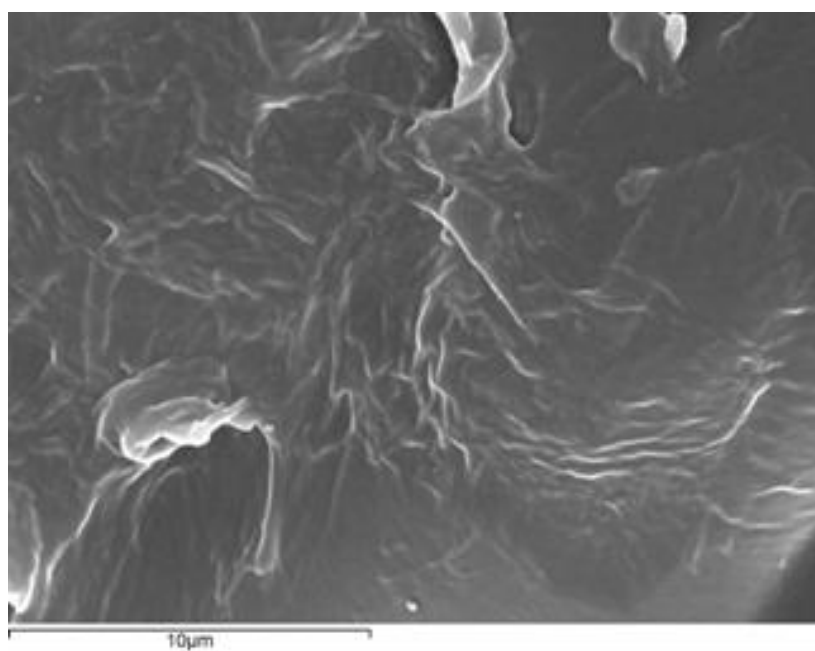


Figure 7.6. SEM analysis for Polyethylene, 10 μm

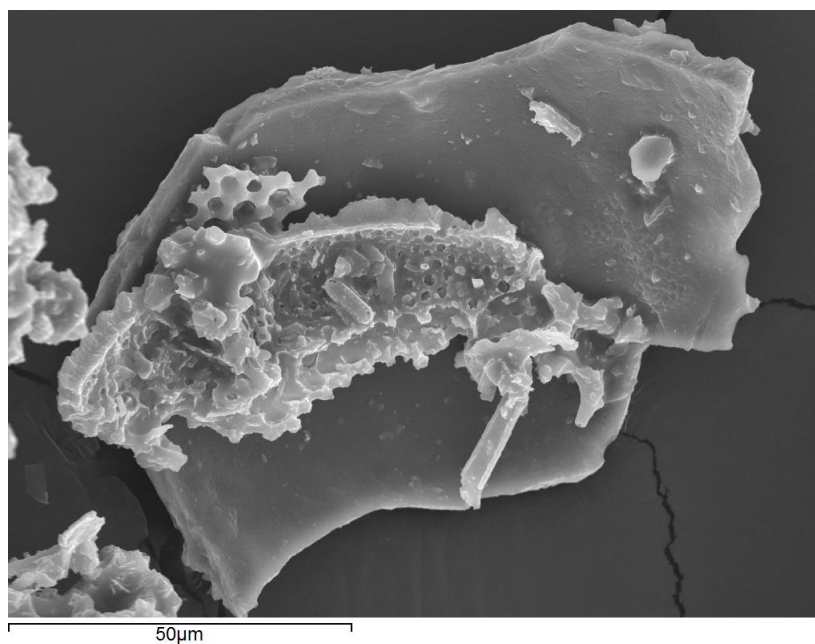


Figure 7.5. SEM analysis for Polyethylene impregnated in Chromosorb, 50 μm

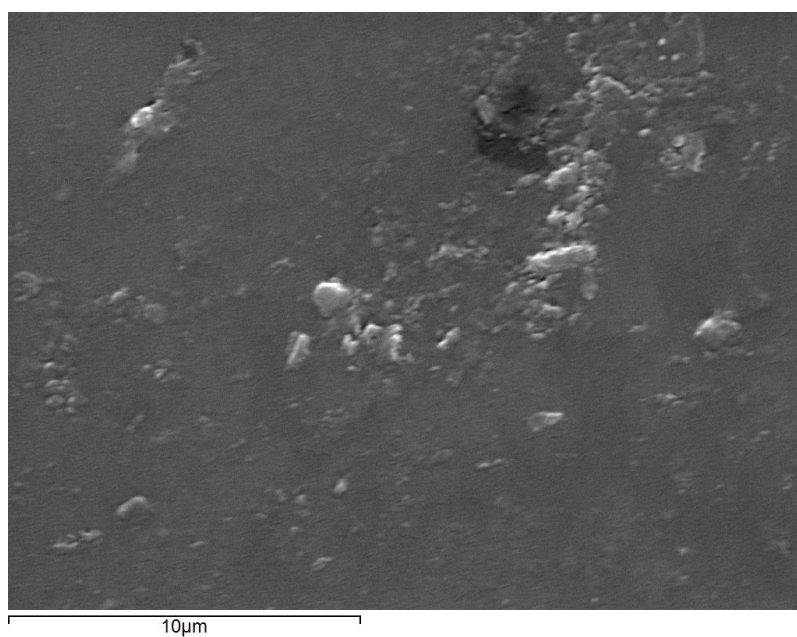


Figure 7.6. SEM analysis for Polyvinylacetate, 10 μm

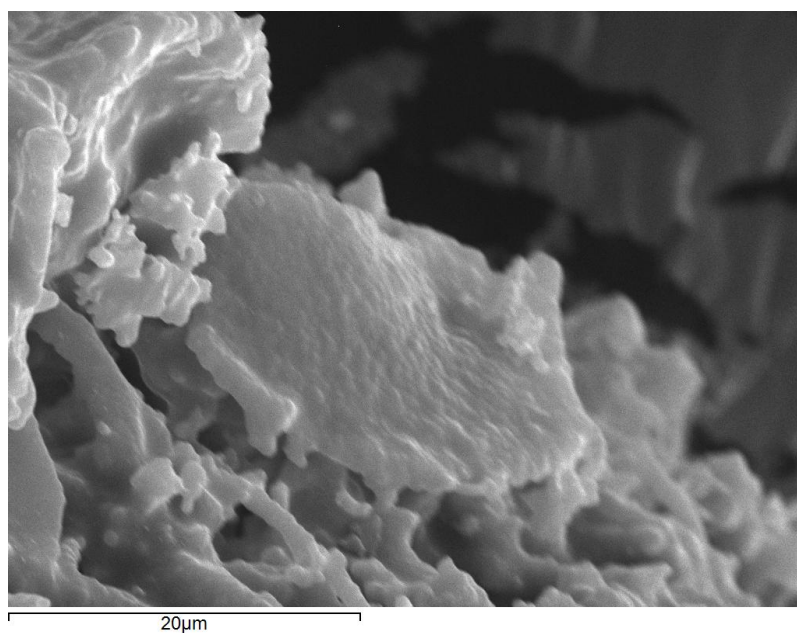


Figure 7.5. SEM analysis for Polyvinylacetate impregnated in Chromosorb, 20 μm